

# Epigenetic Modulation of Small Airway Fibrosis in Chronic Obstructive Pulmonary Disease

A thesis submitted for the degree of  
Doctor of Philosophy

Razia Zakarya  
B. Med.Sci. (hons)  
B.Ec.

School of Life Sciences  
Faculty of Science

University of Technology Sydney  
2019

## CERTIFICATE OF ORIGINAL AUTHORSHIP

I, Razia Zakarya, declare that this thesis, is submitted in fulfilment of the requirements for the award of Doctor of Philosophy, in the Faculty of Science at the University of Technology Sydney.

This thesis is wholly my own work unless otherwise referenced or acknowledged. In addition, I certify that all information sources and literature used are indicated in the thesis.

This document has not been submitted for qualifications at any other academic institution.

This research is supported by an Australian Government Research Training Program Scholarship.

Production Note:

Signature removed prior to publication.

11/09/2019

## Abstract

Chronic Obstructive Pulmonary Disease is commonly associated with cigarette smoke exposure in developed nations. However, research demonstrating that a minority proportion of smokers develop COPD alongside findings that show a stronger correlation between lung function and familial relation than smoke exposure demonstrates that the link between cigarette smoking and airway obstruction is not linear. Previous work from our lab has shown that airway mesenchymal cells of COPD patients produced more extracellular matrix (ECM), thereby contributing to small airway fibrosis. We hypothesise that the mechanisms underpinning increased ECM production in COPD was epigenetic.

Using primary human airway smooth muscle cells, we carried out a microarray gene analysis to determine which ECM genes were aberrantly upregulated in COPD. We determined that transforming growth factor  $\beta$ 1 (TGF- $\beta$ 1) stimulation lead to significantly higher induction of *COL15A1* and *TNC* in COPD *in vitro*. Further, we carried out IHC analysis to show that collagen 15 $\alpha$ 1 and tenascin-C were deposited in the airway smooth muscle (ASM) layer in small airways of COPD patients. Upon quantifying amount of ECM protein deposited within the ASM layer, we determined that collagen 15 $\alpha$ 1 deposition was significantly higher in COPD airways; demonstrating that the ECM protein was aberrantly expressed *in vivo*.

Investigating epigenetic modulations directed us towards studying specific acetyl-lysine histone modifications at the target gene promoter regions. We, for the first time, demonstrated that increased ECM expression in COPD is modulated by histone H4 acetylation induced upon stimulation with TGF- $\beta$ 1. Further, we found that the epigenetic reader, Brd4, plays a role in propagating the epigenetic mark to sustain prolonged *COL15A1* and *TNC* expression.

## Acknowledgements

My PhD candidature will remain a time that I look back on fondly thanks to all those I met over the years. I feel privileged to have been guided by a fantastic supervisory team of A/Professor Brian Oliver and A/Professor Hui Chen.

My heartfelt gratitude goes to Brian, whom I hold in the highest regard as a scientist and a mentor. Brian was always there with feedback and support when I needed him whilst simultaneously allowing me to freely pursue scientific lines of enquiry. A true gift to any budding scientist.

I extend an earnest thank you to Hui, who has always kept my career interests and progression in mind. Hui has given me many opportunities and shown me the ropes within academia and for that I am forever grateful.

I extend a heartfelt thank you to all my colleagues – new and old – within the Respiratory Research Group at the Woolcock Institute. Namely, Dia, Sandra, Jack, and Jeremy – whom I have relied upon at one point or another throughout my candidature and who have always proved to be a source of support. To Jeremy, Diren, and Sandra who helped with work directly contributing to this thesis. And Penny for showing me the wonderful world of online graphics.

I'd like to thank my mum for teaching me that hard work and perseverance will get you anywhere you set your mind to.

Finally, I would like to extend a sincere thank you to my fiancée, Anh. Thank you for being beside me through all the long days and weekends in the lab, for understanding that experimental protocol takes precedence, and for never letting me lose sight of the bigger picture.



## Presentations and Posters Arising from This Work

**Small airway fibrosis is mediated by histone acetylation. R. Zakarya, H. Chen, C.A.A. Brandsma, I.M. Adcock, B.G.G. Oliver 2019** Poster discussion at the annual International Conference of the American Thoracic Society in 2019

**Role of histone acetylation in fibrosis in chronic obstructive pulmonary disease. R. Zakarya, H. Chen, C.A.A. Brandsma, I.M. Adcock, B.G.G. Oliver 2018** Poster discussion at the annual International Conference of the American Thoracic Society in 2018

**Investigating the effect of histone acetylation on TGF- $\beta$  induced fibrosis in COPD. R. Zakarya, H. Chen, C.A.A. Brandsma, I.M. Adcock, B.G.G. Oliver 2018** Oral Presentation at the Thoracic Society of Australia and New Zealand National Annual Scientific Meeting 2018

**Epigenetic Control of TGF- $\beta$  Induced Fibrosis in COPD. R. Zakarya, H. Chen, C.A.A. Brandsma, I.M. Adcock, B.G.G. Oliver 2017** Oral presentation at the Thoracic Society of Australia and New Zealand NSW Annual Scientific Meeting 2017

**Investigating the Role of Histone Acetylation in TGF- $\beta$  Induced Fibrosis in COPD. R. Zakarya, H. Chen, C.A.A. Brandsma, I.M. Adcock, B.G.G. Oliver 2017** Poster presentation at the European Respiratory Society International Congress 2017

## Publications Included as an Adjunct to This Work

The following publications do not pertain directly to this work but have been included as evidence of research productivity. Articles listed below can be found in Appendix A.

**A Mitochondrial Specific Antioxidant Reverses Metabolic Dysfunction and Fatty Liver Induced by Maternal Cigarette Smoke in Mice.** Gerard Li, Yik Lung Chan, Suporn Sukjamnong, Ayad G Anwer, Howard Vindin, Matthew Padula, Razia Zakarya, Jacob George, Brian G Oliver, Sonia Saad, Hui Chen *Nutrients* 2019

**Dietary fatty acids amplify inflammatory responses to infection through p38 MAP kinase signalling.** Sandra Rutting, Razia Zakarya, Jack Bozier, Dia Xenaki, Jay C Horvat, Lisa G Wood, Philip M Hansbro, Brian G Oliver *American Journal of Respiratory Cell and Molecular Biology* 2019

**MitoQ supplementation prevent long-term impact of maternal smoking on renal development, oxidative stress and mitochondrial density in male mice offspring.** Suporn Sukjamnong, Yik Lung Chan, Razia Zakarya, Long The Nguyen, Ayad G Anwer, Amgad A Zaky, Rachana Santiyanont, Brian G Oliver, Ewa Goldys, Carol A Pollock, Hui Chen, Sonia Saad *Scientific Reports* 2018

**Biomass Smoke Exposure Enhances Rhinovirus-Induced Inflammation in Primary Lung Fibroblasts.** Sarah J. Capistrano, Razia Zakarya, Hui Chen, Brian G. G. Oliver. *International Journal of Molecular Sciences* 2016

## Table of Contents

Abstract.....	iii
Acknowledgements.....	iv
Presentations and Posters Arising from This Work.....	v
Publications Included as an Adjunct to This Work .....	vi
Table of Figures .....	xi
List of Tables .....	xii
List of Abbreviations .....	xiii
Preface .....	1
Publication Declaration.....	2
Publication Declaration.....	11
Chapter 1 Introduction .....	23
1.1 Epidemiology .....	23
1.2 Heritability.....	25
1.3 Symptoms.....	25
1.4 Diagnosis.....	26
1.5 Pathophysiology.....	28
1.5.1 Small airway inflammation .....	30
1.5.2 Structural changes in small airways.....	33
1.5.3 TGF- $\beta$ Signalling.....	35
1.6 Epigenetics.....	38
DNA methylation.....	39
Histone modifications .....	41
Epigenetic readers .....	46
1.7 Hypothesis and aims .....	47
Chapter 2 Determination of Aberrantly Expressed ECM Genes in COPD .....	50
2.1 Introduction.....	50
2.2 Methods .....	52
2.2.1 Ethics statement.....	52
2.2.2 Primary cell isolation.....	52
2.2.3 Study subjects.....	54
2.2.4 Cell culture.....	54
2.2.5 Cell stimulation .....	55
2.2.6 mRNA sample collection .....	55
2.2.7 mRNA purification.....	56

2.2.8 Reverse Transcription.....	56
2.2.9 Microarray analysis .....	57
2.2.10 Reverse Transcriptase Quantitative PCR.....	57
2.2.11 Immunohistochemistry .....	58
2.2.12 Statistical analysis .....	59
2.3 Results.....	60
2.3.1 Microarray Analysis .....	60
2.3.2 RT-qPCR Determination of Target Gene Expression.....	61
2.3.3 Immunohistochemical Localisation & Quantification of Collagen 15 $\alpha$ 1 and Tenascin-C .....	62
2.4 Discussion .....	65
Chapter 3 Investigations into Epigenetic Aberrations Underlying ECM Expression in COPD .....	69
3.1 Introduction.....	69
3.2 Methods .....	80
3.2.1 Ethics statement.....	80
3.2.2 Primary cell isolation.....	80
3.2.3 Study subjects.....	80
3.2.4 Cell culture.....	80
3.2.5 Stimulation & Epigenetic Enzyme Inhibition .....	80
3.2.6 Nuclear Extraction.....	82
3.2.7 HAT activity assay .....	82
3.2.8 HDAC activity assay .....	83
3.2.9 Quantitative PCR.....	83
3.2.10 Statistical analysis .....	83
3.3 Results.....	84
3.3.1 Effect of DNMT1 inhibition on <i>COL15A1</i> and <i>TNC</i> expression .....	84
3.3.2 Effect of HDAC inhibition on <i>COL15A1</i> and <i>TNC</i> expression.....	85
3.3.3 Effect of HAT inhibition on <i>COL15A1</i> and <i>TNC</i> expression.....	86
3.3.4 Effect of inhibited KTMs and KDM on <i>COL15A1</i> and <i>TNC</i> expression.....	86
3.3.5 Investigation into basal HAT activity .....	87
3.3.6 Investigation into basal HDAC activity.....	88
3.4 Discussion .....	90
Chapter 4 Chromatin Targeted Investigation of Histone Acetylation.....	95
4.1 Introduction.....	95
4.2 Methods .....	99

4.2.1 Ethics statement.....	99
4.2.2 Primary cell isolation.....	99
4.2.3 Study subjects.....	99
4.2.4 Cell culture.....	99
4.2.5 Stimulation & Brd4 Inhibition.....	99
4.2.6 mRNA sample collection .....	100
4.2.7 mRNA purification.....	100
4.2.8 Reverse Transcription.....	100
4.2.9 Quantitative PCR (cDNA).....	100
4.2.10 ChIP Sample Collection .....	101
4.2.11 Chromatin Sonication.....	101
4.2.12 Chromatin Immunoprecipitation Assay.....	102
4.2.13 Primer Design.....	105
4.2.14 Polymerase Chain Reaction.....	107
4.2.15 Optimisation of PCR Primer Conditions .....	107
4.2.16 Optimisation of SYBR qPCR conditions.....	108
4.2.17 Quantitative PCR (gDNA).....	109
4.2.18 Statistical analysis .....	110
4.2.19 In silico genomic analysis.....	110
4.3 Results.....	111
4.3.1 Quantification of <i>TNC</i> template bound to acetylated histone H3.....	111
4.3.2 Quantification of <i>COL15A1</i> template bound to acetylated histone H3 .....	112
4.3.3 Quantification of <i>TNC</i> template bound to acetylated histone H4.....	114
4.3.4 Quantification of <i>COL15A1</i> template bound to acetylated histone H4 .....	116
4.3.5 Vehicle test.....	117
4.3.6 Dose-response relationship between Brd4 inhibition and <i>TNC</i> expression.....	118
4.3.7 Dose-response relationship between Brd4 inhibition and <i>COL15A1</i> expression .....	119
4.3.8 Quantification of <i>TNC</i> template bound to acetylated histone H4 post Brd4 inhibition.....	121
4.3.9 Quantification of <i>COL15A1</i> template bound to acetylated histone H4 post Brd4 inhibition.....	123
4.3.10 Chromosomal location of ECM target genes in microarray analysis .....	124
4.4 Discussion .....	126
Chapter 5 Summary, Future Directions, and Conclusion .....	130
5.1 Introduction.....	130
5.2 Determination of aberrantly expressed ECM genes in COPD .....	131

5.3 Investigations into epigenetic aberrations underlying ECM expression in COPD .....	132
5.4 Chromatin targeted investigation of histone acetylation.....	134
5.5 Future Directions.....	140
5.6 Conclusion .....	143
Appendix A –	
Publications Included as an Adjunct to This Work .....	144
Appendix B –	
Genes Located on ECM Microarray.....	196
Appendix C –	
Data from Study into Off-target Effects of Epigenetic Inhibitors.....	200
Appendix D –	
Genome Data Viewer: Chromosomal Proximity of COL15A1 and TGFBR1 .....	202
Chapter 6 Reference.....	204

## Table of Figures

Figure 1.1 Rate of decline in FEV1 .....	24
Figure 1.2 Small airway obstruction. ....	29
Figure 1.3 Sites of epigenetic marks on histones.....	42
Figure 2.1 Microarray analysis.....	60
Figure 2.2 qPCR Validation of TGF- $\beta$ 1 induced ECM gene expression .....	62
Figure 2.3 Immunohistochemical Staining.....	63
Figure 2.4 Quantification of ECM protein deposition in ASM layer.....	64
Figure 3.1 Maintenance of DNA Methylation by DNMT .....	70
Figure 3.2 Schematic representation of Histone Tails .....	72
Figure 3.3 Histone Acetylation Mediated by HAT and HDAC. ....	73
Figure 3.4 Effect of DNMT1 inhibition with 5-azacytidine (10 $\mu$ M) on (a) <i>COL15A1</i> and (b) <i>TNC</i> expression.....	84
Figure 3.5 Effect of HDAC inhibition with Trichostatin A (TSA) (100nM) on (a) <i>COL15A1</i> and (b) <i>TNC</i> expression.....	85
Figure 3.6 Effect of HAT inhibition with Curcumin (10 $\mu$ M) on (a) <i>COL15A1</i> and (b) <i>TNC</i> expression. ....	86
Figure 3.7 Effect of lysine specific demethylase 1 (LSD1) inhibition with GSK-LSD1 (100nM) on (a) <i>COL15A1</i> and (b) <i>TNC</i> expression.....	87
Figure 3.8 Histone acetyltransferase activity assay. ....	88
Figure 3.9 Histone deacetylase (HDAC) activity assay.....	89
Figure 4.1 Schematic Representation of Transcriptional Triad. ....	97
Figure 4.2 Chromatin Fragments Post-Sonication.....	102
Figure 4.3 Detection of gDNA via PCR against <i>GAPDH</i> . ....	104
Figure 4.4 Temperature Optimisation for <i>COL15A1</i> primer set. ....	108
Figure 4.5 <i>TNC</i> bound to acetylated H3 determined via ChIP-PCR.....	112
Figure 4.6 <i>COL15A1</i> bound to acetylated H3 determined via ChIP-PCR.. ....	113
Figure 4.7 <i>TNC</i> bound to acetylated H4 determined via ChIP-PCR.....	115
Figure 4.8 <i>COL15A1</i> bound to acetylated H4 determined via ChIP-PCR. ....	117
Figure 4.9 Dose response of <i>TNC</i> mRNA expression post-Brd4 inhibition.....	119
Figure 4.10 Dose response of <i>COL15A1</i> mRNA expression post-Brd4 inhibition. ....	120
Figure 4.11 <i>TNC</i> bound to acetylated H4 post-Brd4 inhibition determined via ChIP-PCR. ....	122
Figure 4.12 <i>COL15A1</i> bound to acetylated H4 post-Brd4 inhibition determined via ChIP-PCR.....	124
Figure 4.13 Chromosome 9.....	125
Figure 5.1 ASM cells produce more ECM in COPD <i>in vitro</i> and <i>in vivo</i> . ....	137
Figure 5.2 Summary of Aim 2 Findings.....	138
Figure 5.3 TGF- $\beta$ 1 induces Brd4 mediated H4ac in COPD.. ....	139

## List of Tables

Table 1.1 GOLD Categories 1-4. ....	27
Table 1.2 The Refined ABCD Assessment Tool. ....	28
Table 1.1.3 List of known TGF- $\beta$ receptors and their respective encoding gene. ....	<b>Error!</b>
<b>Bookmark not defined.</b>	
Table 2.1 Patient information. ....	53
Table 3.1 HAT Substrate Specificity. ....	74
Table 3.2 Classes & subcellular distribution of histone deacetylases (HDACs). ....	75
Table 3.3 Lysine methyltransferases (KMTs), lysine demethylases (KDMs), and protein arginine methyltransferases (PRMTs). ....	78
Table 4.1 Immunoprecipitations (IPs) Per Sample. ....	103
Table 4.2 List of <i>COL15A1</i> and <i>TNC</i> transcription variants. ....	106
Table 4.3 SYBR qPCR Reaction Setup. ....	109



## List of Abbreviations

5mC	5-methylcytosine
ANOVA	Analysis of variance
ASM	Airway smooth muscle
BAL	Bronchoalveolar lavage
BALT	Bronchial associated lymphoid tissue
BCA	Bicinchoninic acid
BET	Bromodomain and extraterminal domain protein
BID	Basic residue-enriched interaction domain
BSA	Bovine serum albumin
CAT	COPD Assessment Test
CDK	Cyclin dependant kinase
cDNA	Complementary DNA
ChIP	Chromatin immunoprecipitation
COPD	Chronic Obstructive Pulmonary Disease
CSE	Cigarette smoke extract
DC	Dendritic cell
DEPC	Diethylpyrocarbonate
DMEM	Dulbecco's modified eagle medium
DNA	Deoxynucleic acid
DNMT	DNA methyltransferase
DSIF	DRB-sensitivity-inducing factor
DTT	Dithiothreitol
ECM	Extracellular matrix
EMA	European Medicines Agency
FBS	Foetal bovine serum
FEV <sub>1</sub>	Forced expiratory volume in 1 second
FOT	forced oscillation technique
FOXP3	Forkhead box P3
FVC	Forced vital capacity
FVC	Forced vital capacity
GDV	Genome data viewer
GOLD	Global Initiative for Chronic Obstructive Lung Disease
GSK-3 $\beta$	Glycogen synthase kinase- $\beta$
GWAS	Genome wide association study
H3ac	Histone H3 acetylation
H3K27me3	Trimethylation of lysine 27 on histone 3
H4ac	Histone H4 acetylation
H4K9me2	Dimethylation of lysine 9 on histone 4
H4K9me3	Trimethylation of lysine 9 on histone 4
HAT	Histone acetyltransferase
HDAC	Histone deacetylase

HDM	House dust mite
IL	Interleukin
IL-5	Interleukin 5
IL-5R $\alpha$	Interleukin 5 receptor subunit alpha
IP	Immunoprecipitation
IPF	Idiopathic pulmonary fibrosis
K	Lysine
KAT	Lysine acetyltransferase
KDAC	Lysine deacetylase
KMT	Lysine methyltransferase
LPS	Lipopolysaccharide
Me-DIP	Methylated DNA precipitation
mMRC	modified MRC dyspnea scale
mRNA	Messenger ribonucleic acid
NAD <sup>+</sup>	Nicotinamide adenine dinucleotide
NCBI	National Center of Biotechnology Information
NELF	Negative elongation factor
NF- $\kappa$ B	Nuclear factor kappa B
PBS	Phosphate buffered saline
PCR	Polymerase chain reaction
PDID	Phosphorylation dependent interaction domain
PGP	Proline-glycine-proline matrikine
PIC	Protease inhibitor cocktail
PRMT	Arginine methyltransferase
pTEFb	Positive transcription elongation factor
PTM	Post-translational modification
R	Arginine
SAHA	Suberoylanilide hydroxamic acid
SAM	S-adenosyl-L-methionine
SNP	Single nucleotide polymorphism
TGF- $\beta$	Transforming growth factor beta
TNF- $\alpha$	Tumour necrosis factor alpha
TSA	Trichostatin A
TSLP	Thymic stromal lymphopoeitin
TSS	Transcriptional start sites
VEGF	Vascular endothelial growth factor
WNT	Wingless/integrase 1

I hereby state that this submission is a thesis by compilation.

## Preface

An investigation into epigenetic modulation includes investigations into hereditary impacts of environmental insults. The following published works investigate the intergenerational effects of cigarette smoke and e-cigarette vapour on established respiratory outcomes and are included in this thesis:

**The effect of long-term maternal smoking on the offspring's lung health.** Razia Zakarya\*, Suporn Sukjamnong\*, Yik Lung Chan\*, Sonia Saad, Pawan Sharma, Rachana Santiyanont, Hui Chen, Brian G. G. Oliver. *American Journal of Physiology - Lung Cellular and Molecular Physiology* 2017

**Epigenetic impacts of maternal tobacco and e-vapour exposure on the offspring lung.** Razia Zakarya, Ian Adcock, Brian G Oliver. *Clinical Epigenetics* 2019

## Publication Declaration

**The effect of long-term maternal smoking on the offspring's lung health. Razia Zakarya\*, Suporn Sukjamnong, Yik-Lung Chan, Sonia Saad, Pawan Sharma, Rachana Santiyanont, Hui Chen, Brian G. G. Oliver. *American Journal of Physiology – Lung Cellular and Molecular Physiology* 2017**

**Status:** Published

**Authors' contributions:** S. Sukjamnong, Y.L.C., and R.Z. performed experiments; S. Sukjamnong, Y.L.C., R.Z., and B.G.O. analyzed data; S. Sukjamnong, Y.L.C., R.Z., S. Saad, P.S., H.C., and B.G.O. interpreted results of experiments; S. Sukjamnong prepared figures; S. Sukjamnong, Y.L.C., and B.G.O. drafted manuscript; S. Sukjamnong, Y.L.C., R.Z., S. Saad, P.S., R.S., H.C., and B.G.O. approved final version of manuscript; Y.L.C., R.Z., S. Saad, P.S., R.S., H.C., and B.G.O. edited and revised manuscript; R.Z., S. Saad, R.S., H.C., and B.G.O. conceived and designed research.

### Signatures:

Name	Signature	Date
Razia Zakarya	Production Note: Signature removed prior to publication.	10/9/2019
Suporn Sukjamnong	Production Note: Signature removed prior to publication.	11/9/2019
Yik-Lung Chan	Production Note: Signature removed prior to publication.	11/9/2019
Sonia Saad	Production Note: Signature removed prior to publication.	11/9/2019
Pawan Sharma	Production Note: Signature removed prior to publication.	11/9/2019
Rachana Santiyanont	Production Note: Signature removed prior to publication.	11/9/2019
Hui Chen	Production Note: Signature removed prior to publication.	10/9/2019
Brian G. G. Oliver	Production Note: Signature removed prior to publication.	10/9/2019

## RAPID REPORT

# Effect of long-term maternal smoking on the offspring's lung health

Surpon Sukjamnong,<sup>1,4\*</sup> Yik Lung Chan,<sup>1,2\*</sup> Razia Zakarya,<sup>1,2\*</sup> Sonia Saad,<sup>1,3</sup> Pawan Sharma,<sup>1,2</sup>  
Rachana Santianont,<sup>4</sup> Hui Chen,<sup>1</sup> and Brian G. Oliver<sup>1,2</sup>

<sup>1</sup>Centre for Health Technologies & Molecular Biosciences, School of Life Sciences, University of Technology Sydney, Sydney, New South Wales, Australia; <sup>2</sup>Respiratory Cellular and Molecular Biology, Woolcock Institute of Medical Research, University of Sydney, Sydney, New South Wales, Australia; <sup>3</sup>Renal Group Kolling Institute, Royal North Shore Hospital, St. Leonards, New South Wales, Australia; and <sup>4</sup>Department of Clinical Chemistry, Chulalongkorn University, Bangkok, Thailand

Submitted 24 March 2017; accepted in final form 11 May 2017

Sukjamnong S, Chan YL, Zakarya R, Saad S, Sharma P, Santianont R, Chen H, Oliver BG. Effect of long-term maternal smoking on the offspring's lung health. *Am J Physiol Lung Cell Mol Physiol* 313: L416–L423, 2017. First published May 18, 2017; doi: 10.1152/ajplung.00134.2017.—Maternal smoking during pregnancy contributes to long-term health problems in offspring, especially respiratory disorders that can manifest in either childhood or adulthood. Receptors for advanced glycation end products (RAGE) are multiligand receptors abundantly localized in the lung, capable of responding to by-products of reactive oxygen species and proinflammatory responses. RAGE signaling is a key regulator of inflammation in cigarette smoking-related pulmonary diseases. However, the impact of maternal cigarette smoke exposure on lung RAGE signaling in the offspring is unclear. This study aims to investigate the effect of maternal cigarette smoke exposure (SE), as well as mitochondria-targeted antioxidant [mitoquinone mesylate (MitoQ)] treatment, during pregnancy on the RAGE-mediated signaling pathway in the lung of male offspring. Female Balb/c mice (8 wk) were divided into a sham group (exposed to air), an SE group (exposed to cigarette smoke), and an SE + MQ group (exposed to cigarette smoke with MitoQ supplement from mating). The lungs from male offspring were collected at 13 wk. RAGE and its downstream signaling, including nuclear factor- $\kappa$ B and mitogen-activated protein kinase family consisting of extracellular signal-regulated kinase 1, ERK2, c-JUN NH<sub>2</sub>-terminal kinase (JNK), and phosphorylated JNK, in the lung were significantly increased in the SE offspring. Mitochondrial antioxidant manganese superoxide dismutase was reduced, whereas IL-1 $\beta$  and oxidative stress response nuclear factor (erythroid-derived 2)-like 2 were significantly increased in the SE offspring. Maternal MitoQ treatment normalized RAGE, IL-1 $\beta$ , and Nrf-2 levels in the SE + MQ offspring. Maternal SE increased RAGE and its signaling elements associated with increased oxidative stress and inflammatory cytokines in offspring lungs, whereas maternal MitoQ treatment can partially normalize these changes.

receptors for advanced glycation end products

MATERNAL SMOKING DURING PREGNANCY CONTRIBUTES TO various long-term health problems in offspring, especially respiratory disorders (21, 37). Several human studies have indicated that maternal smoking is associated with lung underdevelopment, airflow limitations, increase in the risk of respiratory infec-

tions, and development of airway hypersensitivity and asthma (7, 62, 64). Several mechanisms have been proposed, including a reduction in the development or physical size of the lung, such as reduced elastic tissue and the number of alveolar attachments to the airway, an increase in oxidative stress, and alteration to the inflammatory response and immune system (14, 17, 41, 42).

Receptors for advanced glycation end products (RAGE) are multiligand receptors abundantly localized in the lung (16). Recent studies have implied a role of RAGE in cigarette smoking-related diseases, where RAGE signaling is a key regulator of inflammatory response in pulmonary diseases (13, 48). Cigarette smoke induces the formation of advanced glycation end products (AGEs), resulting in the development of diseases through the AGEs-RAGE axis (8, 44). Indeed, it has been reported that serum levels of AGEs are elevated in smokers, including both current and past smokers (40), and RAGE levels are elevated in pulmonary tissue from mice exposed to cigarette smoke (20, 65). AGEs can interact with RAGE, leading to proinflammatory responses via several downstream kinases, such as the mitogen-activated protein kinase (MAPK) family consisting of extracellular signal-regulated kinase-1/2 (ERK1/2), c-JUN NH<sub>2</sub>-terminal kinase (JNK), and p38 MAPK. The transcription factor nuclear factor- $\kappa$  light chain enhancer of activated B cells (NF- $\kappa$ B) can also be activated, which results in the expression of a variety of proinflammatory mediators and cytokines, including IL-1, IL-6, and tumor necrosis factor (TNF)- $\alpha$  (30, 32, 45). Thus, the activation of RAGE-mediated signaling pathways is likely to play a key role to mediate the inflammatory response in many pulmonary disorders (47). In a previous study, short-term maternal cigarette smoke exposure during *embryo days 14.5–18.5* was shown to increase RAGE level in the fetal lung tissue at *embryo day 18.5* (63). However, whether such changes are still present at adulthood is unknown.

Pathological responses induced by the AGEs-RAGE axis are mediated by the generation of intracellular reactive oxygen species (ROS), the ensuing oxidative stress (15), and the activation of ROS-induced cytokine production and inflammation. Mitochondria are the major cellular source of ROS (59) and as such are a pharmacological target for ROS production. It is well established that oxidative stress can induce the secretion of inflammatory cytokines and the expression of adhesion molecules and inflammatory mediators in the lung (3,

\* S. Sukjamnong, Y. L. Chan, and R. Zakarya contributed equally to this work.

Address for reprint requests and other correspondence: B. G. Oliver, Centre for Health Technologies, School of Life Sciences, Faculty of Science, Univ. of Technology Sydney, NSW 2007, Australia (e-mail: brian.oliver@uts.edu.au).

24, 27). It has also been shown that maternal smoking can significantly increase oxidative stress in the offspring, including the lung tissue (4). Therefore, reducing oxidative stress may reduce pulmonary inflammatory responses in the lungs of offspring from smoking parents.

Coenzyme Q10 (CoQ10) is a mitochondrial endogenous antioxidant. It has been shown that CoQ10 dietary supplementation (1%) in mice with diet-induced obesity can lower liver markers of inflammation and oxidative stress (55). Plasma CoQ10 levels are reduced in smokers (1). However, mitochondrial intake of commercial CoQ10 is very low via oral supplementation; thus, a superphysiological dose was used in the abovementioned study. Mitoquinone mesylate, also known as MitoQ, is a mitochondria-targeted antioxidant. It consists of a ubiquinone moiety, the same structure to the ubiquinone found in CoQ10 that is linked to a triphenylphosphonium moiety by a 10-carbon alkyl chain that allows its rapid uptake and accumulation in the mitochondria to restore the antioxidant efficacy of the mitochondrial respiratory complex (26). As such, it has been reported that MitoQ has a protective role against oxidative damage-related pathologies in metabolic disease (36) and neurodegenerative diseases (34). Amniotic fluid CoQ10 levels are significantly lower among women delivering preterm babies, a risk that is increased by maternal smoking (29, 60). Therefore, MitoQ might be a suitable intervention option since it is already marketed for human consumption.

Thus, the main aim of this study was to investigate the long-term impact of maternal cigarette smoke exposure (SE) on lung RAGE signaling elements in adult offspring. In addition, whether MitoQ supplementation during gestation can mitigate the adverse impact of maternal SE was also investigated.

#### MATERIALS AND METHODS

**Animal experiments.** The animal experiments were approved by the Animal Care and Ethics Committee at the University of Technology Sydney (ACEC nos. 2014-638 and 2016-419). All protocols were performed according to the Australian National Health & Medical Research Council Guide for the Care and Use of Laboratory Animals. Female Balb/c mice (8 wk) were housed at  $20 \pm 2^\circ\text{C}$  and maintained on a 12:12-h light-dark cycle with ad libitum access to standard laboratory chow and water. After the acclimatization period, mice were divided into the following three groups: sham (exposed to air), SE (exposed to 2 cigarettes two times daily, 6 wk before mating and throughout gestation and lactation, as previously described; see Ref. 2), and SEMQ [SE mothers supplied with MitoQ (1.5 g/l in drinking water) during gestation and lactation]. This dose was chosen, since it has previously shown to be effective, safe, and maintain steady-state tissue concentrations of 1–100 pmol MitoQ/g of tissue (36, 49) (depending on the organ analyzed; MitoQ accumulates in liver and heart but is effective in the lung with this dosing regimen; see Ref. 33). Male breeders and suckling pups stayed in the home cage when mothers were exposed to sham or cigarette smoke. Pups were weaned at *postnatal day 20* and maintained without additional intervention. Male offspring were euthanized (4% isoflurane, 1%  $\text{O}_2$ ; Veterinary Companies of Australia, Kings Park, NSW) at 13 wk (mature age), and the lung tissues were collected and stored at  $-80^\circ\text{C}$  for later analysis.

**Western blot analysis.** Lung tissues were homogenized in lysis buffer with phosphatase inhibitors (Thermo Fisher Scientific). Protein concentrations were measured using DC Protein assay (Bio-Rad, Hercules, CA). Equal amounts of proteins (20  $\mu\text{g}$ ) were separated on NuPage Novex 4–12% Bis-Tris gels (Thermo Fisher Scientific) and transferred to PVDF membranes. The membranes were blocked with TBS-0.05% Tween 20 containing 5% BSA or skim milk for 1 h,

before incubation with primary antibodies against phospho-Erk1/2 (1:1,000; Cell Signaling Technology), Erk1/2 (1:1,000; Cell Signaling Technology), phospho-JNK (1:1,000; Cell Signaling Technology), JNK (1:500; Cell Signaling Technology), phospho-p38 MAPK (1:1,000; Cell Signaling Technology), p38 MAPK (1:1,000; Cell Signaling Technology), NF- $\kappa\text{B}$  and phospho-NF- $\kappa\text{B}$  (1:1,000; Cell Signaling Technology), IL-6 (1:1,000; Cell Signaling Technology), IL-1 $\beta$  (1:1,000; Cell Signaling Technology), RAGE (1:1,000; GeneTex), TNF- $\alpha$  (1:1,000; GeneTex), antioxidant response element nuclear factor (erythroid-derived 2)-like 2 (Nrf-2; 1:500; Aviva System Biology), endogenous antioxidant manganese superoxide dismutase (MnSOD; 1:1,000; Santa Cruz Biotechnology), transforming growth factor- $\beta$ 1 (TGF- $\beta$ 1; 1:500; R&D Systems), and collagen 1A (1:1,000; Santa Cruz Biotechnology) overnight at  $4^\circ\text{C}$ , which was followed by secondary antibodies (peroxidase-conjugated goat anti-mouse or anti-rabbit IgG; 1:2,000; Santa Cruz Biotechnology). The blots were then incubated in Super Signal West Pico Chemiluminescent substrate (Thermo Fisher Scientific), and the membranes were then visualized by an Amersham Imager 600 (GE Healthcare, NSW, Australia). Protein band density was determined using ImageJ software (National Institute of Health) for densitometry, and  $\beta$ -actin (1:5,000; Santa Cruz Biotechnology) was used as the housekeeping protein.

**Quantitative real-time PCR.** Total mRNA was isolated from lung tissues using TRIzol Reagent (Life Technologies). First-strand cDNA was generated using M-MLV Reverse Transcriptase, RNase H, and the Point Mutant Kit (Promega, Madison, WI). Real-time PCR was performed using the manufacturer's preoptimized and validated TaqMan primers and probes (Thermo Fisher Scientific). Only the RAGE probe sequence is provided by the manufacturer (CCAGGCGTGAGGAGAGGAAGGCC, NCBI gene references: NM\_001271422.1, NM\_001271424.1, NM\_007425.3; ID: Mm01134790.g1). RAGE probes were labeled with FAM dye and those for housekeeping 18S rRNA were labeled with VIC dye. Gene expression was standardized to 18S RNA. The average expression of the control group was assigned as the calibrator against which all other samples were expressed as fold difference.

**Statistical analysis.** Results are presented as means  $\pm$  SE. The data were analyzed by one-way ANOVA followed by post hoc Bonferroni test (Prism 7; Graphpad). Differences were considered statistically significant at  $P < 0.05$ .

#### RESULTS

**Effect on the body weight of offspring.** At *postnatal day 1*, as expected, male offspring from the SE mothers ( $1.30 \pm 0.07$  g,  $n = 11$ ) were significantly smaller than those from the sham mothers ( $1.49 \pm 0.03$  g,  $P < 0.01$ ,  $n = 17$ ). Smaller body weight was maintained until 13 wk of age (SE  $24.3 \pm 0.2$  g,  $n = 21$ ; sham  $25.3 \pm 0.3$  g,  $n = 20$ ,  $P < 0.01$ ), which was consistent with our previous study using the same model (25).

MitoQ supplementation during gestation and lactation significantly reversed in the impact of maternal SE on small birth weight in the male pups ( $1.65 \pm 0.02$  g,  $P < 0.05$  vs. sham,  $P < 0.01$  vs. SE,  $n = 7$ ). In adulthood, the body weight of SEMQ offspring was also normalized to the sham level ( $25.2 \pm 0.2$  g,  $P = 0.01$  vs. SE,  $n = 12$ ).

**Effect on lung RAGE and MAPK signaling elements in offspring.** Maternal smoking increased the amount of RAGE protein in adult offspring lungs ( $P < 0.05$  vs. sham; Fig. 1A), which was reduced by MitoQ. At the mRNA level, RAGE was only slightly reduced in the SE offspring at 13 wk but increased by MitoQ (Fig. 1B). RAGE downstream signaling molecules, including total Erk1, Erk2, JNK, and phospho-JNK protein levels, were increased in SE offspring ( $P < 0.05$  vs. sham; Fig. 2, A–C); however, phospho-Erk1 and phospho-Erk2 levels

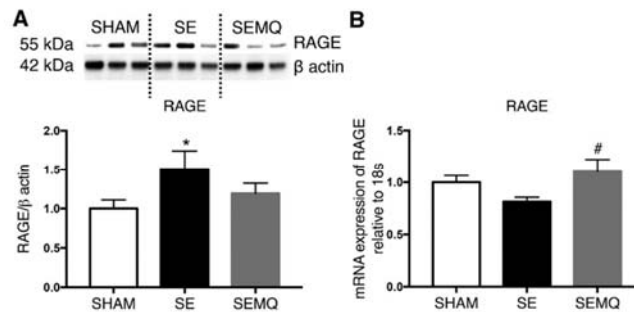


Fig. 1. Receptors for advanced glycation end products (RAGE) in the lung. Protein (A) and mRNA (B) expression of RAGE in lung from male offspring at 13 wk. Results are expressed as means  $\pm$  SE; of  $n = 9$  mice. Data were analyzed by one-way ANOVA followed by post hoc Bonferroni test. \* $P < 0.05$  vs. sham; # $P < 0.05$  vs. smoke exposed (SE); SEMQ, smoke exposed with dietary supplementation of mitoquinone mesylate (MitoQ).

were not different between sham and the SE group. There was no change in total or phosphorylated p38 MAPK between the sham and SE groups (Fig. 2D). Maternal MitoQ supplementation during gestation marginally reduced total ERK1 and ERK2, as well as phospho-ERK1 and phospho-ERK2 levels, although without statistical significance (Fig. 2).

**Effects on lung antioxidant enzyme in offspring.** MnSOD is the primary endogenous mitochondrial antioxidant that plays a key role in protecting cells against oxidative stress. As shown in Fig. 3, mitochondrial levels of MnSOD were significantly reduced in the SE offspring ( $P < 0.05$ ), which was only slightly enhanced by maternal MitoQ treatment. Furthermore, Nrf-2, a transcription factor that is highly sensitive to oxidative stress, was significantly increased in the SE offspring ( $P < 0.05$  vs. sham; Fig. 4A), which was normalized by maternal MitoQ supplementation ( $P < 0.05$  vs. SE; Fig. 4B).

**Effects on lung proinflammatory mediators in offspring.** RAGE-induced release of proinflammatory cytokines is mainly via the activation of NF- $\kappa$ B, a redox-sensitive transcription factor that regulates the transcription of several proinflammatory cytokines. There was a nonsignificant trend toward increasing levels of phosphorylated NF- $\kappa$ B in SE offspring, and the total NF- $\kappa$ B level was significantly increased in SE offspring compared with sham offspring ( $P < 0.05$ ; Fig. 4, A and B). As a result, the ratio of phosphorylated NF- $\kappa$ B to total NF- $\kappa$ B was unchanged. Similarly, IL-1 $\beta$  protein level was more than doubled in SE offspring ( $P < 0.05$ ; Fig. 4B), whereas TNF- $\alpha$  level was increased by 50%, albeit without statistical significance (Fig. 4D). However, IL-6 levels were similar between the sham and SE group (Fig. 4C). Maternal MitoQ supplementation normalized phosphorylated and total NF- $\kappa$ B and IL-1 $\beta$  levels in SEMQ offspring (Fig. 4, A and B), without any effect on IL-6 and TNF- $\alpha$  (Fig. 4, C and D).

**Effect on lung fibrotic markers in offspring.** A prolonged increase in TGF- $\beta$ 1 activity can lead to persistent lung fibrosis, resulting in excessive production of collagen-1A (11). Here, neither TGF- $\beta$ 1 nor collagen-1A proteins levels were changed in 13-wk-old SE offspring (Fig. 5). Maternal MitoQ treatment also showed no impact on these two proteins (Fig. 5).

## DISCUSSION

Maternal smoking during pregnancy has been shown to adversely affect fetal lung development and has also been linked to an increased risk of long-term respiratory disorders

(21, 37). In this study, we found that SE offspring had reduced body weight at birth that was maintained until adulthood. The protein levels of RAGE and its downstream signaling, including NF- $\kappa$ B and MAPK family consisting of ERK1, ERK2, JNK, and phospho-JNK, were significantly increased in the lung of SE offspring, with increased inflammatory cytokine IL-1 $\beta$  level. Mitochondrial antioxidant MnSOD levels were reduced, and the oxidative stress response Nrf-2 was significantly increased in the SE offspring. Maternal MitoQ treatment reversed the impact of maternal SE on birth weight and normalized RAGE, NF- $\kappa$ B, IL-1 $\beta$ , and Nrf-2 levels in offspring.

RAGE plays an important role in cigarette smoking-related diseases as a key regulator in maintaining and promoting inflammatory responses (13, 48, 57). It has been shown that the expression of RAGE is increased in pulmonary epithelial cells after exposure to cigarette smoke extract (46), whereas increased inflammatory cytokines have been found in the lung lavage fluid of smokers and mice exposed to cigarette smoke (25, 28). To our knowledge, this is the first study to demonstrate that continuous maternal SE from pregestation to lactation leads to increased RAGE expression in the offspring's lung at adulthood, with increased downstream signaling elements and inflammatory cytokines. The study by Winden et al. only showed RAGE augmentation in the fetal lung following 4 days of maternal SE during the pseudoglandular period of lung development (63). This suggests that the changes in RAGE and signaling elements by maternal SE can begin in the intrauterine period and last long into adulthood. In our study, RAGE mRNA expression was marginally suppressed (nonsignificantly) in the SE offspring, which may be because of a negative feedback loop. This suggests that the level of RAGE may be regulated at a transcriptional level. Additional studies will be required to determine the exact mechanism, such as the involvement of transcriptional regulator noncoding RNAs.

The activation of RAGE signaling pathways can influence alveolar remodeling characteristics of pulmonary disease (50). Several studies have indicated that cigarette smoke induces the expression of RAGE and promotes the phosphorylation of ERK1/2, p38, and JNK in primary human gingival epithelial cells and in the lungs of rats exposed to cigarette smoke (52, 65, 66). Therefore, here we investigated the signal transduction pathways and fibrotic markers in lung tissue. In the present study, we demonstrated that maternal SE can increase the



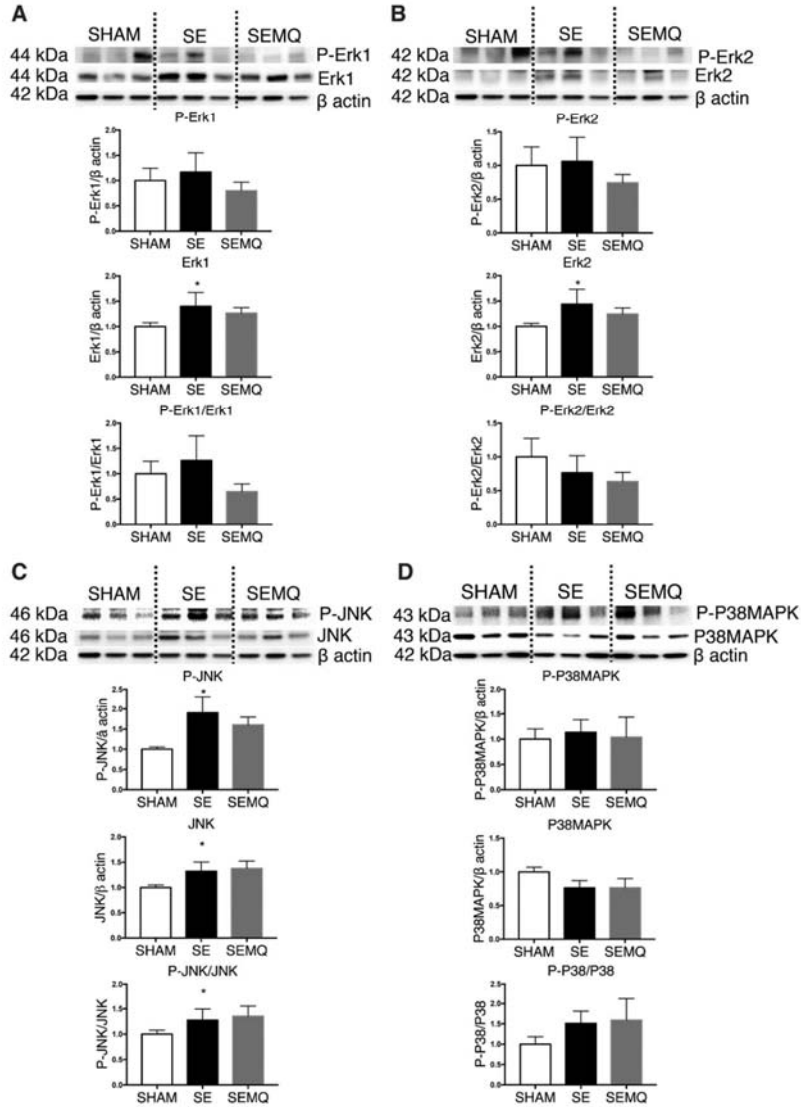
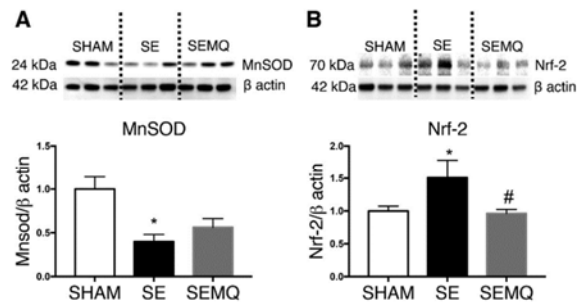


Fig. 2. Lung extracellular signal-regulated kinase (Erk) 1, Erk2, c-JUN NH<sub>2</sub>-terminal kinase (JNK), and p38 mitogen-activated protein kinase (MAPK) expression. Protein expression of phosphorylated and total Erk1 (A), Erk2 (B), JNK (C), and p38 MAPK (D) in the lung from male offspring at 13 wk. Results are expressed as means  $\pm$  SE of  $n = 9$  mice. Data were analyzed by one-way ANOVA followed by post hoc Bonferroni test. \* $P < 0.05$  vs. sham.

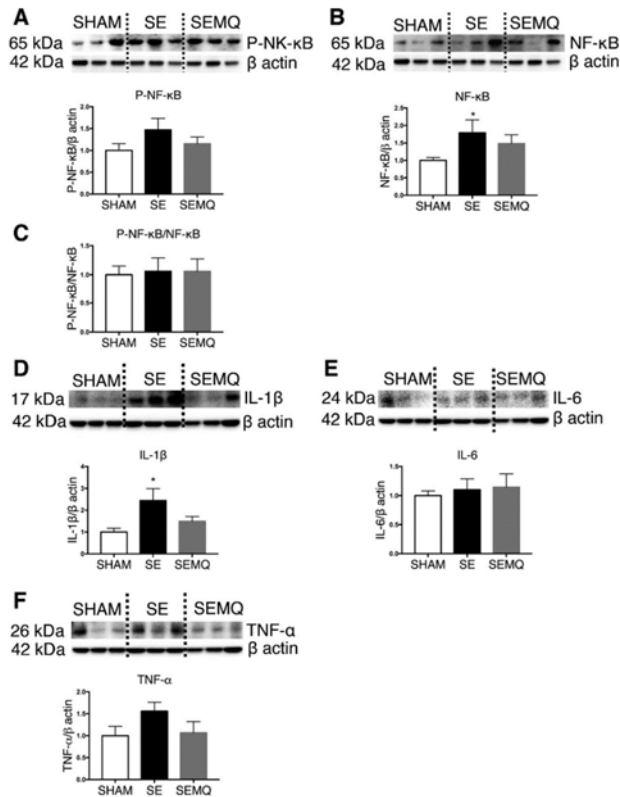
Fig. 3. Lung oxidative stress markers. Mitochondrial manganese superoxide dismutase (MnSOD, *A*) and total tissue nuclear factor erythroid 2-related factor 2 (Nrf-2, *B*) protein level in the lung from male offspring at 13 wk. Results are expressed as means  $\pm$  SE of  $n = 8$  mice. Data were analyzed by one-way ANOVA followed by post hoc Bonferroni test. \* $P < 0.05$  vs. sham; # $P < 0.05$  vs. SE.



expression of RAGE-dependent signaling protein kinases, including Erk1, Erk2, and JNK. However, the phosphorylation of these molecules was not significantly increased by maternal SE. Therefore, the impact of maternal SE on the health outcome of the offspring's lung may prime the lung to be hyper-

responsive to certain stimuli, but the pathways themselves are not intrinsically activated. This is consistent with studies in humans, where smoking during pregnancy is a risk factor for the development of lung diseases such as asthma and chronic obstructive pulmonary disease (COPD), but in both of these

Fig. 4. Lung inflammatory markers. Nuclear factor- $\kappa$ B (NF- $\kappa$ B, *A-C*), interleukin (IL)-1 $\beta$  (*D*), IL-6 (*E*), and tumor necrosis factor (TNF- $\alpha$ , *F*) protein levels in the lung from male offspring at 13 wk. Results are expressed as means  $\pm$  SE of  $n = 9$  mice. Data were analyzed by one-way ANOVA followed by post hoc Bonferroni test. \* $P < 0.05$  vs. sham.



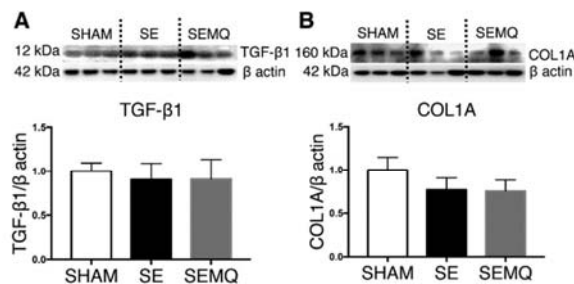


Fig. 5. Markers of lung fibrosis. Transforming growth factor- $\beta$ 1 (TGF- $\beta$ 1, A) and collagen-1A (B) protein levels in the lung from male offspring at 13 wk. Results are expressed as means  $\pm$  SE of  $n = 9$  mice. Data were analyzed by one-way ANOVA.

diseases other environmental stimuli are mostly needed to develop the disease in children.

The two fibrotic markers measured in this study were not affected by maternal SE. This is consistent with the changes in fibrotic markers in the kidney in our previous study using the same model of maternal SE (2). Increased collagen deposition has been found in fetal lung tissue of monkeys due to maternal nicotine administration (51). Such differences may be the result of the dose of nicotine administered. In our study the nicotine dose was low (equivalent to a human smoking 1 to 2 cigarettes/day). The other significant difference is that cigarette smoke is a complex mixture of chemicals that may inhibit or enhance the effects of nicotine.

Cigarette smoke contains free radicals and itself can stimulate the production of ROS in lung tissues, leading to oxidative damage in both pregnant women and newborns (12, 18). MnSOD is an enzyme present in mitochondria that is one of the first-line enzymes to detoxify the superoxide radicals generated during ATP synthesis (6). Here we showed that the level of mitochondrial MnSOD was reduced in the offspring's lung in response to maternal SE. This is consistent with our findings in the brain and kidneys of SE offspring in adulthood in our previous studies (10, 56). RAGE activation by multiple ligands, such as ceramides, cigarette smoke (39), or intracellular amyloid- $\beta$  peptide (58), results in mitochondrial damage, likely mediated via mitochondrial ROS production (22). Given this, it is likely that reduced MnSOD in the current experiments is the result of mitochondrial damage.

Additionally, Nrf2 is a transcription factor that responds to oxidative stress and contributes to the induction of several protective enzymes to scavenge excess free radicals during oxidative stress. Nrf2 was found to be increased in moderate smokers in response to increased oxidative stress induced by cigarette smoke (19). Here, we found that Nrf2 was significantly increased in the SE offspring at adulthood, in line with their increased oxidative stress markers. Taken together, maternal cigarette smoking during pregnancy may cause long-lasting oxidative stress in offspring lungs, possibly because of the reduction of protective antioxidative enzymes.

Prolonged oxidative stress can activate the redox-sensitive transcription factor NF- $\kappa$ B (61), which, in turn, results in the transcription of a variety of mRNA encoding proinflammatory cytokines (43). In the present study, the level of NF- $\kappa$ B in offspring from SE mothers was higher than those from the sham mothers. This is in keeping with increased protein levels of the proinflammatory cytokines IL-1 $\beta$  and TNF- $\alpha$ , both of

which are the downstream targets of NF- $\kappa$ B. It has been reported that chronic production of IL-1 $\beta$  can lead to pulmonary inflammation, emphysema, airway remodeling, and bronchial hyperactivity, which are the main features of asthma and COPD (23, 31, 35). Therefore, maternal smoking during pregnancy may increase the risk of chronic inflammatory conditions in offspring lungs, making them more susceptible to certain pulmonary disorders such as COPD in adulthood, which requires further investigation.

Mitochondrial oxidative damage occurs in many disease states. Therefore, strategies to prevent oxidative stress-induced damage may provide new therapeutic options for a range of human disorders, including lung diseases (5). MitoQ is, to date, the best-characterized mitochondria-targeted ubiquinone (53) that reduces the potent antioxidant ubiquinol in the mitochondria (26). MitoQ has been used in several organ systems but as far as we know never before for pulmonary disorders (9, 36, 38, 54). In the present study, we determined the effects of maternal MitoQ supplementation during pregnancy on the health outcome of the lungs in offspring. Although maternal MitoQ treatment in SE mothers did not affect endogenous MnSOD level in the offspring, oxidative stress seems to be reduced, reflected by normalized Nrf-2 level. RAGE levels in the SEMQ offspring were also reduced. The activity of MAPK family members did not seem to be involved in the action of MitoQ. However, NF- $\kappa$ B was normalized by maternal intervention, which can further normalize proinflammatory cytokine levels (including IL-1 $\beta$  and TNF- $\alpha$ ) in the offspring's lung. Taken together, our findings suggest that the administration of the mitochondria-targeted antioxidant MitoQ may be beneficial to lung health outcomes in offspring from SE mothers.

In summary, maternal SE can enhance oxidative stress and the expression of RAGE, as well as promote RAGE-mediated inflammatory responses in offspring lungs. Maternal MitoQ supplementation during pregnancy is beneficial in reducing inflammatory and oxidative stress responses caused by maternal SE. Future human translation may be plausible, since MitoQ is already marketed as an over-the-counter dietary supplement.

#### GRANTS

This work was supported by the National Health and Medical Research Council Australia (APP1110368) and by funding from the University of Technology Sydney and Chulalongkorn University, Bangkok. This study was also supported by postgraduate research support by the Faculty of Science, University of Technology Sydney, and a Research grant awarded by the

Faculty of Allied Health Sciences, Chulalongkorn University to R. Santayanont. R. Zakarya is supported by an Australia Postgraduate Award. S. Sukjamnong is supported by an Overseas Research Experience Scholarship for Graduate Students by the Graduate School, Chulalongkorn University and the 90th Anniversary of Chulalongkorn University Fund (Ratchadaphiseksomphot Endowment Fund). The MitoQ was provided by MitoQ Limited, New Zealand.

#### DISCLOSURES

No conflicts of interest, financial or otherwise are declared by the authors.

#### AUTHOR CONTRIBUTIONS

S. Sukjamnong, Y.L.C., and R.Z. performed experiments; S. Sukjamnong, Y.L.C., R.Z., and B.G.O. analyzed data; S. Sukjamnong, Y.L.C., R.Z., S. Saad, P.S., H.C., and B.G.O. interpreted results of experiments; S. Sukjamnong prepared figures; S. Sukjamnong, Y.L.C., and B.G.O. drafted manuscript; S. Sukjamnong, Y.L.C., R.Z., S. Saad, P.S., R.S., H.C., and B.G.O. approved final version of manuscript; Y.L.C., R.Z., S. Saad, P.S., R.S., H.C., and B.G.O. edited and revised manuscript; R.Z., S. Saad, R.S., H.C., and B.G.O. conceived and designed research.

#### REFERENCES

- Al-Bazi MM, Elshal MF, Khoja SM. Reduced coenzyme Q(10) in female smokers and its association with lipid profile in a young healthy adult population. *Arch Med Sci* 7: 948–954, 2011. doi:10.5114/aoms.2011.26605.
- Al-Odat I, Chen H, Chan YL, Amgad S, Wong MG, Gill A, Pollock C, Saad S. The impact of maternal cigarette smoke exposure in a rodent model on renal development in the offspring. *PLoS One* 9: e103443, 2014. doi:10.1371/journal.pone.0103443.
- Antoniceilli F, Parmentier M, Drost EM, Hirani N, Rahman I, Donaldson K, MacNee W. N-acetylcysteine inhibits oxidant-mediated interleukin-8 expression and NF-kappaB nuclear binding in alveolar epithelial cells. *Free Radic Biol Med* 32: 492–502, 2002. doi:10.1016/S0891-5849(01)00820-6.
- Basigit I, Tugay M, Dilioglugil MO, Yildiz F, Maral H, Sozibir S. Protective effects of N-acetylcysteine on peroxidative changes of the fetal rat lungs whose mothers were exposed to cigarette smoke. *Hum Exp Toxicol* 26: 99–103, 2007. doi:10.1177/0960327107071917.
- Bernardo I, Bozinovski S, Vlahos R. Targeting oxidant-dependent mechanisms for the treatment of COPD and its comorbidities. *Pharmacol Ther* 155: 60–79, 2015. doi:10.1016/j.pharmthera.2015.08.005.
- Candas D, Li JJ. MnSOD in oxidative stress response-potential regulation via mitochondrial protein influx. *Antioxid Redox Signal* 20: 1599–1617, 2014. doi:10.1089/ars.2013.5305.
- Carroll KN, Gebretsadik T, Griffin MR, Dupont WD, Mitchel EF, Wu P, Enriquez R, Hartert TV. Maternal asthma and maternal smoking are associated with increased risk of bronchiolitis during infancy. *Pediatrics* 119: 1104–1112, 2007. doi:10.1542/peds.2006.2837.
- Cerami C, Founds H, Nicholl I, Mitsuhashi T, Giordano D, Vanpatten S, Lee A, Al-Abed Y, Vlassara H, Bucala R, Cerami A. Tobacco smoke is a source of toxic reactive glycation products. *Proc Natl Acad Sci USA* 94: 13915–13920, 1997. doi:10.1073/pnas.94.25.13915.
- Chacko BK, Reily C, Srivastava A, Johnson MS, Ye Y, Ulasova E, Agarwal A, Zinn KR, Murphy MP, Kalyanaram B, Darley-Usmar V. Prevention of diabetic nephropathy in *Ins2(+/-)* (Akita) mice by the mitochondria-targeted therapy MitoQ. *Biochem J* 432: 9–19, 2010. doi:10.1042/BJ20100908.
- Chan YL, Saad S, Pollock C, Oliver B, Al-Odat I, Zaky AA, Jones N, Chen H. Impact of maternal cigarette smoke exposure on brain inflammation and oxidative stress in male mice offspring. *Sci Rep* 6: 25881, 2016. doi:10.1038/srep25881.
- Chan YL, Saad S, Pollock C, Oliver B, Al-Odat I, Zaky AA, Jones N, Chen H. Impact of maternal cigarette smoke exposure on brain inflammation and oxidative stress in male mice offspring. *Sci Rep* 6: 25881, 2016. doi:10.1038/srep25881.
- Chelehowska M, Ambroszkiewicz J, Gajewska J, Laskowska-Klita T, Leischang J. The effect of tobacco smoking during pregnancy on plasma oxidant and antioxidant status in mother and newborn. *Eur J Obstet Gynecol Reprod Biol* 155: 132–136, 2011. doi:10.1016/j.ejogrb.2010.12.006.
- Chen L, Wang T, Guo L, Shen Y, Yang T, Wan C, Liao Z, Xu D, Wen F. Overexpression of RAGE contributes to cigarette smoke-induced nitric oxide generation in COPD. *Lung* 192: 267–275, 2014. doi:10.1007/s00408-014-9561-1.
- Collins MH, Moessinger AC, Kleinerman J, Bassi J, Rosso P, Collins AM, James LS, Blanc WA. Fetal lung hypoplasia associated with maternal smoking: a morphometric analysis. *Pediatr Res* 19: 408–412, 1985. doi:10.1203/00006450-198519040-00018.
- Daffu G, del Pozo CH, O'Shea KM, Ananthakrishnan R, Ramasamy R, Schmidt AM. Radical roles for RAGE in the pathogenesis of oxidative stress in cardiovascular diseases and beyond. *Int J Mol Sci* 14: 19891–19910, 2013. doi:10.3390/ijms141019891.
- Demling N, Ehrhardt C, Kasper M, Laue M, Knels L, Rieber EP. Promotion of cell adherence and spreading: a novel function of RAGE, the highly selective differentiation marker of human alveolar epithelial type I cells. *Cell Tissue Res* 323: 475–488, 2006. doi:10.1007/s00441-005-0069-0.
- Elliot J, Carroll N, Bosco M, McCrohan M, Robinson P. Increased airway responsiveness and decreased alveolar attachment points following in utero smoke exposure in the guinea pig. *Am J Respir Crit Care Med* 163: 140–144, 2001. doi:10.1164/ajrccm.163.1.9805099.
- Ermiş B, Ors R, Yildirim A, Tastekin A, Kardas F, Akcaay F. Influence of smoking on maternal and neonatal serum malondialdehyde, superoxide dismutase, and glutathione peroxidase levels. *Ann Clin Lab Sci* 34: 405–409, 2004.
- Garbin U, Fratta Pasini A, Stranieri C, Cominacini M, Pasini A, Manfro S, Lugoboni F, Mozzini C, Guidi G, Facini G, Cominacini L. Cigarette smoking blocks the protective expression of Nrf2/ARE pathway in peripheral mononuclear cells of young heavy smokers favouring inflammation. *PLoS One* 4: e8225, 2009. doi:10.1371/journal.pone.0008225.
- Gassman JR, Lewis JB, Milner DC, Lewis AL, Bodine JS, Dunaway TM, Monson TD, Broberg DS, Arroyo JA, Reynolds PR. Spatial expression of receptor for advanced glycation end-products (RAGE) in diverse tissue and organ systems differs following exposure to secondhand cigarette smoke. *FASEB J* 30: 1b741, 2016.
- Gilliland FD, Li YF, Peters JM. Effects of maternal smoking during pregnancy and environmental tobacco smoke on asthma and wheezing in children. *Am J Respir Crit Care Med* 163: 429–436, 2001. doi:10.1164/ajrccm.163.2.2006009.
- Guo C, Sun L, Chen X, Zhang D. Oxidative stress, mitochondrial damage and neurodegenerative diseases. *Neural Regen Res* 8: 2003–2014, 2013. doi:10.3969/j.issn.1673-5374.2013.21.009.
- Hernandez A, Omini C, Daffonchio L. Interleukin-1 beta: a possible mediator of lung inflammation and airway hyperreactivity. *Pharmacol Res* 24: 385–393, 1991. doi:10.1016/1043-6618(91)90043-W.
- Hsu WH, Lee BH, Pan TM. Monascin attenuates oxidative stress-mediated lung inflammation via peroxisome proliferator-activated receptor-gamma (PPAR-γ) and nuclear factor-erythroid 2 related factor 2 (Nrf-2) modulation. *J Agric Food Chem* 62: 5337–5344, 2014. doi:10.1021/jf501373a.
- John G, Kohse K, Orasche J, Reda A, Schnelle-Kreis J, Zimmermann R, Schmid O, Eickelberg O, Yildirim AO. The composition of cigarette smoke determines inflammatory cell recruitment to the lung in COPD mouse models. *Clin Sci Lond* 126: 207–221, 2014. doi:10.1042/CS20130117.
- Kelso GF, Porteous CM, Coulter CV, Hughes G, Porteous WK, Ledgerwood EC, Smith RA, Murphy MP. Selective targeting of a redox-active ubiquinone to mitochondria within cells: antioxidant and antiapoptotic properties. *J Biol Chem* 276: 4588–4596, 2001. doi:10.1074/jbc.M009093200.
- Kim SR, Lee KS, Park SJ, Min KH, Lee KY, Choe YH, Hong SH, Koh GY, Lee YC. Angiopoietin-1 variant, COMP-Ang1 attenuates hydrogen peroxide-induced acute lung injury. *Exp Mol Med* 40: 320–331, 2008. doi:10.3858/emmm.2008.40.3.320.
- Kuschner WG, D'Alessandro A, Wong H, Blanc PD. Dose-dependent cigarette smoking related inflammatory responses in healthy adults. *Eur Respir J* 9: 1989–1994, 1996. doi:10.1183/09031936.96.09101989.
- Kyrkheid-Blomberg NB, Granath F, Cnattingius S. Maternal smoking and causes of very preterm birth. *Acta Obstet Gynecol Scand* 84: 572–577, 2005. doi:10.1111/j.0001-6349.2005.00848.x.
- Lander HM, Tauras JM, Ogiste JS, Hori O, Moss RA, Schmidt AM. Activation of the receptor for advanced glycation end products triggers a p21(ras)-dependent mitogen-activated protein kinase pathway regulated by oxidant stress. *J Biol Chem* 272: 17810–17814, 1997. doi:10.1074/jbc.272.28.17810.

31. Lappalainen U, Whitsett JA, Wert SE, Tichelaar JW, Bry K. Interleukin-1 $\beta$  causes pulmonary inflammation, emphysema, and airway remodeling in the adult murine lung. *Am J Respir Cell Mol Biol* 32: 311–318, 2005. doi:10.1165/ajrcmb.2004-0309OC.
32. Lin L, Park S, Lakatta EG. RAGE signaling in inflammation and arterial aging. *Front Biosci (Landmark Ed)* 14: 1403–1413, 2009. doi:10.2741/3315.
33. Lowes DA, Thottakam BM, Webster NR, Murphy MP, Galley HF. The mitochondria-targeted antioxidant MitoQ protects against organ damage in a lipopolysaccharide-peptidoglycan model of sepsis. *Free Radic Biol Med* 45: 1559–1565, 2008. doi:10.1016/j.freeradbiomed.2008.09.003.
34. Manczak M, Mao P, Calkins MJ, Cornea A, Reddy AP, Murphy MP, Szeto HH, Park B, Reddy PH. Mitochondria-targeted antioxidants protect against amyloid-beta toxicity in Alzheimer's disease neurons. *J Alzheimers Dis* 20, Suppl 2: S609–S631, 2010. doi:10.3233/JAD-2010-100564.
35. McKay S, Sharma HS. Autocrine regulation of asthmatic airway inflammation: role of airway smooth muscle. *Respir Res* 3: 11, 2002. doi:10.1186/rm160.
36. Mercer JR, Yu E, Figg N, Cheng KK, Prime TA, Griffin JL, Masoodi M, Vidal-Puig A, Murphy MP, Bennett MR. The mitochondria-targeted antioxidant MitoQ decreases features of the metabolic syndrome in ATM+/-/ApoE-/- mice. *Free Radic Biol Med* 52: 841–849, 2012. doi:10.1016/j.freeradbiomed.2011.11.026.
37. Milner AD, Rao H, Greenough A. The effects of antenatal smoking on lung function and respiratory symptoms in infants and children. *Early Hum Dev* 83: 707–711, 2007. doi:10.1016/j.earhunde.2007.07.014.
38. Mukhopadhyay P, Horvath B, Zsengeller Z, Zielonka J, Tanchian J, Holovac E, Kechrid M, Patel V, Stillman IE, Parikh SM, Joseph J, Kalyanaram B, Pacher P. Mitochondrial-targeted antioxidants represent a promising approach for prevention of cisplatin-induced nephropathy. *Free Radic Biol Med* 52: 497–506, 2012. doi:10.1016/j.freeradbiomed.2011.11.001.
39. Nelson MR, Swensen AC, Winden DR, Bodine JS, Bikman BT, Reynolds PR. Cardiomyocyte mitochondrial respiration is reduced by receptor for advanced glycation end-product signaling in a ceramide-dependent manner. *Am J Physiol Heart Circ Physiol* 309: H63–H69, 2015. doi:10.1152/ajpheart.00043.2015.
40. Nicholl ID, Bucala R. Advanced glycation endproducts and cigarette smoking. *Cell Mol Biol (Noisy-le-grand)* 44: 1025–1033, 1998.
41. Noakes PS, Holt PG, Prescott SL. Maternal smoking in pregnancy alters neonatal cytokine responses. *Allergy* 58: 1053–1058, 2003. doi:10.1034/j.1398-9995.2003.00290.x.
42. Noakes PS, Thomas R, Lane C, Mori TA, Barden AE, Devadason SG, Prescott SL. Association of maternal smoking with increased infant oxidative stress at 3 months of age. *Thorax* 62: 714–717, 2007. doi:10.1136/thx.2006.061630.
43. Perkins ND. Integrating cell-signalling pathways with NF-kappaB and IKK function. *Nat Rev Mol Cell Biol* 8: 49–62, 2007. doi:10.1038/nrm2083.
44. Prasad K, Dhar I, Caspar-Bell G. Role of advanced glycation end products and its receptors in the pathogenesis of cigarette smoke-induced cardiovascular disease. *Int J Angiol* 24: 75–80, 2015. doi:10.1055/s-0034-1396413.
45. Ramasamy R, Vanucci SJ, Yan SS, Herold K, Yan SF, Schmidt AM. Advanced glycation end products and RAGE: a common thread in aging, diabetes, neurodegeneration, and inflammation. *Glycobiology* 15: 16R–28R, 2005. doi:10.1093/glycob/cwi053.
46. Reynolds PR, Kasteler SD, Cosio MG, Sturrock A, Huecksteadt T, Hoidal JR. RAGE: developmental expression and positive feedback regulation by Egr-1 during cigarette smoke exposure in pulmonary epithelial cells. *Am J Physiol Lung Cell Mol Physiol* 294: L1094–L1101, 2008. doi:10.1152/ajplung.00318.2007.
47. Reynolds PR, Kasteler SD, Schmitt RE, Hoidal JR. Receptor for advanced glycation end-products signals through Ras during tobacco smoke-induced pulmonary inflammation. *Am J Respir Cell Mol Biol* 45: 411–418, 2011. doi:10.1165/ajrcmb.2010-0231OC.
48. Robinson AB, Stogsdill JA, Lewis JB, Wood TT, Reynolds PR. RAGE and tobacco smoke: insights into modeling chronic obstructive pulmonary disease. *Front Physiol* 3: 301, 2012. doi:10.3389/fphys.2012.00301.
49. Rodriguez-Cuenca S, Cochemé HM, Logan A, Abakumova I, Prime TA, Rose C, Vidal-Puig A, Smith AC, Rubinsztein DC, Fearnley IM, Jones BA, Pope S, Heales SJ, Lam BY, Neogi SG, McFarlane I, James AM, Smith RA, Murphy MP. Consequences of long-term oral administration of the mitochondria-targeted antioxidant MitoQ to wild-type mice. *Free Radic Biol Med* 48: 161–172, 2010. doi:10.1016/j.freeradbiomed.2009.10.039.
50. Schmidt AM, Yan SD, Yan SF, Stern DM. The multiligand receptor RAGE as a progression factor amplifying immune and inflammatory responses. *J Clin Invest* 108: 949–955, 2001. doi:10.1172/JCI200114002.
51. Sekhon HS, Keller JA, Proskocil BJ, Martin EL, Spindel ER. Maternal nicotine exposure upregulates collagen gene expression in fetal monkey lung. Association with alpha7 nicotinic acetylcholine receptors. *Am J Respir Cell Mol Biol* 26: 31–41, 2002. doi:10.1165/ajrcmb.26.1.4170.
52. Semlali A, Witold C, Alanazi M, Rouabhia M. Whole cigarette smoke increased the expression of TLRs, HBDS, and proinflammatory cytokines by human gingival epithelial cells through different signaling pathways. *PLoS One* 7: e2614, 2012. doi:10.1371/journal.pone.0052614.
53. Smith RA, Hartley RC, Cochemé HM, Murphy MP. Mitochondrial pharmacology. *Trends Pharmacol Sci* 33: 341–352, 2012. doi:10.1016/j.tips.2012.03.010.
54. Snow BJ, Rolfe FL, Lockhart MM, Frampton CM, O'Sullivan JD, Fung V, Smith RA, Murphy MP, Taylor KM. A double-blind, placebo-controlled study to assess the mitochondria-targeted antioxidant MitoQ as a disease-modifying therapy in Parkinson's disease. *Mov Disord* 25: 1670–1674, 2010. doi:10.1002/mds.23148.
55. Sohet FM, Neyrinck AM, Pachikian BD, de Backer FC, Bindels LB, Niklowitz P, Menke T, Cani PD, Delzenne NM. Coenzyme Q10 supplementation lowers hepatic oxidative stress and inflammation associated with diet-induced obesity in mice. *Biochem Pharmacol* 78: 1391–1400, 2009. doi:10.1016/j.bcp.2009.07.008.
56. Stangenberg S, Nguyen LT, Chen H, Al-Odat I, Killingsworth MC, Gosnell ME, Anwer AG, Goldys EM, Pollock CA, Saad S. Oxidative stress, mitochondrial perturbations and fetal programming of renal disease induced by maternal smoking. *Int J Biochem Cell Biol* 64: 81–90, 2015. doi:10.1016/j.biocel.2015.03.017.
57. Stogsdill MP, Stogsdill JA, Bodine BG, Fredrickson AC, Sefcik TL, Wood TT, Kasteler SD, Reynolds PR. Conditional overexpression of receptors for advanced glycation end-products in the adult murine lung causes airspace enlargement and induces inflammation. *Am J Respir Cell Mol Biol* 49: 128–134, 2013. doi:10.1165/ajrcmb.2013-0013OC.
58. Takuma K, Fang F, Zhang W, Yan S, Fukuzaki E, Du H, Sosunov A, McKhann G, Funatsu Y, Nakamichi N, Nagai T, Mizoguchi H, Ibi D, Hori O, Ogawa S, Stern DM, Yamada K, Yan SS. RAGE-mediated signaling contributes to intraneuronal transport of amyloid-beta and neuronal dysfunction. *Proc Natl Acad Sci USA* 106: 20021–20026, 2009. doi:10.1073/pnas.0905686106.
59. Tang D, Kang R, Zeh HJ III, Lotze MT. High-mobility group box 1, oxidative stress, and disease. *Antioxid Redox Signal* 14: 1315–1335, 2011. doi:10.1089/ars.2010.3356.
60. Terán E, Racines-Orbe M, Toapanta J, Valdivieso L, Vega Z, Vivero S, Moya W, Chedraui P, Pérez-López FR. Maternal plasma and amniotic fluid coenzyme Q10 levels in preterm and term gestations: a pilot study. *Arch Gynecol Obstet* 283, Suppl 1: 67–71, 2011. doi:10.1007/s00404-011-1894-x.
61. Vlahos R, Bozinovski S, Jones JE, Powell J, Gras J, Lilja A, Hansen MJ, Gualano RC, Irving L, Anderson GP. Differential protease, innate immunity, and NF- $\kappa$ B induction profiles during lung inflammation induced by subchronic cigarette smoke exposure in mice. *Am J Physiol Lung Cell Mol Physiol* 290: L931–L945, 2006. doi:10.1152/ajplung.00201.2005.
62. Wickström R. Effects of nicotine during pregnancy: human and experimental evidence. *Curr Neuropharmacol* 5: 213–222, 2007. doi:10.2174/157015907781695955.
63. Winden DR, Barton DB, Betteridge BC, Bodine JS, Jones CM, Rogers GD, Chavarria M, Wright AJ, Jergensen ZR, Jimenez FR, Reynolds PR. Antenatal exposure of maternal secondhand smoke (SHS) increases fetal lung expression of RAGE and induces RAGE-mediated pulmonary inflammation. *Respir Res* 15: 129, 2014. doi:10.1186/s12931-014-0129-7.
64. Zacharasiewicz A. Maternal smoking in pregnancy and its influence on childhood asthma. *ERJ Open Res* 2: pii: 00042-2016, 2016. doi:10.1183/23120541.00042.2016.
65. Zhang SP, Wu YW, Wu ZZ, Liu HY, Nie JH, Tong J. Up-regulation of RAGE and S100A6 in rats exposed to cigarette smoke. *Environ Toxicol Pharmacol* 28: 259–264, 2009. doi:10.1016/j.etap.2009.04.013.
66. Zhong CY, Zhou YM, Douglas GC, Witschi H, Pinkerton KE. MAPK/AP-1 signal pathway in tobacco smoke-induced cell proliferation and squamous metaplasia in the lungs of rats. *Carcinogenesis* 26: 2187–2195, 2005. doi:10.1093/carcin/bgi189.



## Publication Declaration

**Epigenetic impacts of maternal tobacco and e-vapour exposure on the offspring lung.**

**Razia Zakarya**, Ian Adcock, Brian G Oliver. *Clinical Epigenetics* 2019

**Status:** Published

**Authors' contributions:** All Authors conceived the ideas, read the manuscript and edited the final version. **RZ** drafted the manuscript. All authors read and approved the final manuscript.

### Signatures:

<b>Name</b>	<b>Signature</b>	<b>Date</b>
Razia Zakarya	Production Note: Signature removed prior to publication.	<b>10/9/2019</b>
Ian M. Adcock	Production Note: Signature removed prior to publication.	<b>10/9/2019</b>
Brian G. G. Oliver	Production Note: Signature removed prior to publication.	<b>10/9/2019</b>

REVIEW

Open Access

# Epigenetic impacts of maternal tobacco and e-vapour exposure on the offspring lung



Razia Zakarya<sup>1,2</sup>, Ian Adcock<sup>3,4</sup> and Brian G. Oliver<sup>1,2\*</sup>

## Abstract

In utero exposure to tobacco products, whether maternal or environmental, have harmful effects on first neonatal and later adult respiratory outcomes. These effects have been shown to persist across subsequent generations, regardless of the offspring's smoking habits. Established epigenetic modifications induced by in utero exposure are postulated as the mechanism underlying the inherited poor respiratory outcomes. As e-cigarette use is on the rise, their potential to induce similar functional respiratory deficits underpinned by an alteration in the foetal epigenome needs to be explored. This review will focus on the functional and epigenetic impact of in utero exposure to maternal cigarette smoke, maternal environmental tobacco smoke, environmental tobacco smoke and e-cigarette vapour on foetal respiratory outcomes.

**Keywords:** Epigenetics, Airway, Lung development, Asthma, COPD, E-cigarette, Tobacco, Foetal

## Background

Foetal lung organogenesis is an extensive and multi-stage process, commencing with the development of the lung bud by the 4th gestational week, with lobar and vascularised subsegmental branching occurring by the 6th week [1]. Genesis of conducting airways, with airway cartilage, smooth muscle, mucous glands and epithelial cell differentiation commences as early as gestational week 7 [1]. Completion of a full-term pregnancy allows for formation of true alveoli and maturation of surfactant in Type II epithelial cells [1, 2], allowing for healthy gas exchange. Upon delivery, lung development will continue postnatally, with significant alveolar growth occurring during the first 2 years of life [3] and into adolescence [4]. This protracted period of development, commencing in utero and continuing into adolescence, makes the pulmonary system particularly vulnerable to environmental insults affecting normal lung development. Harmful exposures during development can alter the course of healthy lung

development and set the child on a trajectory making them more vulnerable to disease [5–7].

Asthma and chronic obstructive pulmonary disease (COPD) are diseases of the airway, wherein patients experience common symptoms such as shortness of breath, cough and wheeze, and share some similar pathological changes collectively termed airway remodelling. What sets them apart at a functional level is the age of onset of symptoms, etiological causes, progression of the disease and response to existing therapeutics.

Asthma is a heterogeneous disease experienced by 235 million people worldwide [8] and is the most prevalent chronic disease in developed countries. Asthma typically develops early in life with patients experiencing symptoms during an exacerbation episode known as an 'asthma attack', which typically responds well to bronchodilators and can be controlled using corticosteroids. Overall, asthmatic mortality rates have fallen but deaths during asthma attacks persist, with higher prevalence in the elderly [9]. Atopy is common in asthma, mediated by CD4<sup>+</sup> Th2 cells and infiltration of mast cells and eosinophils in the airway walls. Inflammation and increased smooth muscle bulk comprise airway wall remodelling in asthma, causing airway obstruction [9, 10].

\* Correspondence: [brian.oliver@uts.edu.au](mailto:brian.oliver@uts.edu.au)

<sup>1</sup>Respiratory Cellular and Molecular Biology, Woolcock Institute of Medical Research, The University of Sydney, Sydney, Australia

<sup>2</sup>School of Life Sciences, University of Technology Sydney, Sydney, Australia  
Full list of author information is available at the end of the article



© The Author(s). 2019 **Open Access** This article is distributed under the terms of the Creative Commons Attribution 4.0 International License (<http://creativecommons.org/licenses/by/4.0/>), which permits unrestricted use, distribution, and reproduction in any medium, provided you give appropriate credit to the original author(s) and the source, provide a link to the Creative Commons license, and indicate if changes were made. The Creative Commons Public Domain Dedication waiver (<http://creativecommons.org/publicdomain/zero/1.0/>) applies to the data made available in this article, unless otherwise stated.

COPD is the fourth most common cause of death worldwide with prevalence increasing in concert with the ageing population [11, 12]. In contrast to the age of onset in asthma, COPD—except anti- $\alpha$ -trypsin COPD—develops later in life. COPD patients generally show a limited response to corticosteroids and upon manifestation of the disease, lung function progressively declines until death or transplantation. Inflammation in small airway walls of COPD patients is mediated by CD8<sup>+</sup> Tc1 cells, consists of neutrophils and macrophages [9, 10] and is most prevalent in peripheral airways [13]. In conjunction with small airway obstruction, COPD patients may experience emphysema, which manifests as loss of alveolar space. Pathologically, patients can be clustered into predominantly experiencing either small airway obstruction or emphysematous destruction [9].

Both asthma and COPD have an inherited component, but the aetiology and risk factors for the two are different. Typically, asthma is an allergic disease and COPD is the result of inhalation of noxious gases; however, there is considerable overlap of the two diseases, and in some cases, asthma and COPD can co-exist and asthma can progress into COPD. The differences between COPD and asthma are attributed to different gene environment interactions and different genetic risk factors. Pathologically the two diseases are distinct, for example differing inflammatory profiles and sites of inflammation within the airway wall [9, 14], but asthmatics and COPD patients both experience obstruction of the airways. A useful diagnostic tool for airway obstruction is spirometry, wherein patients' forced expiratory volume in 1 second (FEV<sub>1</sub>) demonstrates how quickly a patient can expel air from their lungs. A lower FEV<sub>1</sub> indicates greater airway obstruction. The main spirometric difference is that asthma has reversible airway obstruction, but COPD has incomplete reversal of airway obstruction. However, spirometry alone cannot differentially diagnose the two diseases. In severe forms of asthma, for example asthma with fixed airflow limitation, lung physiology can resemble COPD, and similarly patients with COPD can be highly responsive to bronchodilators.

This review will focus on the epigenetic impact of specific environmental insults such as environmental tobacco smoke (ETS), maternal exposure to ETS (METS), maternal use of tobacco smoke (MTS) and maternal e-cigarette vapour (MEV) exposure on the offspring's lung development and function, with a focus on asthma and COPD.

#### Epigenetics in asthma and COPD

Studies have shown that family history of COPD is a risk factor for manifestation of the disease [15, 16]. Similarly, siblings and first-degree relatives of asthmatics are often affected with lower FEV<sub>1</sub> [17, 18], thereby suggesting a

heritability factor in asthma and COPD. The absence of a correlation between findings of a COPD or asthma SNP in genome-wide associations studies (GWAS) suggests that the hereditary effect is likely established at the epigenomic level rather than genomic and might have greater impact on gene expression in cells at the site of disease [19].

Epigenome-wide association studies (EWAS) have found that leukocytes from COPD patients have 349 differentially methylated CpG sites compared to those from non-COPD smokers [20]. A similar study using small airway epithelial cells found 1260 differentially methylated CpGs related to COPD [21]. DNA methylation status at the promoter of *GATA4* measured in sputum samples has been associated with impaired lung function [22, 23] and health outcomes in COPD [22]. Whilst augmented mRNA expression of *DEFB1*, a gene associated with COPD [24], has been attributed to trimethylation of H3K4 [25].

The balance of Type 1 helper T-cells (Th1) and Type 2 helper T-cells (Th2) is crucial in the development of atopic asthma [26]. Epigenetic changes, such as methylation at the interferon- $\gamma$  (*IFN- $\gamma$* ) promoter, have been associated with skewing naïve T-cells towards an atopic Th2 phenotype [27]. Murine models of asthma have shown that genetic components involved in transcription of Th2 cytokine, IL-13, are regulated by DNA methylation and miRNAs with predicted targets essential in allergic airways disease [28].

The innate immune system is naturally plastic and therefore particularly vulnerable to epigenetic modifications. Further, aberrant accumulation of leukocytes such as neutrophils and eosinophils has been implicated in both asthma and COPD [9] suggesting that dysregulated epigenetic modulation of these cells could contribute to disease pathology. A study using bronchoalveolar lavage (BAL) macrophages from patients with COPD found lower expression of *HDAC2* mRNA and showed decreased histone deacetylase (HDAC) activity in smokers that correlated with significantly higher levels of IL-1 $\beta$  and TNF $\alpha$  [29]. There was an altered ability of the BET mimic JQ1 to suppress specific cytokine gene expression in COPD BAL macrophages [30] which together demonstrate that epigenetic changes contribute to disease pathology. For a comprehensive review on epigenetics in airways disease, it is recommended to read Durham et al [31].

#### Functional and epigenetic outcomes of maternal tobacco smoke (MTS), maternal environmental tobacco smoke (METS) and environmental tobacco smoke (ETS) exposure

Although awareness campaigns have led to a general decline in smoking rates across the world, MTS is an ongoing issue [32, 33]. Rates vary widely between countries, with some EU nations as low as 5% (Sweden,



Austria, Switzerland) and others as high as 40% (Greece) [34–36]; in the US 10.7% of mothers smoke during the last trimester [33]. Together, these data demonstrate that maternal smoking is a worldwide problem. Maternal tobacco use is not the only means of foetal tobacco exposure with epidemiological studies reporting up to 50% of women in China are exposed to ETS while pregnant [37]. Further, it is estimated that the aforementioned MTS and ETS exposure rates do not accurately reflect the true extent of the problem as smoking parents have been shown to falsely report their habit [38] and 50% of smokers continue to smoke throughout their pregnancy [39].

Studies have quantified levels of cotinine in amniotic fluid of pregnant smokers and blood from neonates exposed to MTS [40, 41], confirming that nicotine can cross the placenta in utero [40, 42]. An investigation of nicotine exposure in neonates found cotinine levels comparable to that observed in active smoking adults [43, 44]. It is presumed that the antenatally exposed infant will continue to be exposed to nicotine postnatally through ETS exposure and breast milk [45, 46] with 40% of children reportedly exposed to ETS [47]. Studies have found a positive correlation between concentration of nicotine in maternal blood and foetal growth retardation [48].

Harmful effects of MTS on lung development have been detected early on with a slower pace of septal growth, subsequent alveolarisation [49, 50], and foetal lung size of MTS-exposed babies reduced by the 33rd gestational week [51]. Mothers continuing to smoke during pregnancy have a 25% higher likelihood of preterm labour [52], causing a disruption of healthy lung organogenesis leading to aberrant development [53].

MTS exposure also increases risk of asthma [54, 55] and wheeze [54, 56] in the offspring, with paternal smoking being an additive risk [55]. Negative respiratory outcomes for infants exposed to MTS include irregular tidal breathing patterns, decreased passive respiratory compliance, and decreased forced expiratory flows [51, 57], with decreased lung function persisting into adolescence [55, 57] and early adulthood [58, 59]. Paternal smoking during puberty, when spermatogonia are developing, increases the risk for asthma in offspring [60], thereby demonstrating that parental smoking behaviour has a long-term effect on respiratory outcomes in the offspring.

Exposure to ETS significantly decreases FEV<sub>1</sub> [61, 62] and is an independent risk factor for developing asthma [63]. Asthmatic children exposed to ETS have more severe asthma [64] and frequent exacerbations requiring hospitalisation [65] and tend to have slower recoveries than those not exposed to ETS [66]. Indeed, urinary cotinine levels positively correlate with ETS exposure levels and the severity of asthma exacerbations [67] and higher blood cotinine concentrations are linked to bronchial hyperresponsiveness [68]. Removing ETS from an

asthmatic child's environment has shown positive health outcomes by lessening symptoms [69]. Women exposed to ETS during childhood were twice as likely to develop COPD whilst men showed a slightly increased risk of reduced lung function when compared with those not exposed to ETS during childhood [70]. Childhood ETS exposure combined with previous MTS exposure has been shown to have compounding effects that leave the offspring more vulnerable to harmful effects of active smoking and decline in lung function [58, 71]. The effect of MTS and ETS on COPD patients' outcomes persists long into their lives, with adult patients of smoking mothers having significantly lower FEV<sub>1</sub> than those of non-smoking mothers [72].

Investigations into epigenetic aberrations in human airway cells exposed to tobacco smoke found small airway epithelial cells experience dose-dependent changes in histone acetylation and methylation, alongside decreased expression of DNA methyltransferases (DNMT) [73]. Tobacco smoke-exposed H292 cells, derived from human lung epithelia, showed augmented expression of genes for enzymes involved with chromatin modifications, such as the histone deacetylase (HDAC), *HDAC2*, and the histone acetyltransferase (HAT), *Myst4*, within 60 min of exposure to tobacco smoke extract with expression of other HATs and HDACs upregulated at the 24-h time point [74]. Exposure of human bronchial epithelial cells to the vapour phase of tobacco smoke, rather than a tobacco smoke extract, found that tobacco smoke induces acetylation at H3K27 and demonstrate that these changes have a downstream effect on transcription of genes related to stress responses [75].

COPD is a known risk factor for lung cancer and the latter is also associated with an altered epigenome, and several specific changes in miRNA expression, histone modifications and DNA methylation profiles have been reported in lung cancer and even proposed as biomarkers of disease [76]. For example, the methylation status of PGAM5 in human sperm cells is altered by cigarette smoking which affects its expression [77]. PGAM5 expression was dysregulated in epithelial cells and specific macrophage subtypes of COPD patients with lung cancer with the latter associated with mortality [78].

Epidemiological evidence supports the notion that the effects of MTS are heritable with further generations continuing to manifest poor respiratory outcomes. Grandmaternal smoking has been shown to affect the grandchild's lung development [60, 79] and increase the risk of asthma independent of maternal smoking [80–82]. Furthermore, MTS exposure experienced by the father in utero has been shown to affect the respiratory outcome of his daughter, independent of his smoking habits [83]. Murine models confirm the direct effects of MTS on the offspring with in utero smoke exposure decreasing lung volume [84, 85]

and increasing airway resistance [85] and provide insights into the mechanisms underlying these changes. The developmental differences are evident in MTS-exposed mice offspring with significantly lower lung weights [86] and increased ASM layer thickness and collagen deposition upon allergen challenge with HDM compared to those exposed to ambient air [87]. An intergenerational murine model demonstrates that METS exposure lead to increases in airway hyperactivity, airway resistance and decreases in lung compliance in offspring, which was then passed down to the next generation in the absence of METS exposure [88]. Similarly, allergen challenge elicited an ameliorated atopic response demonstrated by eosinophilia and significantly higher IL-13 levels in two subsequent generations when compared to the progeny of ambient air exposed animals [88]; METS exposure and allergen challenge were shown to deregulate miR-130, miR-16 and miR-221 exposure and are postulated as the epigenetic mechanism modulating the augmented IL-13 response induced by METS exposure [88].

Cigarette smoke constituents have been detected in both the placenta and cord blood [43, 44] of newborns and MTS exposure has been shown to cause changes in global DNA methylation [89–93] and alter miRNA levels in germline cells [94]. Hence, there is no question that MTS exposure alters the foetal epigenome. The effects of aberrant DNA methylation patterns in cord blood and placenta are demonstrated by tissue-specific DNA methylome analyses showing that MTS can induce specific changes to DNA methylation within the placenta in genes crucial to foetal growth and development [92, 95]. Further, blood DNA methylation changes have been associated with lower FEV<sub>1</sub> [96] and have been shown to persist into childhood and adolescence [90, 97–101], demonstrating that epigenetic modulations induced by MTS have long-lasting effects on offspring's lung function (Table 1). Various studies have shown that DNA methylation changes caused by MTS occur at loci specific to established outcomes of maternal smoking such as reduced foetal growth and wheeze [102, 103].

EWAS findings have shown MTS induced altered methylation of *DPP10* [104], a candidate gene identified in GWASs [105, 106], in human foetal lung tissue. Genes playing a role in attenuating the harmful effects of tobacco smoke and its toxic constituents, such as *CYP1A1* [91] and *AHRR* [107], are modulated by DNA methylation and have been shown to be altered by MTS exposure. Immune cells from active smoking adults and cord blood from neonates exposed to MTS both show differential methylation of *CYP1A1* and *AHRR* promoter regions compared to non-smoke-exposed subjects [91, 108]. MTS exposure has been shown to cause demethylation of the promoter region for receptor of insulin-like growth factor 1 (*Igf1R*) in the murine lung [109] and methylation

**Table 1** Summary of respiratory function-specific epigenetic changes in the offspring categorised by exposure

Epigenetic changes induced by MTS	
Altered global DNA methylation	Whole blood, cord blood, placenta [89–93]
Genes associated with foetal growth— <i>LINE-1</i> , <i>AluYb8</i> , <i>IGF2DMR</i> , <i>Igf1R</i> , <i>Igf2</i> —differentially methylated	Placenta, cord WBC, cord blood, murine lung [95, 102, 103, 109, 110]
COPD candidate gene in GWAS, <i>DPP10</i> , hypomethylated	Foetal lung [104–106]
Genes associated with detoxification of tobacco smoke, <i>CYP1A1</i> and <i>AHRR</i> , show altered methylation	Placenta, cord blood [91, 107]
miRNA involved in transcription of <i>Igf1</i> upregulated	Murine lung [86]
Epigenetic changes induced by METS	
<i>IL-4</i> and <i>IL-13</i> hypomethylated at promoter region	Murine lung [118]
miR-155-5p, miR-21-3p and miR-18a-5p positively correlate with Th2 cytokines	Murine lung [118]
Epigenetic changes induced by MEV	
Global DNA hypermethylation	Murine lung [130]

of insulin-like growth factor 2 (*Igf2*) in human cord blood [110], which both play an important role in lung development and can contribute to asthma later in life. Interestingly, the differentially methylated regions in *Igf1R* and *Igf2* induced by MTS have been shown to be sex dependent, with the former only evident in females and the latter males [109, 110]. Taken together with studies showing MTS exposure affecting organs differently [111], the findings fortify the requirement for specificity in epigenetic investigations as stimuli causing demethylation in one organ or gender can have inverse effects in another.

Further investigations have shown that MTS exposure dysregulated 133 miRNAs expressed in foetal murine lungs, some of which played a role in transcription of *Igf1* which was significantly increased in female offspring [86]. The authors validated these findings in humans by showing increased *Igf1* mRNA expressed from leukocytes of school-aged children exposed to MTS [86], demonstrating that the mechanism is conserved between species and persists beyond infancy. METS alters lung structure [112] and lowers birth weight in murine models of exposure [88, 113]. Upon allergen challenge, METS-exposed murine offspring express significantly higher levels of Th2 cytokines in BAL fluid and lung, lung eosinophilia and airway hyperreactivity when compared to offspring exposed to ambient air antenatally [114, 115] which corresponds with strong hypomethylation at the *IL4* and *IL13* promoters [114]. Augmented expression of IL-13 in airways of METS-exposed murine

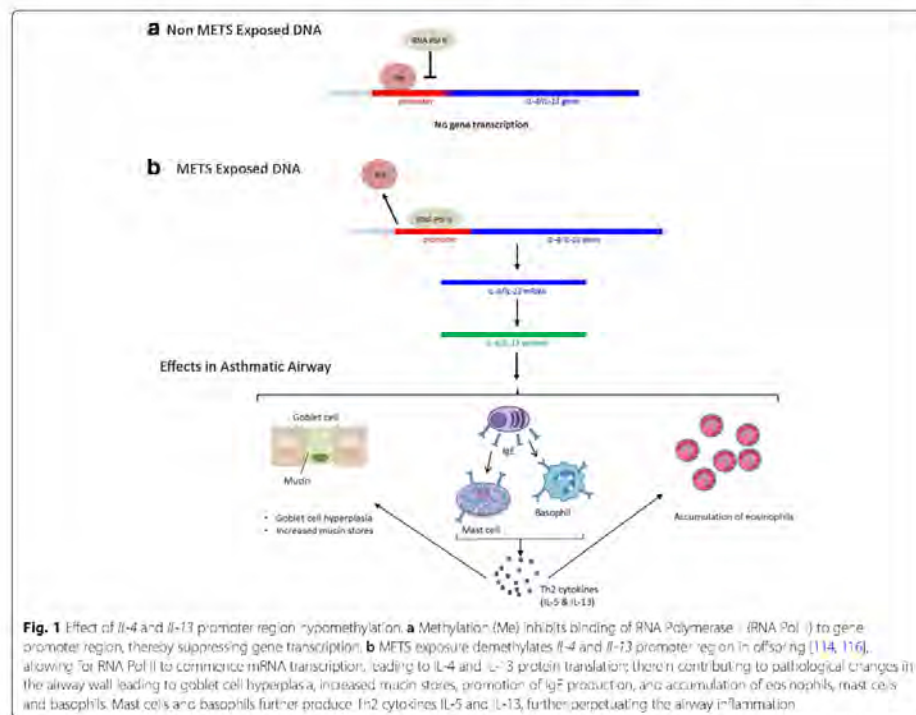
offspring correspond with demethylation at the *IL13* promoter [116] demonstrating alterations to DNA methylation induced by METS exposure contribute to pathology in allergic asthma. Specific miRNAs are implicated as regulators of the Th1/Th2 balance with ablation of miR-21 expression significantly augmenting expression of Th1 cytokine IFN $\gamma$  and ameliorating expression of Th2 cytokine, IL-4 [117] in mice (Fig. 1). A study of allergen-challenged mice exposed to METS found a strong correlation between miR-155-5p, miR-21-3p and miR-18a-5p and expression of Th2 cytokines in BAL [118], implicating miRNAs in the modulation of METS-induced atopy in offspring. These findings are compelling when conjoined with the previously discussed study by Singh et al. [88] implicating miRNAs in METS-induced augmented IL-13 production.

#### Functional and Epigenetic effects of MEV exposure

The negative health impacts of cigarette smoking are well documented and agreed upon. As cigarette consumption declines, an opening in the market has

formed. In response, established tobacco companies and entrepreneurs alike have flooded the market with new nicotine delivery devices. The most successful thus far being the e-cigarette. Briefly, an e-cigarette is a hand-held device comprised of a reservoir for an “e-liquid” and a heating element connected to a battery. Upon use, the e-liquid passes through the heating element, forming an “e-vapour” to be inhaled by the user. Unlike a cigarette, there is no combustion in an e-cigarette and it is subsequently marketed as a “healthier” alternative to cigarette smoking. However, the declaration of healthiness is premature as the effects of long-term e-cigarette use and indirect exposure to e-vapour remain to be elucidated. The illusion of a healthier alternative leaves the population at risk of enduring damaging effects with at-risk groups being the most vulnerable. It has been reported that pregnant women have started to use e-cigarettes during pregnancy at increasing rates [119].

The basic composition of an e-liquid is a mixture of propylene glycol, glycerol and flavourings, which may





include nicotine but some e-liquids contain no nicotine [120]. Notwithstanding coming under the jurisdiction of the EU Tobacco Products Directive in May 2016, e-liquid compositions continue to vary widely, and studies have identified discrepancies in actual versus reported nicotine concentrations [121, 122]. Independent analyses have detected harmful compounds such as phthalates, diacetyl and acrolein in e-liquids [122–124]. Whilst indoor air quality studies have found that levels of aerosolised polycyclic aromatic hydrocarbons (PAHs), formaldehyde, acetaldehyde, acrolein and particulate matter  $\leq 2.5\mu\text{m}$  [120, 122] are significantly increased when e-cigarettes are used indoors.

As established, the ingredients in an e-liquid vary widely, with some shown to be capable of epigenetic modifications. An *in vitro* experiment using EA.hy926 cells found that DNMT3b transcript was decreased following acrolein exposure [125]. Maternal exposure to benzylbutylphthalate (BBP) caused global DNA hypermethylation in CD4+ T cells of the exposed dam and to a greater extent in her offspring in a murine model of exposure [126]. This hypermethylation significantly correlated with attenuated expression of the GATA-3 repressor zinc finger protein 1 (*Zfpml*)—a gene that represses GATA-3 mediated Th2 cell development—thereby promoting the Th2 phenotype. The authors further validated the link between maternal urinary BBP metabolite levels and *Zfpml* in humans using whole blood samples from 4-year-old children in the lifestyle and environmental factors and their influence on newborns allergy (LINA) cohort. Although only trace levels of BBP were detected in e-liquids compared to other phthalates [123], it is of import to note that BBP shares a common metabolite—mono-n-butyl phthalate (MnBP)—with phthalates more abundant in e-liquids, such as diethyl phthalate. Therefore, it is imperative to elucidate whether BBP, MnBP, or other phthalate metabolites induce specific epigenetic modifications. A significant correlation between maternal urinary MnBP levels during pregnancy and asthma symptoms in the child persisting until at least 6 years of age has been reported [126].

Direct e-cigarette vapour exposure leads to impaired innate immune responses in murine lungs [127], whilst murine models of MEV exposure have shown inimical effects of e-cigarette vapour on neonatal lung development [128]. There is a current paucity of studies on the impact of MEV exposure on the foetal epigenome but those that have been published thus far demonstrate that MEV exposure leads to epigenetic aberrations in the offspring. A murine model of MEV exposure with and without nicotine on cognitive function found that exposure to MEV without nicotine significantly increased global DNA methylation in the offspring when compared to ambient air-exposed offspring, whilst MEV with nicotine

did not [129]. The study further showed that *DNMT3a* and *DNMT3b* mRNA were ameliorated by MEV without nicotine. Furthermore, mRNA for genes involved in histone modifications *Carm1*, *Ayf2*, *Aurka*, *Aurkb* and *Aurkc* were also augmented by MEV without nicotine only. Thereby suggesting that e-cigarette vapour is capable of epigenetic modulation in the offspring independent of nicotine.

An investigation into the impact of MEV exposure on respiratory outcomes found that MEV exposure with and without nicotine induced significant global DNA hypermethylation in offsprings' lungs compared to air-exposed controls [130]. Interestingly, MEV without nicotine elicited significantly greater DNA hypermethylation compared to those induced by MEV with nicotine with enhanced expression of the pro-inflammatory cytokines IL-5, IL-13, TNF- $\alpha$  mRNA only seen in the lungs of offspring exposed to MEV without nicotine [130]. The analysis of changes in global DNA methylation patterns demonstrates that exposure to MEV is inducing heritable epigenetic changes that manifest in the offspring. Although nicotine-containing e-vapour has been shown to induce less hypermethylation than non-nicotine containing e-vapour, the profile of which genes are being methylated or demethylated is not yet known. Therefore, further investigation is necessary to elucidate where in the genome the modifications are taking place and the roles these genes play in pathophysiology before making a congruent decision on the role of e-vapour with and without nicotine plays in epigenetics and respiratory disease.

Nicotine concentrations in e-liquid in the EU are permitted to be as high as 20 mg/ml; although, some samples exceed that limit [121] leaving users susceptible to higher nicotine exposure than anticipated. Studies on indoor air quality have detected increased levels of nicotine and carcinogenic nitrosamines, such as *N*-nitrosonornicotine (NNN) and nicotine-derived nitrosamine ketone (NNK) in the atmosphere after e-cigarette use [131]. Serum cotinine levels measured in non-smoking and non-vaping individuals exposed to environmental e-vapour found elevated cotinine levels that equated to ETS exposure and persisted at the same rate as ETS [61, 132], suggesting that e-vapour remains in the atmosphere in a similar fashion to ETS. Further, nicotine remaining in the indoor environment can react with oxidant gases in the atmosphere to form added levels of NNN and NNK [133]. Nitrosamines have been shown to methylate DNA and induce methylation DNA damage [134], which is a mechanism believed to be behind their carcinogenicity [135, 136].

Studies have shown that foetal nicotine levels equate to those in the mother [137] with nicotine capable of accumulating in the respiratory tract in the foetus [42]. Animal models of nicotine-only exposure show that offspring exhibit increased smooth muscle and collagen

bulk in the airway, and augmented airway hyperreactivity [138–140]. Altered lung development was shown to persist in second-generation offspring not exposed to nicotine [141]. A murine model of nicotine exposure showed that perinatal nicotine exposure altered DNA methylation and histone modification in the lung and gonads of offspring and induced asthma-like changes that persisted into the third generation of offspring [142], thereby demonstrating functional respiratory and epigenetic effects induced by maternal nicotine exposure, together with direct epigenetic changes to the germline. Corroborating with these changes was a decrease in mRNA and protein expression of peroxisome proliferator-activated receptor  $\gamma$  (PPAR $\gamma$ ) which plays an essential role in lung development and repair [142–144]. Interestingly, when Rosiglitazone, a known PPAR $\gamma$  agonist, was administered in concert with nicotine to pregnant dams, asthma-like changes and H3 acetylation induced by nicotine exposure was prevented whilst nicotine induced global H4 acetylation and DNA methylation persisted [145], further reinforcing the significance of PPAR $\gamma$ 's role in healthy lung development. These seemingly paradoxical effects of nicotine in e-liquids compared to those described earlier in relation to cigarette smoking may relate to the dose and duration of exposure and to its well-known anti-inflammatory effects [146].

#### The future of epigenetic therapeutics

The established role of epigenetics in pathophysiology naturally implores exploring its therapeutic potential. Using 5-azacytidine to inhibit DNMT1 in a murine model of asthma augmented numbers of Treg cells and effectively reduced airway inflammation [147]. The pan-HDAC inhibitor, Trichostatin-A, has similarly shown efficacy in asthma models [148], as has the allosteric activator of SIRT1, SRT1720 [149]. Targeting HDAC classes 1–3 with MS-275 abrogated neutrophil infiltration of the lungs and expression of proinflammatory cytokines KC, IL-6 and IL-1 $\beta$  [150]. An in vitro model of asthma using human airway smooth muscle cells attenuated TGF- $\beta$ -induced proliferation and pro-inflammatory cytokine production with bromodomain inhibitors JQ1(+) and I-BET762 [151]. Using inhibitors to target proteins and enzymes active in epigenetic modulation are useful tools in demonstrating the effect of certain classes of epigenetic changes. However, due to the nature of their targets, it is difficult to determine the complete extent of which genes are within the purview of the inhibitors.

To overcome this impediment, epigenetic therapeutics may focus on the use of DNA targeting systems capable of binding to genes of interest in a directed manner. The three most well-understood DNA targeting systems are zinc finger proteins (ZFPs), transcriptional-activator-like

effectors (TALEs), and clustered regularly interspaced short palindromic repeats (CRISPR) and CRISPR-associated protein 9 (Cas9, 152); the latter of which being the most recent advance in the field and most efficient as it is less cumbersome than ZFPs and TALEs [152]. A study of *SPDEF*—a regulator of mucus production in COPD known to be hypomethylated [153]—in human lung epithelial cells effectively used ZFPs and CRISPR/dCas to attenuate mucus-related gene expression and reduce mucus production by silencing *SPDEF* [154]. Therein demonstrating that targeted silencing of genes using epigenetic editing can reverse disease pathologies in vitro.

#### Conclusion

The evidence summarised in this review demonstrates that maternal use of tobacco cigarettes and e-cigarettes and exposure to environmental tobacco smoke induces epigenetic changes in the offspring. These changes have been demonstrated to contribute to disease pathology and be passed down to further generations independent of exposure. The all-encompassing nature of epigenetic modifications implores research to consider using cell types specifically implicated in disease pathologies, as findings across differing cell types may obfuscate pathological epigenetic differences with inherent epigenetic differences dictating cell phenotype. Further, it is imperative to continue exploring intergenerational effects of maternal e-cigarette use and exposure using animal models on DNA methylation at specific genomic regions and specific chromatin modifications to relate the changes being induced to genes implicated in disease pathology, thereby elucidating targets for the use of advanced DNA targeting systems in therapy. Finally, it is recommended that further longitudinal studies on the impacts of e-cigarettes are carried out, thereby allowing us to distinguish between epigenetic modifications that are biomarkers of exposure, such as the aforementioned *CYP1A1* and *AHRR* versus those that are likely to mediate airway disease susceptibility.

#### Abbreviations

ASM: Airway smooth muscle; BAL: Bronchoalveolar lavage; BBP: Benzylbutylphthalate; BET: Bromo- and extra-terminal domain; CAS9: CRISPR-associated protein 9; COPD: Chronic Obstructive Pulmonary Disease; CRISPR: Clustered regularly interspaced short palindromic repeats; DNA: Deoxyribonucleic acid; DNMT: DNA methyltransferase; ETS: Environmental tobacco smoke; EU: European Union; EWAS: Epigenome-wide association study; FEV1: Forced Expiratory Volume in one second; GWAS: Genome-wide association study; HAT: Histone acetyltransferase; HDAC: Histone deacetylase; HDM: House dust mite; IFN $\gamma$ : Interferon gamma; *Igf1*: Gene for insulin growth factor 1; *Igf2*: Gene for insulin growth factor 2; IL: Interleukin; LINA: Lifestyle and environmental factors and their influence on newborns allergy; METS: Maternal exposure to environmental tobacco smoke; MEV: Maternal e-cigarette vapour; miRNA: MicroRNA; MnBP: Mono-n-butyl phthalate; mRNA: Messenger RNA; MTS: Maternal use of tobacco smoke; NNK: Nitrosamine ketone; NNN: N-nitrososarcosine; PAHs: Polycyclic aromatic hydrocarbons; SNP: Single-nucleotide polymorphism; TALEs: Transcriptional-activator-like effector; TGF- $\beta$ : Transforming growth factor beta; ZFP: Zinc finger protein

**Acknowledgements**

NA.

**Funding**

BGO is supported by a fellowship from the NHMRC Australia and Ms Zakarya is supported by a post graduate scholarship from the University of Technology Sydney.

**Availability of data and materials**

NA.

**Authors' contributions**

All Authors conceived the ideas, read the manuscript and edited the final version. RZ drafted the manuscript. All authors read and approved the final manuscript.

**Ethics approval and consent to participate**

NA.

**Consent for publication**

All Authors consent to publication of this paper.

**Competing interests**

The authors declare that they have no competing interests.

**Publisher's Note**

Springer Nature remains neutral with regard to jurisdictional claims in published maps and institutional affiliations.

**Author details**

<sup>1</sup>Respiratory Cellular and Molecular Biology, Woolcock Institute of Medical Research, The University of Sydney, Sydney, Australia. <sup>2</sup>School of Life Sciences, University of Technology Sydney, Sydney, Australia. <sup>3</sup>Airway Diseases Section, National Heart and Lung Institute, Imperial College London, London, UK. <sup>4</sup>Biomedical Research Unit, Section of Respiratory Diseases, Royal Brompton and Harefield NHS Trust, London, UK.

Received: 19 December 2018 Accepted: 11 February 2019

Published online: 19 February 2019

**References**

- Gibbs K, Collaco JM, McGrath-Morrow SA. Impact of tobacco smoke and nicotine exposure on lung development. *Chest*. 2016;149(2):552–61.
- Clements JA. Lung surfactant: a personal perspective. *Annu Rev Physiol*. 1997;59:1–21.
- Thurlbeck WM. Postnatal human lung growth. *Thorax*. 1982;37(8):564–71.
- Herring MJ, Putney LF, Wyatt G, Finkbeiner WE, Hyde DM. Growth of alveoli during postnatal development in humans based on stereological estimation. *Am J Phys Lung Cell Mol Phys*. 2014;307(4):L338–L44.
- Guerra S, Martinez FD. Epidemiology of the origins of airflow limitation in asthma. *Proc Am Thorac Soc*. 2009;6(8):707–11.
- Martinez FD. The origins of asthma and chronic obstructive pulmonary disease in early life. *Proc Am Thorac Soc*. 2009;6(3):272–7.
- Stern DA, Morgan WJ, Wright AL, Guerra S, Martinez FD. Poor airway function in early infancy and lung function by age 22 years: a non-selective longitudinal cohort study. *Lancet*. 2007;370(9589):758–64.
- Organisation WH. Key facts: asthma 2017 [updated 31 Aug 2017].
- Barnes PJ. Cellular and molecular mechanisms of asthma and COPD. *Clin Sci*. 2017;131(13):1541–58.
- Hirota N, Martin JG. Mechanisms of airway remodeling. *Chest*. 2013;144(3):1026–32.
- Barnes PJ, Shapiro S, Pauwels R. Chronic obstructive pulmonary disease: molecular and cellular mechanisms. *Eur Respir J*. 2003;22(4):672–88.
- Lozano R, Naghavi M, Foreman K, Lim S, Shibuya K, Aboyans V, et al. Global and regional mortality from 235 causes of death for 20 age groups in 1990 and 2010: a systematic analysis for the Global Burden of Disease Study 2010. *Lancet*. 2012;380(9859):2095–128.
- Barnes PJ. Inflammatory mechanisms in patients with chronic obstructive pulmonary disease. *J Allergy Clin Immunol*. 2016;138(1):16–27.
- Hogg JC, Chu F, Utokaparch S, Woods R, Elliott WM, Buzatu L, et al. The nature of small-airway obstruction in chronic obstructive pulmonary disease. *N Engl J Med*. 2004;350(26):2645–53.
- Hersh CP, Holanson JE, Lynch DA, Washko GR, Make BJ, Crapo JD, et al. Family history is a risk factor for COPD. *Chest*. 2011;140(2):343–50.
- McCLOSKEY SC, Patel BD, Hinchliffe SJ, Reid ED, Wareham NJ, Lomas DA. Siblings of patients with severe chronic obstructive pulmonary disease have a significant risk of airflow obstruction. *Am J Respir Crit Care Med*. 2001;164(8):1419–24.
- Cantani A, Micera M. A study on 300 asthmatic children, 300 controls and their parents confirms the genetic transmission of allergy and asthma. *Eur Rev Med Pharmacol Sci*. 2011;15(9):1051–6.
- Kurzus-Spencer M, Guerra S, Sherrill DL, Halonen M, Elston RC, Martinez FD. Familial aggregation of allergen-specific sensitization and asthma. *Pediatr Allergy Immunol*. 2012;23(1):21–7.
- Shrine N, Portelli MA, John C, Artigas MS, Bennett N, Hall R, et al. Moderate-to-severe asthma in individuals of European ancestry: a genome-wide association study. *Lancet Respir Med*. 2019;7(1):20–34.
- Qiu W, Baccarelli A, Carey VJ, Boutaouil N, Bacherman H, Klanderman B, et al. Variable DNA methylation is associated with chronic obstructive pulmonary disease and lung function. *Am J Respir Crit Care Med*. 2012;185(4):373–81.
- Vuckc EA, Chari R, Thu KL, Wilson IM, Cotton AM, Kennett JY, et al. DNA methylation is globally disrupted and associated with expression changes in chronic obstructive pulmonary disease small airways. *Am J Respir Cell Mol Biol*. 2014;50(5):912–22.
- Meek PM, Sood A, Petersen H, Belinsky SA, Tesfaigzi Y. Epigenetic change (GATA-4 gene methylation) is associated with health status in chronic obstructive pulmonary disease. *Biol Res Nurs*. 2015;17(2):191–8.
- Sood A, Petersen H, Blanchette CM, Meek P, Picchi MA, Belinsky SA, et al. Wood smoke exposure and gene promoter methylation are associated with increased risk for COPD in smokers. *Am J Respir Crit Care Med*. 2010;182(9):1098–104.
- Matsushita I, Hasegawa K, Nakata K, Yasuda K, Tokunaga K, Keicho N. Genetic variants of human β-defensin-1 and chronic obstructive pulmonary disease. *Biochem Biophys Res Commun*. 2002;291(1):17–22.
- Andresen E, Günther G, Bullwinkel J, Lange C, Heine H. Increased expression of beta-defensin 1 (DEFB1) in chronic obstructive pulmonary disease. *PLoS One*. 2011;6(7):e21898.
- Wenzel SE. Asthma phenotypes: the evolution from clinical to molecular approaches. *Nat Med*. 2012;18(5):716.
- Jones B, Chen J. Inhibition of IFN-γ transcription by site-specific methylation during T helper cell development. *EMBO J*. 2006;25(11):2443–52.
- Ooi AT, Ram S, Kuo A, Gilbert JL, Yan W, Pellegrini M, et al. Identification of an interleukin 13-induced epigenetic signature in allergic airway inflammation. *Am J Transl Res*. 2012;4(2):219.
- Ito K, Lim S, Caramori G, Chung K, Barnes P, Adcock I. Cigarette smoking reduces histone deacetylase 2 expression, enhances cytokine expression, and inhibits glucocorticoid actions in alveolar macrophages. *FASEB J*. 2001;15(6):1110–2.
- Malhotra R, Kurian N, Zhou X-H, Jiang F, Monkley S, DeMicco A, et al. Altered regulation and expression of genes by BET family of proteins in COPD patients. *PLoS One*. 2017;12(3):e0173115.
- Durham A, Chou PC, Kirkham P, Adcock IM. Epigenetics in asthma and other inflammatory lung diseases. *Epigenomics*. 2010;2(4):523–37.
- Rockhill KM, Tong VT, Farr SL, Robbins CL, D'Angelo DV, England LJ. Postpartum smoking relapse after quitting during pregnancy: pregnancy risk assessment monitoring system, 2000–2011. *J Women's Health*. 2016;25(5):480–8.
- Tong VT, Dietz PM, Morrow B, D'Angelo DV, Farr SL, Rockhill KM, et al. Trends in smoking before, during, and after pregnancy—Pregnancy Risk Assessment Monitoring System, United States, 40 sites, 2000–2010. *Morb Mortal Wkly Rep Surveill Summ*. 2013;62(6):1–19.
- Neuman A, Hohmann C, Orsini N, Pershagen G, Eller E, Kjær HF, et al. Maternal smoking in pregnancy and asthma in preschool children: a pooled analysis of eight birth cohorts. *Am J Respir Crit Care Med*. 2012;186(10):1037–43.
- Smedberg J, Lupattelli A, Månby A-C, Nordeng H. Characteristics of women who continue smoking during pregnancy: a cross-sectional study of pregnant women and new mothers in 15 European countries. *BMC Pregnancy Childbirth*. 2014;14(1):213.
- Vivilaki VG, Diamanti A, Tzeli M, Patelarou E, Bick D, Papadakis S, et al. Exposure to active and passive smoking among Greek pregnant women. *Tob Induc Dis*. 2016;14(1):12.



37. Zhang L, Hsia J, Tu X, Xia Y, Zhang L, Bi Z, et al. Exposure to secondhand tobacco smoke and interventions among pregnant women in China: a systematic review. *Prev Chronic Dis*. 2015;12:140377. <https://doi.org/10.5888/pcd12.140377>.
38. Shipton D, Tappin DM, Vadevelo T, Crossley JA, Aitken DA, Chalmers J. Reliability of self reported smoking status by pregnant women for estimating smoking prevalence: a retrospective, cross sectional study. *BMI*. 2009;339:b4347.
39. Alkharawy O, Anthony JC. Month-wise estimates of tobacco smoking during pregnancy for the United States, 2002–2009. *Matern Child Health J*. 2015;19(5):1010–5.
40. Jauniaux E, Gulbis B, Acharya G, Thiny P, Rodeck C. Maternal tobacco exposure and cotinine levels in fetal fluids in the first half of pregnancy. *Obstet Gynecol*. 1999;93(1):25–9.
41. Luck W, Nau H, Hansen R, Steldinger R. Extent of nicotine and cotinine transfer to the human fetus, placenta and amniotic fluid of smoking mothers. *Dev Pharmacol Ther*. 1985;8:384–95.
42. Szöcs T, Olsson S, Lindquist NG, Ullberg S, Pilotti A, Enzeli C. Long-term fate of [<sup>14</sup>C] nicotine in the mouse: retention in the bronchi, melanin-containing tissues and urinary bladder wall. *Toxicology*. 1978;10:207–20.
43. Chazeron I, Daval S, Ughetto S, Richard D, Nicolay A, Lermey D, et al. GC-MS determined cotinine in an epidemiological study on smoking status at delivery. *Pulm Pharmacol Ther*. 2008;21(3):485–8.
44. Ivorra C, García-Vicent C, Ponce F, Ortega-Evangelio G, Fernández-Formoso JA, Lurbe E. High cotinine levels are persistent during the first days of life in newborn second hand smokers. *Drug Alcohol Depend*. 2014;134:275–9.
45. Schulte-Hobein B, Schwartz-Bickenbach D, Abt S, Plum C, Nau H. Cigarette smoke exposure and development of infants throughout the first year of life: influence of passive smoking and nursing on cotinine levels in breast milk and infant's urine. *Acta Paediatr*. 1992;81(6–7):550–7.
46. Schwartz-Bickenbach D, Schulte-Hobein B, Abt S, Plum C, Nau H. Smoking and passive smoking during pregnancy and early infancy: effects on birth weight, lactation period, and cotinine concentrations in mother's milk and infant's urine. *Toxicol Lett*. 1987;35(1):73–81.
47. Öberg M, Jaakkola MS, Woodward A, Peruga A, Prüss-Ustün A. Worldwide burden of disease from exposure to second-hand smoke: a retrospective analysis of data from 192 countries. *Lancet*. 2011;377(9760):139–46.
48. Bardy AH, Seppälä T, Lillsunde P, Kataja JM, Koskela P, Piikarainen J, et al. Objectively measured tobacco exposure during pregnancy: neonatal effects and relation to maternal smoking. *BJOG Int J Obstet Gynaecol*. 1993;100(8):721–6.
49. Vidić B, Ujević N, Shabahang MM, van de Zande F. Differentiation of interstitial cells and stromal proteins in the secondary septum of early postnatal rat: effect of maternal chronic exposure to whole cigarette smoke. *Anat Rec*. 1989;223(2):165–73.
50. Feng J-h, Yan Y-e, Liang G, Liu Y-s, Li X-j, Zhang B-j, et al. Maternal and fetal metabonomic alterations in prenatal nicotine exposure-induced rat intrauterine growth retardation. *Mol Cell Endocrinol*. 2014;394(1):59–69.
51. Hoo A-F, Henschen M, Dezateux C, Costeloe K, Stocks J. Respiratory function among preterm infants whose mothers smoked during pregnancy. *Am J Respir Crit Care Med*. 1998;158(3):700–5.
52. Ion R, Bernal AL. Smoking and preterm birth. *Reprod Sci*. 2015;22(8):918–26.
53. Stocks J, Hislop A, Sonnappa S. Early lung development: lifelong effect on respiratory health and disease. *Lancet Respir Med*. 2013;1(9):728–42.
54. Gilliland FD, Li Y-F, Peters JM. Effects of maternal smoking during pregnancy and environmental tobacco smoke on asthma and wheezing in children. *Am J Respir Crit Care Med*. 2001;163(2):429–36.
55. Mitchell EA, Beasley R, Keil U, Montefort S, Odhiambo J, Group IPTS. The association between tobacco and the risk of asthma, rhinoconjunctivitis and eczema in children and adolescents: analyses from phase three of the ISAAC programme. *Thorax*. 2012;67(11):941–9.
56. Herman T, Sonnenschein-van der Voort AM, de Jongste JC, Reiss IK, Hofman A, Jaddoe VW, et al. Tobacco smoke exposure, airway resistance, and asthma in school-age children: the generation R study. *Chest*. 2015;148(3):607–17.
57. Cunningham J, Dockery DW, Speizer FE. Maternal smoking during pregnancy as a predictor of lung function in children. *Am J Epidemiol*. 1994;139(12):1139–52.
58. Guerra S, Stern DA, Zhou M, Sherrill DL, Wright AL, Morgan WJ, et al. Combined effects of parental and active smoking on early lung function deficits: a prospective study from birth to age 26 years. *Thorax*. 2013. <https://doi.org/10.1136/thoraxjnl-2013-203538>.
59. Hayatbakhsh MR, Sadasivam S, Mamun AA, Najman JM, O'Callaghan MJ. Maternal smoking during and after pregnancy and lung function in early adulthood: a prospective study. *Thorax*. 2009;64(9):810–4.
60. Miller LL, Henderson J, Northstone K, Pembrey M, Golding J. Do grandmaternal smoking patterns influence the etiology of childhood asthma? *Chest*. 2014;145(6):1213–8.
61. Flouris AD, Chorti MS, Poulantaki KP, Jamurtas AZ, Kostikas K, Tzatzarakis MN, et al. Acute impact of active and passive electronic cigarette smoking on serum cotinine and lung function. *Inhal Toxicol*. 2013;25(2):91–101.
62. He Q-Q, Wong T-W, Du L, Jiang Z-Q, Yu T-si, Qiu H, et al. Environmental tobacco smoke exposure and Chinese schoolchildren's respiratory health: a prospective cohort study. *Am J Prev Med*. 2011;41(5):487–93.
63. Castro-Rodriguez JA, Forno E, Rodriguez-Martinez CE, Celedón JC. Risk and protective factors for childhood asthma: what is the evidence? *J Allergy Clin Immunol Pract*. 2016;4(6):1111–22.
64. Pyle RC, Divekar R, May SM, Narla N, Pianosi PT, Hartz MF, et al. Asthma-associated comorbidities in children with and without secondhand smoke exposure. *Ann Allergy Asthma Immunol*. 2015;115(5):205–10.
65. Wang Z, May SM, Charoenlap S, Pyle R, Ott NL, Mohammed K, et al. Effects of secondhand smoke exposure on asthma morbidity and health care utilization in children: a systematic review and meta-analysis. *Ann Allergy Asthma Immunol*. 2015;115(5):396–401.e2.
66. Andrews AL, Shirley N, Ojukwu E, Robinson M, Torok M, Wilson KM. Is secondhand smoke exposure associated with increased exacerbation severity among children hospitalized for asthma? *Hosp Pediatr*. 2015;5(5):249–55.
67. Hassanzad M, Khalilzadeh S, Nobari SE, Bloursaz M, Shafiqi H, Mohajerani SA, et al. Cotinine level is associated with asthma severity in passive smoker children. *Iran J Allergy Asthma Immunol*. 2015;14(1):67–73.
68. Carlsen K-H, Carlsen KCL. Respiratory effects of tobacco smoking on infants and young children. *Paediatr Respir Rev*. 2008;9(1):11–20.
69. Landau L. Parental smoking: asthma and wheezing illnesses in infants and children. *Paediatr Respir Rev*. 2001;2(3):202–6.
70. Johannessen A, Bakke PS, Hardie JA, Eagan TM. Association of exposure to environmental tobacco smoke in childhood with chronic obstructive pulmonary disease and respiratory symptoms in adults. *Respirology*. 2012;17(3):499–505.
71. Dratva J, Zemp E, Dharmage SC, Accordini S, Burdet L, Gislason T, et al. Early life origins of lung ageing: early life exposures and lung function decline in adulthood in two European cohorts aged 28–73 years. *PLoS One*. 2016;11(1):e0145127.
72. Beyer D, Mittelsel H, Gillissen A. Maternal smoking promotes chronic obstructive lung disease in the offspring as adults. *Eur J Med Res*. 2009;14(4):27.
73. Liu F, Killian J, Yang M, Walker R, Hong J, Zhang M, et al. Epigenomic alterations and gene expression profiles in respiratory epithelia exposed to cigarette smoke condensate. *Oncogene*. 2010;29(25):3650.
74. Sundar IK, Rahman I. Gene expression profiling of epigenetic chromatin modification enzymes and histone marks by cigarette smoke: implications for COPD and lung cancer. *Am J Phys Lung Cell Mol Phys*. 2016;31(6):L1245–L58.
75. Glass K, Thibault D, Guo F, Mitchell JA, Pham B, Qiu W, et al. Integrative epigenomic analysis in differentiated human primary bronchial epithelial cells exposed to cigarette smoke. *Sci Rep*. 2018;8(1):12750.
76. Mateu-Jimenez M, Curull V, Rodriguez-Fuster A, Aguiló R, Sánchez-Font A, Pijuan L, et al. Profile of epigenetic mechanisms in lung tumors of patients with underlying chronic respiratory conditions. *Clin Epigenetics*. 2018;10(1):7.
77. Alkhaled Y, Laqqan M, Tierling S, Lo Porto C, Amor H, Hammadeh M. Impact of cigarette-smoking on sperm DNA methylation and its effect on sperm parameters. *Andrologia*. 2018;50(4):e12950.
78. Kwong FNK, Nicholson A, Pavlidis S, Adcock I, Chung K. PGAM5 expression and macrophage signatures in non-small cell lung cancer associated with chronic obstructive pulmonary disease (COPD). *BMC Cancer*. 2018;18(1):1238.
79. Li Y-F, Gilliland FD, Berhane K, McCONNELL R, James Gauderman W, Rappaport EB, et al. Effects of in utero and environmental tobacco smoke exposure on lung function in boys and girls with and without asthma. *Am J Respir Crit Care Med*. 2000;162(6):2097–104.
80. Li Y-F, Langholz B, Salam MT, Gilliland FD. Maternal and grandmaternal smoking patterns are associated with early childhood asthma. *Chest*. 2005;127(4):1232–41.
81. Lodge CJ, Bråbäck L, Lowe AJ, Dharmage S, Olsson D, Forsberg B. Grandmaternal smoking increases asthma risk in grandchildren: a nationwide Swedish cohort. *Clin Exp Allergy*. 2018;48(2):167–74.

82. Magnus MC, Häberg SE, Karlstad Ø, Nafstad P, London SJ, Nystad W. Grandmother's smoking when pregnant with the mother and asthma in the grandchild: the Norwegian mother and child cohort study. *Thorax*. 2015;70(3):237–43.
83. Svanes C, Koplin J, Skulstad SM, Johannessen A, Bertelsen RJ, Benediktsdottir B, et al. Father's environment before conception and asthma risk in his children: a multi-generation analysis of the respiratory health in northern Europe study. *Int J Epidemiol*. 2016;46(1):235–45.
84. Collins MH, Moessinger AC, Kleinerman J, Bassi J, Rosso P, Collins AM, et al. Fetal lung hypoplasia associated with maternal smoking: a morphometric analysis. *Pediatr Res*. 1985;19(4):408–12.
85. Larcombe AN, Foong RE, Berry LJ, Zosky GR, Sly PD. In utero cigarette smoke exposure impairs somatic and lung growth in BALB/c mice. *Eur Respir J*. 2011;38(4):952–8.
86. Dehmel S, Nathan P, Bartel S, El-Merhie N, Scherb H, Milger K, et al. Intrauterine smoke exposure deregulates lung function, pulmonary transcriptomes, and in particular insulin-like growth factor (IGF)-1 in a sex-specific manner. *Sci Rep*. 2018;8(1):7547.
87. Blacquierre MJ, Timens W, Melgert BN, Geerlings M, Postma DS, Hylkema MN. Maternal smoking during pregnancy induces airway remodelling in mice offspring. *Eur Respir J*. 2009;33(5):1133–40.
88. Singh SP, Chand HS, Langley RJ, Mishra N, Barnett T, Rudolph K, et al. Gestational exposure to sidestream (secondhand) cigarette smoke promotes transgenerational epigenetic transmission of exacerbated allergic asthma and bronchopulmonary dysplasia. *J Immunol*. 2017;198(10):3815–22.
89. Breiting LP, Yang R, Korn B, Burwinkel B, Brenner H. Tobacco-smoking-related differential DNA methylation: 27K discovery and replication. *Am J Hum Genet*. 2011;88(4):450–7.
90. Shorey-Kendrick LE, McEvoy CT, Ferguson B, Burchard J, Park BS, Gao L, et al. Vitamin C prevents offspring DNA methylation changes associated with maternal smoking in pregnancy. *Am J Respir Crit Care Med*. 2017;196(6):745–55.
91. Suter M, Abramovici A, Showalter L, Hu M, Do Shope C, Varner M, et al. In utero tobacco exposure epigenetically modifies placental CYP1A1 expression. *Metab Clin Exp*. 2010;59(10):1481–90.
92. Suter M, Ma J, Harris AS, Patterson L, Brown KA, Shope C, et al. Maternal tobacco use modestly alters correlated epigenome-wide placental DNA methylation and gene expression. *Epigenetics*. 2011;6(11):1284–94.
93. Zeilinger S, Kühnel B, Klopp N, Baurecht H, Kleinschmidt A, Gleiger C, et al. Tobacco smoking leads to extensive genome-wide changes in DNA methylation. *PLoS One*. 2013;8(5):e63812.
94. Marczylo EL, Amoako AA, Konje JC, Gant TW, Marczylo TH. Smoking induces differential miRNA expression in human spermatozoa: a potential transgenerational epigenetic concern? *Epigenetics*. 2012;7(5):432–9.
95. Wilhelm-Benartzi CS, Houseman EA, Maccani MA, Poage GM, Koestler DC, Langevin SM, et al. In utero exposures, infant growth, and DNA methylation of repetitive elements and developmentally related genes in human placenta. *Environ Health Perspect*. 2011;120(2):296–302.
96. den Dekker HT, Bumows K, Felix JF, Salas LA, Nedeljkovic I, Yao J, et al. Newborn DNA-methylation, childhood lung function, and the risks of asthma and COPD across the life course. *Eur Respir J*. 2019. <https://doi.org/10.1183/13993003.01795-2018>.
97. Breton CV, Byun H-M, Wang X, Salam MT, Siegmund K, Gilliland FD. DNA methylation in the arginase-nitric oxide synthase pathway is associated with exhaled nitric oxide in children with asthma. *Am J Respir Crit Care Med*. 2011;184(2):191–7.
98. Breton CV, Vora H, Salam MT, Islam T, Wenten M, Gauderman WJ, et al. Variation in the GST mu locus and tobacco smoke exposure as determinants of childhood lung function. *Am J Respir Crit Care Med*. 2009;179(7):601–7.
99. Ladd-Acosta C, Shu C, Lee BK, Gidaya N, Singer A, Schieve LA, et al. Presence of an epigenetic signature of prenatal cigarette smoke exposure in childhood. *Environ Res*. 2016;144:139–48.
100. Novakovic B, Ryan J, Pereira N, Boughton B, Craig JM, Saffery R. Postnatal stability, tissue, and time specific effects of AHRH methylation change in response to maternal smoking in pregnancy. *Epigenetics*. 2014;9(3):377–86.
101. Richmond RC, Simpkin AJ, Woodward G, Gaunt TR, Lyttleton O, McArdle WL, et al. Prenatal exposure to maternal smoking and offspring DNA methylation across the lifecourse: findings from the Avon longitudinal study of parents and children (ALSPAC). *Hum Mol Genet*. 2015;24(8):2201–17.
102. Bouwland-Both MJ, van Mil NH, Tolhoek CP, Stolk L, Eilers PH, Verbiest MM, et al. Prenatal parental tobacco smoking, gene specific DNA methylation, and newborns size: the Generation R study. *Clin Epigenetics*. 2015;7(1):83.
103. Morales E, Bustamante M, Vilahur N, Escarimís G, Montfort M, de Cid R, et al. DNA hypomethylation at ALOX12 is associated with persistent wheezing in childhood. *Am J Respir Crit Care Med*. 2012;185(9):937–43.
104. Chhabra D, Sharma S, Kho AT, Gaedigk R, Vyhldal CA, Leeder JS, et al. Fetal lung and placental methylation is associated with in utero nicotine exposure. *Epigenetics*. 2014;9(11):1473–84.
105. Liang P, Song F, Ghosh S, Morien E, Qin M, Mahmood S, et al. Genome-wide survey reveals dynamic widespread tissue-specific changes in DNA methylation during development. *BMC Genomics*. 2011;12(1):231.
106. Wu H, Romieu I, Shi M, Hancock DB, Li H, Sienna-Monge J-J, et al. Evaluation of candidate genes in a genome-wide association study of childhood asthma in Mexicans. *J Allergy Clin Immunol*. 2010;125(2):321–7.e13.
107. Joubert BR, Häberg SE, Nilsen RM, Wang X, Vollet SE, Murphy SK, et al. 450K epigenome-wide scan identifies differential DNA methylation in newborns related to maternal smoking during pregnancy. *Environ Health Perspect*. 2012;120(10):1425.
108. Monick MM, Besch SR, Plume J, Sears R, Gerrard M, Brody GH, et al. Coordinated changes in AHRH methylation in lymphoblasts and pulmonary macrophages from smokers. *Am J Med Genet B Neuropsychiatr Genet*. 2012;159(2):141–51.
109. Meyer KF, Krauss-Etschmann S, Koostra W, Reindens-Luinge M, Timens W, Kobzik L, et al. Prenatal exposure to tobacco smoke sex dependently influences methylation and mRNA levels of the Igf axis in lungs of mouse offspring. *Am J Phys Lung Cell Mol Phys*. 2017;312(4):L542–L55.
110. Murphy SK, Adigun A, Huang Z, Overcash F, Wang F, Jirtle RL, et al. Gender-specific methylation differences in relation to prenatal exposure to cigarette smoke. *Gene*. 2012;494(1):36–43.
111. Meyer KF, Verlaak-Schakel RN, Timens W, Kobzik L, Plosch T, Hylkema MN. The fetal programming effect of prenatal smoking on Igf1r and Igf1 methylation is organ- and sex-specific. *Epigenetics*. 2017;12(12):1076–91.
112. Noël A, Xiao R, Perveen Z, Zaman H, Le Donne V, Penn A. Sex-specific lung functional changes in adult mice exposed only to second-hand smoke in utero. *Respir Res*. 2017;18(1):104.
113. Mejia C, Lewis J, Jordan C, Mejia J, Ogden C, Monson T, et al. Decreased activation of placental mTOR family members is associated with the induction of intrauterine growth restriction by secondhand smoke in the mouse. *Cell Tissue Res*. 2017;367(2):387–95.
114. Christensen S, Jaffar Z, Cole E, Porter V, Ferrini M, Postma B, et al. Prenatal environmental tobacco smoke exposure increases allergic asthma risk with methylation changes in mice. *Environ Mol Mutagen*. 2017;58(6):423–33.
115. Xiao R, Perveen Z, Rouse RL, Le Donne V, Paulsen DB, Ambalavanan N, et al. In utero exposure to second-hand smoke aggravates the response to ovalbumin in adult mice. *Am J Respir Cell Mol Biol*. 2013;49(6):1102–9.
116. Lee JW, Jaffar Z, Pinkerton KE, Porter V, Postma B, Ferrini M, et al. Alterations in DNA methylation and airway hyperreactivity in response to in utero exposure to environmental tobacco smoke. *Inhal Toxicol*. 2015;27(13):724–30.
117. Lu TX, Hartner J, Lim E-J, Fabry V, Mingler MK, Cole ET, et al. MicroRNA-21 limits in vivo immune response-mediated activation of the IL-12/IFN- $\gamma$  pathway, Th1 polarization, and the severity of delayed-type hypersensitivity. *J Immunol*. 2011;187(6):3362–73.
118. Xiao R, Noel A, Perveen Z, Penn AL. In utero exposure to second-hand smoke activates pro-asthmatic and oncogenic miRNAs in adult asthmatic mice. *Environ Mol Mutagen*. 2016;57(3):190–9.
119. Wagner NJ, Carerota M, Propper C. Prevalence and perceptions of electronic cigarette use during pregnancy. *Matern Child Health J*. 2017;21(8):1655–61.
120. Beauval N, Verrièle M, Garat A, Fronval I, Dusautoir R, Anthérieu S, et al. Influence of puffing conditions on the carbonyl composition of e-cigarette aerosols. *Int J Hyg Environ Health*. 2019;222(1):136–46.
121. Givalakí C, Tzatzarakis M, Kyriakos CN, Vardavas AJ, Stivaktakis PD, Kavalakis M, et al. Composition and chemical health hazards of the most common electronic cigarette liquids in nine European countries. *Inhal Toxicol*. 2018;30(9–10):361–9.
122. Schober W, Szendrei K, Matzen W, Osländer-Fuchs H, Heltmann D, Schettgen T, et al. Use of electronic cigarettes (e-cigarettes) impairs indoor air quality and increases FeNO levels of e-cigarette consumers. *Int J Hyg Environ Health*. 2014;217(6):628–37.



123. Moldoveanu SC, Yerabolu R. Critical evaluation of several techniques for the analysis of phthalates and terephthalates: application to liquids used in electronic cigarettes. *J Chromatogr A*. 2018;1540:77–86.
124. Oh J-A, Shin H-S. Identification and quantification of several contaminated compounds in replacement liquids of electronic cigarettes by gas chromatography-mass spectrometry. *J Chromatogr Sci*. 2014;53(6):841–8.
125. Moon K, Lee P, Kim B, Park M, Jang A. Claudin 5 transcripts following acrolein exposure affected by epigenetic enzyme. *J Clin Toxicol*. 2015;5(268):2161–0495.1000268.
126. Jahreis S, Trump S, Bauer M, Bauer T, Thurnmann L, Feltens R, et al. Maternal phthalate exposure promotes allergic airway inflammation over 2 generations through epigenetic modifications. *J Allergy Clin Immunol*. 2018;141(2):741–53.
127. Sussan TE, Gajghate S, Thimmulappa RK, Ma J, Kim J-H, Sudini K, et al. Exposure to electronic cigarettes impairs pulmonary anti-bacterial and antiviral defenses in a mouse model. *PLoS One*. 2015;10(2):e0116861.
128. McGrath-Morrow SA, Hayashi M, Ahemera A, Lopez A, Malinina A, Collaco JM, et al. The effects of electronic cigarette emissions on systemic cotinine levels, weight and postnatal lung growth in neonatal mice. *PLoS One*. 2015;10(2):e0118344.
129. Nguyen T, Li GE, Chen H, Cranfield CG, McGrath KC, Gorrie CA. Maternal E-cigarette exposure results in cognitive and epigenetic alterations in offspring in a mouse model. *Chem Res Toxicol*. 2018;31(7):601–11.
130. Chen H, Li G, Chan YL, Chapman DG, Sukjammong S, Nguyen T, et al. Maternal E-cigarette exposure in mice alters DNA methylation and lung cytokine expression in offspring. *Am J Respir Cell Mol Biol*. 2018;58(3):366–77.
131. McAuley TR, Hopke P, Zhao J, Balaian S. Comparison of the effects of e-cigarette vapor and cigarette smoke on indoor air quality. *Inhal Toxicol*. 2012;24(12):850–7.
132. Balbè M, Martínez-Sánchez JM, Sureda X, Fu M, Pérez-Ortuño R, Pascual JA, et al. Cigarettes vs e-cigarettes: passive exposure at home measured by means of airborne marker and biomarkers. *Environ Res*. 2014;135:76–80.
133. Burton A. Does the smoke ever really clear? Thirdhand smoke exposure raises new concerns. *Environ Health Perspect*. 2011;119(2):A70.
134. Hecht SS. Tobacco smoke carcinogens and lung cancer. *J Natl Cancer Inst*. 1999;91(14):1194–210.
135. Bartsch H, Montesano R. Relevance of nitrosamines to human cancer. *Carcinogenesis*. 1984;5(11):1381–93.
136. Xue J, Yang S, Seng S. Mechanisms of cancer induction by tobacco-specific NNK and NNN. *Cancers*. 2014;6(2):1138–56.
137. McEvoy CT, Spindel ER. Pulmonary effects of maternal smoking on the fetus and child: effects on lung development, respiratory morbidities, and life long lung health. *Paediatr Respir Rev*. 2017;21:27–33.
138. Sandberg KL, Pinkerton KE, Poole SD, Minton PA, Sundell HW. Fetal nicotine exposure increases airway responsiveness and alters airway wall composition in young lambs. *Respir Physiol Neurobiol*. 2011;176(1–2):57–67.
139. Sekhon H, Proskocil B, Clark J, Spindel E. Prenatal nicotine exposure increases connective tissue expression in foetal monkey pulmonary vessels. *Eur Respir J*. 2004;23(6):906–15.
140. Wongtrakool C, Wang N, Hyde DM, Roman J, Spindel ER. Prenatal nicotine exposure alters lung function and airway geometry through  $\alpha 7$  nicotinic receptors. *Am J Respir Cell Mol Biol*. 2012;46(5):695–702.
141. Maritz GS, Muterwa M. The effect of grand maternal nicotine exposure during gestation and lactation on lung integrity of the F2 generation. *Pediatr Pulmonol*. 2014;49(1):67–75.
142. Rehan VK, Liu J, Sakurai R, Torday JS. Perinatal nicotine-induced transgenerational asthma. *Am J Phys Lung Cell Mol Phys*. 2013;305(7):L501–L7.
143. Rehan VK, Torday JS. PPARgamma signaling mediates the evolution, development, homeostasis, and repair of the lung. *PPAR Res*. 2012;2012:289867.
144. Rehan VK, Liu J, Naeem E, Tian J, Sakurai R, Kwong K, et al. Perinatal nicotine exposure induces asthma in second generation offspring. *BMC Med*. 2012;10(1):129.
145. Liu J, Sakurai R, O'Roark EM, Kenyon NJ, Torday JS, Rehan VK. PPARgamma agonist rosiglitazone prevents perinatal nicotine exposure-induced asthma in rat offspring. *Am J Physiol Lung Cell Mol Physiol*. 2011;300(5):L710–7.
146. Lathan SE, Kirchgessner A. Anti-inflammatory effects of nicotine in obesity and ulcerative colitis. *J Transl Med*. 2011;9:129.
147. Wu C-J, Yang C-Y, Chen Y-H, Chen C-M, Chen L-C, Kuo M-L. The DNA methylation inhibitor 5-azacytidine increases regulatory T cells and alleviates airway inflammation in ovalbumin-sensitized mice. *Int Arch Allergy Immunol*. 2013;160(4):356–64.
148. Choi JH, Oh SW, Kang MS, Kwon H, Oh GT, Kim DY. Trichostatin A attenuates airway inflammation in mouse asthma model. *Clin Exp Allergy*. 2005;35(1):89–96.
149. Ichikawa T, Hayashi R, Suzuki K, Imanishi S, Kambara K, Okazawa S, et al. Sirtuin 1 activator SRT1720 suppresses inflammation in an ovalbumin-induced mouse model of asthma. *Respirology*. 2013;18(2):332–9.
150. Leus NG, Van Den Bosch T, Van Der Wouden PE, Krist K, Ouralidou ME, Eleftheriadis N, et al. HDAC1-3 inhibitor MS-275 enhances IL10 expression in RAW264. 7 macrophages and reduces cigarette smoke-induced airway inflammation in mice. *Sci Rep*. 2017;7:45047.
151. Perry MM, Durham AL, Austin PJ, Adcock IM, Chung KF. BET bromodomains regulate transforming growth factor- $\beta$ -induced proliferation and cytokine release in asthmatic airway smooth muscle. *J Biol Chem*. 2015;290(14):9111–21.
152. Wu D-D, Song J, Bartel S, Krauss-Etschmann S, Rots MG, Hylkema MN. The potential for targeted rewriting of epigenetic marks in COPD as a new therapeutic approach. *Pharmacol Ther*. 2018;182:1–14.
153. Song J, Hejlink I, Kistemaker L, Reinders-Luinge M, Kooistra W, Noordhoek J, et al. Aberrant DNA methylation and expression of SPDEF and FOXA2 in airway epithelium of patients with COPD. *Clin Epigenetics*. 2017;9(1):42.
154. Song J, Cano-Rodriguez D, Winkler M, Gjaltema RAF, Goubert D, Jurkowski TP, et al. Targeted epigenetic editing of SPDEF reduces mucus production in lung epithelial cells. *Am J Phys Lung Cell Mol Phys*. 2016;312(3):L334–L47.

Ready to submit your research? Choose BMC and benefit from:

- fast, convenient online submission
- thorough peer review by experienced researchers in your field
- rapid publication on acceptance
- support for research data, including large and complex data types
- gold Open Access which fosters wider collaboration and increased citations
- maximum visibility for your research: over 100M website views per year

At BMC, research is always in progress.

Learn more [biomedcentral.com/submissions](https://biomedcentral.com/submissions)



## Chapter 1 Introduction

Chronic obstructive pulmonary disease (COPD) is a disease wherein patients experience persistent shortness of breath (airflow limitation) that worsens over time (2). It is postulated that worsening airflow limitation in COPD patients is the result of a heightened inflammatory response to inhaled noxious particles in the airways (2), but it is also probable that novel inflammatory mechanisms are important (3). The World Health Organisation has reported COPD to be the third leading cause of death in the world (4). The disease affects at least 1 in 10 Australians over the age of 40 and is the only chronic disease with ongoing increasing mortality (5). The direct healthcare costs attributed to COPD was \$0.9 billion nationally in 2008 and this figure was projected to increase over time (6). Inevitable disease progression leads to disability, preventing the patient from joining the productive workforce, and ultimately death. When considering this loss of human capital and productivity, the economic cost of COPD was reported as \$8.8 billion in 2008 (6).

### 1.1 Epidemiology

In the developed world, cigarette smoking is the most common cause of COPD (2, 7) but other inhaled irritants such as occupational dusts, vapours, fumes and use of biomass fuels indoors are also important causes of COPD, especially in developing countries (2, 7-10). Gender skew in patients was initially towards males, with very few females being diagnosed with the disease. However, this is thought to have been a consequence of variance in exposure to the aforementioned irritants as women in the developed world traditionally did not smoke or perform tasks that would expose them to inhaled noxious particles in the past. This theory is supported by data that shows that COPD rates amongst women has now equated that of men

as it has become more socially acceptable for women to smoke as much as their male counterparts (2). Research carried out using a murine model of COPD found that female mice had higher levels of small airway remodelling and transforming growth factor (TGF)- $\beta$ 1 activation than their male counterparts, suggesting that females are more at risk of COPD when exposure to irritants is controlled for (11).

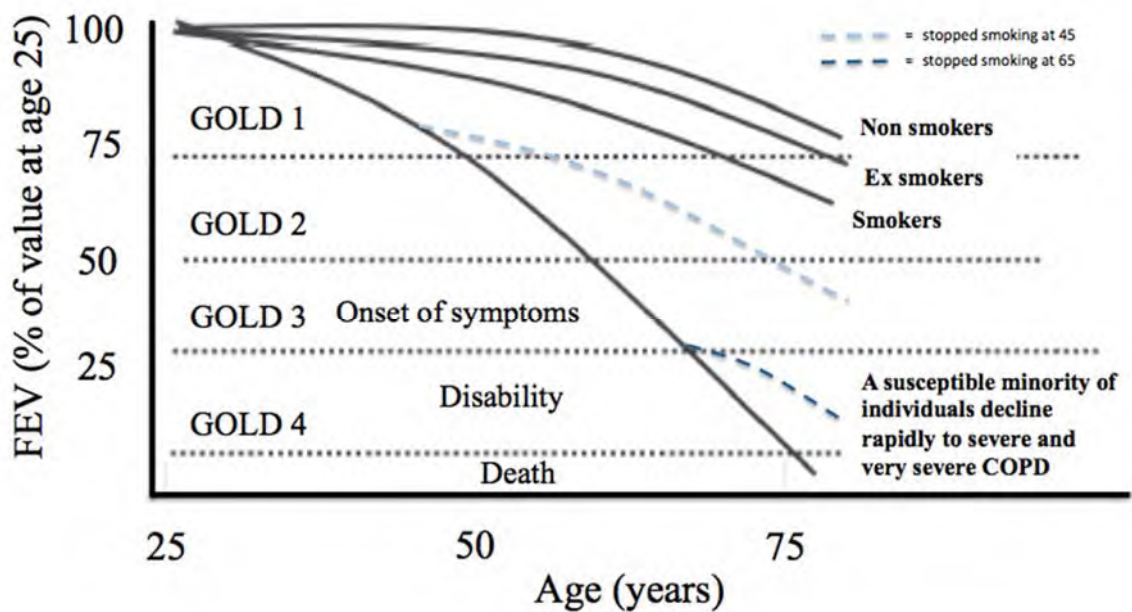


Figure 1.1 Rate of decline in FEV1 with age in non-smokers, ex-smokers, smokers, smoking COPD patients, smoking COPD patients quit at 45, smoking COPD patients quit at 65. Adapted from Fletcher & Peto (12).

In 1977, Fletcher and Peto (12) carried out a prospective epidemiological study of the early stages of development of COPD. The study followed 792 men (non-smokers, ex-smokers, non-COPD smokers, smokers with COPD) aged 30-59 over eight years. During the course of this time, the men attended biannual appointments wherein the following three parameters were assessed: mucus hypersecretion, bronchial infections, and airflow obstruction by measuring

forced expiratory volume in one second (FEV<sub>1</sub>). This was considered a landmark study for two primary reasons: firstly, the study revealed that there was a phenotype of smokers susceptible to rapid progressive lung functional decline (COPD), losing more than 50 mL of lung capacity per year compared to other smokers losing 20 mL per year. Secondly, the study demonstrated the effect of quitting smoking on slowing down the rapid decline in lung function during COPD progression. Further information that was derived from this study included the knowledge that smoking caused rapid and irreversible obstructive changes in COPD susceptible individuals. See Figure 1 for a graph adapted from aforementioned study.

## 1.2 Heritability

Studies have shown that family history of COPD is a risk factor for manifestation of the disease (13, 14). Similarly, siblings and first-degree relatives of asthmatics are often affected with lower FEV<sub>1</sub> (15, 16). Therefore suggesting a heritability factor in both asthma and COPD. The absence of a correlation between findings of a causative COPD or asthma single nucleotide polymorphism (SNP) in genome wide associations studies (GWAS) suggests that the hereditary effect is likely established at the epigenomic level rather than genomic and might have greater impact on gene expression in cells at the site of disease (17).

## 1.3 Symptoms

The progressive nature of COPD means that there is a grace period in which symptoms of airflow limitation are absent and only appear after substantial lung function decline has taken place (18). For most smokers this means that they have lost up to 50% of their lung function before noticing any aberrant effects (Fig. 1). Upon experiencing significant decline in lung

function, patients begin to suffer from the classic triad of COPD symptoms: dyspnoea, chronic cough and excessive sputum production (19, 20). These symptoms will progress over time as the hallmark of COPD, causing extreme distress and disability to the patient and subsequent death from respiratory failure (12). Symptoms may worsen during exercise as a result of increased respiratory demands (2). This chronic disease is punctuated by acute periods of intense symptoms known as exacerbations. Patients may also suffer from non-specific respiratory symptoms such as wheezing and chest tightness as well as non-respiratory symptoms such as weight loss, nutritional abnormalities and skeletal muscle dysfunction. COPD is now considered by many to be a systemic disease.

#### 1.4 Diagnosis

Symptoms alone are not enough to confirm the diagnosis of COPD. However, if a patient exhibits symptoms and has a history of exposure to COPD risk factors, such as exposure to the aforementioned noxious particles, clinical diagnosis with use of spirometry should be considered. Spirometry is capable of measuring a number of parameters relating to how well the lungs work. Those most relevant to COPD are (i) the volume of air forcibly exhaled from the point of maximal capacity (FVC) and (ii) the volume of air exhaled during the first second of this manoeuvre ( $FEV_1$ ) (2). Simply put, the test is a measurement of the functional size of a person's lung and how fast air can travel through their airways, respectively. The two parameters, FVC and  $FEV_1$  are then used to calculate the  $FEV_1/FVC$  ratio, which is used as a diagnostic figure. A  $FEV_1/FVC$  ratio of  $<0.70$  combined with the aforementioned symptoms and risk factors results in a diagnosis of COPD. The accuracy of using these figures to diagnose the extent of airway obstruction has been verified by histological analysis suggesting that the extent of small airway destruction (a pathological feature of COPD) correlates with the decline

in FEV<sub>1</sub> and the FEV<sub>1</sub>/FVC ratio (21). Given that COPD is progressive, the Global Initiative for Chronic Obstructive Lung Disease (GOLD) has developed a classification of severity of airflow limitation in COPD by comparing the patient's post-bronchodilator FEV<sub>1</sub> with a predicted FEV<sub>1</sub> value adjusted by height, sex, and ethnicity. The classification ranges from GOLD 1 (mild) to GOLD 4 (very severe) COPD (Table 1). These categories are then combined with results from a questionnaire to assess symptoms – either the modified MRC dyspnea scale (mMRC) or the COPD Assessment Test (CAT) – and history of exacerbations in the ABCD assessment tool (table 1.2). The combined numerical and lettered grading represents severity of airflow limitation and symptom burden/exacerbation risk, respectively (1).

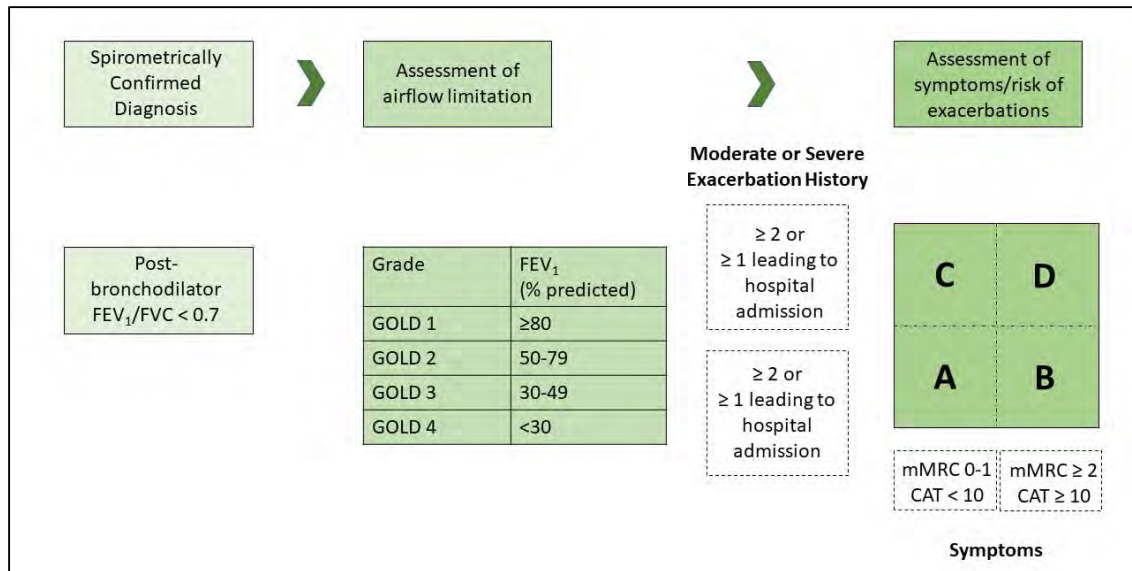
**Table 1.1 GOLD Categories 1-4.** Upon showing symptoms and obtaining an FEV<sub>1</sub>/FVC ratio of <0.70, patients' FEV<sub>1</sub> figures are calculated against predicted FEV<sub>1</sub> for gender, height, weight, and ethnicity. This percentage is used to class the patient into GOLD groups 1-4 as outlined (1).

<b>In patients with FEV<sub>1</sub>/FVC &lt; 0.70:</b>		
<b>GOLD 1:</b>	<b>Mild</b>	<b>FEV<sub>1</sub> ≥ 80% predicted</b>
<b>GOLD 2:</b>	<b>Moderate</b>	<b>50% ≤ FEV<sub>1</sub> &lt; 80% predicted</b>
<b>GOLD 3:</b>	<b>Severe</b>	<b>30% ≤ FEV<sub>1</sub> &lt; 50% predicted</b>
<b>GOLD 4:</b>	<b>Very Severe</b>	<b>FEV<sub>1</sub> &lt; 30% predicted</b>

Modern diagnostic methods, such as the forced oscillation technique (FOT), have been shown to have great clinical promise with much greater sensitivity to detect airway obstruction and the capacity to delineate between small airway obstruction and emphysema (22). However,

FOT currently lacks available robust reference values. Therefore, spirometry still currently remains the primary diagnostic tool to this date.

**Table 1.2 The Refined ABCD Assessment Tool.** Combined assessment tool considering spirometry results with symptoms and exacerbation history. Numerical grading (GOLD 1-4) is based on spirometry, whilst letter grade describes symptom burden and risk of exacerbation. Adapted from (1).



## 1.5 Pathophysiology

The symptoms experienced by COPD patients are attributed to three mechanisms:

- Emphysematous destruction of the alveoli
- Mucus hypersecretion; and
- Small airway (<2mm diameter) remodelling & destruction



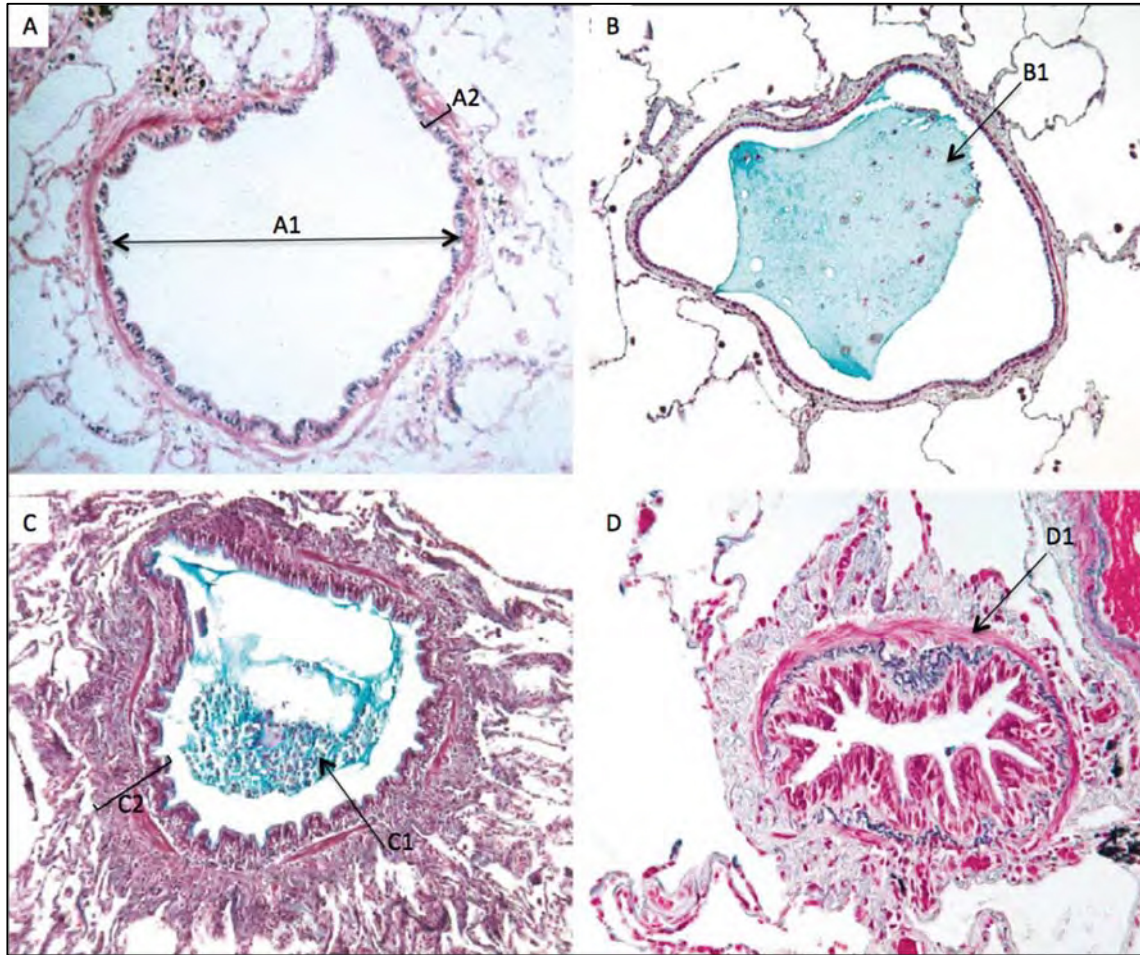


**Figure 1.2 Small airway obstruction.** A) Normal small airway with lumen (A1) and width of airway wall (A2) shown. B) Evidence of a mucus plug (B1) in small airway. Acutely inflamed airway with mucus plug containing immune cells (C1) and thickened airway wall (C2). D) Thickened small airway with evidence of fibrosis (D1). Adapted from (16).

In a healthy lung the alveoli are attached to the small airway walls, and interconnectivity helps to keep both the airways and alveoli open. Emphysematous destruction contributes to a loss of terminal support of small airways culminating in closure of the airway during expiration causing air to be trapped (23). Excess mucus produced in the airways (Fig. 2B and Fig. 2C) would further obstruct small airways by acting as a plug. Small airway remodelling is a term that is used to explain the thickening of the small airway walls (Fig. 2C) that occurs as a result of inflammation and structural changes (Fig. 2D) within the airway wall (23, 24). The structural



changes documented include increased thickness of smooth muscle layer and fibrosis of the basement membrane (24), therefore, resulting in a narrower airway.

In order to elucidate the progression of the aforementioned features of COPD, McDonough *et al* carried out a micro-CT study comparing a number of small airways from 78 patients with varying degrees of COPD (25). They found that small airway destruction and remodelling precedes emphysematous destruction. It has also been shown that the major site of obstruction in COPD is found in the smaller airways (26-28). Therefore, it is argued that small airway remodelling is fundamental to the pathophysiology of COPD and investigating its underlying mechanisms would reveal a therapeutic target that would mitigate the primary pathological insult in COPD.

#### 1.5.1 Small airway inflammation

Typically, the airways of COPD patients have been continuously exposed to noxious particles that trigger the patients' innate and adaptive immune responses (2, 24). The effect of cigarette smoking on these host defence mechanisms has been well studied. *In vivo* studies carried out in guinea pigs and humans have shown that cigarette smoke exposure can increase epithelial permeability in the airway (29-31), therein initiating an inflammatory response in the airway wall leading to the infiltration of polymorphonuclear cells, macrophages, natural killer cells and mast cells into the airway wall (24). This finding correlates with another study showing an increased number of macrophages in the airways, bronchoalveolar lavage (BAL) fluid, and sputum from COPD patients (32). Thus, the level of macrophage infiltration correlates with the disease severity (33). The interactions between cigarette smoke exposure and macrophage potency have been investigated. It has been found that the macrophages from smokers had an extended survival rate due to the release of an anti-apoptotic protein, Bcl-XL stimulated by

cigarette smoke (34). Cigarette smoke exposure can also induce a more activated form of macrophages, with a study showing that the alveolar macrophages from COPD patients secreted more inflammatory proteins and exhibited enhanced proteolytic activity in response to the stimulation by cigarette smoke (35).

The changes in eosinophil infiltration in the lungs of patients with COPD however are not as well understood. The analyses of bronchial biopsies and BAL fluid obtained from COPD patients experiencing acute exacerbations found elevated eosinophil levels (36). However, overall eosinophil levels tend to be much lower in COPD patients compared to those with asthma (32). Post-hoc analysis has shown that levels of eosinophilia may be able to predict which patients will respond to steroids, as patients with higher blood eosinophil counts were more likely to have their exacerbations controlled by inhaled corticosteroids (37). This is a new area in COPD research; therefore, the underlying molecular mechanisms remain to be elucidated. Interleukin-5 (IL-5) plays a significant role in the production and maintenance of eosinophils, therefore biologics targeting the IL-5 receptor subunit alpha (IL-5R $\alpha$ ) are a predominant area of interest. Examples of such biologics include Benralizumab and Mepolizumab, which have been investigated in phase 3 clinical trials (38, 39). Overall, although the biologics have been shown to reduce eosinophilia, their use has yet to be shown to contribute to functional outcomes such as reduced exacerbations (40), suggesting that COPD treatment options based on blood eosinophils remains to be accomplished.

Airway epithelial cells have been shown to work in concert with lymphoid tissue (41) and dendritic cells (DCs) (42) in order to propagate a powerful acquired immune response (43). Noxious particles either act as antigens on the airway epithelial surface that are transported across intact epithelia in specialised transport cells known as M cells, or penetrate the epithelia

at the site of injury (24). DCs are the primary antigen presentation cells in the acquired immune response, picking up antigen at the base of epithelium (42-44) and transporting them to the bronchial associated lymphatic tissue (BALT) (24). As a result, a robust inflammatory event in the walls of the conducting airways is initiated and sustained. The evidence shows that COPD patients expressed elevated total number of T lymphocytes (1), CD8<sup>+</sup> T lymphocytes, and inflammatory factors such as neutrophilic chemoattractant CXCL8, tumour necrosis factor (TNF)- $\alpha$ , and TGF- $\beta$ , IL-4 and IL-13 (24, 33, 45-50). Noxious particles have an oxidised nature and may contain LPS within them, allowing for direct activation of epithelia and other cells independent of antigen presentation (51).

Many different mediators of inflammation are increased in the lungs of patients with COPD, and it is beyond the scope of this literature review to discuss all factors. However, some cytokines and chemokines that are important in the pathogenesis of COPD and targets for the pharmaceutical industry are described below.

Neutrophils are consistently elevated in COPD, and their recruitment to the airway is principally through the chemokine, CXCL8. CXCL8 is secreted by macrophages, neutrophils, airway smooth muscle cells, fibroblasts, and airway epithelial cells (32, 52, 53). This chemokine signals through two receptors: CXCR1 and CXCR2. The former is associated with neutrophil chemotaxis and degranulation which is specific to CXCL8. The latter can be activated by the other CXC chemokines, such as GRO- $\alpha$  and ENA-78 (32).

TNF- $\alpha$  is a major pro-inflammatory cytokine elevated in patients with COPD. TNF- $\alpha$  activates nuclear transcription factor kappa B (NF- $\kappa$ B), which in turn, increases the transcription of the genes for cytokine production, such as CXCL8 and IL-6, and proteases in macrophages and

epithelial cells (32). Furthermore, the activation of NF- $\kappa$ B promotes cachexia, which is a common feature of patients with severe COPD (54). Supporting this, a study found that serum TNF- $\alpha$  concentration and TNF- $\alpha$  production from stimulated peripheral blood monocytes was significantly higher in COPD patients experiencing characteristic weight loss (55).

TGF- $\beta$  plays several roles in the immune response. This cytokine promotes isotype switching in B cells (56), suppresses the immune system and induces the production of extracellular matrix (ECM) components (57). The characterised TGF- $\beta$  isoforms include: TGF- $\beta$ 1, TGF- $\beta$ 2, and TGF- $\beta$ 3 (58), all of which are expressed in the lung (59). Of these, TGF- $\beta$ 1 is the most well understood overall and in the context of lung diseases. Many cells within the lung have been shown to express TGF- $\beta$ 1, such as fibroblasts, endothelial, epithelial, ASM, and immune cells (58). Post-intracellular synthesis, TGF- $\beta$ 1 is secreted into and stored in a latent state in the ECM (60, 61).

Other inflammatory mediators have been associated with COPD, such as the cytokine thymic stromal lymphopoietin (TSLP) which has been linked to the development of COPD (62) and shown to be elevated in COPD epithelial cells (63). It is understood that TSLP contributes to atopic asthma by stimulating type 2 immune cells but its mechanism in COPD pathogenesis remains to be understood (64).

### 1.5.2 Structural changes in small airways

#### Thickening of airway smooth muscle (ASM) layer

Smooth muscle layer thickening, as shown in Figure 1C, is a characteristic feature of obstructive airway diseases, including asthma and COPD (21, 24). However, what sets the two

diseases apart is the manner by which the ASM layer expands. In asthma, it has been shown that the means by which ASM thickens is hypertrophy and hyperplasia (65, 66). Whereas in the case of COPD, recent findings have demonstrated that FEV<sub>1</sub> directly correlates with increased ECM production by airway smooth muscle cells, rather than hypertrophy or hyperplasia (67). An *in vitro* study using primary human ASM cells found that there is significantly higher collagen VIII $\alpha$ 1 deposition in the cells from patients with COPD in comparison with the cells from non-COPD patients when treated with cigarette smoke extract (CSE) (68). Appropriately, we surmise that excess ECM production from ASM cells in response to cigarette smoke exposure is a central feature of COPD pathophysiology.

#### Extracellular matrix (ECM) deposition

The ECM provides the necessary structure for adequate function of the airway, it is a heterogeneous mix of proteins and within the lung the primary components are collagen, elastic fibres, fibronectin, and perlecan (69). Pathogenesis occurs when excessive ECM deposition occurs, resulting in tissue fibrosis. Excess ECM is evident in COPD (24, 70) where 50-85% of the total wall composition is comprised of ECM proteins. Excess ECM deposition within the airway wall is a rigid barrier to efficient air conduction as it envelops the lumen, decreasing its size and contributing to poor bronchodilator responsiveness (24).

In addition to causing structural changes in the airway, the ECM molecules are also bioactive. An *in vitro* study using primary human parenchymal fibroblasts showed that cells from COPD patients produced fibronectin and perlecan in response to CSE, whilst those from non-COPD patients did not, and that this ECM then had pro-proliferative effects on the cells. Similar effects have also been found in human asthmatic and bovine tracheal smooth muscle cells (71,

72). It has been shown that the pro-proliferative signals in human ASM cells occur via the integrin family of transmembrane receptors (73) and are enhanced with cell contact to the substrata ECM components, such as fibronectin and collagen (74, 75). In addition, the ECM components fibronectin and perlecan augment cytokine production from human ASM cells (76). A study using mink lung epithelial cells found that ECM can modulate fibrotic signals by sequestering growth factors, such as the pro-fibrotic cytokine TGF- $\beta$ 1 (77). It is further understood that the c-terminal fragment of collagens can become cleaved and have their own bioactive properties, therein acting as 'matrikines' that further propagate fibrosis and inflammation (78-80). We assert that the production of ECM in COPD triggers a positive feedback loop that promotes proliferation of cells and subsequent further deposition of ECM from these cells, therein explaining the aetiology of rapid decline in lung function in patients with COPD.

Structural airway cells of COPD patients respond to cigarette smoke differently compared to cells of non-COPD smokers *in vitro* (3, 68) and it is known that some smokers develop COPD whilst majority do not (12). These points have us posit that there is an intrinsic and specific difference in airway cells in COPD. Further, keeping in mind that there is a hereditary association in COPD and in light of research demonstrating cigarette smokers having unique epigenetic profiles (81, 82), we further posit that the underlying molecular mechanism in COPD can be attributed to epigenetic marks unique to COPD pathogenesis.

### 1.5.3 TGF- $\beta$ Signalling

There are two classes of transmembrane extracellular receptors for active TGF- $\beta$ 1 ligand and they are known as the type I and type II TGF- $\beta$  receptors (58). Investigations have identified

that there are seven type I receptors and five type II receptors (61). See table 1.2 for a list of these receptors and their respective encoding genes. TGF- $\beta$ 1 binds to the type II receptor, which heterodimerizes with type I receptor through phosphorylation (83). TGF- $\beta$ 1 receptor binding initiates subsequent recruitment of TGF- $\beta$  specific intracellular signal mediators, known as SMADs, to propagate the signal cascade (84, 85). There are eight known SMAD proteins (SMAD 1-8), the majority of which propagate the signal with the exception of SMADs 6 & 7 which are known as inhibitory SMADs (86). SMADs have been shown to be phosphorylated by kinases outside of the SMAD pathway such as MAPKs, glycogen synthase kinase-3 $\beta$  (GSK-3 $\beta$ ) (87), and cyclin dependant kinases (CDKs) (88).

**Table 1.1.3 List of known TGF- $\beta$  receptors and their respective encoding gene Source:(61).**

<b>Receptor</b>	<b>Encoding Gene</b>
<i>Type I receptors</i>	
ALK7	<i>ACVR1C</i>
ALK5	<i>TGFBR1</i>
ALK4	<i>ACVR1B</i>
ALK6	<i>BMPR1B</i>
ALK3	<i>BMPR1A</i>
ALK1	<i>ACVRL1</i>
ALK2	<i>ACVR1</i>
<i>Type II receptors</i>	
TGF $\beta$ RII	<i>TGFBR2</i>
MISRII	<i>AMHR2</i>
BMPRII	<i>BMPR2</i>
ACTRII	<i>ACVR2</i>
ACTRIIB	<i>ACVR2B</i>

*In vitro* experiments wherein cells were treated with TGF- $\beta$  with subsequent washing out of the ligand demonstrated a sustained TGF- $\beta$  induced response demonstrating a “memory effect” of TGF- $\beta$  stimulation that was abrogated with pre-treatment of a pharmacological inhibitor (89). This sustained TGF- $\beta$  receptor activity is mediated via activated receptor internalization



through endocytosis (90, 91). It has been established that the TGF- $\beta$  receptors are constitutively internalized in response to – and independent of – receptor activation (92). Internalization is mediated by either clathrin-dependant mechanism, wherein receptors are endocytosed into EEA1-positive endosomes, or a caveolin-dependant lipid-raft pathway into a distinct endocytic compartment (61, 93, 94). It has been shown that EEA1-positive endosomes can anchor SMAD2 and SMAD3, allowing interaction with the activated receptor and therefore it is thought the clathrin-dependant pathway play a role in the “memory effect”. Conversely, it is thought that the caveolin dependant pathway promotes receptor degradation (95). However, this is likely to be an oversimplification as inhibition of the clathrin-dependant mechanism had a subordinate attenuating effect on TGF- $\beta$ 1 induced signalling compared to inhibiting caveolae-mediated endocytosis (96, 97).

Although these two pathways have commonly been described to be distinct, investigations using live cell fluorescent microscopy on HeLa cells have shown that clathrin-coated and caveolar vesicles are fused post-internalisation (98). Post-internalisation fusion forms a caveolin-1 and clathrin positive hybrid vesicle, suggesting there may be crosstalk between these two endocytic pathways. It was further shown that these hybrid vesicles were likely involved in TGF- $\beta$  receptor I degradation (98), indicating that a larger proportion of endocytosed receptors are degraded in the cytoplasm rather than recycled. Although it is established that TGF- $\beta$  receptor endocytic trafficking plays a role in mediating the TGF- $\beta$  ligand induced signal, the mechanisms underlying why activated receptors are shuttled towards one endocytic pathway over the other remains to be elucidated.

Studies have found that tissue-specific overexpression of TGF- $\beta$ 1 in transgenic mice results in fibrosis in several organs, including the lungs (99). The effect of TGF- $\beta$ 1 on airway

remodelling has been demonstrated by *in vivo* administration of TGF- $\beta$ 1 inducing increased ECM protein deposition within the airway wall (100). Whilst treatment with an anti-TGF- $\beta$  antibody significantly reduced bronchiolar ECM deposition in a murine model (100). Investigations have determined increased expression of TGF- $\beta$ 1 in the airway epithelium of smokers, and patients with chronic bronchitis or COPD (101-104). An *in vitro* study using primary human epithelial cells showed that TGF- $\beta$ 1 levels positively correlated with basal membrane thickness (104). TGF- $\beta$ 1 induced ECM production in human ASM cells has been shown to be induced by both the canonical pathway – mediated by SMAD proteins (84, 85, 105) – and non-canonical pathways that recruit  $\beta$ -catenin (106) and the wingless/integrase 1 ligand, WNT-5A (107). The existence of multiple known induction mechanisms demonstrates that this cytokine contributes to ECM production in the lung in a pleiotropic manner not yet entirely elucidated.

## 1.6 Epigenetics

Epigenetics as a term encompasses heritable changes related to genome function that are not changes to the genome sequence. Epigenetic changes either repress or promote gene expression. These changes may occur *de novo* or under influence of the environment (108). Epigenetic changes may occur directly to the DNA, such as in the case of DNA methylation, or as a post-translational modification (PTM) of the histones. Histone PTMs may take the form of methylation, acetylation, ubiquitination, and/or phosphorylation (109), some of which fall beyond the scope of this project. The primary focus of this project is on methylation of both DNA and histones and acetylation of histones. The field of epigenetics within COPD is not yet well understood, however research in asthma has been carried out. As a result, many examples available in the literature and provided in this review are from asthma studies.

## DNA methylation

DNA methylation occurs at complementary pairs of cytosine residues directly followed by guanine (CpG) in mammals (110). Dense CpG regions known as CpG islands were initially thought to be the primary site of DNA methylation, but some evidence of methylation outside of these areas has been shown (111). Although the effect of epigenetic marks might be cell and location specific, DNA methylation is commonly associated with gene repression (110). Methylation is carried out by various DNA methyltransferase genes (112) and the underlying molecular mechanisms have been studied with the aid of *in vivo* studies using gene knockout animals. *Dnmt1*<sup>-/-</sup> mice display a DNA hypomethylation phenotype (113). During replication, DNMT1 acts by converting hemi-methylated DNA into fully methylated DNA (114). DNA methylation was thought to be a permanent mark, however it has also been shown to be reversible (115).

Investigations into unique epigenetic patterns in lung pathologies have been carried out. Kwon and colleagues (116) carried out a study that found naïve CD4<sup>+</sup> T cells had methylated CpG regions in the promoter for IL-4, which initiates immunoglobulin isotype switching (117) and enhances cytokine secretion (118), suggesting that the transcription of IL-4 protein was repressed. Interestingly, after stimulation with the common allergen, house dust mite (HDM), T cells obtained from asthmatics became demethylated at the IL-4 promoter, whilst those from healthy controls did not. Microarray analysis of lung tissue showed that samples from patients with idiopathic pulmonary fibrosis (IPF) have unique CpG methylation patterns that differ from healthy control and carcinoma groups (119). Other studies have also directly linked six altered DNA methylation regions to the fibrotic pathogenesis of IPF (120, 121).

Investigations into the DNA methylation status of COPD patients have found numerous CpG methylation sites that are associated with both the presence and severity of COPD symptoms (111). A number of genes for ECM proteins were methylated in small airways of the patients with COPD (122). However, homogenised samples were used in those studies, thereby rendering the study unable to identify which cell type methylation occurred suggesting that further studies are necessary to elucidate cell specific methylation patterns.

The association between cigarette smoke exposure and DNA methylation has been investigated in an epigenome-wide study. It has been found that cigarette smoke exposure alters methylation patterns within the epigenome and; interestingly, the cessation of tobacco smoke allows restoration to the methylation profile to that of the non-smokers (82). A similar study using small airway epithelial cells found 1260 differentially methylated CpGs related to COPD (123). DNA methylation status at the promoter of *GATA4* measured in sputum samples has been associated with impaired lung function (124, 125) and health outcomes in COPD (124). However, a study using blood found that ex-smokers retained 10% of a smokers' epigenetic signature even after smoking cessation (81). This suggests that there may be a difference between the local and systemic effects of cigarette smoke which requires further investigation. Nevertheless, these findings do suggest that DNA methylation could be a causal factor in cigarette smoke induced COPD pathogenesis and the reason why quitting smoking slows down the rapid decline in lung function in patients with COPD.

## Histone modifications

Histones are structural proteins that act as ‘spools’ for DNA. Pairs of histone H2A, H2B, H3 and H4 form an octomeric complex known as the nucleosome (126, 127). Precisely 146kbp of DNA is wrapped around and stored around a nucleosome and held together by histone H1 (128). The histones can regulate transcription by either tightly coiling the DNA in an inaccessible “heterochromatin” state or loosely in a “euchromatin” state (129, 130). The heterochromatin state leads to gene repression as RNA polymerase II (RNA Pol II) and transcriptional activators are unable to access DNA to generate mRNA (131); whilst euchromatin encourages transcription by ensuring DNA is readily accessible to transcription factors and RNA Pol II (130). The transition between heterochromatin and euchromatin states is affected by PTMs (132), which can alter charge of the histones resulting in either repulsion or stronger attraction between histones and DNA (127, 133). PTMs are made to the N-terminal tail of the histone proteins by adding an acetyl or methyl group to lysine (132). Furthermore, PTMs can act as epitopes, by recruiting transcription factors and co-factors to the site of modification (134).

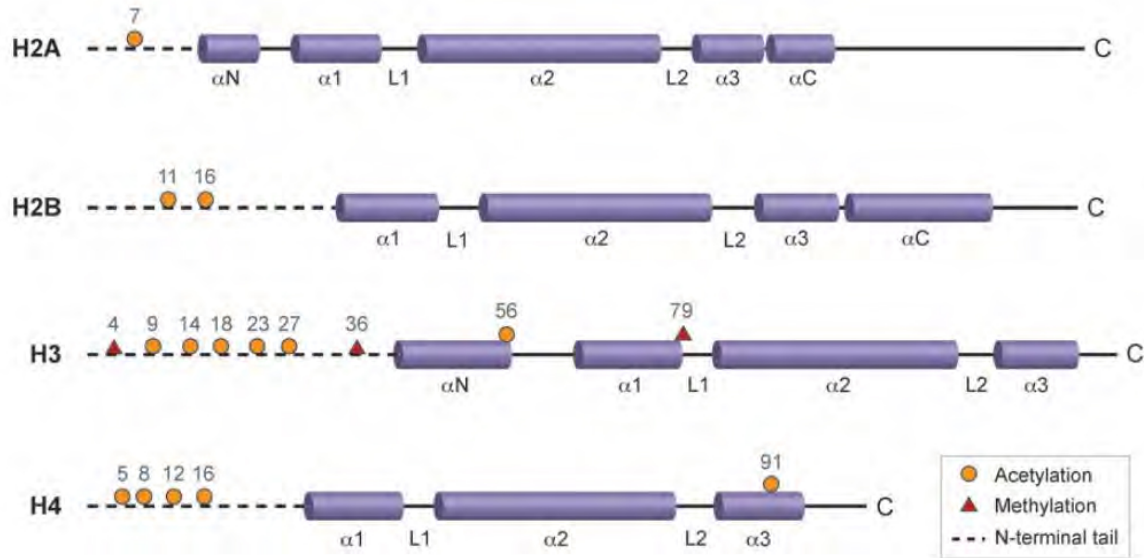


**Figure 1.3 Sites of epigenetic marks on histones H2A, H2B, H3, and H4 in yeast.** The N-terminal tails are denoted by the dashed lines where most of acetylation (orange circles) and methylation (red triangles) of histones occur (127)

### *Histone methylation*

Unlike DNA methylation, the expression pattern of methylated histones is not considered exclusively as gene silencing or promoting (135). Firstly, lysine residues on histone tails can be mono-, di-, or tri-methylated, with each status offering different functional outcomes (131, 135). Secondly, the expression of histone methylation patterns vary widely depending on the location of the amino acid residue targeted (131). Therefore, elucidating the effects of methylation on gene expression or repression via histone methylation is a challenge. Two contradictory histone modifications can be bound to the same promoter, leading to transcriptional pause at the promoter until the inhibitory mark is removed (136).

It has been shown that trimethylation of lysine 4 on histone 3 (H3K4me3) is linked to increased transcription of the IL-4 coding gene, IL-4 (137). Whilst dimethylation of the same histone

(H3K4me2) investigated in T cell studies has shown to influence asthmatic pathogenesis during T cell differentiation (138). These findings show that the number of methylations at the same lysine residue can have differing pathological outcomes, further adding to the complexity of epigenetic modifications.

Zhu and colleagues (139) have found that trimethylation of lysine 9 on histone 4 (H4K9me3) is associated with overall gene repression by preventing RNA polymerase II from binding to the promoter (131). Vascular endothelial growth factor (VEGF) is a key angiogenic molecule, which is overexpressed by asthmatic human ASM cells (140). Clifford and colleagues (140) showed that these cells had significantly lower levels of the H4K9me3 repression complex at the VEGF promoter. Whilst augmented mRNA expression of *DEFB1*, a gene associated with COPD (141), has been attributed to trimethylation of H3K4 (142). The examples of differential mediation demonstrate altered epigenetic regulation in an airway disease.

Chromatin immunoprecipitation (ChIP) analysis on trimethylation of lysine 27 on histone 3 (H3K27me3) has revealed the location dependent functional effects on gene transcription (143). It was found that H3K27me3 inhibits gene expression when modified residues are located within the body of the genes, whilst H3K27me3 located at the promoter ameliorates transcription. However, H3K27me3 modified residues at the transcriptional start site would lead to transcriptional pause (143). Current research has only just begun to uncover the specific effects of histone methylation patterns within airway diseases whilst much remains to be elucidated.

### *Histone acetylation*

The most frequently occurring PTM is the  $\epsilon$ -N-Acetylation of lysine residue (144). Histone acetyltransferases (HATs) transfer the acetyl moiety from acetyl co-enzyme A (127). The



addition of an acetyl moiety to the lysine residue neutralises the positive charge of the  $\epsilon$ -amino group (127, 130, 145). Consequently, the histone's electrostatic attraction to negatively charged DNA is attenuated and the euchromatin state is induced (127, 130). In contrast to HATs, histone deacetylases (HDACs) remove acetyl moieties from lysine residues (127, 130). HATs and HDACs are enzyme families working to control cellular acetylation levels (127). There are four classes of enzymes within the HDAC family – class I, class II, class III, and class IV. The primary identified roles of class I HDACs are to regulate innate immunity, while class IIa HDACs predominantly regulate adaptive immune functions (146).

**Table 2: The role of HDAC isoforms in regulating immunity (adapted from (146))**

Class	HDACs	Negative regulation	Positive regulation
I	HDAC1	TLR signalling Cytokine production T cell function	IFN signalling Cytokine production
	HDAC2	TLR signalling Cytokine production	IFN signalling Cytokine production
	HDAC3	TLR signalling Cytokine production	IFN signalling Cytokine production
IIa	HDAC4	--	T cell function
	HDAC7	T reg cell function	TLR signalling Cytokine production T cell function T cell development
	HDAC9	T reg cell development T reg cell function	T cell function
IIb	HDAC6	T reg cell function	IFN signalling Cytokine production Immune synapse formation

Enzymes from neither HAT nor the HDAC family (Table 2) work alone; rather, they are parts of large multiprotein complexes (127, 147). HDACs have been shown to be the catalytic site at the core of large multiprotein complexes (147). CoREST, NuRD, and Sin3 are some examples of these mega Dalton complexes that each form around an HDAC1 and HDAC2 dimer core (147).

HDAC is associated with repressing the production of pro-inflammatory cytokines in alveolar macrophages (148, 149). HDAC activity levels have been found to be significantly lower in immune cells and peripheral lung samples of patients with COPD when compared to normal controls (129, 150). There was no alteration in the level of HAT activity in COPD patients; however HAT activity was increased in specimens obtained from asthmatic patients (149, 150). HDAC2 expression in particular is attenuated in immune cell and peripheral lung samples obtained from COPD patients (23, 149), with smoking status being an attenuating factor (151). A study using alveolar macrophages showed reduced HDAC2 activity in cells from patients with COPD, with the reduction in HDAC2 corresponding with disease severity and resistance to corticosteroid therapy (152). The anti-inflammatory effects of corticosteroids are carried out via HDAC (148). Corticosteroids bind to the glucocorticoid receptor, which recruits HDAC to deacetylate histones, thereby silencing inflammatory genes (148). Therefore, the reduction of HDAC expression in immune cells from COPD patients can be associated with the corticosteroid insensitivity experienced in COPD. Further studies have shown that deletion of HDAC1 in T cells leads to enhanced airway inflammation (153) and broad spectrum HDAC inhibitors compromise host defence and exacerbate COPD (154).

Further to the already noted intricacies in epigenetic modifications, cross talk between modified residues is another area of complexity and interest. In the study of the fungus

*Neurospora crassa*, it has been shown that methylation of histone H3 at lysine 9 is fundamental in establishing DNA methylation (155). The aforementioned multiprotein complex, CoREST, has been shown to couple histone acetylation to demethylation (156), suggesting that these complexes have an important role in epigenetic cross talk. Cross talk has been studied with regard to the transcription factor modulating development and function of T-regulatory (T reg) cells, FOXP3 (157). Alterations in the methylation status of FOXP3 have been shown to affect T reg development and activity (157, 158). Methylation of the CpG island in the promoter region of FOXP3 leads to repression, whilst inhibiting methylation with knockdown of *Dmmt1* or using DNMT1 inhibitor, 5-azacytidine ameliorated expression of FOXP3, whilst stimulation with TGF- $\beta$ 1 produced the same effect (157, 158). However, in order to obtain a robust, long term expression of FOXP3 and T reg function, DNA methylation needs to be stabilised by changes in histone H3 acetylation and lysine 4 methylation (158). Providing a further example of epigenetic marks interacting to produce a coordinated functional outcome.

### Epigenetic readers

Epigenetic modifiers can be classed into three groups: writers (lay marks on DNA or histones e.g. DNMT1 or HAT), erasers (remove marks laid on DNA or histones e.g. HDAC) and readers (recognise epigenetic marks). The activities of writers and erasers have been described in prior sections; therefore, this section will focus on a reader class: bromodomain and extra-terminal domain (BET) proteins. BET proteins specifically recognise acetylated  $\epsilon$ -N-lysine motifs (159). BET proteins contain two hydrophobic cavities containing an H-bond linking to an asparagine residue (160); it is these sites that recognise acetylated lysine residues (160). The most well understood BET protein is Brd4 (161). Brd4 can bind to acetylated histones in the euchromatin state (161) as well as non-histone proteins such as NF- $\kappa$ B (162). Thus, BET

proteins are classically associated with the constitutive function of recruitment of transcription factors and RNA polymerase II to initiate gene transcription (163). However, research has shown that Brd4 may also act by directly targeting specific genes to maintain acetylation at their respective promoter regions, therein modulating gene expression in a specific and discretional manner (164-167).

The novel Brd4 inhibitor, JQ1, has been shown to reduce IL-1 $\beta$  induced inflammation in asthma (168), and TGF- $\beta$  induced cell proliferation and cytokine release from asthmatic human ASM cells (169). JQ1 works by competitively binding to Brd4, displacing acetylated lysine residues (170). A study has demonstrated that the release of TLSP by COPD fibroblasts can be attenuated with the use of JQ1, suggesting the existence of a unique epigenome that may be manipulated for therapeutic benefit (171). Further studies showing an altered ability of the BET mimic JQ1 to suppress specific cytokine gene expression in COPD BAL macrophages(172) underpins this position.

## 1.7 Hypothesis and aims

In summary, COPD is a disease characterised by persistent and rapidly declining lung function, of which the primary site of obstruction is shown to be in the small airways. In the developed world, cigarette smoking is the primary cause of the disease. However, not all smokers experience the rapid decline in lung function characteristic of COPD. In those smokers with COPD, cessation of smoking can drastically improve prognosis and slows down loss of lung function. It has been established that cigarette smoking leads to an altered epigenome and that stopping smoking reverts the epigenome to one more resembling that of a non-smoker. Furthermore, altered epigenetic expression is evident in COPD and other lung diseases, such

as asthma and idiopathic pulmonary fibrosis. Altering epigenetic writers, erasers or readers can lead to positive outcomes by reducing inflammation; however the epigenetic mechanisms underlying fibrosis during the development of COPD remain to be elucidated. Previous studies in my research group have found that primary human airway cells from COPD patients have augmented production of ECM in response to cigarette smoke extract (CSE) stimulation compared to the healthy controls (3, 68). Furthermore, recent findings have shown that excessive ECM production by human ASM cells has a more significant role in small airway remodelling in the development of obstructive airway disorders than previously thought (67). The aetiology of excessive ECM production in COPD is currently unknown.

Therefore, I hypothesise that ASM cells in the small airways in patients with COPD are epigenetically reprogrammed, allowing the excessive production of ECM proteins upon stimulation with known pro-fibrotic cytokine shown to be elevated in COPD, TGF- $\beta$ 1, leading to airway wall thickening.

The overall aim of the project is to determine why COPD cells show aberrant ECM production.

The specific aims are:

Aim 1: Determine differentially expressed ECM genes between human ASM cells of COPD and non-COPD smokers in response to TGF- $\beta$ 1 stimulation

Aim 2: Assess and contrast the potential role of modifications to histones or DNA in primary human ASM cells from COPD and non-COPD smokers

Aim 3: Confirm specific modifications at single ECM gene promoters using chromatin immunoprecipitation (ChIP) and/or methylated DNA immunoprecipitation (MeDIP)

## Chapter 2 Determination of Aberrantly Expressed ECM Genes in COPD

### 2.1 Introduction

It is well established that remodelling within the small airway walls contributes to airway obstruction in COPD patients (21). Research has shown that increased ECM deposition within the ASM layer in small airways positively correlates with a loss in lung function (67). *In vitro* research carried out within our group has demonstrated that airway mesenchymal cells from patients with COPD deposit more ECM proteins upon stimulation, when compared to those cells from smokers without obstructed airways (3, 68). Further, it is established that TGF- $\beta$ 1 is a potent inducer of ECM proteins, with increased expression in COPD (101-104).

This Chapter aims to investigate aberrant ECM production from primary human ASM cells induced by TGF- $\beta$ 1. In order to control for any aberrations induced by the donor's smoking behaviour, all cells were obtained from explanted tissue of patients with positive smoking history, with written formal consent. Selecting from donors with positive smoking history ensured that both cohorts were matched for smoke exposure. Further, we ensured to use primary human ASM cells from males and females to account for any epigenetic skew that may be attributable to gender. This Chapter contains the results pertaining to *in vitro* investigations using primary human ASM cells, and *in vivo* determination of localisation of ECM proteins in airways using immunohistochemical techniques. We posit that the ECM gene aberrantly expressed by human ASM cells in response to stimulation with TGF- $\beta$ 1 is a



contributing agent to small airway disease and subsequent manifestation of patient airway obstruction.

## 2.2 Methods

### 2.2.1 Ethics statement

The use of human tissue was approved by the Ethics Review Committee of St Vincent's Hospital Sydney and the University of Technology Sydney Human Research Ethics Committee (UTS HREC: ETH16-0507; St Vincent's Hospital HREC/15/SVH/351). Written informed consent has been obtained from all volunteers or next of kin.

### 2.2.2 Primary cell isolation

Airways were isolated from the lung and small airways (<2 mm) of patients undergoing lung transplantation or lung resection for thoracic malignancies, as previously described (68). Primary human ASM cells were grown in a T175 flask with Dulbecco modified eagle medium (DMEM, Thermo Fisher Scientific, Waltham MA, USA) enriched with 10% FBS, 1% antibiotic/anti-mycotic (Thermo Fisher Scientific, Waltham MA, USA), and buffered with 2.5% HEPES (Amresco, Solon OH USA). The cells were incubated at 37 °C/5% CO<sub>2</sub>. Cells were passaged at 80% confluence. Cells were first washed with Hanks salt solution (Sigma-Aldrich, Castle Hill, NSW) and incubated with 3ml Trypsin (0.05% w/v, Thermo Fisher Scientific, Waltham MA, USA) at 37°C/5% CO<sub>2</sub> for 3 min. Trypsin was inactivated with the addition of 9ml of growth medium, and the cells were centrifuged at 201 g for 5 min. Cells were resuspended in the growth medium and grown under required experimental conditions.

**Table 2.1 Patient information.** All tissue specimens were obtained with written formal consent from patients or next of kin. Experiment key: 1 = microarray analysis; 2 = qPCR of TGF-β1 induced ECM gene expression; 3 = HAT activity assay; 4 = HDAC activity assay; 5 = Epigenetic inhibition; 6 = ChIP-PCR experiments; 7 = JQ1 dose-response relationship with *COL15A1* and *TNC* mRNA.

Patient ID	Experiments used	Disease	Gender	Age	Sample type	FEV% pred	FVC% Pred	FEV1/FVC	Hospital	Meds	Smoking history
1	1, 2, 5, 6, 7	malignant neoplasm of upper lobe bronchus lung	F	71	Resection	86% (2.13L)	99% (2.19L)	96%	Strathfield private	Grisolvon, Temase, Locacortem, Vioform, Centrum, Fish Oil	5-6/day, 30 years, quit 2 months prior
2	1-7	emphysema	M	54	Tx	(0.56L)	(2.15L)	-	StV	-	Ex smoker, 50 pack years
3	3, 4, 6	COPD	F	62	Tx	-	-	-	StV	-	Current/Ex smoker
4	1-7	emphysema	F	44	Tx	23% (0.59L)	95% (2.9L)	20%	StV	-	15 pack years
5	3, 4, 6	malignant neoplasm of upper lobe bronchus lung	M	75	Resection	85% (2.15L)	79% (2.66L)	81%	Strathfield private	zocor, diabex xr, novasc, allopurino coversyl, serc, stemetil, gangfort 0.3/5	ex smoker, 20-30/day, quit 2002 (sample collected 2012)
6	1-7	Adenocarcinoma, NOS/metastatic, secondary and unspecified malignant neoplasm of intrathoracic lymph nodes	M	61	Resection	88% (3.15L)	90% (4.26L)	73.90%	RPA	telmesartan	30 pack years
7	1-7	NSSCa	M	66	Resection	pre-BD=3.44 (102%), post-BD=3.44 (102%)	pre-BD=4.79 (106%) post-BD=4.97 (110%)	FEV1/FVC pre=72 (97%), post= 69 (94%)		Other resp con: CAL	
8	3, 4, 6	COPD	F	52	Tx	-	-	-	StV	-	Current/Ex smoker
9	1-6	NSSCa	F	60	Resection	92% (2.24L)	94% (2.9L)	83%	Strathfield private	effexor 75mg, lipitor 20mg	ex smoker, quit 1/8/2010, sample collected 31/8/2010
10	1, 2, 5, 6, 7	Emphysema	F	56	Tx	0.51 (20%) 0.49 (20%) post	2.03 (69%), 2.14 (72%) post		StV	Prednisolone, Augmentin, Tiotropium bromide, aspirin, doxycycline, perindopril, Fluticasone - Salmeterol	Ex-smoker <10 yrs, 30 pack years
11	7	Adenocarcinoma	M	60	Resection	-	-	-	RPAH	-	Current/Ex smoker
12	6	emphysema	M	59	Tx	-	-	-	StV	-	Current/Ex smoker
13	2, 5, 7	COPD	F	60	Tx	-	-	-	StV	-	Current/Ex smoker
14	1, 2, 5	Emphysema	M	64	Tx	-	-	-	StV	-	Current/Ex smoker
15	1, 2, 5, 7	Emphysema + adenocarcinoma, COPD	M	70	Resection	66% (3.19L)	(4.32L)	-	RPA	-	ex-smoker, 20/day X 50 years, quit 3 weeks prior
16	1, 2, 5, 7	Emphysema	M	60	Tx	(0.34L)	(1.31L)	-	StV	-	60 pack years
17	2, 5, 7	Adenocarcinoma	F	64	Resection	2.4L	4.15L	-	RPA	-	ex-smoker, 50/day * 50 years = 100 pack years, stopped 6 weeks prior
18	1, 2, 5	NsCCa malignant neoplasm of upper lobe	F	65	resection	pre-BD=2.91 (94%) post-BD=2.98 (96%)	pre-BD=5.01 (126%) post-BD=5.24 (132%)	FEV1/FVC 3.11/3.98 = 76%PRED	RPA	candesartan 16mg daily oral, celebrex 200mg daily oral, durogesic 25mcg/hr q3rd day topical, alprazolam 1mg bd oral, omeprazole 20mg daily oral, dothiepin 75mg daily oral, pindolol 15mg daily oral, simvastatin 40mg nocte oral	yes current 40 pack years, 20/d 40yrs
19	2, 5, 7	Adenocarcinoma	M	70	resection	2.14	3.84		RPA		ex-smoker 100 pack years stopped 1 year prior

### 2.2.3 Study subjects

To identify aberrations specifically attributable to COPD, human ASM cells were obtained from bronchial airways of subjects with COPD or with no obstructive lung disease as determined by FEV<sub>1</sub> values. Patient information regarding sex, diagnosis, smoking history and lung function were obtained. Those subjects with diagnosis of asthma, infectious diseases, or interstitial lung disease were excluded. Considering that smoke exposure significantly alters the epigenome (81, 82), all subjects were smokers to normalise the effects of cigarette smoke on the epigenome of our non-COPD and COPD groups. Subjects were classified as follows according to severity of airflow limitation. Non-COPD susceptible: n = 8, FEV<sub>1</sub>/FVC >70% and FEV<sub>1</sub> % predicted >80%. 2). COPD: n = 11, FEV<sub>1</sub>/FVC < 70% and FEV<sub>1</sub> % predicted <80%. All studies were carried out with a targeted 1:1 gender balance, when possible. Table 2.1 contains full patient information.

### 2.2.4 Cell culture

Primary human ASM cells were seeded at a density of  $4.2 \times 10^4$  cells/mL into 6 well plates. Briefly, an 80% confluent T175 flask first washed with Hanks salt solution (Sigma-Aldrich, Castle Hill, NSW) and incubated with 3 mL Trypsin (0.05% w/v, Thermo Fisher Scientific, Waltham MA, USA) at 37°C/5% CO<sub>2</sub> for 3 minutes. Trypsin was inactivated with the addition of 9 ml of growth medium, and the cells were centrifuged at 201 g for 5 min. Cells were resuspended in the growth medium and an aliquot removed to be stained with Trypan Blue and loaded onto a hemocytometer for manual cell counting. Growth medium is added to cell suspension to obtain correct concentration of cells ( $4.2 \times 10^4$  cells/mL). 3 mL of cell suspension

was carefully added to each well of a 6 well plate and grown at 37°C/5% CO<sub>2</sub> for 72 hours or until reaching 80% confluency.

### 2.2.5 Cell stimulation

Upon reaching 80% confluency, cell cycle was arrested in DMEM buffered with 2.5% HEPES and supplemented with 0.1% Bovine Serum Albumin (BSA), and 1% antibiotic/antimycotic at 37°C /5% CO<sub>2</sub> for 24 hours. Quiescent medium was removed and cells were stimulated with recombinant human TGF-β1 (10ng/ml; R&D Systems, Noble Park North, VIC) in quiescent medium at 37°C/5% CO<sub>2</sub> for 48 hours as it was previously determined in our lab that this was the optimal time point for ECM mRNA expression in cells of this type (68).

### 2.2.6 mRNA sample collection

Upon treating cells as detailed in section 2.2.5, cell culture supernatant was carefully removed, and the cells were washed twice with ice cold sterile 1x PBS. To effectively lyse cells and stabilise mRNA, cell lysis buffer provided as part of the Isolate II Mini RNA Kit (BIO52073; Bioline, NSW Australia) was supplemented with β-mercaptoethanol (BME) (MB148; Sigma Aldrich, Germany) to a final concentration of 1% (v/v). 350 μL of the cell lysis buffer (BME 1% v/v) was added to each well. Cells were manually agitated with the use of a sterile scraper to aid lysis and ensure all cells were removed from well bottom. Resultant RNA lysate was stored at -20°C.

### 2.2.7 mRNA purification

mRNA lysates collected according to section 2.2.6 were defrosted on ice and purified using a commercial kit (Isolate II Mini RNA Kit; BIO52073) according to manufacturer's instructions. Briefly, samples were separated via centrifugation at 11,000 g for 1 min to allow for removal of cell fragments and protein contaminants. Nucleic acid binding conditions were adjusted with the addition of 350  $\mu$ L of 70% EtOH (made up in RNase-free diethylpyrocarbonate (DEPC) treated H<sub>2</sub>O). After briefly (2 sec) vortexing the sample + 70% EtOH to ensure adequate mixing of the solution, it was loaded onto a column containing a silica membrane filter to which nucleic acids bind and centrifuged (30 sec@11,000 g). To ensure only RNA remained, it was essential to carry out a DNA digest. Membrane desalting preceded DNA digestion, which was carried out using DNase I (provided with kit). Following the DNA digest, the column filter was washed over numerous steps with a series of wash buffers provided as part of the kit. Total mRNA was eluted in 60  $\mu$ L of RNase-free DEPC-treated H<sub>2</sub>O. UV-Vis Spectrophotometry was used to assess mRNA purity levels and concentration through use of a Nanodrop 2000 (Thermo Fisher Scientific, NSW, Australia).

### 2.2.8 Reverse Transcription

Complementary DNA (cDNA) to our RNA template purified in section 2.2.6 was synthesized using the SensiFAST cDNA Synthesis Kit (BIO-65053; Bioline, NSW, Australia) according to manufacturer's instructions. Each reaction had a minimum of 50 ng purified mRNA added to 4  $\mu$ L 5x TransAmp Buffer, 1  $\mu$ L reverse transcriptase, and n  $\mu$ L RNase-free DEPC-treated H<sub>2</sub>O to make up to 20  $\mu$ L total volume. An Eppendorf Mastercycler (Eppendorf, NSW, Australia) was used to run the PCR cycle as follows:

Primer annealing: 10 mins @ 25°C

cDNA synthesis: 15 mins @ 42°C

Inactivation: 5 mins @ 85°C

Synthesized cDNA was stored at -20° C until use in RT-qPCR.

### 2.2.9 Microarray analysis

Prior to our microarray analyses, cDNA as prepared in section 2.2.8 from basal and TGF- $\beta$ 1 treated cells was pooled into respective non-COPD (n=7) and COPD (n=7) groups to reduce the effects of biological variation. Microarray analysis was carried out with Taqman® Fast Array Plates targeting human ECM matrix & adhesion molecules (Life Technologies, Carlsbad, CA) cycled on a StepOnePlus Real-Time PCR System (Applied Biosystems, Branchburg, NJ). The array targeted 96 genes, four of which were housekeeping genes and the remaining two were ECM. See Appendix B for complete list of all genes on the microarray. Microarray findings were confirmed with quantitative PCR.

### 2.2.10 Reverse Transcriptase Quantitative PCR

cDNA was synthesised as described in section 2.2.8. A pre-developed, specific primer set for *COL15A1* Hs00266332\_m1, *COL5A1* Hs00609088\_m1, *ITGA1* Hs00235006\_m1, or *TNC* Hs01115665\_m1 with SensiFAST™ Probe Hi-ROX Master Mix (Bioline, Castle Hill, NSW), and the StepOnePlus Real-Time PCR System (Applied Biosystems, Branchburg, NJ) was used for real-time PCR (Applied Biosystems, Branchburg, NJ). A pre-developed TaqMan reagent human 18S rRNA (Cat. #4319413; Life Technologies) was included in each real-time RT-



qPCR reaction as an endogenous control. Data from the reactions were analyzed using StepOne Software, v 2.3 (Applied Biosystems, Branchburg, NJ).

#### 2.2.11 Immunohistochemistry

Airway identification and accumulation of col 15 $\alpha$ 1 and tenascin-C proteins was assessed in formalin fixed paraffin embedded sections using hematoxylin & eosin, col 15 $\alpha$ 1, and tenascin-C staining (n = 4-5). For hematoxylin and eosin staining, the slides were stained with Mayer's hematoxylin and eosin staining after hydration. Immunohistochemistry were performed according to manufacturer's instruction with Dako Envision+ System (K400311-2, Dako, USA). In brief, slides were first hydrated from xylene to water in gradually decreasing concentrations of ethanol, followed by phosphate buffered saline. Heat-induced epitope retrieval was applied by microwaving on 'high' in citric acid buffer (pH6.0) for 15 mins. The slides were then blocked with Dako peroxidase block (S202386-2, Dako, USA). The slides were then incubated with diluted primary antibodies for 1 hour (col 15 $\alpha$ 1 (1:500; Sigma-Aldrich, Castle Hill, NSW); tenascin-C (1:50; Sigma-Aldrich, Castle Hill, NSW)) in antibody diluent (K8006, Dako, USA). Negative controls were incubated with antibody diluent only (K8006, Dako, USA). The slides were then incubated with secondary antibody (K400311-2, EnVision+/HRP Rabbit, Dako, USA) for 40 min at RT, followed and then visualised using liquid DAB+ (K436811-2, Dako, USA) for 8 min. Sections were subsequently counterstained with hematoxylin and cover slipped. Imaging was conducted using a Hamamatsu NanoZoomer (40x) and stain intensity quantified using Fiji Image J.

### 2.2.12 Statistical analysis

The data were analysed for parametric distribution, with differences identified by either unpaired t-test or 2way ANOVA followed by Tukey post-hoc tests as specified. Data analysis was carried out using Graphpad Prism 8 software wherein a p-value  $< 0.05$  is considered significant.

## 2.3 Results

### 2.3.1 Microarray Analysis

As a screening step to target aberrant ECM genes attributable to COPD status, rather than smoking, we treated primary human ASM cells from our cohorts identified in section 2.2.1 with TGF- $\beta$ 1 (10ng/mL) for 48 hours. It is of import to note that TGF- $\beta$ 1 stimulation induced upregulation of all ECM genes in the COPD and non-COPD groups, and our primary objective was to determine which of those were aberrantly expressed in the COPD susceptible population. Microarray analyses results in Figure 2.1, expressed as TGF- $\beta$ 1 induced expression over basal expression, showed *COL15A1* and *COL5A1* expression upregulated in COPD. Whilst, other ECM genes *TNC* and *ITGA1* were shown to have augmented expression in non-COPD susceptible smokers.

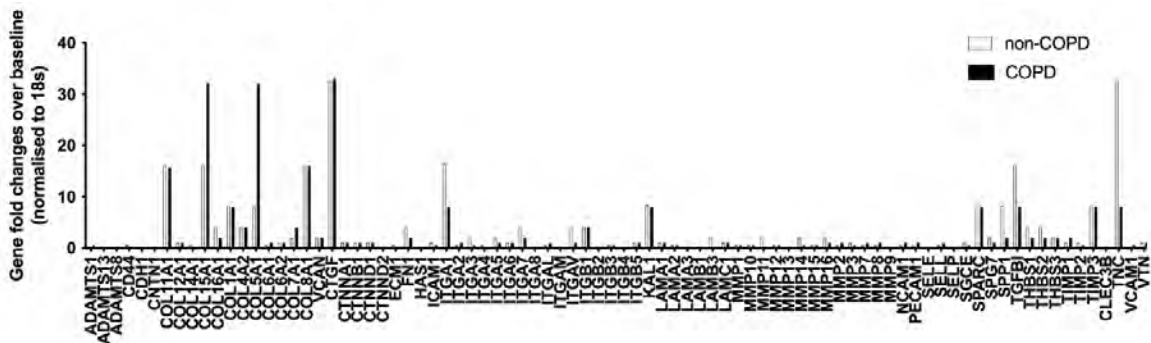


**Figure 2.1 Microarray analysis.** Primary human ASM cells from COPD (n=5) and non-COPD (n=6) susceptible smokers were cultured  $\pm$  TGF- $\beta$ 1 (10ng/ml) for 48 hours. mRNA lysates were collected, and cDNA was reverse transcribed using RT-PCR. Resultant cDNA from treated and non-treated groups was pooled and ran on a microarray targeting a panel of 92 ECM genes. Results are expressed as TGF- $\beta$ 1 induced fold change over baseline. *COL15A1* & *COL5A1* expression was higher in COPD, whilst *TNC* and *ITGA1* expression in non-COPD smokers was shown to be higher.

### 2.3.2 RT-qPCR Determination of Target Gene Expression

In section 2.3.1, four ECM gene targets were identified to be aberrantly expressed in COPD. As is the nature of microarrays (173), these results were based on pooled cDNA samples applied to numerous genes without technical replicates. Therefore, in order to grant prudent statistical power to our findings, we used RT-qPCR to quantitate the fold change in each individual patient cDNA sample in triplicate.

In doing so, we found that *COL15A1* expression was significantly ( $p=0.0155$ ;  $63.21\pm 15.19$ ) upregulated in COPD, as shown in the microarray analyses. The RT-qPCR results for *COL5A1* ( $p<0.9999$ ) and *ITGAI* ( $p=0.4555$ ) showed no significant difference between cohorts. Whilst, contrary to the microarray findings, *TNC* ( $p=0.0482$ ;  $13.65\pm 3.651$ ) expression was shown to be significantly upregulated in COPD.

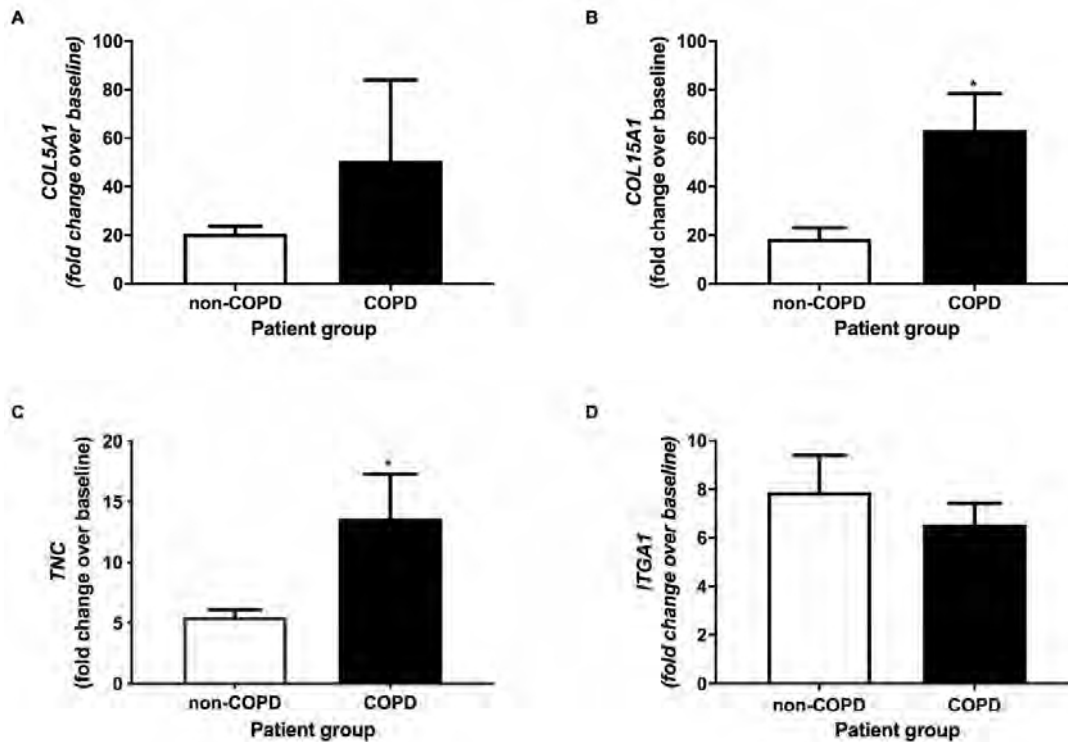


**Figure 2.2 RT-qPCR Validation of TGF- $\beta$ 1 induced ECM gene expression.** Primary human ASM cells from COPD (n=7) and non-COPD (n=7) smokers were stimulated  $\pm$  TGF- $\beta$ 1 (10ng/ml) for 48 hours. At which point mRNA lysates were collected, and cDNA was reverse transcribed using RT-PCR. Probe-based RT-qPCR was carried out on *COL5A1* (a), *COL15A1* (b), *TNC* (c), and *ITGA1* (d). Results were normalised to an endogenous gene (18s) and are expressed as TGF- $\beta$ 1 induced expression over basal expression. Data were analysed using unpaired t-test, (\*=p<0.05). *COL5A1* and *TNC* expression were found to be significantly upregulated in COPD. (mean  $\pm$  SEM)

### 2.3.3 Immunohistochemical Localisation & Quantification of Collagen 15 $\alpha$ 1 and Tenascin-C

The aberrantly expressed mRNA identified in section 2.3.2 includes *COL15A1* and *TNC*. These genes encode for collagen type 15 $\alpha$ 1 and tenascin-C, respectively. We have shown in sections 2.3.1 and 2.3.2 that *COL15A1* and *TNC* mRNA is expressed *in vitro*, and in this section, we aim to demonstrate that the proteins encoded by these genes are located amongst the ASM layer in human small airways *in vivo*. To do so we stained sections cut from paraffin embedded COPD-diagnosed human airways with anti-collagen 15 $\alpha$ 1 and anti-tenascin-C antibody.

Positive DAB staining within the concentric smooth muscle layer for collagen 15 $\alpha$ 1 (Fig. 2.3a) and tenascin-c (Fig. 2.3b) was noted, thereby confirming that these proteins are deposited in the small airways of COPD patients *in vivo*. It is of note that the deposition of collagen 15 $\alpha$ 1 was exclusively localised to the ASM layer.

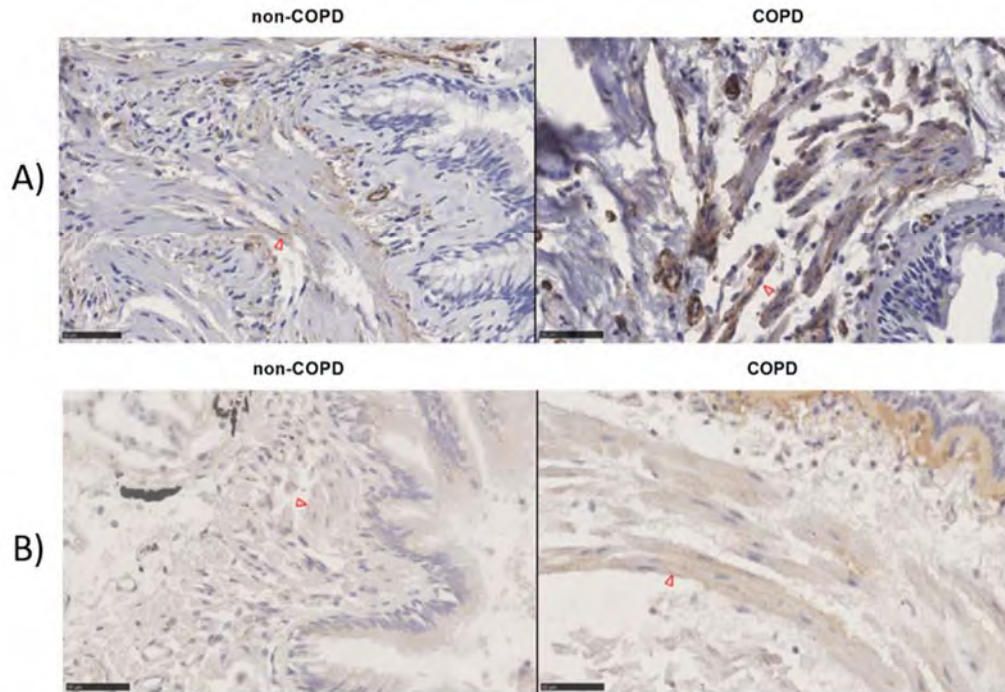


**Figure 2.3 Immunohistochemical Staining.** Paraffin embedded human lung tissue from a COPD and non-COPD patient containing small airways was sectioned and stained with (A) anti-collagen 15 $\alpha$ 1 antibody and (B) anti-tenascin-C antibody. Red  $\Delta$  denotes positive staining within the concentric airway smooth muscle layer surrounding the small airway; black bar = 50  $\mu$ m

Further, upon quantifying stain intensity within the ASM layer of COPD airways versus control samples, we found that collagen 15 $\alpha$ 1 deposition was significantly ( $p=0.0242$ ) higher in COPD airways ( $0.1969 \pm 0.05643$ ) compared to control ( $0.1022 \pm 0.02856$ ) (Fig 2.4a). Although the results for tenascin-C deposition were not statistically significant ( $p=0.1947$ ), we found that

there was a trend of increased deposition in COPD ( $0.1456 \pm 0.0490$ ) compared to control ( $0.1076 \pm 0.02100$ ) (Fig. 2.4b).

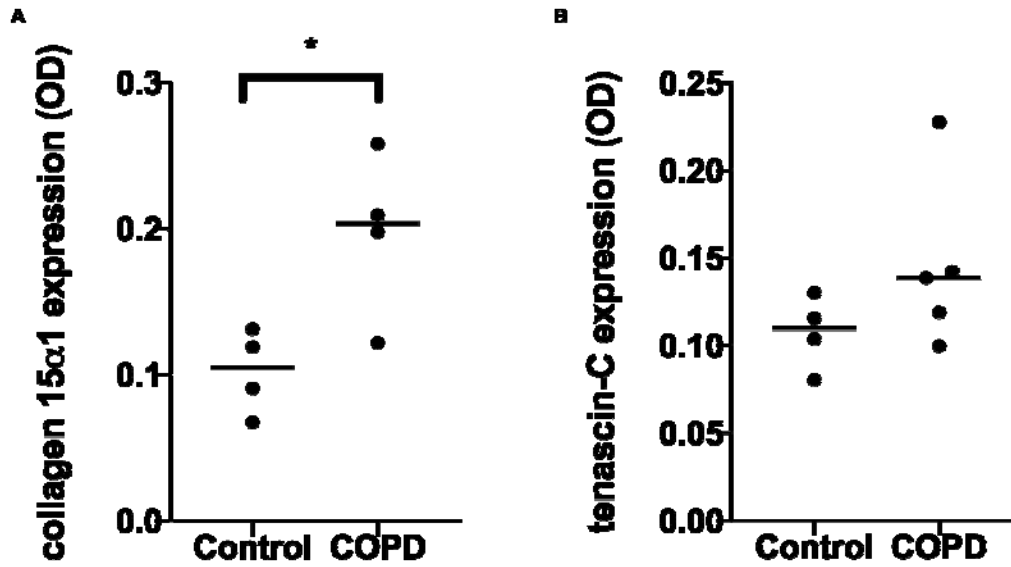


**Figure 2.4** Quantification of ECM protein deposition in ASM layer. Airway section from control and COPD patients were stained with (a) anti-collagen 15α1 and (b) anti-tenascin-C and quantified. Collagen 15α1 deposition is significantly higher in COPD airways (\*= $p < 0.05$ ; mean  $\pm$  SEM)

## 2.4 Discussion

The aim of this section was to take the first step in elucidating the mechanism underpinning the rapid decline in lung function experienced by COPD patients. As it is known that (i) increased ECM deposition within the airway smooth muscle layer is the primary contributing factor to fibrosis, and that (ii) the extent of fibrosis positively correlates with airway obstruction experienced by COPD patients, we focused our experiments on isolating those ECM genes that may be aberrantly expressed.

As expected, our microarray analyses showed an overall upregulation in each ECM gene upon stimulation with TGF- $\beta$ 1 (Fig. 2.1) in both groups. However, the genes for *COL15A1* and *COL5A1* were shown to be further upregulated in COPD. Whilst *TNC* and *ITGAI* mRNA was shown to be downregulated in COPD than in non-COPD susceptible smokers. Leading into our microarray analyses, we pooled cDNA from each cohort to identify the characteristics of each cohort whilst reducing the effects of biological variation. The latter of which is quite prevalent when using primary cells. Therefore, we took the information from these arrays into the next phase of experiments wherein we repeated our model of 48-hour TGF- $\beta$ 1 exposure with a higher n number and use of quantitative PCR to ensure the sound practice of biological and technical replicates is fulfilled.

Upon carrying out the aforementioned outlined in section 2.3.2, it was determined that *COL15A1* (Fig. 2.2b) expression was significantly upregulated in COPD susceptible smokers. Whilst *ITGAI* (Fig. 2.2d) and *COL5A1* (Fig. 2.2a) upregulation was not validated. Interestingly, the results for *TNC* (Fig. 2.2c) upon the addition of biological and technical replicates contradicted the microarray analyses and it was determined that *TNC* mRNA was



significantly upregulated in COPD susceptible smokers. It is of particular importance to note that these were not the *only* genes upregulated by TGF- $\beta$ 1 in COPD, but rather those that expressed significantly higher upregulation than human ASM of non-COPD smoking patients. In light of our findings showing that only two of the ninety-two ECM genes on the array showed significantly higher expression in COPD, we assert that the underlying mechanism is attributable to individual gene expression rather than TGF- $\beta$ 1 signalling.

In Figure 2.3 we demonstrate that the ECM proteins encoded by *COL15A1* and *TNC* are deposited within the concentric smooth muscle layer surrounding the small airway of a COPD patient. ECM localised to the ASM layer affirms that *in vitro* modelling using primary human ASM cells is the best course to investigate the molecular pathophysiology underlying small airway fibrosis in COPD. We further demonstrated in Figure 2.4a that there is a measured increase in amount of collagen 15 $\alpha$ 1 deposited within the ASM layer in COPD airways compared to those of non-COPD patients. Demonstrating that our *in vitro* findings translate to *in vivo* outcomes within the COPD airway. We note that tenascin-C deposition (Fig. 2.4b) followed a similar increased trend in COPD, however the results did not attain statistical significance due to low statistical power.

These findings are consistent with literature showing increased ECM mRNA expression and protein deposition from COPD smokers (3, 68, 174, 175) in response to stimuli. The most evident mechanism in which these findings underpin COPD pathophysiology would be the obstructive effect of increased ECM protein deposition within the airway wall, which would impose upon the lumen and physically impede conduction of air through the small airways.

Further, it is well understood that ECM proteins have inherent bioactive properties in addition to adding bulk to provide structural support. Tenascin-C is a glycoprotein that has been identified as a driver of fibrosis (176) with tenascin-C deficient mice demonstrating lower levels of fibrosis in models of acute lung injury (177). The ECM protein has also been shown to induce myofibroblast formation (178), increase cell migration (179), and ameliorate the production of other ECM proteins such as collagen from fibroblasts (178), demonstrating that tenascin-C plays an active role in sustained fibrosis.

Collagen XV $\alpha$ 1 has been detected in basement membranes, and smooth and striated muscle of numerous organ systems (180) but is one of the lesser understood collagens. Although increased levels of collagen XV $\alpha$ 1 have been noted in other fibrotic diseases (181), little is understood of its role in COPD or other pulmonary pathologies. It is known that the C-terminal fragment of collagens may become cleaved and act as signalling molecules known as matrikines (78-80). A matrikine comprised of amino acid residue sequence Proline-Glycine-Proline (PGP) has been described as a damage associated molecular pattern shown to exacerbate neutrophilic inflammation and induce protease imbalance in the lung (182, 183). PGP has been considered as a biomarker in COPD (184). Collagens are considered the primary source of PGPs as they are typically rich with PGP sequences; collagen XV  $\alpha$ 1 contains 15 PGP sequences, most of which are located near the C-terminus (Uniprot ID: p39059). The C-terminal fragment of collagen XV $\alpha$ 1 is known as restin. Like collagen XV $\alpha$ 1, restin is not yet well understood, but has been shown to inhibit migration of endothelial cell line, ECV 304, cells *in vitro* (185). High levels of restin has been detected in tumor cells of patients with in Hodgkin's lymphoma (186). The paucity of information regarding collagen XV $\alpha$ 1 and its bioactive potential highlights a need for further investigation into this protein, particularly in the context of fibrosis.

The findings described in this section are significant as they identify aberrant ECM genes unique to COPD patients, rather than smokers. Further, they do so in primary human cells from the site of pathological insult within the small airway wall. The method of ECM gene induction using TGF- $\beta$ 1 further bolsters this work as TGF- $\beta$ 1 is a known pro-fibrotic cytokine that has been shown to be elevated in COPD. Therein ensuring that using TGF- $\beta$ 1 is biologically relevant to real-world COPD outcomes, enabling us to effectively investigate the molecular mechanisms underlying increased small airway fibrosis in Chapters 3 & 4.

# Chapter 3 Investigations into Epigenetic Aberrations Underlying ECM Expression in COPD

## 3.1 Introduction

In Chapter 2, it was established that ECM genes *COL15A1* and *TNC* are significantly upregulated in COPD, compared to non-COPD susceptible smokers. In this Chapter, the aim is to screen for any epigenetic variances between the groups.

The epigenome comprises many different epigenetic marks, some of which are made directly onto the DNA, and others that bind to histones. The overall understanding is that the former directly blocks transcription factors from accessing transcriptional start sites (TSS) and promoter regions whilst the latter directly affects chromatin compaction to modulate promoter accessibility. Of those understood epigenetic mechanisms, we chose to focus on those most well understood and previously shown to be involved in numerous pathologies:

- DNA Methylation
- Histone Acetylation
- Histone Methylation

DNA methylation refers to the transfer of a methyl (CH<sub>3</sub>) group from universal methyl donor *S*-adenosyl-L-methionine (SAM) to the fifth carbon on cytosine, culminating in 5-methylcytosine (5mC). 5mC commonly occurs on CpG sites, which are typically clustered together in regions dense in guanine and cytosine, known as CpG islands. CpG islands are

often located within or close to TSS and promoter regions of many genes, including housekeeping and tissue-specific genes (187). When unmethylated, CpG islands play an active role in transcriptional initiation by destabilising the nucleosome and therefore promoting chromatin decompaction (188). Upon becoming densely methylated, CpGs become silenced and gene expression is subsequently repressed (188).

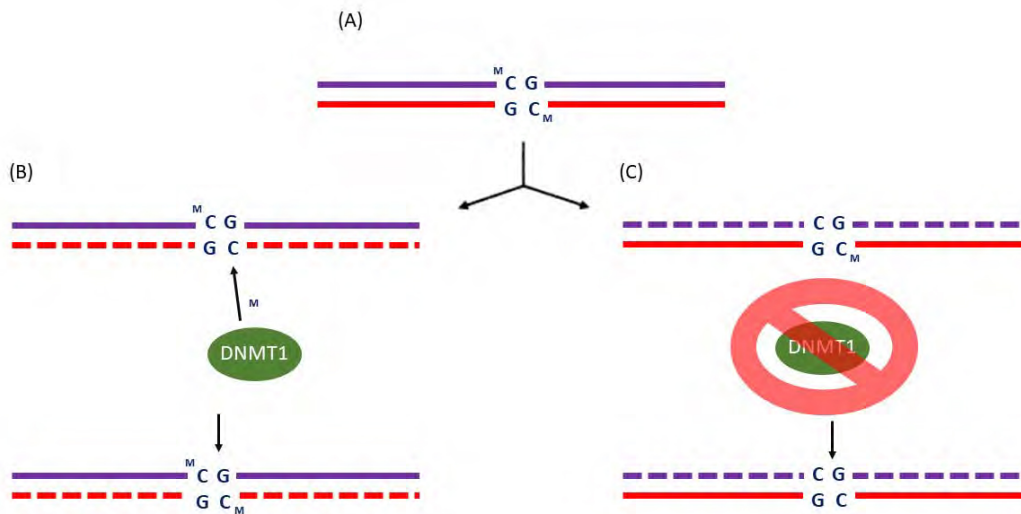


**Figure 3.1 Maintenance of DNA Methylation by DNA Methyltransferase 1 (DNMT1).** During mitosis, fully methylated DNA (A) undergoes replication. Post-replication, the template strand (solid line) carries on the inherent epigenetic mark whilst the complementary strand (dashed line) is unmethylated, resulting in hemi-methylated DNA. (B) DNMT1 transfers a methyl group from S-adenosyl-L-methionine (SAM) onto the complementary strand, resulting in a fully methylated daughter DNA strand. (C) Upon treatment with 5-azacytidine, DNMT1 is inhibited and the transient hemi-methylated mark is lost passively, resulting in a non-methylated daughter DNA strand.

Cytosine methylation is mediated by enzymes known as DNA Methyltransferases (DNMTs). Among mammals, DNMT1, DNMT3A, DNMT3B, and DNMT3L have been identified (189). All DNMTs are essential for human development, however DNMT1 plays the predominant role in maintaining methylation markers to induce mitotic heritability (190) (Fig. 3.1), whilst

DNMT3A and DNMT3B induce *de novo* methylation marks (189); with this in mind, the DNMTs are classed as either methylation maintenance molecules or *de novo* methylators. To investigate the evidence of a methylation mark contributing to COPD pathophysiology, we sought to inhibit the maintenance of established epigenetic marks in our study groups to reflect DNA methylation patterns acquired by the patients. To do so we used a well-established inhibitor of DNMT1, 5-azacytidine (191).

5-azacytidine – trading under brand name Vidaza – is an FDA approved drug for treatment of subtypes of myelodysplastic syndrome (192) and further approved for chronic myelomonocytic leukaemia, and acute myeloid leukaemia by the European Medicines Agency (EMA). Vidaza's mechanism of action is attributed to 5-azacytidine's DNMT1 inhibition, with use culminating in demethylated regions wherein methylation has contributed to pathology.

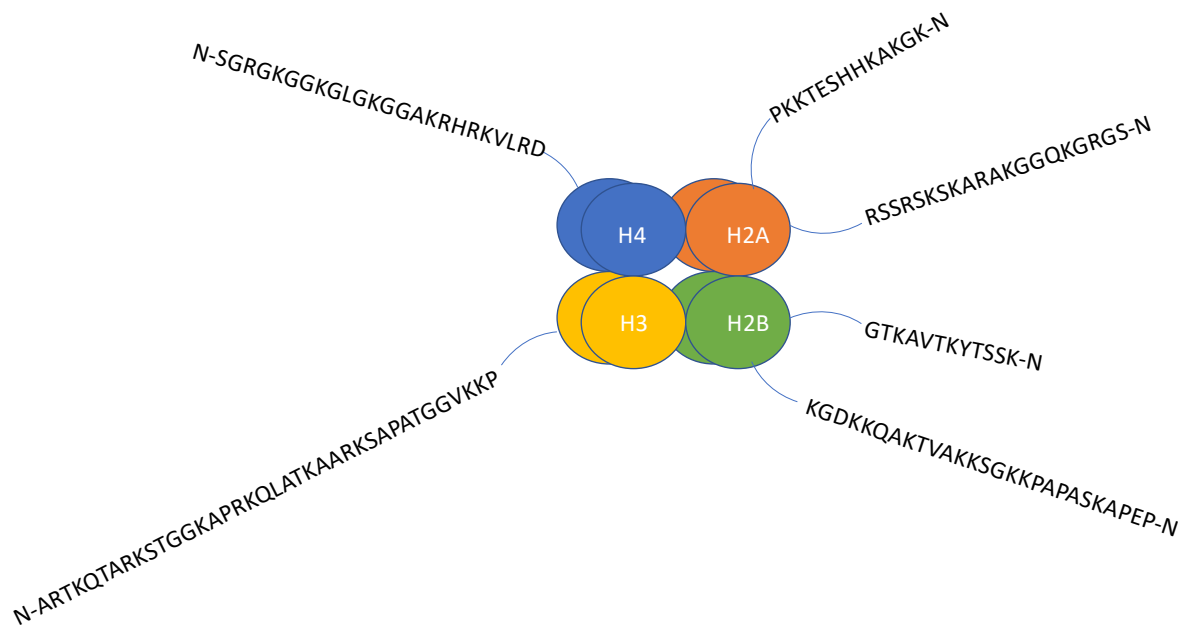


**Figure 3.2 Schematic representation of Histone Tails.** The octameric protein complex at the centre of a nucleosome is comprised of duplicates of histone H2A, H2B, H3, and H4. Each of these histones has an N-terminal tail (two in the case of histones H2A and H2B) comprised of amino acid residues. These residues are the sites of PTMs made to histones, with lysine (K) and arginine (R) understood to be the most commonly modified residues. Numerical allocation of residues begins at the N-terminus.

Histone acetylation is a post-translation modification which refers to the addition of an acetyl-moiety to the lysine residue on a histone tail. Core histones play a significant role in nucleosome stability, and their inherent positive charge contributes to this function. As DNA is negatively charged, it is attracted to the histone ‘spools’ thus 146 bps wind tightly around the histone octameric complex (comprised of histones H2A, H2B, H3, and H4) and are tethered by histone H1. This tightly wound nucleosomal complex is referred to as heterochromatin. Due to its tight coils, heterochromatin is less accessible to transcriptional mediators such as NF- $\kappa$ B and RNA Polymerase II. The acetyl moiety ( $C_2H_3O$ ), however, is negatively charged and consequently, histones with acetylated lysine residues have a less positive charge (193). Although DNA remains wound around acetylated histones, it is no longer tightly coiled; this

loosely bound state is known as euchromatin. Euchromatin is inherently more accessible to transcriptional mediators allowing for transcriptional activation and initiation, therefore histone acetylation is strongly linked to upregulation in gene transcription. This link was first identified in 1964 (194) and has since been proven both *in vitro* and *in vivo* (145, 195-197).

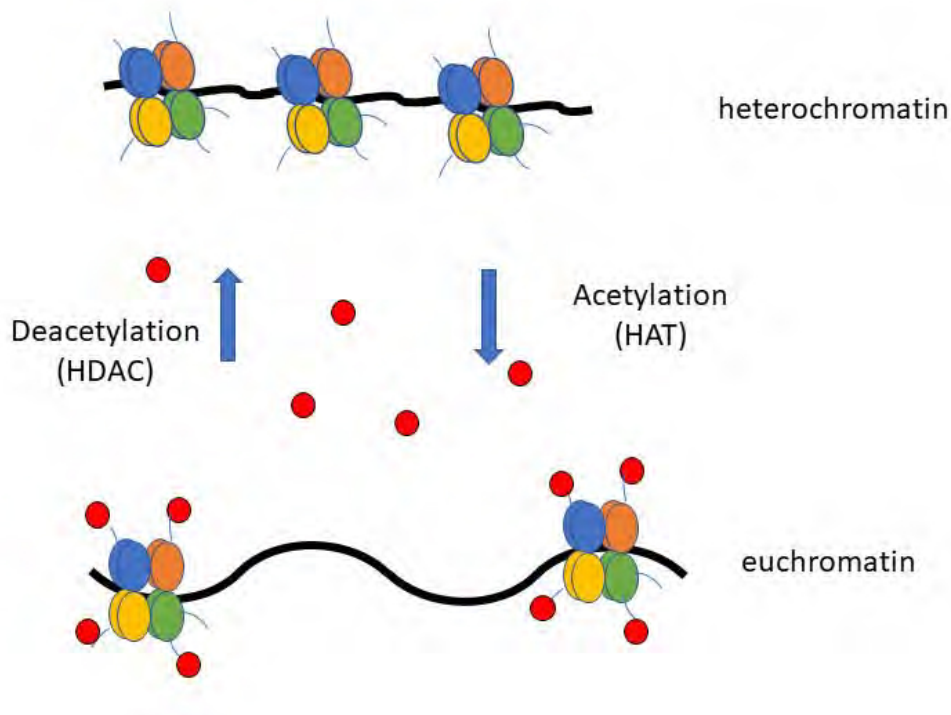


**Figure 3.3 Histone Acetylation Mediated by HAT and HDAC.** Histone acetylation occurs when acetyl moiety (red) is added on to the histone by a HAT enzyme, whilst deacetylation occurs when the acetyl moiety is removed by an HDAC enzyme. The former promotes the tightly wound heterochromatin state, whilst the latter promotes the euchromatin state.

The addition and removal of acetyl moieties to lysine residues is modulated by enzymes histone acetyltransferase (HAT) and histone deacetylase, respectively. The aforementioned may also be referred to as lysine acetyltransferases (KATs) and lysine deacetylases (KDACs) as they have been shown to acetylate non-histone proteins. In the interest of clarity, we will continue



to use the term HATs and HDACs in this work. HATs use acetyl-CoA as the acetyl donor to acetylate the  $\epsilon$ -amine of lysine residues and are classed into three families:

- GNAT
- MYST
- P300/CBP

**Table 3.1 HAT Substrate Specificity.** Identified histone specificity of HATs within the three well-understood classes. It is of import to note that factors that may affect the specificity of an enzyme include method of isolation & purification, biological context, and nature of histone substrate (i.e. histone peptide fragments, core histones). Source: (198-200). \*yeast homolog

Family/HAT name	Target residue(s)
<b>GNAT family</b>	
Gcn5*	H3K9K14K36; H3K9K14K18K23KK27K36
p/CAF	H3K14
<b>MYST family</b>	
Tip60	H4K5K8K12K16
MOF	H4K16
Sas3	H3K14K23
MOZ	H3K14
<b>p300/CBP family</b>	
p300	H2AK5; H2B; H3K4K9K14K18K27K56;
Rtt109*	H3K56K9K23
CBP	H2AK5; H2B

Each HAT employs acetyl-CoA to act on a lysine substrate to form acetyl-lysine, however the difference between classes becomes evident upon examining the sequence of acetylation. Suggesting that each class demonstrates distinct substrate specificity and biological activity (198). Although, the exact pattern can vary depending on the biological context and the nature of the substrates (198, 200, 201). Table 3.1 outlines the identified patterns of histone acetylation by different HATs.

In our investigations, we aimed to inhibit HAT activity using a natural inhibitor derived from turmeric: curcumin. Curcumin's capacity as a HAT inhibitor has been well demonstrated *in vitro* (202-204) and *in vivo* (202, 204); with its mechanism of action being linked to inhibition of p300 HAT activity (202, 204).

**Table 3.2 Classes & subcellular distribution of histone deacetylases (HDACs).**

Source: (205, 206)

<b>Family/HDAC</b>	<b>Subcellular distribution</b>
<b>Class I</b>	
HDAC1	Nucleic
HDAC2	Nucleic
HDAC3	Nucleic
HDAC8	Nucleic & cytoplasmic
<b>Class II</b>	
<b>Class IIa</b>	
HDAC4	Nucleic & cytoplasmic
HDAC5	Nucleic & cytoplasmic
HDAC7	Nucleic, cytoplasmic & mitochondrial
HDAC9	Nucleic & cytoplasmic
<b>Class IIb</b>	
HDAC6	Cytoplasmic
HDAC10	Cytoplasmic
<b>Class III</b>	
Sirt1	Nucleic & cytoplasmic
Sirt2	Nucleic & cytoplasmic
Sirt3	Mitochondrial
Sirt4	Mitochondrial
Sirt5	Mitochondrial
Sirt6	Nucleic & cytoplasmic
Sirt7	Nucleic & cytoplasmic
<b>Class IV</b>	
HDAC11	Nucleic & cytoplasmic

Acetylation levels are not solely mediated by HATs, as the removal of the acetyl mark by enzymes known as histone deacetylases (HDACs) also plays a significant role. Like HATs,

HDACs are at times referred to as protein deacetylases but we will continue to refer to them as HDACs in this work. HDACs are classed into four families (I-IV), with table 3.2 outlining the members of each family. HDAC classes I, II, and IV have Zn dependent catalytic mechanisms (207), whilst class III HDACs, also known as Sirtuins, depend on oxidized nicotinamide adenine dinucleotide (NAD<sup>+</sup>) as a cofactor during catalysis (208). HDAC activity has been shown to correlate with transcriptional repression (209). Aberrant recruitment of HDACs has been mechanistically linked to numerous malignancies *in vitro* (210, 211), and a potent HDAC inhibitor suberoylanilide hydroxamic acid (SAHA), trading under the name Vorinostat, has been FDA approved for the treatment of cutaneous T-cell lymphoma. Studies investigating HDAC activity in COPD have shown that immune cells and peripheral lung tissue obtained from COPD patients had decreased levels of HDAC2 activity which correlate with disease severity (149). Further, it was shown that restoring HDAC2 activity in immune cells resulted in a resolution of the impaired glucocorticoid response typical of COPD (129, 148). These findings underpin the reemergence of interest in Theophylline as a COPD therapeutic. Previously used as a bronchodilator at high therapeutic concentrations, Theophylline fell out of favour with patients and prescribers due to its many side effects (212). However, upon demonstrating that Theophylline activates HDACs and thereby enhances the anti-inflammatory effect of corticosteroids *in vitro* (213, 214), the drug has been considered a likely contender for treatment in COPD exacerbations. Although recent evidence from a pilot clinical trial shows no improvement in exacerbations in severe COPD patients (215) thus far.

In this Chapter, we inhibited HDAC activity with Trichostatin A (TSA). We chose TSA over other HDAC inhibitors, such as SAHA, due to its enhanced inhibitory activity at lower concentrations (216), thereby exerting less cytotoxic effects on primary human ASM cells. Treatment with TSA has been shown to lead to accumulation of acetylated histones *in vitro*

and *in vivo* (217). TSA's mechanism is attributed to its capacity as a zinc scavenger, thereby effectively inhibiting the catalytic properties of HDACs within classes I, II, and IV.

Histone methylation refers to a PTM wherein a methyl (CH<sub>3</sub>) group is covalently attached to amino acid residues on histone lysine tails. It is modulated by enzymes known as histone methyltransferases and demethylases, which demonstrate affinity for methylating lysine (K) and arginine (R) residues (218). These are known as lysine methyltransferases (KMTs) and protein arginine N-methyltransferases (PRMTs). Lysine demethylation is modulated by lysine specific demethylases (KDMs). Methylated histone tails affect gene transcription by acting as docking sites for transcriptional upregulators (219) and have been shown to act in concert with other epigenetic marks to affect chromatin structure (220). Lysine and arginine methylations have been shown to be involved in multiple cellular processes such as cell signalling, cell fate determination, X chromosome inactivation, *Hox* gene patterns, transcriptional regulation, RNA metabolism, and DNA repair (196, 221-228).

**Table 3.3 Lysine methyltransferases (KMTs), lysine demethylases (KDMs), and protein arginine methyltransferases (PRMTs).** Epigenetic enzymes mediating histone methylation to lysine (K) residues are classed as either KMTs or KDMs, whilst those methylating arginine (R) residues are PRMTs.

<b>KMT</b>	<b>Target residue(s)</b>	<b>KDM</b>	<b>Target residue(s)</b>	<b>PRMT</b>	<b>Target residue(s)</b>
ASH1L	H3K4K36	JARID1a-	H3K4	CARM1	H3R17R26R42
DOT1L	H3K79	JMJD1a-c	H3K9	PRMT1	H4R3; H2AR3R11
ESET	H3K9	JMJD2b,d	H3K9	PRMT2	H3R8
EZH1	H3K27	JMJD2a,c	H3K9K36	PRMT5	H3R2R3R8; H2AR3
EZH2	H3K27	JMJd3	H3K27	PRMT6	H3R2R3R42; H2AR3R29
G9a	H3K9	JMJD5	H3K36	PRMT7	H3R2
GLP	H3K9	KDM2A	H3K36	PRMT7	H3R2; H4R3R17R19; H2AR3;
MLL1-4	H3K4	KDM2B	H3K36		
NSD1	H3K20K36	KIA1718	H3K9K20K27		
NSD2	H3K36	LSD1	H3K4		
NSD3	H3K36	LSD2	H3K4		
PRDM19	H3K9	NO66	H3K4K36		
PRDM3	H3K9	PHF2	H3K9		
PRDM9	H3K4	PHF8	H3K9K20K27		
RIZ	H3K9	UTX	H3K27		
SET1A	H3K4				
SET1B	H3K4				
SET2	H3K36				
SET3	H3K36				
SET7	H3K4				
SET8	H4K20				
SET9	H3K4				
SETMAR	H3K4K36				
SMYD1,2	H3K4				
SUV-4-20h1	H4K20				
SUV-4-20h2	H4K20				
SUV39h1	H3K9				
SUV39h2	H3K9				
SYMD2	H3K36				

Histone methylation marks are not as well understood as DNA methylation and histone acetylation as there is far more complexity in the nature of histone methylation and the resultant outcomes. For example, a particular residue may be mono-, di-, or tri-methylated and each outcome may be linked to either transcriptional upregulation or downregulation depending on the target residue (218, 229). Aberrancies in these enzymes have been linked to disease. For example, the KMT, G9a, has been shown to contribute to lung cancer metastasis *in vivo* (230); whilst increased expression of SETDB1 was shown to contribute to lung tumorigenesis (231). In the context of respiratory disorders, it was shown that a gene associated with COPD, *DEFB1* (232), has been attributed to trimethylation of H3K4 (233).

Due to the large number of enzymes involved in histone methylation we used two small molecule inhibitors designed by the Structural Genomics Consortium (SGC) to investigate differences in lysine specific demethylation. The first, GSK-LSD1, was shown to be a potent inactivator of KDM, LSD1 (234). Whilst the second, UNC0642, was an inhibitor of KMTs, G9a and GLP(235).

## 3.2 Methods

### 3.2.1 Ethics statement

Ethics approval was obtained as previously stated in section 2.2.1

### 3.2.2 Primary cell isolation

Primary cells were collected & cultured as previously indicated in section 2.2.2

### 3.2.3 Study subjects

Study subjects were identified as previously stated in section 2.2.3

### 3.2.4 Cell culture

Primary human ASM cells were seeded as described in section 2.2.4.

### 3.2.5 Stimulation & Epigenetic Enzyme Inhibition

Cells were stimulated as previously described in section 2.2.5.

HAT activity was inhibited with Curcumin (10  $\mu$ M; Sigma-Aldrich, Germany) for 1 hour prior to stimulation with TGF- $\beta$ 1. HDAC activity was inhibited with Trichostatin A (TSA; 100 nM; Sigma-Aldrich, Germany) for 1 hour prior to stimulation with TGF- $\beta$ 1. LSD was inhibited with

GSK-LSD1 (100 nM; Sigma-Aldrich, Germany) for 1 hour prior to stimulation. DNMT1 activity was inhibited with 5-azacytidine (10  $\mu$ M) for 48 hours prior to stimulation with TGF- $\beta$ 1. All inhibitors were dissolved in dimethylsulfoxide (DMSO; Sigma-Aldrich, Germany) vehicle.

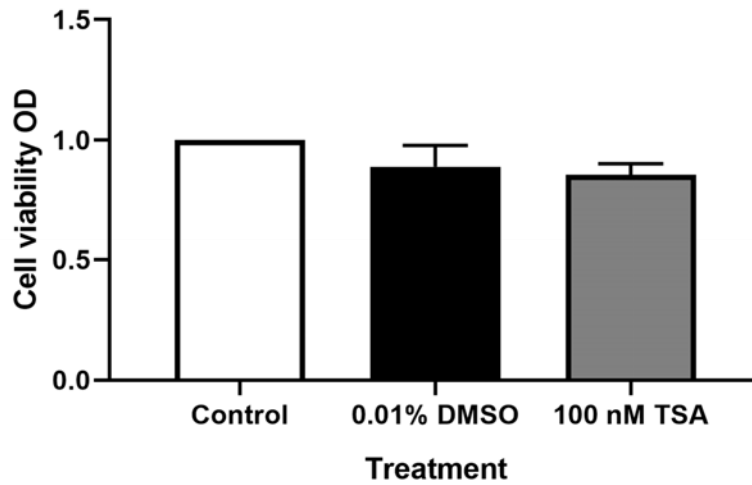


**Figure 3.4 Effect of DMSO and TSA on cell viability.** Primary human ASM cells were grown to 85% confluence and inhibited with TSA and DMSO at the above noted concentrations. Cell viability was assessed using an LDH assay. Results are normalised to non-treated control, no significant difference between all groups (n = 4). This experiment was carried out for each inhibitor used in this chapter.

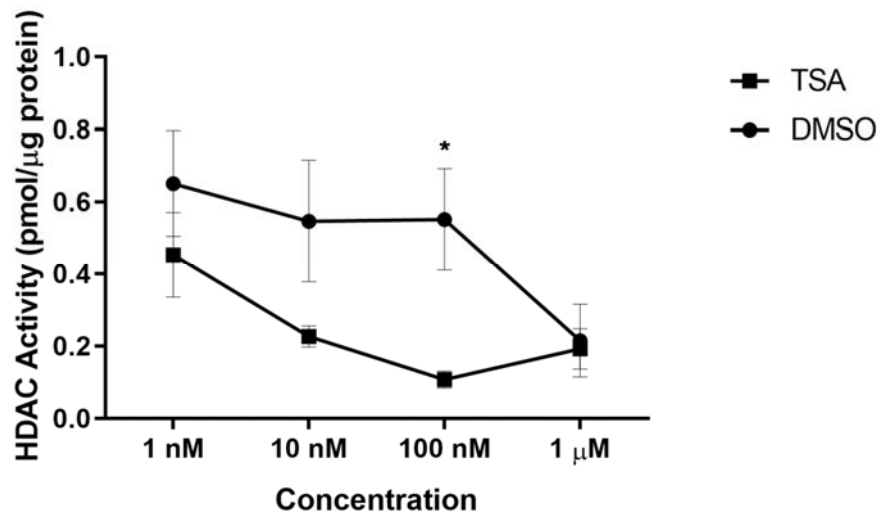


**Figure 3.5 Effect of TSA inhibition on HDAC activity over vehicle.** Primary human ASM cells were grown to 85% confluence and inhibited with TSA at the above noted concentrations prior to stimulation. Nuclear fraction was isolated and immediately used in HDAC activity assay to determine HDAC activity. At 100nM, there was significantly lower HDAC activity compared to the equivalent volume of DMSO vehicle (n = 5, p = 0.4441). This experiment was carried out for each inhibitor used in this chapter.



### 3.2.6 Nuclear Extraction

Cells were seeded and grown as mentioned above. Nuclear protein fractions were collected using a commercial nuclear extraction kit (ab113474; Abcam, UK). Briefly, cells were trypsinised and twice washed in sterile 1x phosphate buffered solution (PBS). Cell numbers were quantified by manual cell count, and cell lysis buffer – containing freshly added protease inhibitor cocktail (PIC) and dithiothreitol (DTT) – was added at a concentration of 100  $\mu$ L per  $10^6$  cells. Cells in cell lysis were kept on ice before being vortexed vigorously and centrifuged (13,400 g/1 min/4°C). The nuclear pellet was then resuspended in nuclear lysis buffer – containing freshly added PIC & DTT – at a concentration of 10  $\mu$ L per  $10^6$  cells and vortexed every 3 mins for 15 mins to facilitate nuclear protein extraction. At which point the suspension is centrifuged (16,300 g/10 mins/4°C). The protein concentration of the nuclear extract was quantified using a bicinchoninic acid (BCA) assay (Sigma-Aldrich, St Louis, MO) against a bovine serum albumin (BSA; Sigma-Aldrich, St Louis, MO) standard.

### 3.2.7 HAT activity assay

Histone acetyltransferase activity was determined by a commercial kit (ab239713; Abcam, UK) according to the manufacturer's instructions. Results are expressed as amount of catalytic byproduct (CoA-SH) per  $\mu$ g protein.

### 3.2.8 HDAC activity assay

Histone deacetylase activity was determined with an established assay (566328; Calbiochem, Germany) used according to the manufacturer's instructions. The results are expressed as amount of deacetylated histone substrate per  $\mu\text{g}$  protein.

### 3.2.9 Quantitative PCR

Cells were cultured as described above in section 3.2.4 and RT-qPCR was carried out as outlined in section 2.2.6 for *COL15A1* and *TNC*.

### 3.2.10 Statistical analysis

The data were analysed for parametric distribution, with differences identified by either unpaired t-test or 2way ANOVA followed by Tukey post-hoc tests as specified. Data analysis was carried out using Graphpad Prism 8 software wherein a p-value  $< 0.05$  is considered significant.

### 3.3 Results

#### 3.3.1 Effect of DNMT1 inhibition on *COL15A1* and *TNC* expression

To inhibit DNMT1, we cultured cells with 10 $\mu$ M 5-azacytidine prior to stimulation with TGF- $\beta$ 1. Upon measuring *COL15A1* (Fig. 3.6a) and *TNC* (Fig. 3.6b) expression with RT-qPCR, it was shown that DNMT1 inhibition significantly attenuates *COL15A1* expression in both COPD (p=0.0015) and non-COPD (p=0.0017) smokers. Whilst *TNC* expression showed no significant effect upon DNMT1 inhibition.

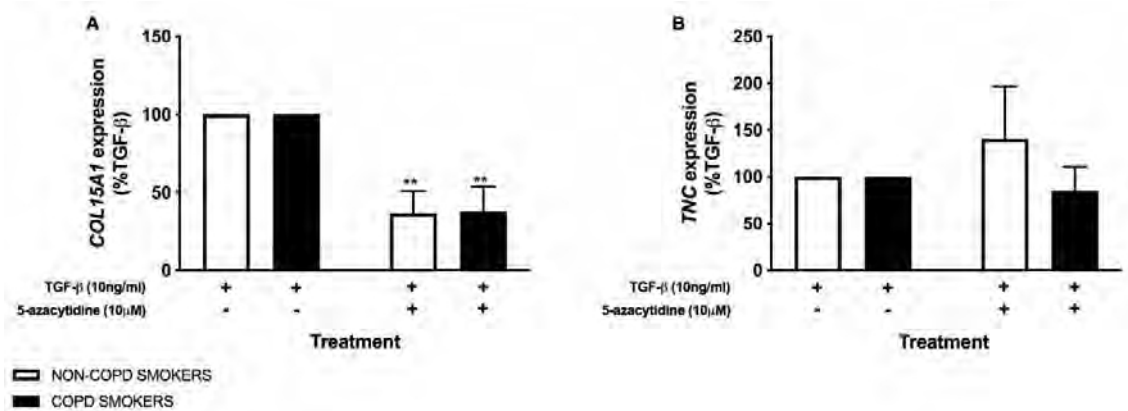


**Figure 3.6 Effect of DNMT1 inhibition with 5-azacytidine (10 $\mu$ M) on (a) *COL15A1* and (b) *TNC* expression.** Primary human ASM cells from COPD (n=5) and non-COPD (n=5) susceptible smokers were grown in the presence of 5-azacytidine for 48 hours prior to stimulation with TGF- $\beta$ 1 (10ng/ml). mRNA was collected after 48 hours of treatment, and cDNA was reverse transcribed using RT-PCR. Results are expressed as percentage of TGF- $\beta$ 1 induced expression to control for variations in TGF- $\beta$ 1 induction capacity demonstrated in Chapter 2. Data was analysed with 2way ANOVA and Bonferroni post-hoc analysis (P<0.05 = significant; mean  $\pm$  SEM).

### 3.3.2 Effect of HDAC inhibition on *COL15A1* and *TNC* expression

Upon inhibiting HDAC activity with TSA (100nM), cells were stimulated with TGF- $\beta$ 1 for 48 hours. Levels of *COL15A1* and *TNC* expression were quantified with RT-qPCR. HDAC inhibition lead to significantly ( $p=0.0104$ ) lower levels of *TNC* (Fig. 3.7b) being expressed by primary human ASM cells from non-COPD susceptible individuals, when compared to those cells from COPD susceptible patients. Although the results for *COL15A1* (Fig. 3.7a) are not statistically significant, they follow a similar trend to those statistically significant results for *TNC*, suggesting that a similar underlying mechanism be in place.

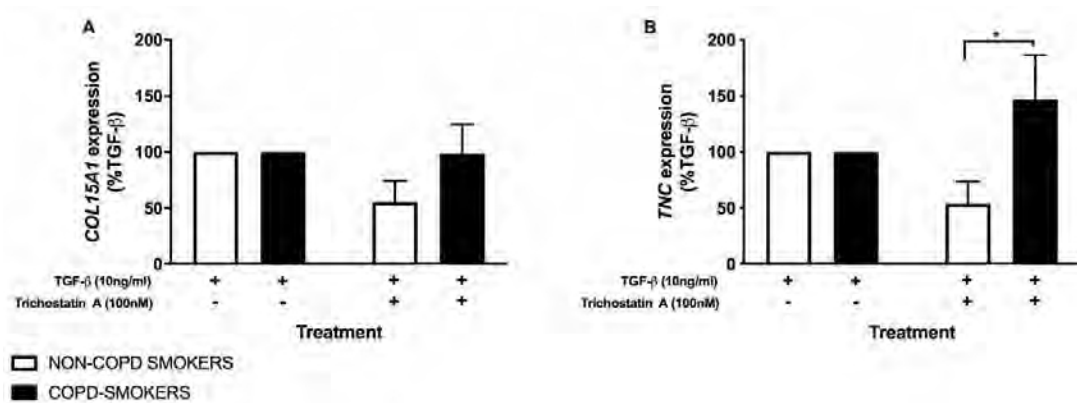


**Figure 3.7 Effect of HDAC inhibition with Trichostatin A (TSA) (100nM) on (a) *COL15A1* and (b) *TNC* expression.**

Primary human ASM cells from COPD ( $n=6$ ) and non-COPD ( $n=7$ ) susceptible smokers were treated with TSA for 1 hour prior to stimulation with TGF- $\beta$ 1 (10ng/ml). mRNA was collected after 48 hours of treatment, and cDNA was reverse transcribed using RT-PCR. Results are expressed as percentage of TGF- $\beta$ 1 induced expression to control for variations in TGF- $\beta$ 1 induction capacity demonstrated in Chapter 2. Data was analysed with 2way ANOVA and Bonferroni post-hoc analysis ( $P<0.05$  = significant;  $\pm$  SEM).

### 3.3.3 Effect of HAT inhibition on *COL15A1* and *TNC* expression

Histone acetyltransferase activity was inhibited with Curcumin prior to stimulation with TGF- $\beta$ 1. Upon quantifying *COL15A1* and *TNC* expression with RT-qPCR, it was evident that HAT inhibition lead to no significant difference in TGF- $\beta$ 1 induced *COL15A1* (Fig. 3.8a) or *TNC* (Fig. 3.8b) expression.

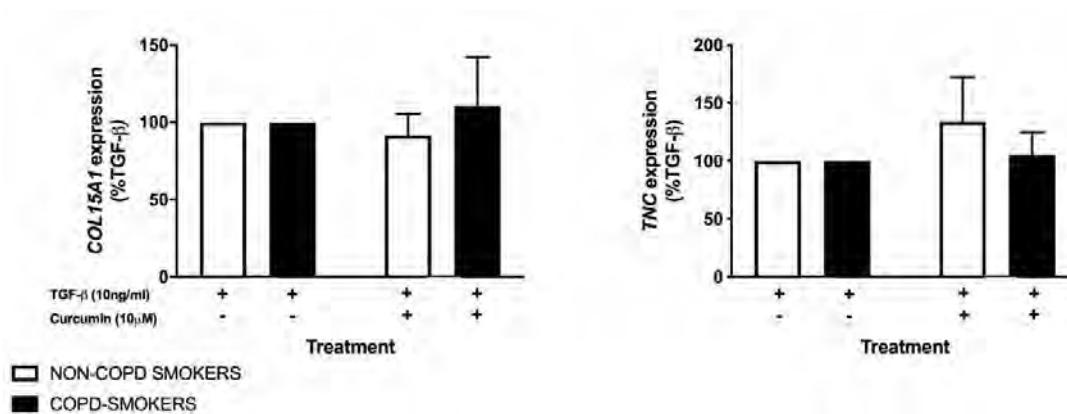


**Figure 3.8** Effect of HAT inhibition with Curcumin (10 $\mu$ M) on (a) *COL15A1* and (b) *TNC* expression. Primary human ASM cells from COPD (n=6) and non-COPD (n=7) susceptible smokers were treated with curcumin for 1 hour prior to stimulation with TGF- $\beta$ 1 (10ng/ml). mRNA was collected after 48 hours of treatment, and cDNA was reverse transcribed using RT-PCR. Results are expressed as percentage of TGF- $\beta$ 1 induced expression to control for variations in TGF- $\beta$ 1 induction capacity demonstrated in Chapter 2. Data was analysed with 2way ANOVA and Bonferroni post-hoc analysis (P<0.05 = significant;  $\pm$  SEM).

### 3.3.4 Effect of inhibited KTMs and KDM on *COL15A1* and *TNC* expression

To determine the effect of histone methylation on *COL15A1* and *TNC* expression, we aimed to inhibit the KTMs G9a and GLP with UNC0642 and the KDM LSD1 with GSK-LSD1.

However, during our cell viability investigations it was determined that UNC0642 was cytotoxic to primary human ASM cells at concentrations ranging from 10 nM-10  $\mu$ M.

Treatment with GSK-LSD1, showed no significant effect on TGF-  $\beta$ 1 induced *COL15A1* (Fig. 3.9a) and *TNC* (Fig. 3.9b) expression in human ASM cells from either COPD or non-COPD cohorts.

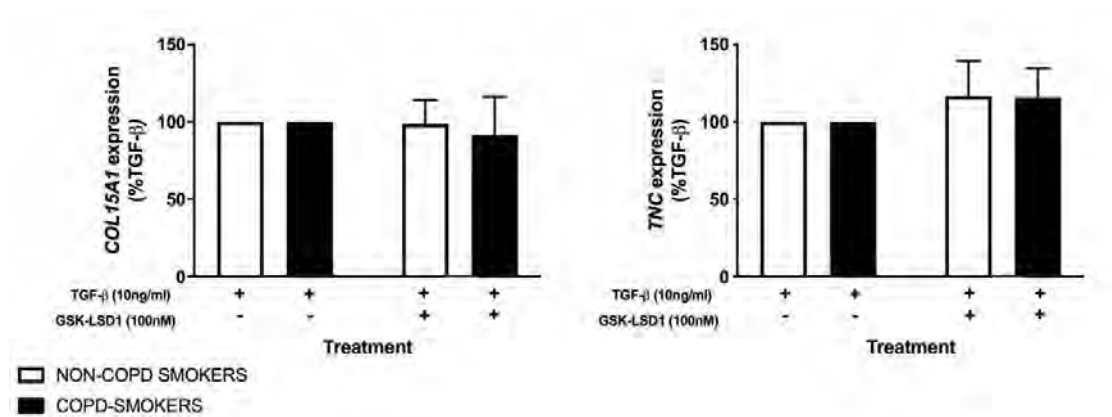


**Figure 3.9** Effect of lysine specific demethylase 1 (LSD1) inhibition with GSK-LSD1 (100nM) on (a) *COL15A1* and (b) *TNC* expression. Primary human ASM cells from COPD (n=6) and non-COPD (n=7) susceptible smokers were treated with GSK-LSD1 for 1 hour prior to stimulation with TGF-  $\beta$ 1 (10ng/ml). mRNA was collected after 48 hours of treatment, and cDNA was reverse transcribed using RT-PCR. Results are expressed as percentage of TGF-  $\beta$ 1 induced expression to control for variations in TGF-  $\beta$ 1 induction capacity demonstrated in Chapter 2. Data was analysed with 2way ANOVA and Bonferroni post-hoc analysis (P<0.05 = significant;  $\pm$  SEM).

### 3.3.5 Investigation into basal HAT activity

Our investigations determined that there was no significant difference in baseline levels of HAT activity (Fig. 3.10) between non-COPD and COPD susceptible smokers.

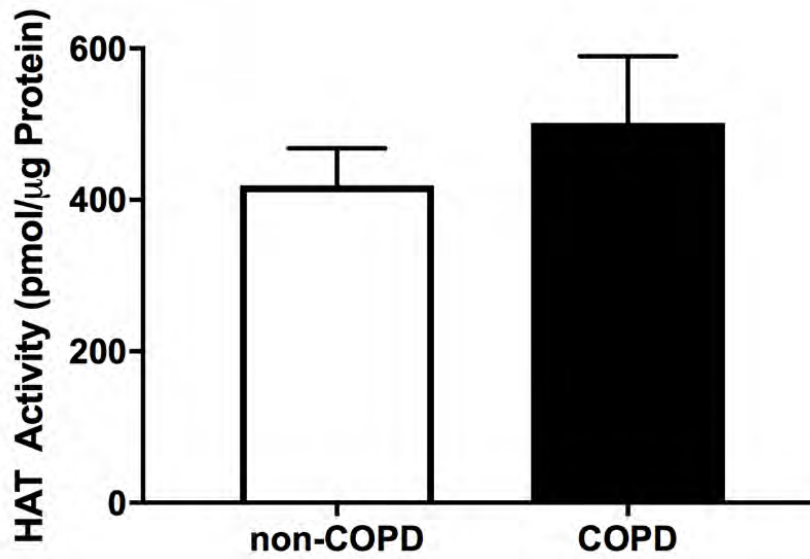


**Figure 3.10 Histone acetyltransferase activity assay.** Nuclear fractions were isolated from primary human ASM cells from COPD (n=4) and non-COPD (n=5) susceptible individuals and used in a commercial enzyme activity assay. Results are expressed as amount of catalytic byproduct (CoA-SH) per  $\mu\text{g}$  of protein. Data was analysed with unpaired t-test ( $p < 0.05$  = significant;  $\pm$  SEM).

### 3.3.6 Investigation into basal HDAC activity

Results expressed in Figure 3.11 found that there was no significant difference in overall basal level of HDAC enzyme activity between non-COPD and COPD susceptible smokers.

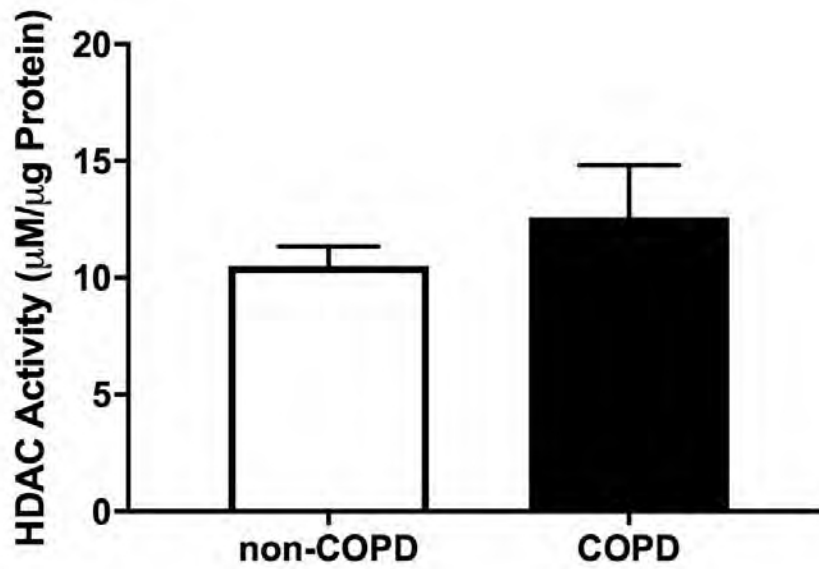


**Figure 3.11 Histone deacetylase (HDAC) activity assay.** Nuclear fractions were isolated from primary human ASM cells from COPD (n=4) and non-COPD (n=5) susceptible individuals and used in a commercial enzyme activity assay. Results are expressed as amount of deacetylated histone substrate per µg of protein. Data was analysed with unpaired t-test ( $p < 0.05$  = significant;  $\pm$  SEM).



### 3.4 Discussion

In this Chapter we aimed to identify epigenetic aberrations between our non-obstructed smokers and COPD study subjects to highlight a potential target for specific DNA or chromatin immunoprecipitation investigations. To screen for such differences, we chose established inhibitors of enzymes shown to affect DNA methylation, histone acetylation, and histone methylation.

Our results showed that inhibiting the maintenance of DNA methylation by targeting DNMT1 lead to a significant attenuation of *COL15A1* expression whilst *TNC* expression remained unaffected. In looking at histone acetylation, our results found no effect of inhibiting HAT activity; whilst inhibiting HDACs lead to a differential *TNC* expression between human ASM cells from COPD and non-COPD susceptible smokers. Finally, when investigating histone methylation, we found that inhibiting G9a and GLP was cytotoxic at a range of concentrations, suggesting that these enzymes are essential in cell survival. Whilst inhibiting LSD1, thereby inhibiting the removal of a histone methyl mark, had no significant effect on *COL15A1* or *TNC* expression from either cohort.

Our results shown in Figure 3.6a show that TGF- $\beta$ 1 induced *COL15A1* expression was significantly attenuated in response to pre-treatment with 5-azacytidine. The mechanism of 5-azacytidine is to reduce DNA methylation levels. Therefore, when overall levels of DNA methylation had been reduced, human ASM from COPD and non-COPD susceptible smokers expressed less *COL15A1*. As discussed in section 3.1, the overall effect of DNA methylation is transcriptional repression, therefore our results do not suggest that there is DNA methylation at the *COL15A1* promoter region as DNMT1 inhibition would have augmented *COL15A1*

expression rather than attenuating it. We postulate that DNMT1 inhibition lead to an alteration in expression of a protein involved in the transcriptional regulation of *COL15A1*, causing a decrease in gene expression. Further, it is of importance to note that this effect was not different between human ASM cells from non-COPD and COPD susceptible patients. Therefore, we conclude that the underlying mechanism revealed by DNMT1 inhibition is attributed to inherent *COL15A1* regulation and not likely to contribute to increased ECM deposition.

Our results shown in Figure 3.7b show that HDAC inhibition leads to a significant difference in TGF-  $\beta$ 1 induced *TNC* expression when comparing human ASM cells from non-COPD and COPD susceptible smokers. This suggests that there is an inherent difference in acetylation patterns at the *TNC* promoter between the cohorts. Further, we find that the gene expression is significantly lower in non-COPD, when comparing to COPD, after HDAC inhibition. To summarise, this infers that when general acetylation levels increase, human ASM of non-COPD patients express comparatively less *TNC* whilst those from COPD express more. We posit that this points to *TNC* gene expression in non-COPD depending on factors outside of acetylation whilst expression in COPD is augmented in line with accumulated acetylation. Although the results for *COL15A1* in Figure 3.7a did not meet statistical significance, there is an evident trend mirroring those results in *TNC*, thereby suggesting that the genes may share a common regulatory mechanism. This is made more likely when considering that both genes reside on the q arm of chromosome 9.

To further delineate any aberrancies that may contribute to the response to HDAC inhibition (Fig. 3.7), we sought to investigate the basal activity of enzymes modulating levels of histone acetylation, HATs and HDACs. As shown in Figures 3.10 and 3.11, there is no significant difference in HAT or HDAC activity in primary human ASM cells from either group. The

results for HDAC activity (Fig. 3.11) sit in contrast to a published study wherein HDAC activity detected in isolated airway macrophages and homogenised peripheral lung tissue from COPD patients was significantly lower than those samples obtained from non-obstructed patients. We believe the difference being attributed to the types of cells investigated. Based on the previously mentioned study (149), we can conclude that immune cells from COPD patients have altered HDAC activity, however the method of using peripheral lung tissue as a representation of mesenchymal cells within this study is not robust. In using peripheral lung tissue, the study does not delineate between the type of mesenchymal cell or control for macrophages and other immune cells residing in the peripheral tissue that may contribute to the result. Therefore, we assert that our findings are a more robust investigation into the inherent HDAC activity when comparing COPD smokers to non-COPD susceptible smokers. There is no evidence in the literature that sits in contrast with our results for HAT activity (Fig. 3.10). Further, no baseline difference between HAT and HDAC activity implores us to posit that the aberrant results in response to HDAC inhibition with TSA (Fig. 3.7) is likely to be the result of a gene specific mechanism, rather than a consequence of a global disparity in epigenetic enzymatic activity. Based on this evidence, we surmise that the epigenetic mark most likely to contribute to increased expression of ECM protein genes, *COL15A1* and *TNC*, is histone acetylation.

However, it is of import to note that epigenetic inhibitors have many off-target effects. For example, curcumin has been shown to have antioxidant and anti-inflammatory effects (236, 237). Further, enzymes HAT and HDAC have been shown to act on non-histone proteins that are active in gene transcription, such as NF- $\kappa$ B (238, 239), therefore by inhibiting the enzymes we may be inadvertently affecting the activity of numerous proteins involved in gene transcription. A separate study investigating the off-target effects of epigenetic inhibitors on

transcriptional activators and mediators showed that treatment with TSA alone leads to significantly higher levels of NF- $\kappa$ B p65 phosphorylation and p38 MAPK phosphorylation in non-COPD smokers, when compared to COPD smokers (Appendix C). These findings confirm that results from studies using these inhibitors cannot immediately be attributed to direct epigenetic modifications without further investigation. Consequently, it is imperative that any robust investigations into aberrations in histone acetylation would include methods directly assessing the incidence of an acetyl mark on the histones. The most robust of which involving chromatin immunoprecipitation (ChIP).

We must further acknowledge and assert that in this investigation we do not conclusively exclude the role that other epigenetic marks may play in overall pathology. For example, when investigating histone methylation, we used inhibitors focused on lysine methylation but not arginine methylation. In a thorough investigation of DNA methylation it would be ideal to include PRMT inhibition with a specific inhibitor such as RM65 (240). However, considering the range of epigenetic enzymes outlined in tables 3.1-3.3 a thorough investigation would need to employ high-throughput methods. Further, the proposed study would need to be underpinned by further advancement in the field of epigenetic inhibitors as there is a current dearth of specific inhibitors for each epigenetic enzyme listed in tables 3.1-3.3.

In this Chapter we used a range of established epigenetic inhibitors on primary human ASM cells from non-COPD and COPD patients to screen for any epigenetic aberrancies between the two groups. Our most promising finding was the significantly different response to HDAC inhibition between COPD and non-COPD human ASM cells. We are further encouraged that this mechanism plays a specific and targeted role in aberrant ECM gene expression as it sits in concert with results showing that overall HDAC activity is not aberrant between the two

groups. Therefore, we resolved to pursue our investigations into aberrant *COL15A1* and *TNC* expression using ChIP rather than Me-DIP.

## Chapter 4 Chromatin Targeted Investigation of Histone Acetylation

### 4.1 Introduction

In Chapters 2 & 3 we have demonstrated that primary human ASM cells from COPD patients show aberrant expression of the ECM genes *COL15A1* and *TNC*, with a likely aberrant epigenetic response attributed to histone acetylation. In this Chapter, we aim to use the gold standard of techniques to confirm or abolish the notion of an acetyl mark associated with the promoter regions for *COL15A1* and *TNC*: ChIP-PCR. We also include the use of a more specific epigenetic inhibitor – JQ1(+) – to investigate the link between an acetyl mark and ECM gene expression.

In section 3.1, we discussed how histone acetylation contributes to an increase in gene expression by altering histone charge, thereby promoting a loosely bound euchromatin state. However, there is also a secondary mechanism through which acetylated histones contribute to gene transcription: through the recruitment of proteins from the bromo- and extra-terminal domain (BET) family.

The mammalian BET family of proteins includes Brd2, Brd3, Brd4, and BrdT (241); each of which contains two bromodomains known as BD1 and BD2 and an extra terminal (ET) domain (242). Brd4 is the most well understood of the BET protein family. The BD1 and BD2 domains in Brd4 have been shown to recognise and bind to acetylated lysine residues on histones H4 and H3, allowing for the BET protein to dock on the histone tail (243, 244). Considering that

Brd4 does not contain a DNA binding domain (162), histone acetylation is essential in recruiting Brd4 to the gene promoter region.

It is common in metazoan genes that are transcribed by RNA Pol II to experience transcriptional pause. This refers to RNA Pol II being paused immediately after transcription initiation (245) through association with negative elongation factor (NELF) and DRB-sensitivity-inducing factor (DSIF) (246). During transcriptional pause, mRNA synthesis is transiently halted, but RNA Pol II remains bound to the DNA template and nascent RNA template already transcribed (246). Brd4 acts to reinitiate transcription through recognition of acetylation marks on histone tails bound to such paused regions. Upon “reading” the acetylated histone mark, Brd4 recruits positive transcription elongation factor (pTEFb) (247, 248), which inhibits DSIF and NELF (249) and subsequently releases promoter-proximal pausing of RNA polymerase II (250, 251); therein initiating gene transcription. Brd4 further contributes to the first stages of transcriptional elongation while remaining bound to the pTEFb/RNA Pol II transcriptional complex until productive elongation >36 nucleotides occurs (252). A study into direct interactions of Brd4 with transcription factors via protein: protein screening found that Brd4 does not directly interact with RNA Pol II (253). The study further demonstrated that Brd4 only directly interacts with the following specific subset of transcription factors: p53, YY1, c-Jun, AP2, C/EBP $\alpha$ , C/EBP $\beta$ , and Myc/Max (253). These findings confirm that transcriptional elongation aided by Brd4 must be part of a “triad” wherein Brd4 associates with one of the aforementioned transcription factors already bound to RNA Pol II. It is by acting as a docking site for Brd4, and Brd4’s subsequent activities in transcriptional elongation, which acetylated lysine residues on histone tails further promote transcriptional upregulation. Therein encapsulating a secondary mechanism of promoting transcriptional upregulation in addition to the primary mechanism of promoting chromatin decompaction to the euchromatin state.

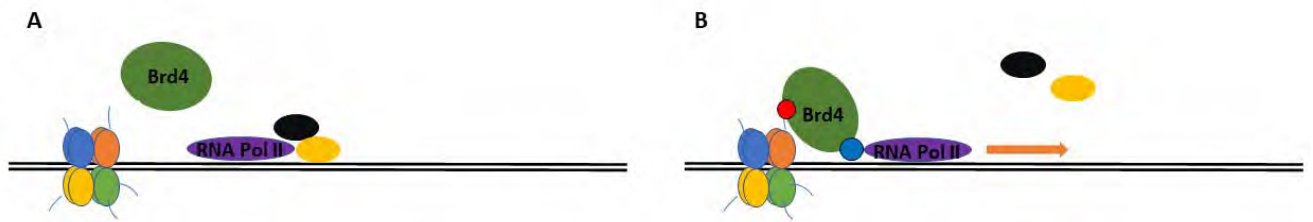


**Figure 4.1 Schematic Representation of Transcriptional Triad.** (A) Without an acetylated histone tail to dock on, Brd4 is unable to associate with chromatin to recruit pTEFb to inhibit DSIF (black) and NELF (yellow) and relieve promoter-proximal pause. (B) Brd4 can “read” acetylated lysine residue (red), thereby docking on chromatin and subsequently recruiting pTEFb (blue) to relieve RNA Pol II pause at the promoter region. Allowing for transcriptional elongation to continue. This is a constitutive function of Brd4. However, Brd4 has been shown to associate with other proteins aside from pTEFb in a more selective manner (253).

Further, Brd4 also plays a role in transmitting epigenetic memory. During mitosis, it is common for majority of transcription factors to become displaced from the chromosome. In high eukaryotes, this correlates with a marked hypoacetylation of histone tails and overall transcriptional silence typical of cells undergoing mitosis (254-256). However, studies have shown that Brd4 – previously known as mitotic chromosome-associated protein (MCAP) – remains bound to acetylated lysine residues on histones H3 and H4 via BD1 and BD2 during mitosis and remains bound during interphase (242, 257). Whilst being bound during interphase, it is proposed that Brd4 acts as a ‘mitotic bookmark’ to transmit epigenetic memory to cell progeny (242, 257). Further, it was shown that post-mitotic chromatin decompaction and transcriptional kinetics were accelerated by Brd4 propagating the epigenetic mark (258). Thus, demonstrating the duality of Brd4 in its capacity to act in functional epigenetic memory as well as transcriptional initiation and elongation.



JQ1 is a molecule designed by the structural genomics consortium as a selective and potent Brd4 inhibitor. Although JQ1 has been shown to bind to other members of the BET family, such as Brd3, it has highest affinity for the acetyl-lysine recognition sites of Brd4 (170). JQ1 does not associate with bromodomain containing proteins outside of the BET family (170). Further, it has been determined using co-crystal structure analysis that JQ1 binds to the acetylated lysine recognition sites of Brd4 (170), demonstrating that JQ1's mechanism is through competitive inhibition of the acetyl lysine recognition motif.

As of August 2019 there are seven clinical trials investigating inhibitors of BET proteins in the treatment of multiple myeloma (NCT03068351; phase I), advanced solid tumors (NCT02259114; phase Ib; NCT02157636; phase I), progressive lymphoma (NCT01949883; phase I), peripheral nerve sheath tumours (NCT02986919; phase II), acute myeloid leukemia (NCT02698189; phase I; NCT02308791; phase I), and myelodysplastic syndrome (NCT02308761; phase I). JQ1 has been shown to exhibit therapeutic effects in the treatment of acute myeloid leukemia (259) and Myc- mediated human malignancies (260, 261). Studies using primary human ASM from asthmatic patients showed pre-treatment with JQ1 prior to stimulation with TGF- $\beta$ 1 reduced Brd4 binding to the *IL6* and *CXCL8* promoters, which correlated with a decrease in IL6 and CXCL8 protein expression (262). Demonstrating the efficacy of this inhibitor in mediating inflammation primary ASM cells.

## 4.2 Methods

### 4.2.1 Ethics statement

Ethics approval was obtained as previously stated in section 2.2.1

### 4.2.2 Primary cell isolation

Primary cells were isolated & cultured as previously indicated in section 2.2.2 (is 6 well plate mentioned).

### 4.2.3 Study subjects

Study subjects were identified as previously stated in section 2.2.3

### 4.2.4 Cell culture

Primary human ASM cells were seeded as described in section 2.2.4.

### 4.2.5 Stimulation & Brd4 Inhibition

Cells were stimulated as previously described in section 2.2.5.

Brd4 inhibition was carried out with JQ1(+) (1 nM, 10 nM, 100 nM, 1  $\mu$ M; Sigma-Aldrich, Germany) for 1 hour prior to stimulation with TGF- $\beta$ 1 (10 ng/ml). JQ1 was made up in

dimethylsulfoxide (DMSO; Sigma-Aldrich, Germany); none of the working concentrations used impacted cell viability. The negative enantiomer JQ1(-) showed no effect in any of the experiments.

#### 4.2.6 mRNA sample collection

Upon treating cells as detailed in section 4.2.5, mRNA samples were collected as detailed in section 2.2.6.

#### 4.2.7 mRNA purification

mRNA lysates collected according to section 4.2.6 were purified as outlined in section 2.2.7.

#### 4.2.8 Reverse Transcription

Complementary DNA (cDNA) to our RNA template purified in section 4.2.6 was synthesized as outlined in section 2.2.7.

#### 4.2.9 Quantitative PCR (cDNA)

qPCR was carried out as described in section 2.2.6 for *COL15A1* and *TNC*.

#### 4.2.10 ChIP Sample Collection

Cells were treated as outlined in section 4.2.4. Prior to collection, 37% formaldehyde was added to the well to a final concentration of 1% (v/v) to cross-link histones to DNA. After 10 mins of fixation, formaldehyde was quenched by adding glycine to a final concentration of 0.2 M. Freshly prepared, filtered, ice-cold PBS containing PIC was added to each well and manual scraping was used to remove cells from well bottom. To ensure enough chromatin was collected for ChiP, all 6 wells of a 6 well plate was dedicated to each treatment (i.e. 6 wells of DMEM only, 6 wells of TGF- $\beta$ 1 stimulated, etc.), and thusly were aggregated into one tube per treatment. This cell extract was spun at 800 g@4° C for five mins. The supernatant was removed, and the cell pellet was snap frozen in liquid nitrogen until sonication.

#### 4.2.11 Chromatin Sonication

Cell pellets containing cross linked protein-DNA complexes prepared as detailed in section 4.2.8 were defrosted on ice and resuspended in 200  $\mu$ L cell lysis buffer with freshly added PIC. These were incubated on ice for fifteen mins, whilst vortexed briefly (3 sec) every five mins. The cell suspension was spun at 800 g@4°C for five mins to separate the nuclear fraction, and the supernatant carefully removed. The nuclear pellet was resuspended in 200  $\mu$ L nuclear lysis buffer with freshly added PIC and vigorously pipetted up and down to promote nuclear release. The nuclear lysates were sonicated using a high throughput Bioruptor Plus (Diagenode, Zurich) with an in-built cooling system, allowing for uniform processing to yield high quality samples. Ideal sonication settings were optimized wherein an equivalent amount of primary human ASM cells suspended in 200  $\mu$ L nuclear lysis buffer were sonicated for 0, 10, 20, 30, 40, and 50 x 30-second cycles on high and visualized on a 2% agarose gel. The optimal size of sheared

chromatin fragments for ChIP is 200-800 bps. For our samples, the majority of chromatin fragments fell in this range after 50 30-second cycles on high. A small quantity of DNA was obtained from each sample post-sonication to ensure chromatin fragments were the correct size before carrying out a ChIP Assay. See Figure 4.1 for a representative image of sonicated chromatin. BCA Assay (Sigma-Aldrich, St Louis, MO) against a BSA standard was used to verify presence of protein.

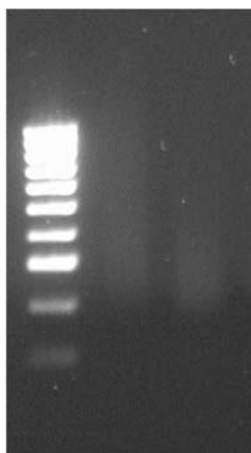


**Figure 4.2 Chromatin Fragments Post-Sonication.** 2% Agarose gel visualisation of chromatin fragments after being sonicated for 50 x 30-second cycles on high. Lane 1 contains a 100 bp standard ladder (1000 bp top, 100 bp bottom), whilst 2 & 3 contain representative samples of sonicated chromatin.

#### 4.2.12 Chromatin Immunoprecipitation Assay

Chromatin Immunoprecipitation (ChIP) assay was carried out as previously described (263) using a commercial kit (EZ-ChIP; Millipore, Bayswater, VIC) according to the manufacturer's protocol. Briefly, 50  $\mu$ L of sheared chromatin prepared as described in section 4.2.9 was placed in a tube with 450  $\mu$ L dilution buffer (containing freshly added PIC) and mixed gently. 5  $\mu$ L of this mixture was removed as sample "input" to normalize for amount of chromatin at beginning of assay. To complete our IP Mix, we added 20  $\mu$ L of well mixed magnetic protein

A/G bead slurry and x µg of antibody of interest. For each sample we carried out four immunoprecipitations as outlined in table 4.1.

**Table 4.1 Immunoprecipitations (IPs) Per Sample.** Four immunoprecipitations were carried out for each sample. Wherein IPs 1 & 2 for our antibodies of interest and IPs 3 & 4 were our positive and negative control. Our antibodies of interest were rabbit polyclonal and their immunogen properties are as follows: acetylated H3 (H3ac): anti-H3K9acK14ac. Acetylated H4 (H4ac): anti-H4K5acK8acK12acK16ac.

	<b>IP 1</b>	<b>IP 2</b>	<b>IP 3</b>	<b>IP 4</b>
<b>Experimental purpose</b>	Ab of interest	Ab of interest	Positive Control	Negative Control
<b>Ab</b>	Anti-H3ac	Anti-H4ac	Anti-RNA Pol II	Rabbit IgG
<b>Amount used</b>	5µg	4µg	4µg	4µg

We used pre-validated purified rabbit polyclonal antibodies to target anti-H3K9acK14ac (5 µg) and anti-H4K5acK8acK12acK16ac (4 µg) antibodies (Millipore, Bayswater, VIC). Each antibody used was pre-validated by the supplier (Millipore, Bayswater, VIC) to work with the kit being used, however preliminary antibody titrations were carried out to confirm the recommend amount against our cell type. We found the suppliers recommended amounts gave the best results and therefore did not deviate from manufacturer's recommendations.

The IP was carried out by incubating the IP Mix at 4°C overnight with rotation. After which, the magnetic bead + ab + protein/chromatin complexes were magnetically separated using a MagnaGrIP Rack (20-400; Millipore, Bayswater, Vic) and washed thoroughly with ice-cold buffers supplied with the kit. Finally, the chromatin/protein complexes were eluted and proteins digested by adding 100 µL elution buffer containing 10 µg proteinase K to washed beads and

incubating at 62°C for two hours with shaking on an Eppendorf ThermoMixer (Eppendorf, NSW, Australia) and finally at 95°C for ten mins to deactivate the proteinase K.

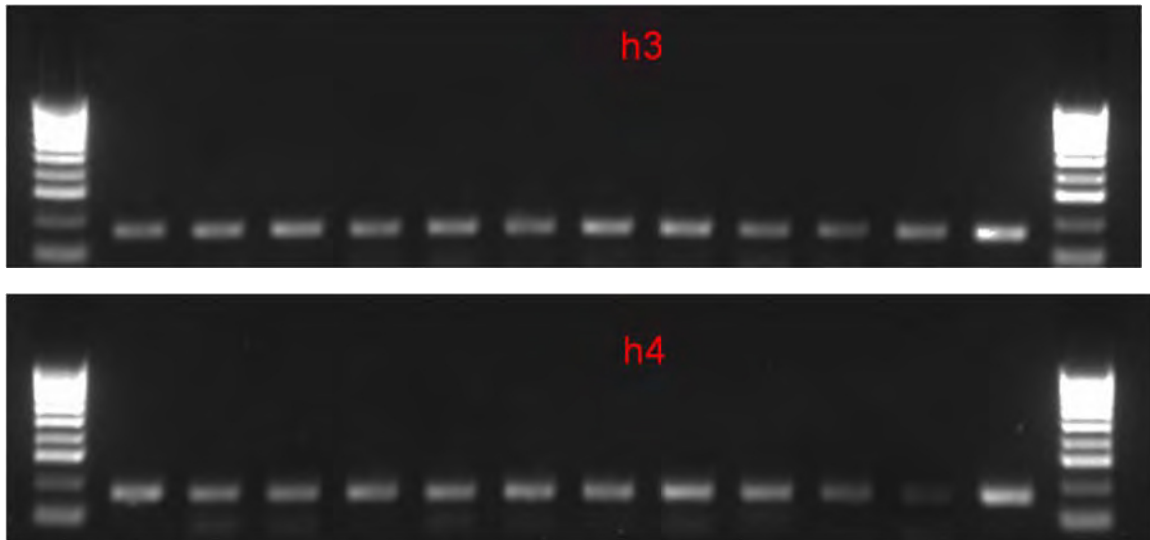


**Figure 4.3 Detection of gDNA via PCR against *GAPDH*.** PCR of immunoprecipitated samples was carried out against human *GAPDH* for positive detection of human gDNA and visualised on a 2% agarose SYBR safe stained gel via electrophoresis. Gel denoted “h3” refers to samples immunoprecipitated with anti-H3ac, whilst “h4” refers to anti-H4ac. Lane 1 & 14 contain a 100 bp standard ladder (1000 bp top, 100 bp bottom), whilst 2 - 13 represents different patients’ immunoprecipitated chromatin sample.

After each IP, eluted chromatin samples were purified using a Nucleospin gDNA Cleanup Kit (740230; Macherey-Nagel, Germany) and analysed via PCR against housekeeping gene *GAPDH* for positive detection of human gDNA (Fig. 4.2). The primer sequence for *GAPDH* was:

Forward: TAC TAG CGG TTT TAC GGG CG

Reverse: TCG AAC AGG AGG AGC AGA GAG

Quantification of *COL15A1* and *TNC* was carried out by real time qPCR using SYBR Green on a StepOnePlus Real-Time PCR System (Applied Biosystems). Data is presented as fold enrichment adjusted for input sample ( $2^{-(Ct(\text{input})-Ct(\text{ChIP}))}$ ) compared with the IgG negative control.

#### 4.2.13 Primer Design

Primers against immunoprecipitated genomic DNA (gDNA) were designed with the aid of the National Centre of Biotechnology Information's (NCBI) Genome Data Viewer (GDV). Using the aforementioned, a search for chromosomal location and sequence for *COL15A1* and *TNC* was carried out within assembly GRCh37.p13. This was used in concert with the Ensembl Genome Browser which provided additional information pertaining to promoter location. To ensure our primers target gDNA and not mRNA transcripts, we designed each primer to straddle at least one intron-exon junction. Keeping in mind that our chromatin was sheared to 200-800 bp fragments, we set 200 bp as the maximal product size. We used the NCBI primer BLAST on selected intron-exon spanning regions with the following parameters:

Minimum product size: 100 bp

Maximum product size: 200 bp

Optimal Tm: 60°C

Minimal GC Clamp: 3

Maximum GC in primer 3' end: 4



**Table 4.2 List of *COL15A1* and *TNC* transcription variants.** Within the known *H. sapien* genome (GRCh38.p12), there are five discovered transcripts of *COL15A1* and fourteen of *TNC*.

Name	Transcript ID	bp	Protein	Biotype	CCDS	UniProt	RefSeq Match
COL15A1-201	ENST00000375001.8	5223	1388aa	Protein coding	CCDS35081	P39059	NM_001855.5
COL15A1-205	ENST00000610452.1	5422	1374aa	Protein coding	-	AOA087X0K0	-
COL15A1-203	ENST00000471477.1	1412	No protein	Retained intron	-	-	-
COL15A1-204	ENST00000496686.1	771	No protein	Retained intron	-	-	-
COL15A1-202	ENST00000467052.1	276	No protein	lncRNA	-	-	-
TNC-202	ENST00000350763.9	8500	2201aa	Protein coding	CCDS6811	P24821	NM_002160.4
TNC-210	ENST00000535648.5	7508	1838aa	Protein coding	-	F5H7V9	-
TNC-201	ENST00000341037.8	6786	2019aa	Protein coding	-	J3QSU6	-
TNC-203	ENST00000423613.6	6281	1928aa	Protein coding	-	E9PC84	-
TNC-212	ENST00000542877.5	5517	1838aa	Protein coding	-	F5H7V9	-
TNC-211	ENST00000537320.5	4946	1564aa	Protein coding	-	P24821	-
TNC-213	ENST00000544972.1	1844	615aa	Protein coding	-	HOYGZ3	-
TNC-209	ENST00000534839.1	734	92aa	Protein coding	-	F5H5D6	-
TNC-214	ENST00000635336.1	69	23aa	Protein coding	-	AOA0U1RR80	-
TNC-207	ENST00000481475.1	823	No protein	lncRNA	-	-	-
TNC-206	ENST00000476680.1	696	No protein	lncRNA	-	-	-
TNC-204	ENST00000460345.1	651	No protein	lncRNA	-	-	-
TNC-208	ENST00000498724.5	566	No protein	lncRNA	-	-	-
TNC-205	ENST00000473855.1	386	No protein	lncRNA	-	-	-

We avoided primers with nucleotide runs >5, high self-complementarity scores, and those forward and reverse sets with large Tm discrepancy. Further, we ensured that the selected genomic region encoded for proteins and was conserved across all transcript variants. See table 4.2 for list of known transcript variants. Based on the aforementioned parameters, we selected two of the best primer sets for *COL15A1* and *TNC* for optimization of primer conditions. Selected primer sets were ordered from and manufactured by Integrated DNA Technologies (Coralville, Iowa) and provided as 100  $\mu$ M concentration in pH 8.0 lab-ready solution.

#### 4.2.14 Polymerase Chain Reaction

cDNA amplification was carried out using a Taqman DNA Polymerase Kit (BIO-21105; Bioron, NSW, Australia). Briefly, in each reaction 1 µL of cDNA was added to 2.1 µL 5x MyTaq Reaction buffer, 0.5 µL each of 10 µM forward and reverse primers, 0.2 µL MyTaq DNA Polymerase, and DEPC-treated H<sub>2</sub>O to make up 10 µL volume. The reaction mix was cycled in an Eppendorf Mastercycler (Eppendorf, NSW, Australia) for 32 cycles at optimal T<sub>m</sub> determined in section 4.2.13 and visualized via SYBR safe (Bioron, NSW, Australia) stained 2% agarose gel electrophoresis. Images were captured under UV light exposure with a Gel Doc EZ Imager (Bioron, NSW, Australia).

#### 4.2.15 Optimisation of PCR Primer Conditions

A 1:10 dilution of provided primers in DEPC-treated H<sub>2</sub>O was made to obtain a 10 µM working solution. Primer sets were optimized for T<sub>m</sub> to determine which primer set would produce the best product – determined by clearest band with minimal non-specific binding – closest to 60°C to facilitate in SYBR qPCR. PCR was carried out in an Eppendorf Mastercycler gradient thermal cycler (Eppendorf, NSW, Australia) at temperatures ranging from 55°C to 65°C. DNA bands were visualized using 2% agarose Gel electrophoresis (Fig. 4.4) using recipe in table 4.3.

Table 4.3 2% Agarose Gel Recipe for Electrophoresis

Reagent	Amount
Agarose gel	4.0 g
1x TBE	200 mL

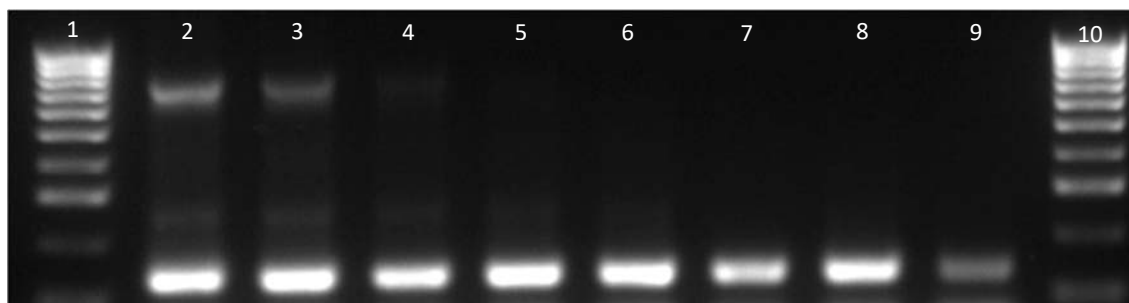


**Figure 4.4 Temperature Optimisation for *COL15A1* primer set.** Forward and reverse primer sets designed as outlined in section 4.2.11 were PCR cycled at temperatures ranging over 55-65°C to determine the optimal PCR temperature for each primer set. Lane 6 (59°C) produced the brightest product, whilst lane 7 (62°C) produced the clearest product, therefore we deemed this a suitable primer to use at 60°C. Lanes 1 & 10 contain 100 bp standard ladder. Products were visualised on a 2% agarose SYBR safe stained gel via electrophoresis.

Upon completion of optimization the decided primer pairs sequences for *COL15A1* and *TNC* were as follows:

*COL15A1* forward: 5'-TCTTTGGTGTGTCACAGGGG-3';

*COL15A1* reverse: 5'-GGAACAGAATGATCGCAGCC-3';

*TNC* forward: 5'-TATGTCCACAGC CCGAAGGC-3'; and

*TNC* reverse: 5'- CTGTCATTATTCAGAACAAGCCCC-3'.

#### 4.2.16 Optimisation of SYBR qPCR conditions

To determine the optimal concentration of our primers designed in section 4.2.11 for SYBR qPCR, we ran each primer with pooled gDNA at concentrations ranging from 100 nM – 500 nM primer. qPCR was carried out using StepOnePlus Real-Time PCR System (Applied Biosystems), followed by a subsequent melt curve analysis to validate sequence specificity. It was determined that 300 nM was the optimal concentration when considering both

amplification and melt curve efficiency. Amplified PCR product was run on a 2% agarose SYBR safe (Bioline, NSW, Australia) gel to validate amplification of a single product of the correct size.

#### 4.2.17 Quantitative PCR (gDNA)

**Table 4.4 SYBR qPCR Reaction Setup.** *COL15A1* and *TNC* templates in ChIP eluted gDNA were quantified using SYBR qPCR set up as outlined below.

<b>Reagent</b>	<b>Volume</b>
KiCqStart SYBR Green qPCR ReadyMix (2X)	5 $\mu$ l
Forward primer (10 $\mu$ M)	0.3 $\mu$ l
Reverse primer (10 $\mu$ M)	0.3 $\mu$ l
DEPC-treated H <sub>2</sub> O	8.6 $\mu$ l
gDNA template	3 $\mu$ l
<b>Final Volume</b>	10 $\mu$ l

Quantification of all gDNA products post-ChIP as outlined in section 4.2.10 were carried out using the intercalating dye system, KiCqStart SYBR Green qPCR Readymix (2x) with ROX (KCQS02; Merck, Germany). Reactions were set up as denoted in table 4.4 and cycled on a StepOnePlus Real-Time PCR System (Applied Biosystems) according to the following protocol:

Initial denaturation: 95°C, 20 seconds

PCR cycling (40 cycles): 95°C, 3 seconds

Post-extension data collection: 60°C, 30 seconds

With the addition of a continuous post-run melting analysis for sequence verification as follows:

Disassociation ramp: 95°C, 15 seconds

Reanneal ramp: 60°C, 1 min

Dissociation ramp: 95°C, 15 seconds

#### 4.2.18 Statistical analysis

The data were analysed for parametric distribution, with differences identified by 2-way ANOVA followed by Bonferroni post-hoc tests as specified. Data analysis was carried out using Graphpad Prism 8 software wherein a p-value < 0.05 is considered significant.

#### 4.2.19 In silico genomic analysis

Information pertaining to chromosomal location, genomic sequence, and transcript variants was obtained with use of National Center for Biotechnology Information (NCBI) Genome Data Viewer (GDV) (Bethesda MD, USA) and the Ensembl Genome Browser (Cambridge, UK). Chromosomal Ideograms representing target genes were generated by overlaying tracks downloaded from the NCBI GDV and Ensembl to the NCBI Genome Decoration Page (Bethesda MD, USA).

## 4.3 Results

### 4.3.1 Quantification of *TNC* template bound to acetylated histone H3

We carried out ChIP-PCR using an anti-H3ac antibody to determine if the promoter region for *TNC* was associated with acetylated histone H3. After IP pull down and subsequent gene amplification using SYBR, it is evident (Fig. 4.4) that there is no significant difference ( $p=0.8469$ ) in the basal levels of H3ac associated with the *TNC* promoter region between COPD ( $5.436 \pm 1.715$ ) and non-COPD ( $2.687 \pm 1.124$ ) smokers. Similarly, stimulation with TGF- $\beta$ 1 ( $p=0.8400$ ) did not induce a significant increase in H3ac levels associated with the *TNC* promoter in COPD ( $6.615 \pm 0.310$ ) or non-COPD ( $9.432 \pm 7.100$ ) smokers.

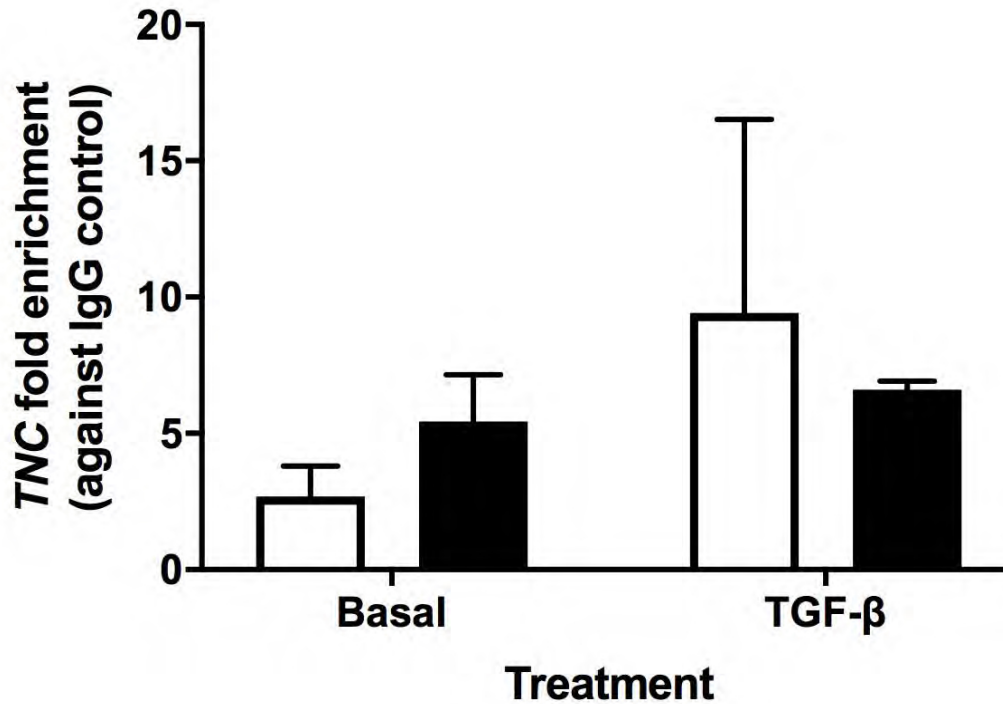


**Figure 4.5** *TNC* bound to acetylated H3 determined via ChIP-PCR. Sonicated chromatin collected from primary human ASM cultured in DMEM ± TGF-β1 (10ng/ml) for 48 hours was immunoprecipitated against anti-H3ac antibody using ChIP assay and *TNC* template was subsequently quantified using SYBR qPCR. It is evident that there is no significant difference between levels of *TNC* bound to acetylated H3 in either group basally or in response to stimulation. Results are expressed as fold change over negative IgG control (mean ± SEM) and analysed by 2way ANOVA followed by Bonferroni post-hoc analysis.

#### 4.3.2 Quantification of *COL15A1* template bound to acetylated histone H3

We carried out ChIP-PCR using an anti-H3ac antibody to determine if the promoter region for *COL15A1* was associated with acetylated histone H3. After IP pull down and subsequent gene amplification using SYBR, it is evident (Fig. 4.5) that there is no significant difference ( $p = 0.9957$ ) in the basal levels of H3ac associated with the *TNC* promoter region between COPD ( $13.760 \pm 9.161$ ) and non-COPD ( $6.423 \pm 3.481$ ) smokers. Similarly, stimulation with TGF-

$\beta$ 1 ( $p=0.7841$ ) did not induce a significant increase in H3ac levels associated with the *TNC* promoter in COPD ( $11.209 \pm 8.585$ ) or non-COPD ( $6.089 \pm 3.439$ ) smokers.

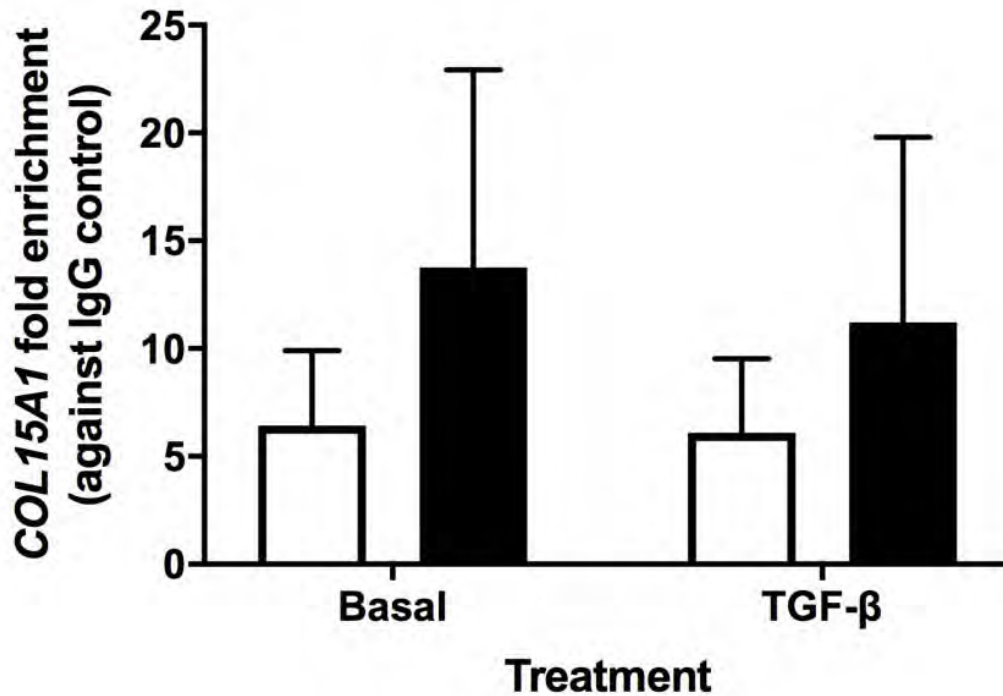


**Figure 4.6** *COL15A1* bound to acetylated H3 determined via ChIP-PCR. Sonicated chromatin collected from primary human ASM cultured in DMEM  $\pm$  TGF- $\beta$ 1 (10ng/ml) for 48 hours was immunoprecipitated against anti-H3ac antibody using ChIP assay and *COL15A1* template was subsequently quantified using SYBR qPCR. Results are expressed as fold change over negative IgG control. It is evident that there is no significant difference between levels of *COL15A1* bound to acetylated H3 in either group basally or in response to stimulation. Results are expressed as fold change over negative IgG control (mean  $\pm$  SEM) and analysed by 2way ANOVA followed by Bonferroni post-hoc analysis.



#### 4.3.3 Quantification of *TNC* template bound to acetylated histone H4

We carried out ChIP-PCR using an anti-H4ac antibody to determine if the promoter region for *TNC* was associated with acetylated histone H4. After IP pull down and subsequent gene amplification using SYBR, it is evident (Fig. 4.6) that there is no significant difference ( $p > 0.9999$ ) in the basal levels of H4ac associated with the *TNC* promoter region between COPD ( $49.393 \pm 6.482$ ) and non-COPD ( $40.811 \pm 10.988$ ) smokers. Interestingly, stimulation with TGF- $\beta$ 1 lead to a significant induction of acetylation of histone H4 at the *TNC* promoter in COPD only ( $p = 0.0339$ ). Causing a significant difference ( $p=0.0074$ ) in levels of H4 acetylation in response to TGF- $\beta$ 1 stimulation when comparing primary human ASM cells from COPD ( $152.378 \pm 42.788$ ) to those from non-COPD ( $31.830 \pm 16.211$ ).

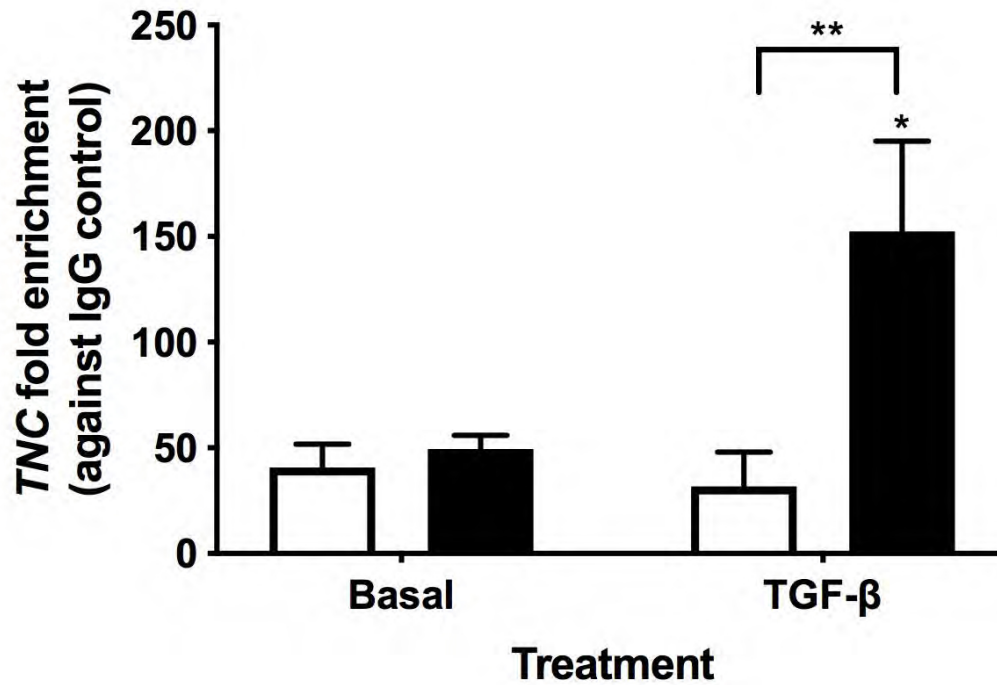


**Figure 4.7** *TNC* bound to acetylated H4 determined via ChIP-PCR. Sonicated chromatin collected from primary human ASM cultured in DMEM ± TGF-β1 (10ng/ml) for 48 hours was immunoprecipitated against anti-H4ac antibody using ChIP assay and *TNC* template was subsequently quantified using SYBR qPCR. It is evident that there is no significant difference between levels of *TNC* bound to acetylated H4 in either group basally whilst TGF-β1 stimulation induced histone H4 acetylation at the *TNC* promoter in COPD only. Results are expressed as fold change over negative IgG control (mean ± SEM) and analysed by 2way ANOVA followed by Bonferroni post-hoc analysis (\* $p < 0.05$ ; \*\* $p < 0.01$ ).

#### 4.3.4 Quantification of *COL15A1* template bound to acetylated histone H4

We carried out ChIP-PCR using an anti-H4ac antibody to determine if the promoter region for *COL15A1* was associated with acetylated histone H4. After IP pull down and subsequent gene amplification using SYBR, it is evident (Fig. 4.7) that there is no significant difference ( $p > 0.9999$ ) in the basal levels of H4ac associated with the *COL15A1* promoter region between COPD ( $3.725 \pm 1.494$ ) and non-COPD ( $14.688 \pm 12.235$ ) smokers. Interestingly, stimulation with TGF- $\beta$ 1 lead to a significant induction of acetylation of histone H4 at the *COL15A1* promoter in COPD only ( $p=0.0326$ ). Causing a significant difference ( $p=0.0355$ ) in levels of H4 acetylation in response to TGF- $\beta$ 1 stimulation when comparing primary human ASM cells from COPD ( $79.584 \pm 26.523$ ) to those from non-COPD ( $21.297 \pm 6.819$ ).

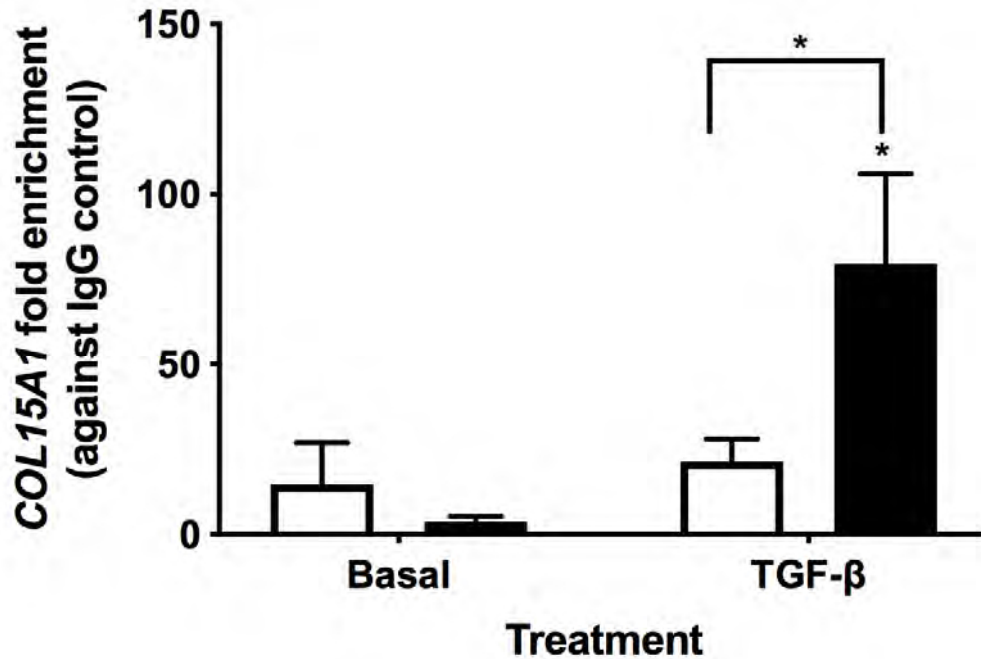


**Figure 4.8** *COL15A1* bound to acetylated H4 determined via ChIP-PCR. Sonicated chromatin collected from primary human ASM cultured in DMEM ± TGF-β1 (10ng/ml) for 48 hours was immunoprecipitated against anti-H4ac antibody using ChIP assay and *COL15A1* template was subsequently quantified using SYBR qPCR. It is evident that there is no significant difference between levels of *COL15A1* bound to acetylated H4 in either group basally whilst TGF-β1 stimulation induced histone H4 acetylation at the *COL15A1* promoter in COPD only. Results are expressed as fold change over negative IgG control (mean ± SEM) and analysed by 2way ANOVA followed by Bonferroni post-hoc analysis (\*p≤0.05).

#### 4.3.5 Vehicle test

Cells were treated with equivalent amounts of DMSO to those used in the JQ1 treatments and analysed alongside the samples in all equivalent assays. We found no significant effect attributed to DMSO only treatment when compared to basal expression (data not shown). Statistical analysis was carried out on Graphpad Prism 8 with differences assessed by unpaired t-tests ( $p \leq 0.05$  deemed significant).

#### 4.3.6 Dose-response relationship between Brd4 inhibition and *TNC* expression

In this section, we used JQ1 to competitively inhibit Brd4's acetyl lysine recognition site. Inhibiting Brd4 acetyl-lysine recognition allows us to determine if acetylated lysine residues play a role in the expression of *TNC* mRNA. JQ1 treatment had no effect on *TNC* mRNA expression at 1nM ( $p > 0.9999$ ) and 10nM ( $p > 0.9999$ ); whilst pre-treatment with 100 nM ( $p \leq 0.0001$ ;  $1.208 \pm 0.375$ ) and 1  $\mu$ M ( $p \leq 0.0001$ ;  $0.552 \pm 0.083$ ) demonstrated robust attenuation of TGF- $\beta$ 1 induced *TNC* mRNA expression in primary human ASM cells of COPD smokers. It should be noted that the suppression of TGF- $\beta$ 1 induced *TNC* mRNA expression in non-COPD susceptible smokers was not significantly abrogated at any of the JQ1 concentrations noted in Figure 4.8, although a trend of decreased *TNC* mRNA expression with increased JQ1 concentration expression is evident.

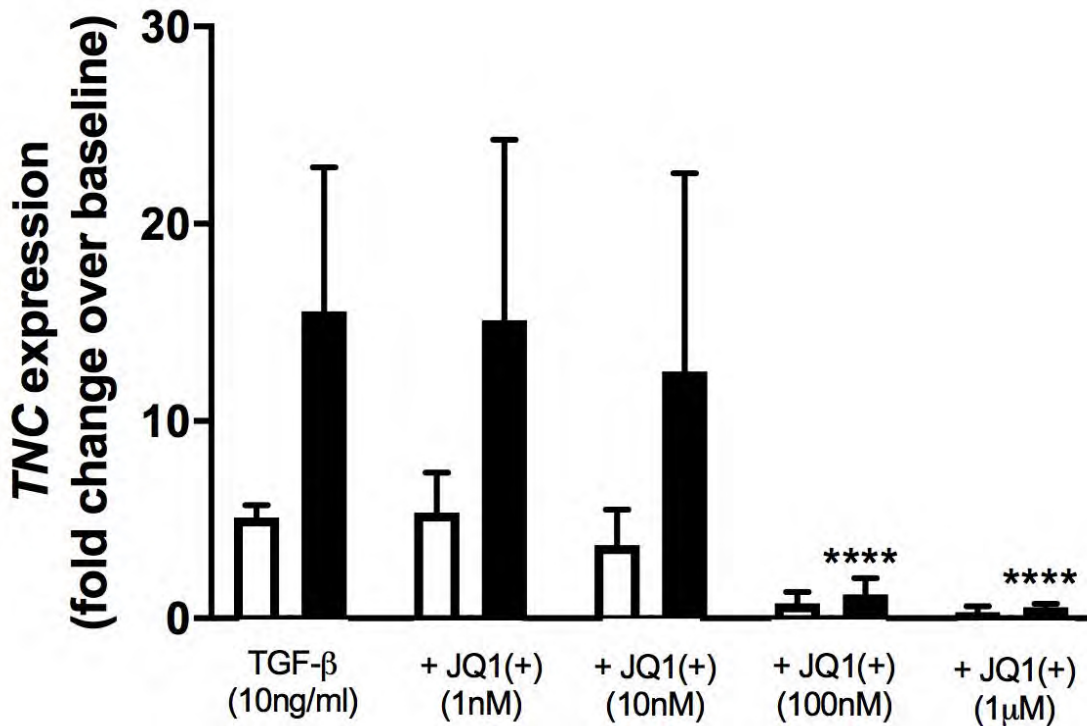


**Figure 4.9 Dose response of *TNC* mRNA expression post-Brd4 inhibition.** Primary human ASM cells were stimulated with TGF-β1 (10ng/ml) ± 1-hour JQ1 pre-treatment (1 nM, 10 nM, 100 nM, 1 μM). RNA lysates were collected at 48 hours and cDNA synthesized via RT-PCR. *TNC* template was quantified using probe-based PCR. All results were normalised against endogenous housekeeping gene 18s and are expressed as TGF-β1 induced fold change over basal expression. Data is expressed as mean ± SEM and analysed by 2way ANOVA followed by Bonferroni post-hoc analysis (\*\*\*\*p ≤ 0.0001).

#### 4.3.7 Dose-response relationship between Brd4 inhibition and *COL15A1* expression

In this section, we used JQ1 to competitively inhibit Brd4's acetyl lysine recognition site. Inhibiting Brd4 acetyl-lysine recognition allows us to determine if acetyl lysine residues play a role in the expression of *COL15A1* mRNA. JQ1 treatment had no effect on *COL15A1* mRNA expression at 1 nM ( $p > 0.9999$ ) and 10 nM ( $p > 0.9999$ ); whilst pre-treatment with 100 nM ( $p = 0.0009$ ;  $3.557 \pm 1.528$ ) and 1 μM ( $p = 0.0003$ ;  $0.309 \pm 0.102$ ) demonstrated robust attenuation of TGF-β1 induced *COL15A1* mRNA expression in primary human ASM cells of COPD

smokers. It should be noted that the suppression of TGF- $\beta$ 1 induced *TNC* mRNA expression in non-COPD susceptible smokers was not significantly abrogated at any of the JQ1 concentrations noted in Figure 4.9, although a trend of decreased *COL15A1* mRNA expression with increased JQ1 concentration is evident.

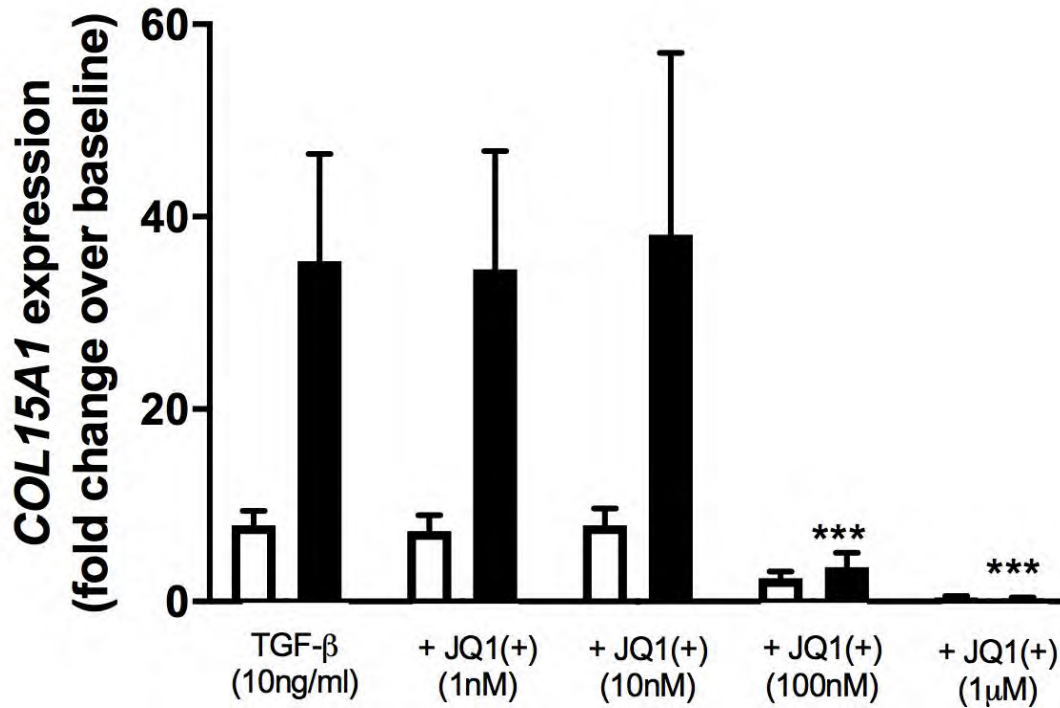


**Figure 4.10 Dose response of *COL15A1* mRNA expression post-Brd4 inhibition.** Primary human ASM cells were stimulated with TGF- $\beta$ 1 (10ng/ml)  $\pm$  1-hour JQ1 pre-treatment (1 nM, 10 nM, 100 nM, 1  $\mu$ M). RNA lysates were collected at 48 hours and cDNA synthesized via RT-PCR. *COL15A1* template was quantified using probe-based PCR. All results were normalised against endogenous housekeeping gene 18s and are expressed as TGF- $\beta$ 1 induced fold change over basal expression. Data is expressed as mean  $\pm$  SEM and analysed by 2way ANOVA followed by Bonferroni post-hoc analysis (\*\*\*) $p$  $\leq$ 0.001).

#### 4.3.8 Quantification of *TNC* template bound to acetylated histone H4 post Brd4 inhibition

We established that pre-treatment with 100 nM and 1  $\mu$ M of JQ1 significantly abrogates TGF- $\beta$ 1 induced *TNC* mRNA expression. To determine whether this effect was isolated to Brd4's recognition of acetyl lysine residues and subsequent transcriptional initiation, we carried out ChIP against acetylated histone H4 on primary human ASM cells that had been pre-treated with JQ1 at the effective concentrations (100 nM and 1  $\mu$ M). Results displayed in figure 4.10 demonstrate that JQ1 pre-treatment lead to a significant abrogation of the TGF- $\beta$ 1 induced acetyl lysine mark on histone H4 associated with the *TNC* promoter in COPD smokers at both 100 nM ( $p = 0.0018$ ;  $33.950 \pm 22.507$ ) and 1  $\mu$ M ( $p = 0.0002$ ;  $6.984 \pm 3.246$ ). Just as with mRNA expression in Figure 4.8, there is a trend of decreased H4 acetylation in response to JQ1 treatment in primary human ASM cells of non-COPD susceptible smokers, however statistical significance was not achieved.



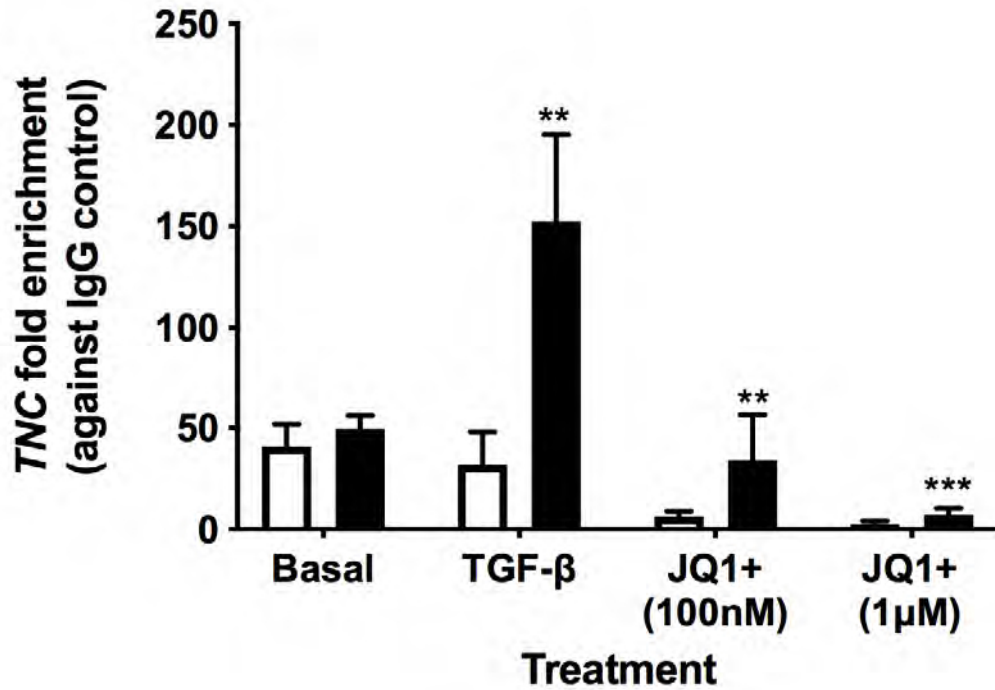


**Figure 4.11 *TNC* bound to acetylated H4 post-Brd4 inhibition determined via ChIP-PCR.** Sonicated chromatin collected from primary human ASM cultured in DMEM ± TGF-β1 (10ng/ml) for 48 hours ± pre-treatment with JQ1 (100 nM & 1 μM) was immunoprecipitated against anti-H4ac antibody using ChIP assay. *TNC* template was subsequently quantified using SYBR qPCR. Pre-treatment with JQ1 at 100 nM and 1 μM significantly abrogates histone H4 acetylation at the *TNC* promoter. Results are expressed as fold change over negative IgG control (mean ± SEM) and analysed by 2way ANOVA followed by Bonferroni post-hoc analysis (\*\*p≤0.01; \*\*\*p≤0.001).

#### 4.3.9 Quantification of *COL15A1* template bound to acetylated histone H4 post Brd4 inhibition

Further, it was established that pre-treatment with 100nM and 1 $\mu$ M of JQ1 significantly abrogates TGF- $\beta$ 1 induced *COL15A1* mRNA expression. To determine whether this effect was isolated to Brd4's recognition of acetyl lysine residues and subsequent transcriptional initiation, we carried out ChIP against acetylated histone H4 on primary human ASM cells that had been pre-treated with JQ1 at the effective concentrations (100 nM and 1  $\mu$ M). Results displayed in Figure 4.10 demonstrate that JQ1 pre-treatment lead to a significant abrogation of the TGF- $\beta$ 1 induced acetyl lysine mark on histone H4 associated with the *COL15A1* promoter in COPD smokers at both 100 nM ( $p = 0.0017$ ;  $6.797 \pm 2.636$ ) and 1  $\mu$ M ( $p = 0.0008$ ;  $1.337 \pm 0.271$ ). Those cells from non-COPD susceptible smokers did not respond to 100 nM treatment with JQ1, whilst 1  $\mu$ M induced a non-significant decrease in histone H4 acetylation bound to the *COL15A1* promoter in non-COPD susceptible smokers. These findings suggest that the level of acetylation that exists at a constant in non-COPD human ASM cells is less dependent on Brd4 to maintain the mark.

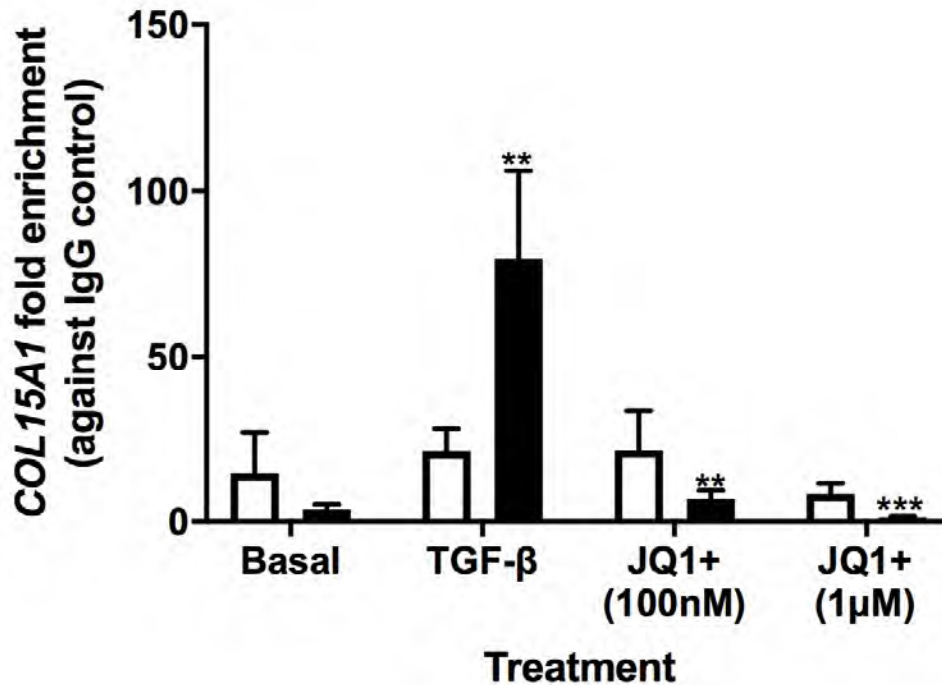


**Figure 4.12 *COL15A1* bound to acetylated H4 post-Brd4 inhibition determined via ChIP-PCR.** Sonicated chromatin collected from primary human ASM cultured in DMEM ± TGF-β1 (10 ng/ml) for 48 hours ± pre-treatment with JQ1 (100 nM & 1 μM) was immunoprecipitated against anti-H4ac antibody using ChIP assay. *COL15A1* template was subsequently quantified using SYBR qPCR. Pre-treatment with JQ1 at 100 nM and 1 μM significantly abrogates histone H4 acetylation at the *COL15A1* promoter. Results are expressed as fold change over negative IgG control (mean ± SEM) and analysed by 2way ANOVA followed by Bonferroni post-hoc analysis (\*\*p ≤ 0.01; \*\*\*p ≤ 0.001).

#### 4.3.10 Chromosomal location of ECM target genes in microarray analysis

Upon investigating the chromosomal location of each ECM gene in the microarray analysis we determined that *COL15A1* and *TNC* were both located on q arm of chromosome 9 with the former encoded by region bp 98,930,652 – 99,083,532, and the latter bp 115,009,706 – 115,128,124. Of all 92 genes assessed by ECM microarray Analysis only four were located on chromosome 9, all of which on the q arm (Fig. 4.9). See Appendix B for complete list of chromosomal location of each ECM gene assessed via microarray Analyses in Chapter 2.

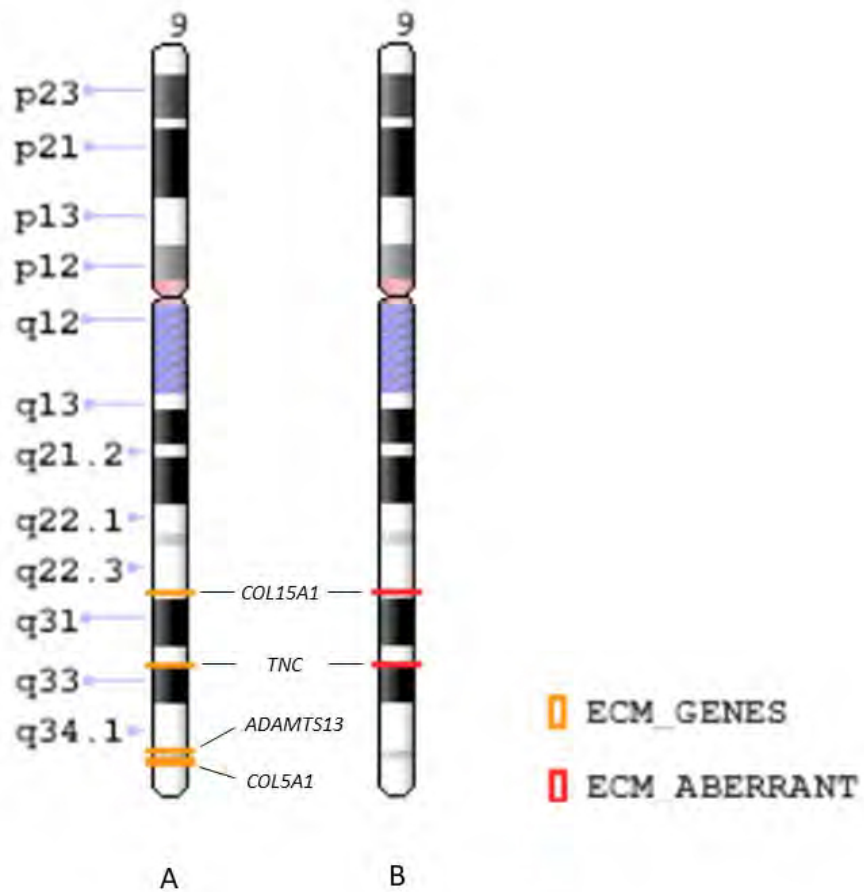


**Figure 4.13 Chromosome 9.** Depiction of chromosomal location of (a) all ECM genes residing on chromosome 9 that were included in our ECM microarray analyses in Chapter 2 (orange); and (b) the genes shown to be aberrantly expressed in COPD smokers in response to stimulation with TGF- $\beta$ 1 (10ng/ml) (red); Chromosomal ideogram was obtained from NCBI's GDP with tracks overlaid from NCBI's GDV and Ensembl Genome Browser (Genome assembly: GRCh38.p12).

## 4.4 Discussion

In this Chapter, we have used ChIP-PCR to detect whether acetylated histones H3 and H4 are bound to the promoter region of genes of *TNC* and *COL15A1*. ChIP-PCR is considered the gold-standard technique used to characterize histone modifications within a defined region of the genome (264). We selected these genes of interest based on evidence presented in Chapter 2, where it was shown that *TNC* and *COL15A1* expression was significantly higher in response to stimulation with TGF- $\beta$ 1. Our choice to focus on the epigenetic mechanism of histone acetylation was based on our findings presented in Chapter 3, where it was shown that HDAC inhibition lead to differential expression of TGF- $\beta$ 1 induced *TNC* mRNA when comparing primary human ASM cells from COPD to non-COPD susceptible smokers.

We have shown that neither histone H3 nor H4 demonstrate differential baseline acetylation levels at the *COL15A1* or *TNC* promoter between cohorts (Fig. 4.4-4.7). These results indicate that the difference in gene expression measured between COPD and non-COPD cohorts is not attributable to a basal difference in acetylation of histone H3 or H4 bound to the promoter region for *COL15A1* or *TNC*. The absence of a basal difference in acetyl-lysine marks corresponds with the absence of aberrant ECM mRNA expression at baseline shown in Chapter 2. However, what should be noted is that although there is no significant difference in basal acetylated histones H3 and H4 bound to the *COL15A1* and *TNC* promoter, there is fold enrichment against the IgG control in all instances, suggesting that a proportion of cells do express acetylation at the *COL15A1* and *TNC* promoters at any given time in COPD and non-COPD.

Upon treating cells with TGF- $\beta$ 1, ChIP-PCR detected no significant induction of histone H3 acetylation bound to the *COL15A1* (Fig. 4.5) or *TNC* (Fig. 4.4) promoter region. When immunoprecipitating against anti-acetyl H4, however, it was shown that TGF- $\beta$ 1 stimulation significantly augmented levels of histone H4 acetylation associated with the promoter region for *COL15A1* (Fig. 4.7) and *TNC* (Fig. 4.6) in COPD only. The differential acetylation patterns established demonstrate a differential response in COPD that follows the pattern of increased expression of *COL15A1* and *TNC* mRNA demonstrated in Chapter 2. These results are induced by TGF- $\beta$ 1 stimulation, rather than during basal expression, suggesting that the differences in response to this cytokine is where the mechanism underlying aberrant ECM expression resides. Using TGF- $\beta$ 1 to stimulate the response is relevant to COPD as levels have been shown to be elevated in COPD (67-70 via koenigshoff). Therefore, studying TGF- $\beta$ 1's effect on COPD is especially pertinent. We propose that SMAD2 and SMAD3 may be involved in the induction of histone acetylation as they have been shown to recruit histone acetyl transferases p300 and CBP to gene promoter regions (265, 266), however we assert that the aberrancy does not lie in overall TGF- $\beta$ 1 signalling as we did not see aberrant expression of all TGF- $\beta$ 1 induced ECM proteins in COPD.

To elucidate whether this acetyl mark directly contributed to the expression of *COL15A1* and *TNC*, we used a competitive inhibitor (JQ1) of the acetyl-lysine binding pockets of Brd4. In doing so we demonstrated that pre-treatment with both 100 nM or 1  $\mu$ M significantly attenuated expression of *COL15A1* and *TNC*, whilst lower concentrations (10 nM and 1 nM) did not. These findings confirm that Brd4 recognition of acetyl-lysine residues plays a direct role in the transcriptional expression of *COL15A1* (Fig. 4.8) and *TNC* (Fig. 4.9) and subsequently, directly linking histone H4 acetylation at the *COL15A1* and *TNC* promoter to the increased expression of these ECM genes in COPD. It should be noted that although only the COPD group showed

statistically significant attenuation of *COL15A1* and *TNC* mRNA expression, there was a trend of reduced expression in non-COPD. These results are compatible with those shown in Figures 4.4-4.7 where basal expression of *TNC* and *COL15A1* was not at zero, indicating that there was a level of histone acetylation associated with the promoter region of these genes at baseline in both groups. Therefore, we posit that the trend of decreased ECM gene expression in non-COPD human ASM cells in response to JQ1 stimulation is via inhibiting recognition of baseline acetylation.

Considering the duality of Brd4's epigenomic function – with a role in epigenetic memory in addition to transcriptional regulation – we decided to investigate the effect of Brd4 inhibition on histone H4 acetylation. Upon performing anti-acetyl H4 ChIP-PCR on cells treated with the effective concentrations of JQ1 (100 nM and 1  $\mu$ M), we demonstrated a significant ablation of the TGF- $\beta$ 1 induced acetyl-lysine mark on histone H4 associated with *COL15A1* (Fig. 4.11) and *TNC* (Fig. 4.10). The loss of acetylated marks post-inhibition with JQ1 demonstrates that Brd4 plays a role in propagating epigenetic memory to underpin aberrant expression of *COL15A1* and *TNC* in COPD. Interestingly, the efficacy in doing so is less potent in cells from non-COPD susceptible smokers in terms of *COL15A1* expression (Fig. 4.11) where it is evident that 100 nM JQ1 pre-treatment had no effect on *COL15A1* mRNA expression. Based on these results we posit that the acetyl histone H4 marks bound to the *COL15A1* promoter detected in the non-COPD susceptible cohort are *de novo* PTMs and not propagated through mitosis after treatment with TGF- $\beta$ 1; whilst the significantly higher levels of TGF- $\beta$ 1 induced histone H4 acetylation in cells from COPD patients is maintained by Brd4 activity. Based on these findings, we infer that cells from COPD patients demonstrate aberrant *COL15A1* and *TNC* expression due to TGF- $\beta$ 1 induced histone H4 acetylation that is dependent on Brd4 to maintain and propagate acetyl H4 marks to cell progeny.

To delineate why certain genes were responding this way to TGF- $\beta$ 1 stimulation without an established inherent difference in acetylation at baseline we considered the chromosomal location of each ECM gene on our microarrays used in investigations detailed in Chapter 2. Upon doing so we determined that our two target genes resided on the same arm (q) of chromosome 9 (Fig. 4.12). Two other genes from the ECM array included on Chr9 included *ADAMTS13*, which encodes for a protease involved in blood clotting by cleaving von Willebrand factor (267), and *COL5A1*, which was initially picked up by our microarray analyses but did not meet statistical significance. It should be noted that our target genes were proximal to one another.

Late research that has shown Brd4 to demonstrate inherent histone acetyltransferase capacities (199) suggests that our findings may be explained by this phenomenon. However, we posit that Brd4 acting as a HAT is an unlikely explanation of our findings as any aberrations in histone acetyltransferase capacity of the COPD ASM cells would have been revealed in our HAT activity assays

In summary, this Chapter demonstrates that TGF- $\beta$ 1 stimulation of primary human ASM cells from COPD patients induces histone H4 acetylation at the promoter region for *COL15A1* and *TNC*. We demonstrate that competitive inhibition of acetyl-lysine recognition by Brd4 significantly attenuates *COL15A1* and *TNC* mRNA expression and leads to a loss of the acetyl-lysine mark on histone H4. These results suggest that Brd4 plays a role in transcriptional regulation and epigenetic memory in specific and targeted manner in COPD. Apart from the data presented in this thesis, no other reports have examined the interaction between TGF- $\beta$ 1 stimulation and acetylation of promoter regions associated with ECM genes in COPD.



## Chapter 5 Summary, Future Directions, and Conclusion

### 5.1 Introduction

COPD is a disease characterised by persistent loss of lung function, manifesting in persistent shortness of breath. COPD is a progressive disease with no current cure, leaving transplantation the only medical intervention available to patients wanting to avoid significant disability and inevitable mortality. Although the disease is characterised by two primary phenotypes: small airways disease prominent and emphysematous destruction prominent, it has been established that small airways disease precedes emphysematous destruction. Thorough investigations into pathophysiological changes underpinning small airways disease have shown that the primary cause of airway obstruction in COPD is increased ECM deposition. It has further been shown that ECM deposition within the ASM layer contributes to small airway obstruction, and the degree of which inversely correlates with FEV<sub>1</sub>. The relationship between ECM, the ASM and FEV<sub>1</sub> demonstrates the role ASM plays in small airway fibrosis and subsequent obstruction. *In vitro* investigations have shown that primary mesenchymal cells from COPD patients deposit more ECM in response to stimuli than those cells from non-COPD patients, independent of differences in transcription factor activity (68). Considering the aforementioned alongside established epidemiological evidence highlighting a hereditary link in COPD and statistics demonstrating that only a small proportion of smokers develop COPD, we hypothesized that there is an underlying epigenetic mechanism modulating small airway fibrosis in COPD and therein bestowing a “COPD susceptible” population.

The aim of this study was to carefully identify study subjects based on known lung function measurements and smoking history. In doing so, we carefully selected a cohort of smokers with and without airway obstruction, which we labelled “COPD susceptible smokers” and “non-

COPD susceptible smokers”, respectively. We used primary ASM cells from these cohorts in all of the investigations in this study.

## 5.2 Determination of aberrantly expressed ECM genes in COPD

To investigate an aberrant ECM gene response, we aimed to use a stimulus that was proven capable to induce ECM expression that was relevant to COPD. We decided upon the cytokine TGF- $\beta$ 1 as it fulfilled the aforementioned criteria. It has been well established in numerous studies in our lab and labs of others that TGF- $\beta$ 1 is an appropriate stimulus to generate an ECM induction response from our cell type. Prior temporal analyses of ECM upregulation demonstrated that the 48-hour time point coincided with peak ECM gene expression in our cell type. Upon carrying out a microarray analysis targeting 92 ECM genes in DMEM only and TGF- $\beta$ 1 stimulated samples, it was shown that four genes (*TNC*, *COL15A1*, *COL5A1*, and *ITGAI*) were differently expressed in response to TGF- $\beta$ 1 stimulation in pooled cDNA samples from COPD susceptible smokers when compared to those sampled from non-COPD susceptible smokers. Further qPCR validation confirmed that *TNC* and *COL15A1* were significantly upregulated in response to TGF- $\beta$ 1 stimulation in COPD susceptible smokers.

To demonstrate that the ECM proteins encoded for by these genes were deposited within the ASM layer *in vivo*, we carried out IHC staining against anti-collagen 15 $\alpha$ 1 and anti-tenascin-c on paraffin embedded sections of small airway from COPD explant tissue. We noted positive staining for collagen 15 $\alpha$ 1 and tenascin-c within the airway wall. Interestingly, collagen 15 $\alpha$ 1 deposition appeared predominantly localised to the ASM layer, suggesting that ASM cells are the primary source of collagen 15 $\alpha$ 1 deposition in the small airway. We further showed that

collagen 15 $\alpha$ 1 deposition was significantly higher in *in vivo* thereby demonstrating that this protein is a primary contributor to increased ECM deposition in COPD airways.

It is of import to note that not every ECM gene induced by TGF- $\beta$ 1 had aberrant expression in COPD, with significantly higher upregulation being unique to *COL15A1* and *TNC*, thereby indicating that the aberrance is gene specific rather than an overall enhanced TGF- $\beta$ 1 response in COPD. We posit that if our results were reflecting the former, many more ECM genes induced by TGF- $\beta$ 1 would be aberrantly expressed.

### 5.3 Investigations into epigenetic aberrations underlying ECM expression in COPD

To identify epigenetic aberrations between COPD and non-COPD susceptible peoples' ASM cells, we used established inhibitors of well understood epigenetic modifications – DNA methylation, histone acetylation, and histone methylation. We used the ECM genes identified to be aberrantly expressed in COPD in Chapter 2 as a target and cultured primary human ASM cells with and without aforementioned inhibitors to screen for different outcomes in target gene expression between our cohorts. Pre-treatment with inhibitors for LSD and HAT showed no significant difference in TGF- $\beta$ 1 induced *COL15A1* or *TNC* expression in cells from either cohort. Whilst DNMT1 inhibition lead to significant abrogation of *COL15A1* expression from each cohort, with no significant difference in expression level between them. HDAC inhibition lead to significantly different expression of *TNC* when comparing non-COPD to COPD susceptible smokers. Although pre-treatment did not lead to significant changes from baseline, the differential response between the two cohorts suggested that histone acetylation mediated transcriptional regulation at the promoter regions for *TNC* differ. Although the differential results for *COL15A1* expression by non-COPD and COPD human ASM cells post-HDAC

inhibition did not attain statistical significance, they followed the same trend as *TNC* which suggested that the underlying mechanisms in expression of our target genes may be shared.

To elucidate whether this was an effect in overall HAT or HDAC activity, we obtained nuclear lysates from human ASM cells of our study groups and carried out enzyme activity assays. Our results found no significant difference in HAT or HDAC activity between non-COPD and COPD susceptible smokers. These findings assert that the mechanism underlying increased *COL15A1* and *TNC* expression isn't a consequence a global dysregulation of histone modifying enzymes and further underpin our earlier supposition that the aberrancy in *TNC* and *COL15A1* expression by COPD human ASM cells is at the gene specific level.

Our results from the HDAC activity assay sit in contrast with a study on immune cells and peripheral lung tissue from COPD patients wherein it was shown that those samples from COPD patients had significantly lower levels of HDAC activity. It was further shown that HDAC2 expression was lower in these samples and other studies demonstrated that restoring HDAC2 expression enhanced the glucocorticoid response in COPD. It is well established that different epigenetic modifications dictate cell fate lineage, therefore different cell types will exhibit different epigenetic modifications. Further, immune cells have been shown to be demonstrate enhanced phenotypic plasticity and therefore are more susceptible to variations in epigenetic enzymes as these variations underpin their role in the innate immune system. Apart from the data presented in this thesis, no other reports have examined epigenetic modulation of small airway fibrosis in COPD.

## 5.4 Chromatin targeted investigation of histone acetylation

To directly assess the level of acetylated histones H3 and H4 we performed ChIP-PCR on TGF- $\beta$ 1 stimulated human ASM cells of our selected cohorts. We found that there was no significant difference in basal H3 and H4 acetylation levels bound to the promoter for *COL15A1* nor *TNC*. However, we did note that there was positive fold change in basally treated human ASM cells of either cohort bound to each target gene's promoter. This finding demonstrates that a proportion of lysine residues are acetylated at baseline.

Upon stimulating with TGF- $\beta$ 1, we measured a significant upregulation in histone H4 acetyl-lysine residues bound to the promoter regions for both *TNC* and *COL15A1*. Whilst there was no significant difference in histone H3 acetylation bound to the target gene promoter regions. This is the first study demonstrating a direct induction of an aberrant epigenetic mark associated with an ECM gene in COPD. Our results showing increased histone acetylation in COPD human ASM whilst global HAT activity remains unaltered between cohorts determines that these findings cannot be attributed to a global shift in enzymatic activity. This correlates with *in vivo* experiments showing cigarette smoke induced histone H3 & H4 acetylation at specific lysine residues independent of global HAT upregulation in a murine model (268, 269). These findings are further corroborated in lungs of non-COPD and COPD susceptible smokers (270). Demonstrating that acetylation can be induced in a targeted and specific manner.

To demonstrate that histone H4 acetylation played a role in the expression of *TNC* and *COL15A1*, we performed dose-response experiments using an inhibitor of the epigenetic reader Brd4: JQ1. JQ1 competitively and selectively binds to the acetyl-lysine recognition motif on Brd4. We showed that pre-treatment with 100 nM of JQ1 was enough to significantly attenuate

both *COL15A1* and *TNC* mRNA expression and the attenuation persisted at a pre-treatment concentration of 1  $\mu$ M. These findings demonstrate that the recognition of acetylated lysine residues by Brd4 is essential in the transcriptional elongation of *COL15A1* and *TNC*. Brd4's role in relieving transcriptional pause and conferring mRNA elongation has been described to be constitutive. Therefore, the aberrancy would not lie in Brd4's transcriptional capacity and the epigenetic reader's role in pathology would be limited to the expression of an aberrant acetyl lysine mark. However, given that Brd4 does not directly interact with DNA or RNA Pol II and subsequently relies on an "interacting partner" (253), the known panel of transcriptional regulators capable of recruiting and interacting with Brd4 should be investigated to delineate any aberrancies in their activity levels in COPD. A detailed protein interaction analysis showed Brd4 capable of interacting with p53, YY1, AP2, c-Jun, C-Myc/Max, C/EBP $\alpha$ , C/EBP $\beta$ , Acfl, and G9a (253). The aforementioned study was the first to identify two conserved regions in Brd4 separate to the acetyl binding residues BD1 and BD2. These were referred to as basic residue-enriched interaction domain (BID) and phosphorylation dependent interaction domain (PDID). It was further shown that the regulatory domain of p53 interacts with Brd4 via PDID to selectively regulate transcription at the gene specific level. The identification of these domains reveal how a transcriptional triad through an interacting partner would work to confer gene specificity to an otherwise constitutive function of Brd4.

Further, Brd4 has been described to have dual roles with its second being that of an epigenetic bookmark to carry acetyl-lysine marks through mitosis. This function has been described to be more gene specific and gives Brd4 the capacity to conservatively propagate specific acetyl-lysine marks to cell progeny. To investigate whether Brd4 was acting in this capacity we carried out ChIP-PCR on cells pre-treated with the effective concentrations of JQ1. Interestingly, JQ1

pre-treatment lead to a complete abrogation of TGF- $\beta$ 1 induced histone H4 acetylation at the *COL15A1* and *TNC* promoter region. This finding demonstrates that Brd4 plays a role in maintaining histone H4 acetylation in COPD. Based on this evidence, we posit that the augmented histone H4 acetylation at the promoter region for *COL15A1* and *TNC* is maintained by Brd4's capacity as an epigenetic bookmark.

Figures 5.1, 5.2, and 5.3 summarise the major findings of the preceding Chapters, in addition to established literature about ECM production and epigenetic modulation in COPD.

# Aim 1

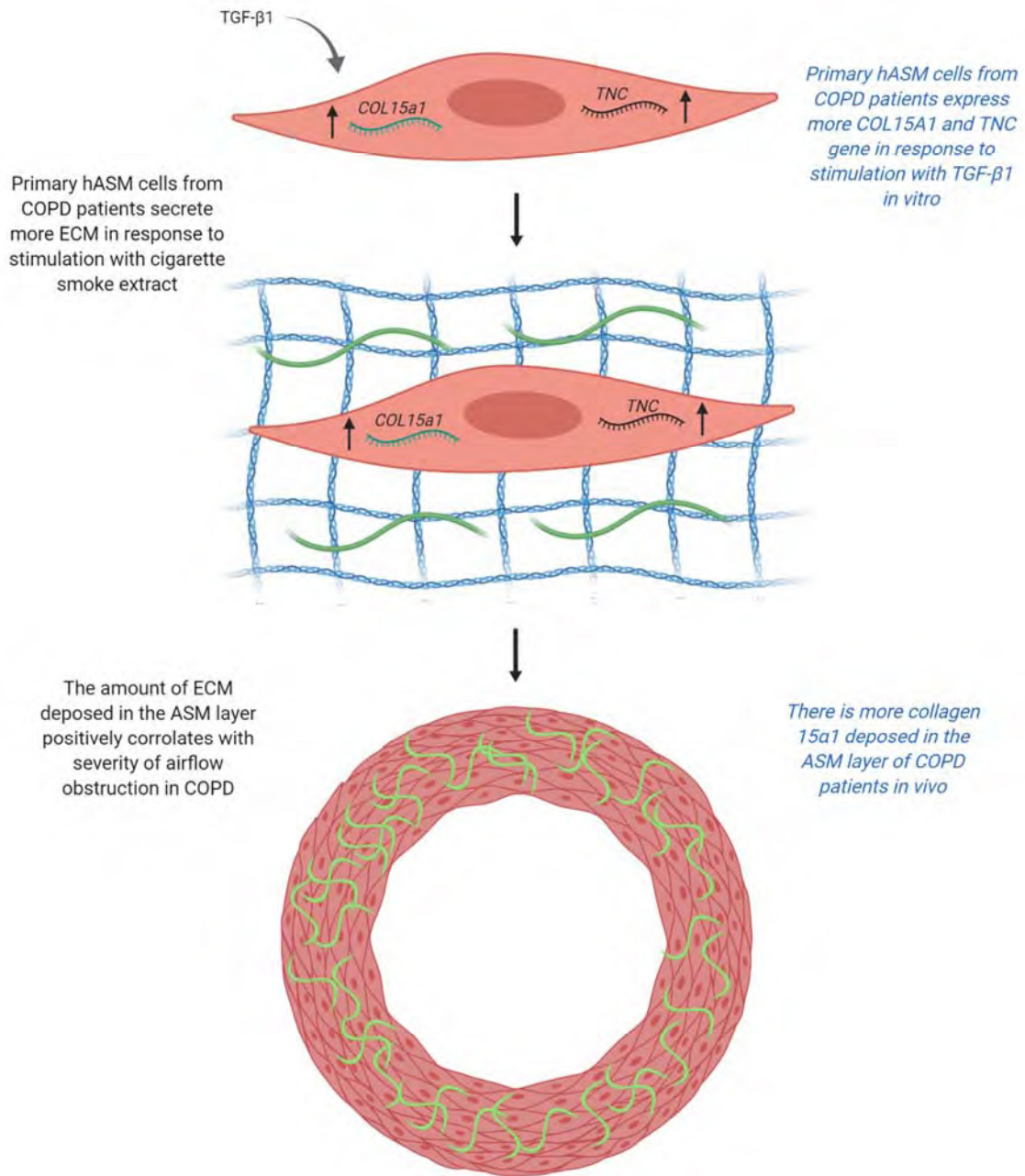


**Figure 5.1** ASM cells produce more ECM in COPD *in vitro* and *in vivo*. Text in black indicates previously known effects.

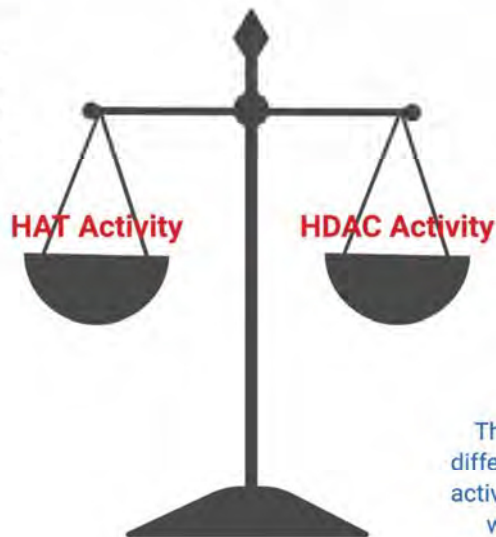
Text in blue indicates new findings presented in this thesis.



# Aim 2

		Dampening acetylation (Curcumin)	Promoting acetylation (Trichostatin A)	Dampening DNA methylation (5-azacytidine)
	TGF- $\beta$ 1 Induction Pattern	Differential response?	Differential response?	Differential response?
<b>COL15A1</b>	Increased in COPD	✗	✗	✗
<b>TNC</b>	Increased in COPD	✗	✓	✗

Macrophages and peripheral tissue samples from COPD patients have higher HDAC activity than non-obstructed smokers; whilst HAT activity does not differ



There is no significant difference in HAT or HDAC activity in COPD ASM cells when comparing to non-obstructed smokers

**Figure 5.2 Summary of Aim 2 Findings.** In this screening step, we found that HDAC inhibition showed a significantly different response in COPD whilst overall activity levels of histone acetyl modifying enzymes did not differ. Therefore, we surmised to investigate targeted chromatin modifications using ChIP-PCR. Text in black indicates previously known effects. Text in blue indicates new findings presented in this thesis.

# Aim 3

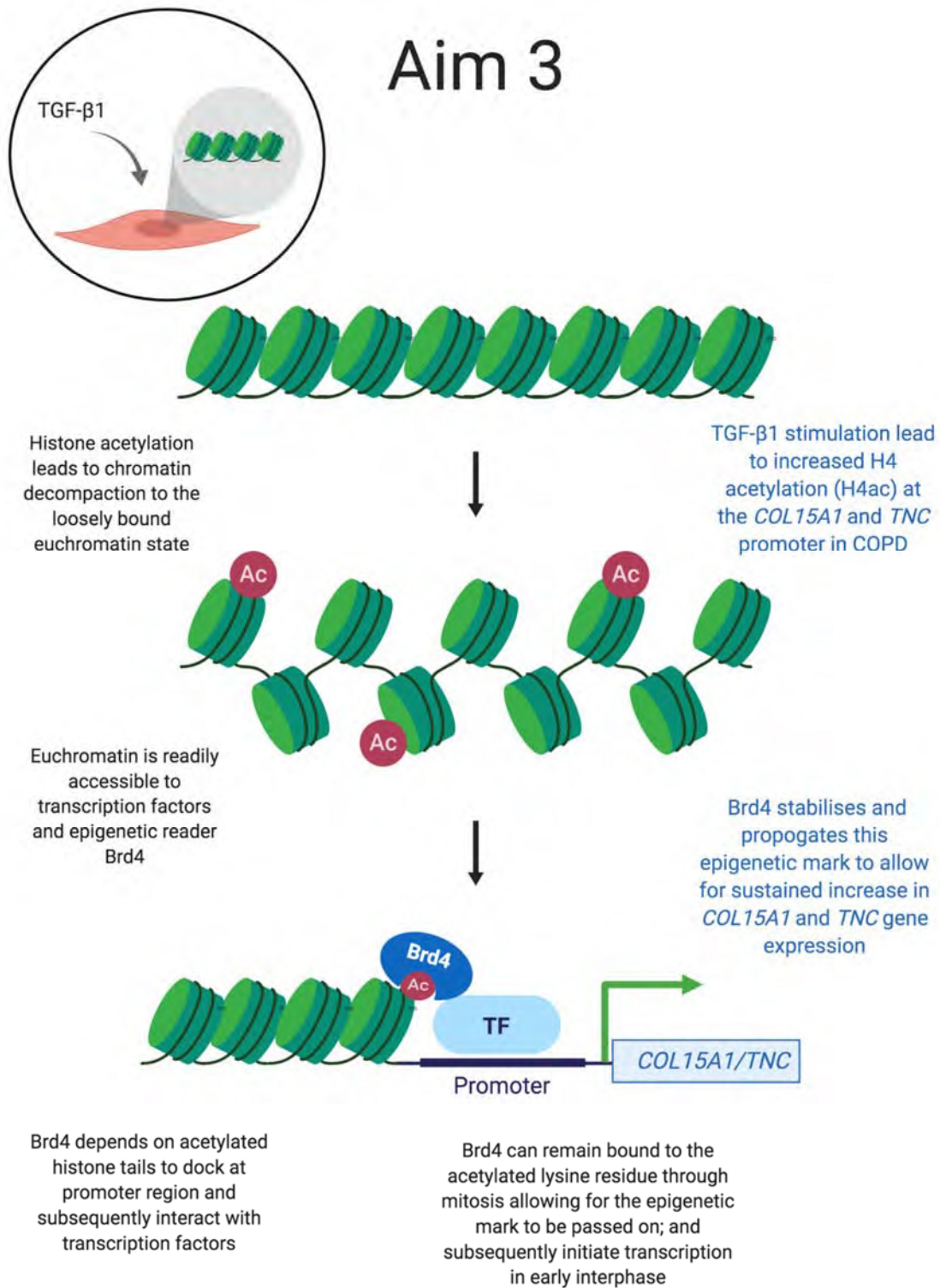


**Figure 5.3 TGF-β1 induces Brd4 mediated H4ac in COPD.** Text in black indicates previously known effects. Text in blue indicates new findings presented in this thesis.

## 5.5 Future Directions

This is the first report on epigenetic modulation of ECM expression in primary human ASM cells. Therefore, our findings can be considered the first step in delineating the intricate epigenetic mechanisms underlying small airway fibrosis in COPD. In Chapter 2, we identify two ECM genes with augmented expression in COPD. It is known that increased ECM deposition contributes to ASM bulk within the airway wall. What remains to be elucidated is the specific bioactive effect of increased *COL15A1* and *TNC* on ASM and other surrounding cells in the airway wall. Therefore, our first recommendation is for future studies to thoroughly investigate the propensity of these ECM proteins to initiate a positive feedback cascade that would accelerate further fibrosis, inflammation, and subsequent airway obstruction. Experiments would focus on cell migration, cytokine production, and ECM deposition from cells cultured on collagen 15 $\alpha$ 1 and tenascin-C substrates. Given the progressive nature of small airway fibrosis and COPD pathogenesis overall, it is likely that such a cascade is contributing to disease progression.

In Chapter 3 we carried out epigenetic screening experiments. The extent of our investigation as a screening step between two cohorts was particular to this study, however we assert that they do not conclusively exclude the role other epigenetic marks may play in overall pathology. It is well established that epigenetic marks have been shown to interact with one another. *In vitro* experiments have shown DNMT1 interacting with G9a to induce DNA methylation (271) and DNA methylation outcomes being dictated by H3K9 methylation (272). Therefore, we recommend ongoing investigation into other epigenetic marks that may interact with the increased histone H4 acetylation mark induced by TGF- $\beta$ 1.

Our findings demonstrate an increase in H4 histone acetylation at the promoter region for *COL15A1* and *TNC* in response to TGF- $\beta$ 1 treatment unique to COPD susceptible smokers. Through use of competitive inhibitor JQ1, it was further shown that Brd4 played a significant role in transcription of *TNC* and *COL15A1*. Most interestingly, Brd4 inhibition lead to a loss of TGF- $\beta$ 1 induced histone H4 acetylation demonstrating that Brd4 plays a role in epigenetic memory of TGF- $\beta$ 1 induced histone H4 acetylation. Another route of inquiry should surround proteins upstream from Brd4 recruitment to the promoter region. It has been shown that Brd4 cannot directly interact with RNA Pol II, but does bind with p53, YY1, c-Jun, AP2, C/EBP $\alpha$ , C/EBP $\beta$ , and Myc/Max (253). These findings underpin the theory that Brd4 dependant gene expression depends on a “triad” of factors at the promoter region (i) RNA Pol II in a state of transcriptional pause; (ii) a transcription factor capable of interacting with Brd4 (“interacting partner”); and (iii) subsequent recruitment of Brd4 by the interacting partner to relieve transcriptional pause and commence elongation. Therefore, it would be beneficial for future investigations to use ChIP-PCR using antibodies for the aforementioned proteins to determine if there is a discrepancy between the levels of these transcription factors bound to the promoter region of our target genes when comparing non-COPD to COPD susceptible smokers. In order to build upon our findings and further delineate specific mechanisms contributing to increased ECM gene expression it is imperative for future reports to investigate the levels of Brd4 interacting molecules in COPD. Future investigations would consider the chromatin targeting specificity of each interacting partner and subsequent recruitment of JQ1.

We established that our target genes share a chromosomal location, highlighting a possible mechanism underlying the mirrored response by the two ECM genes in our investigations. To widen the scope of our investigation outside of those genes on the microarray we identified all known genes nearby *COL15A1* and *TNC* and their established function. We found that

*TGFBR1* which encodes for the type I TGF- $\beta$ 1 receptor AKL5 (table 1.2) resides between *COL15A1* and *TNC*. Furthermore, it is of import to note that *TGFBR1* is directly downstream from *COL15A1*. See Appendix D for a GDV screen excerpt of gene proximity.

Investigations into *TGFBR1* fell out of the scope of this study, however a study using peripheral lung tissue from non-smokers, non-COPD smokers, and COPD susceptible smokers found no significant difference in *TGFBR1* expression between non-COPD and COPD susceptible smokers (273). It should be noted that these results are of homogenized tissue samples and therefore are only indicative of baseline differences, which do not occur in our target genes. Given that an established mechanism of TGF- $\beta$ 1 signal modulation is internalization and subsequent degradation of activated TGF- $\beta$ 1 receptors, we posit that stimulating our primary human ASM may have triggered TGF- $\beta$ 1 receptor endocytic trafficking, leading to eventual degradation of expressed receptors. Ergo, necessitating receptor replenishment which is likely fulfilled via epigenetic activation of *TGFBR1*. Considering that evidence of transgenic acetylation patterns across a chromosomal region has been established (274, 275), this may be one possible mechanism contributing to TGF- $\beta$ 1 induced acetylation at the promoter region for our target genes *COL15A1* and *TNC*. However, it is to be noted that due to the paucity of investigations into the effect of TGF- $\beta$ 1 on *TGFBR1* expression and the mechanism underlying TGF- $\beta$  receptor trafficking, this position is based on indirect evidence and is merely a hypothesis. We infer that this is a promising field of investigation in further elucidating epigenetic mechanisms contributing to COPD.



## 5.6 Conclusion

The overall aim of this investigation was to determine why ASM cells from COPD patients produce more ECM in response to fibrotic stimulus. Our hypothesis was that the aberrancy was epigenetic, which is best described by Riggs (276) as “mitotically or meiotically heritable changes in gene function” not attributable to changes in DNA sequence. What lies at the crux of every epigenetic investigation is the question: which came first, the epigenetic modification or the disease? Investigating a disease that commonly presents in smoking populations, we aimed to address this question by ensuring we were making comparisons between two populations of smokers to control for the confounding effect of cigarette smoke induced epigenetic change. To delineate the epigenetic effect, we identified a pathophysiological mechanism that contributed to small airway fibrosis and subsequent obstruction – ECM deposition within the ASM layer – and modeled our epigenetic investigations around this pathology. We, for the first time, showed that the underlying mechanism of increased ECM gene expression in COPD is induction of histone H4 acetylation at the promoter region for *COL15A1* and *TNC*. Further, we demonstrated that Brd4 plays a role in maintaining histone H4 acetylation, thereby unveiling the molecular mechanism underpinning the mitotic heritability of TGF- $\beta$ 1 induced histone H4 acetylation and a possible therapeutic target for small airway fibrosis in COPD. These findings are bolstered by our model using human mesenchymal cells from the primary site of pathological insult in COPD. The data presented in this thesis are novel in the field of respiratory cell and molecular biology, as no other reports have examined the epigenetic mechanisms modulating small airway fibrosis in COPD.

## Appendix A – Publications Included as an Adjunct to This Work

Article

# A Mitochondrial Specific Antioxidant Reverses Metabolic Dysfunction and Fatty Liver Induced by Maternal Cigarette Smoke in Mice

Gerard Li <sup>1</sup>, Yik Lung Chan <sup>1,2</sup>, Suporn Sukjamnong <sup>3</sup>, Ayad G. Anwer <sup>4</sup>, Howard Vindin <sup>2</sup>, Matthew Padula <sup>1</sup> , Razia Zakarya <sup>1,2</sup>, Jacob George <sup>5</sup>, Brian G. Oliver <sup>1,2</sup>, Sonia Saad <sup>1,6</sup> and Hui Chen <sup>1,\*</sup> 

<sup>1</sup> School of Life Sciences, Faculty of Science, University of Technology Sydney, Sydney, NSW 2007, Australia

<sup>2</sup> Respiratory Cellular and Molecular Biology, Woolcock Institute of Medical Research, The University of Sydney, Sydney, NSW 2037, Australia

<sup>3</sup> Department of Clinical Chemistry, Faculty of Allied Health Sciences, Chulalongkorn University, Pathum Wan, Bangkok 10330, Thailand

<sup>4</sup> Graduate School of Biomedical Engineering, University of New South Wales, Sydney, NSW, 2052, Australia

<sup>5</sup> Storr Liver Centre, The Westmead Institute for Medical Research, Westmead Hospital and The University of Sydney, Sydney, NSW 2037, Australia

<sup>6</sup> Kolling Institute of Medical Research, Royal North Shore Hospital, The University of Sydney, Sydney, NSW 2065, Australia

\* Correspondence: Hui.Chen-1@uts.edu.au; Tel.: +61-2-9514-1328

Received: 23 May 2019; Accepted: 18 July 2019; Published: 21 July 2019



**Abstract:** Maternal smoking leads to glucose and lipid metabolic disorders and hepatic damage in the offspring, potentially due to mitochondrial oxidative stress. Mitoquinone mesylate (MitoQ) is a mitochondrial targeted antioxidant with high bioavailability. This study aimed to examine the impact of maternal cigarette smoke exposure (SE) on offspring's metabolic profile and hepatic damage, and whether maternal MitoQ supplementation during gestation can affect these changes. Female Balb/c mice (eight weeks) were either exposed to air or SE for six weeks prior to mating and throughout gestation and lactation. A subset of the SE dams were supplied with MitoQ in the drinking water (500  $\mu\text{mol/L}$ ) during gestation and lactation. Intraperitoneal glucose tolerance test was performed in the male offspring at 12 weeks and the livers and plasma were collected at 13 weeks. Maternal SE induced glucose intolerance, hepatic steatosis, mitochondrial oxidative stress and related damage in the adult offspring. Maternal MitoQ supplementation reduced hepatic mitochondrial oxidative stress and improved markers of mitophagy and mitochondrial biogenesis. This may restore hepatic mitochondrial health and was associated with an amelioration of glucose intolerance, hepatic steatosis and pathological changes induced by maternal SE. MitoQ supplementation may potentially prevent metabolic dysfunction and hepatic pathology induced by intrauterine SE.

**Keywords:** ROS; liver fibrosis; MitoQ; glucose intolerance

## 1. Introduction

Tobacco cigarette smoking during pregnancy has been associated with an increased risk of metabolic disorders in the offspring, especially type 2 diabetes in adulthood [1]. In utero smoke exposure (SE) increases oxidative stress and damage in the offspring's liver [2], which can lead to mitochondrial dysfunction. Mitochondria are essential for glucose and fatty acid metabolism to generate energy in the form of ATP. The process of mitochondrial oxidative phosphorylation results in the generation of reactive oxygen species (ROS), which are normally cleared by endogenous mitochondrial



antioxidants [3]. Within the mitochondria, the imbalance between excessive ROS and antioxidant capacity leads to oxidative stress and mitochondrial damage. Adaptive mechanisms respond to damaged mitochondria through the processes of mitophagy and mitochondrial biogenesis [4]. However hepatic mitochondrial dysfunction (increased oxidative stress or impaired adaptive mechanisms) can lead to glucose intolerance and triglyceride accumulation, which could underlie the development of type 2 diabetes and non-alcoholic fatty liver disease [5]. Increasing evidence, including our own work, has suggested that in utero SE can induce mitochondrial damage in multiple organs, increasing mitochondrial ROS output and impairing metabolic function [6–9]. Therefore, the impacts of maternal SE on metabolic disorders in the offspring could be related to liver mitochondrial damage. As a result, the liver was chosen as the focus of this study because it represents an important and novel field of investigation.

Mitoquinone mesylate (MitoQ) is a mitochondrial targeted antioxidant with high oral bioavailability, derived from covalently attaching a triphenylphosphonium cation moiety to Coenzyme Q10 (CoQ10) [10]. CoQ10 is an endogenous antioxidant with reduced levels in the plasma of smokers [11] and diabetic patients [12]. The positively charged moiety of MitoQ promotes its accumulation within the negatively charged inner mitochondria membrane, directly reducing mitochondrial oxidative stress [10]. We have demonstrated that maternal MitoQ supplementation during gestation and lactation alleviates the adverse effects of maternal smoking in the offspring's lung and kidney [13,14]. Additionally, in a phase II clinical trial on patients with chronic hepatitis C, oral MitoQ administration decreased plasma alanine aminotransferase (ALT) activity, a marker of liver damage [10]. Thus, in a mouse model, we aimed to determine if maternal MitoQ supplementation during gestation and lactation could ameliorate the metabolic dysfunction and hepatic damage caused by SE.

## 2. Materials and Methods

### 2.1. Animal Model

The animal experiments were approved by the Animal Care and Ethics Committee of the University of Technology Sydney (ACEC #2014-638 and ACEC #2016-419) and carried out according to the Australian National Health and Medical Research Council Guide for the Care and Use of Laboratory Animals. After acclimatisation, virgin female Balb/c mice (eight weeks old, Animal Resource Centre, WA, Australia) were randomly assigned to two groups with equal starting body weight. Mice were either exposed to ambient air (Sham group,  $n = 9$ ) or cigarette smoke (SE group,  $n = 19$ ) generated from two cigarettes (Winfield Red,  $\leq 16$  mg tar,  $\leq 1.2$  mg nicotine, and  $\leq 15$  mg of CO; VIC, Australia) twice daily for six weeks prior to mating and throughout gestation and lactation as previously described [15]. The female mice were exposed to the smoke generated by each cigarette for 15 minutes, with a 5-minute interval between the two cigarettes. As indicated by plasma cotinine concentrations in both mothers and offspring, this model represents light human smokers, as we have previously published [8,16]. At mating, a sub-group of the SE dams were administered with MitoQ in the drinking water (500  $\mu\text{mol/L}$ ) during gestation and lactation (SE + MQ group,  $n = 9$ ) [13]. MitoQ in the drinking water provided to the dams has previously been shown to reach the neonatal liver [17]. Male breeders and suckling pups were not exposed to cigarette smoke.

Male offspring were studied because they are more susceptible to the adverse impacts of maternal smoking, as elucidated in our previous studies [8,15]. Male offspring were weaned at postnatal day 20 and maintained without additional intervention until 12 weeks of age, when an intraperitoneal glucose tolerance test (IPGTT) was performed as previously described [18]. After 5 hours of fasting, baseline blood glucose levels were measured followed by glucose injection (2 g/kg, ip). Blood glucose was measured at 15, 30, 60, and 90 minutes post-injection. The area under the curve (AUC) of the blood glucose curve was calculated for each mouse. At 13 weeks of age, after the induction of deep anaesthesia (4% isoflurane), blood was collected via cardiac puncture and the plasma was stored at  $-20$  °C for further analysis. The livers were weighed and then snap frozen at  $-80$  °C or fixed in 10%

neutral buffered formalin for further analysis. One male offspring from each litter was used for tissue analyses (Figure 1).



**Figure 1.** Schematic diagram of animal experiments. SE: cigarette smoke exposure, SE + MQ: SE with mitoquinone mesylate (MitoQ) supplementation.

## 2.2. Bioassays

Plasma ALT activity was measured using the Alanine Transaminase Colorimetric Activity Assay Kit (Cayman Chemical, Ann Arbor, MI, USA) according to the manufacturer's instructions. Plasma insulin concentration was measured by ELISA (Abnova, Taiwan) according to the manufacturer's instructions. Liver lipids were extracted using the Folch method [19]. Briefly, liver samples were homogenised in a chloroform:methanol (2:1) mixture. After agitation, the samples were washed with 0.6% saline solution and centrifuged at low speeds. The lower organic phase was then extracted and dried. Plasma, liver extracts and glycerol standards (Sigma-Aldrich, MO, USA) were incubated with triacylglycerol reagent (Roche Diagnostics, Basel, Switzerland) using an in-house assay [18].

## 2.3. Real Time-PCR

Total mRNA was extracted from frozen liver tissue with TriZol reagent (Life Technologies, Carlsbad, CA, USA) and first strand cDNA was generated using M-MLV Reverse Transcriptase, RNase H, Point Mutant Kit (Promega, Madison, WI, USA). Target gene expression was quantified with manufacturer pre-optimised and validated TaqMan primers and probes (Table S1, Thermo Fisher, San Jose, CA, USA) and standardised to 18S RNA. The probes of the target genes were labelled with FAM and those for housekeeping 18S RNA were labelled with VIC. The Sham group was assigned the calibrator against which all other results were expressed as fold changes.

## 2.4. Western Blotting

Protein samples were separated on NuPage Novex 4%–12% Bis-Tris gels (Life Technologies, Carlsbad, CA, USA) and transferred to PVDF membranes (Pierce, Rockford, IL, USA). After blocking with 5% skim milk, the membranes were incubated with primary antibodies (microtubule associated 1A/1B light chain protein 3 (LC3A/B, 1:2000, Cat# 4108 S, Cell Signalling Technology, Danvers, MA, USA), manganese superoxide dismutase (MnSOD, 1:2000, Cat# 06-984, Millipore, MA, USA), glutathione peroxidase 1 (GPx1, 1:250, Cat# AF3798, R&D systems, Minneapolis, MN, USA), mitochondrial dynamin like GTPase (OPA-1, 1:2000, Cat# NB110-55290, Novus Biotechnology, Centennial, CO, USA), dynamin related protein 1 (DRP-1, Cat# NB110-55237, 1:2000, Novus Biotechnology, Centennial, CO, USA), fission 1 protein (Fis-1, 1:500, Cat# FL-152, Santa Cruz Biotechnology, Dallas, TX, USA), EGF-like module-containing mucin-like hormone receptor-like 1 (F4/80, 1:1000 Cat# sab5500103, Sigma-Aldrich, St. Louis MO, USA)) followed by the corresponding secondary antibody (Abcam, Cambridge, UK). Bands were detected with SuperSignal West Pico Chemiluminescent substrate (Thermo Fisher Scientific,

CA, USA) and Fujifilm LAS-3000 (Fujifilm, Tokyo, Japan) and then quantified with ImageJ (National Institutes of Health, Bethesda, MD, USA). Results were expressed as a ratio against the housekeeping protein  $\beta$ -actin or cytochrome c oxidase subunit (COX) IV.

### 2.5. Immunohistochemistry

Formalin fixed, paraffin embedded livers were sectioned at 5  $\mu$ m. Sections were deparaffinised and rehydrated in xylene and decreasing grades of ethanol. Antigen retrieval was performed [7] before the sections were incubated with anti-rabbit collagen III (1:50, Cat# NB600-594, Novus Biotechnology, Centennial, CO, USA) or cluster of differentiation 68 (CD68) (1:600, Cat# OABB00472, Aviva Systems Biology, San Diego, CA, USA) primary antibody and horseradish peroxidase anti-rabbit Envision system (Dako Cytochemistry, Tokyo, Japan). Sections were counterstained with haematoxylin and quantified with ImageJ (National Institutes of Health, Bethesda, MD, USA).

### 2.6. Second Harmonic Generation

Images were acquired on a Leica SP8 multi-photon microscope equipped with a Mai Tai DeepSee laser tuned to 930 nm. Second harmonic generation signal was collected between 455–475 nm using a HyD detector in photon counting mode and the autofluorescence was collected from 480–600 nm. Channel separation and stitching were performed within the Leica Application Suite X software (Leica Microsystems, Wetzlar, Germany) controlling the microscope, before being deconvolved with Huygens Professional version 18.04 (Scientific Volume Imaging, Hilversum, The Netherlands). The data was 3D median filtered to remove noise, the background subtracted, and the amount of collagen quantified using ImageJ (National Institutes of Health, Bethesda, MD, USA). A Fast Fourier Transform (FFT) filter was applied to the autofluorescence channel to remove stitching artifacts. Image projections are summed slices of the 3D z stack, and to enable visualisation of the total amount of collagen, spanning the entire dynamic range in a single image, a gamma correction of 0.2 was applied.

### 2.7. Mitochondrial Density and ROS

Frozen livers were sectioned to quantify mitochondrial density and ROS levels. Liver mitochondria were visualised using MitoTracker Green (Thermo Fisher Scientific, Waltham, MA, USA) and images were acquired at 488 nm excitation wavelength and detected in the 510–550 nm emission range as previously reported [14]. For total reactive oxygen species (ROS), CellROX Deep Red (Thermo Fisher Scientific, Waltham, MA, USA) was used and images were acquired at 633 nm excitation wavelength and detected in the 640–680 nm emission range. All imaging parameters including laser intensities, photomultiplier tubes voltage and pinholes were kept constant during imaging. The MitoTracker and CellRox images were overlaid to provide information on mitochondrial specific ROS. Data were generated using ImageJ (National Institutes of Health, Bethesda, MD, USA).

### 2.8. Lipidomics

Lipids were extracted from frozen liver tissue using methyl-tert-butyl ether [20]. Cryohomogenised liver tissues were incubated with methanol and then methyl-tert-butyl ether, before centrifugation to induce phase separation. The top organic phase was dried and then resuspended in methanol:isopropanol (2:1) mixture.

Using a Vanquish Ultra Performance Liquid Chromatography (UPLC) system (Thermo Fisher Scientific, Waltham, MA, USA), 2  $\mu$ L of the sample was loaded at 400 mL/min onto an Accucore™ C30 (2.1  $\times$  150 mm, 2.6  $\mu$ m) column with a 70:30 A:B solvent mix (A: 60% Acetonitrile (ACN)/40% H<sub>2</sub>O containing 10 mM ammonium formate and 0.1% formic acid (FA). B: 90% isopropyl alcohol (IPA)/10% ACN containing 10 mM ammonium formate and 0.1% FA). Retained lipids were eluted from the column and into the Q Exactive Plus mass spectrometer (Thermo Fisher Scientific, Waltham, MA, USA) using the following program: 30–43% B over 2 min, 43–55% B over 0.1 min, 55–65% B for 9.9 min, 65–85% for 6 min, 85–100% B over 2 min, held at 100% B for 5 min, 30%–100% B over 0.1 min

and re-equilibration for 5 min. The eluting peptides were ionised. A data dependent MS/MS and selected ion monitoring (dd-MS2 – dd-SIM) experiment was performed, with a survey scan of 250–1200 Da performed at 140,000 resolution with an AGC target of  $1 \times 10^6$  and maximum injection time of 100 ms. Ions listed on the inclusion list were selected for fragmentation in the higher-energy collisional dissociation cell using an isolation window of 1.0 m/z, an AGC target of  $1 \times 10^5$  and maximum injection time of 100 ms. Fragments were scanned in the Orbitrap analyser at 17,500 resolution and the production fragment masses measured over a mass range of 200–2000 Da. The mass of the precursor peptide was then excluded. The data files were searched using the Lipidex software package [21] in conjunction with Compound Discoverer (Thermo Fisher Scientific, Waltham, MA, USA).

### 2.9. Statistical Analysis

Results are expressed as mean  $\pm$  SEM and were analysed using one-way ANOVA with Fisher's least significant post hoc test if the data were normally distributed. If the data were not normally distributed, they were log transformed to achieve normality of distribution before analysis (GraphPad Prism 7.03, San Diego, CA, USA).  $p < 0.05$  was considered the threshold for statistical significance.

## 3. Results

### 3.1. Body and Liver Weights

Birth weight and body weight can be used as an indication of intrauterine and postnatal development in mice. Male offspring from SE mothers had lower birth weight compared to male offspring from Sham mothers, which was normalised when MitoQ was administered to the SE mothers ( $p < 0.01$ , SE + MQ vs. SE, Table 1). At 13 weeks, SE offspring remained smaller compared to the Sham offspring ( $p < 0.05$ ), which was reversed in the SE + MQ group ( $p < 0.01$ , Table 1). SE offspring also had reduced liver weights when compared to the Sham offspring ( $p < 0.05$ ) at 13 weeks; again, this was reversed by maternal MitoQ supplementation ( $p < 0.01$ , SE + MQ vs. SE, Table 1). However, when liver weights were expressed as a percentage of body weight, there were no differences among the three groups. Maternal SE resulted in intrauterine growth restriction in male offspring, which was reversed by MitoQ supplementation during pregnancy.

**Table 1.** Birth weight and parameters in 13 weeks old male offspring.

	Sham (n = 19)	SE (n = 20)	SE + MQ (n = 14)
Birth weight (g)	1.51 $\pm$ 0.03	1.30 $\pm$ 0.06 **	1.65 $\pm$ 0.05 ##
Body weight at 13 weeks (g)	25.2 $\pm$ 0.2	24.2 $\pm$ 0.2 **	25.1 $\pm$ 0.2 ##
Liver weight (g)	1.12 $\pm$ 0.019	1.05 $\pm$ 0.019 *	1.15 $\pm$ 0.02 ##
Liver weight (% of body weight)	4.42 $\pm$ 0.073	4.37 $\pm$ 0.079	4.55 $\pm$ 0.08
Liver triglycerides (mg/g liver)	4.08 $\pm$ 0.41	6.03 $\pm$ 0.49 *	4.04 $\pm$ 0.61 #
Liver PE 34:1 intensity (cps)	121,000 $\pm$ 8900	203,000 $\pm$ 29,000 *	170,000 $\pm$ 19,000
Liver PE 38:1 intensity (cps)	13,100 $\pm$ 1600	21,700 $\pm$ 3000 *	17,000 $\pm$ 1900
Liver PE 38:2 intensity (cps)	12,500 $\pm$ 2400	23,000 $\pm$ 4700 *	12,700 $\pm$ 1200 #
Liver PE 40:5 intensity (cps)	88,200 $\pm$ 7000	156,000 $\pm$ 25,000 *	104,000 $\pm$ 15,000
Plasma triglycerides (mg/mL)	2.36 $\pm$ 0.19	2.31 $\pm$ 0.21	2.40 $\pm$ 0.29
Plasma ALT (U/L)	8.03 $\pm$ 1.1	11.2 $\pm$ 0.9 *	7.75 $\pm$ 0.7 #
Plasma insulin (ng/mL)	0.0702 $\pm$ 0.014	0.103 $\pm$ 0.083	0.111 $\pm$ 0.010
AUC of IPGTT (mM·min)	1150 $\pm$ 20	1280 $\pm$ 41 *	1130 $\pm$ 38 #

Data are expressed as mean  $\pm$  SEM (n = 14–20 for birth weight, body weight at 13 weeks, liver weight, and AUC of IPGTT; n = 6–8 for liver triglycerides, plasma triglycerides, plasma ALT, plasma insulin; n = 5 for liver PE). \*  $p < 0.05$ , \*\*  $p < 0.01$  vs. Sham. #  $p < 0.05$ , ##  $p < 0.01$  vs. SE. ALT: alanine aminotransferase, AUC: area under the curve, IPGTT: intraperitoneal glucose tolerance test, PE: phosphatidylethanolamine, SE: cigarette smoke exposure, SE + MQ: SE with MitoQ supplementation.

### 3.2. Glucose Metabolic Markers

Impaired glucose clearance is associated with insulin resistance and type 2 diabetes. The IPGTT demonstrated that blood glucose was increased in the SE group compared to Sham group ( $p < 0.05$ ) which was normalised in the SE + MQ group ( $p < 0.05$  vs. SE, Table 1). However, hepatic expression of glucose transporters (Glut1, Glut2, and Glut4), glycolysis marker phosphofructokinase (PFK), gluconeogenesis markers (phosphoenolpyruvate carboxykinase 1 (PCK1), and forkhead box protein O1 (FOXO1)), and liver insulin sensing marker peroxisome proliferator-activated receptor gamma (PPAR- $\gamma$ ) were not different among the groups (Figure 2a–g). Maternal MitoQ supplementation reversed glucose intolerance induced by intrauterine tobacco smoke exposure, however, hepatic glucose metabolic markers were not affected.

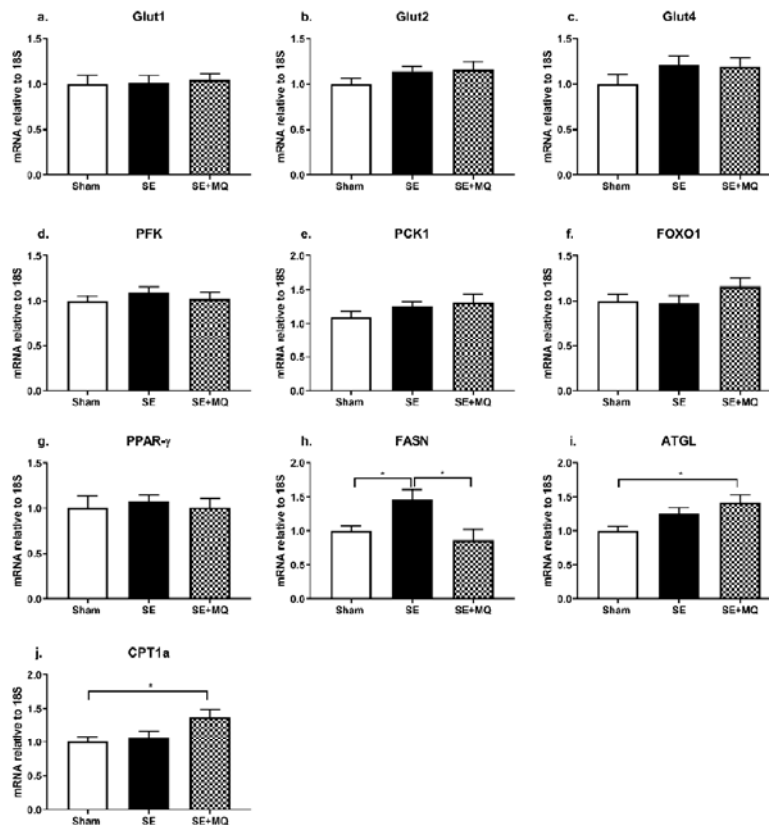


**Figure 2.** Liver mRNA expression of markers involved in glucose metabolism (a–g) and lipid metabolism (h–j) in 13 weeks old male offspring. Results are expressed as mean  $\pm$  SEM ( $n = 6$ –8). \*  $p < 0.05$ . ATGL: adipose triglyceride lipase, CPT1a: carnitine palmitoyltransferase 1a, FASN: fatty acid synthase, FOXO1: forkhead box protein O1, Glut: glucose transporter, PFK: phosphofructokinase, PPAR- $\gamma$ : peroxisome proliferator-activated receptor gamma, SE: cigarette smoke exposure, SE + MQ: SE with MitoQ supplementation.



### 3.3. Lipid Metabolic Markers

Since blood glucose was increased in the SE group and hepatic steatosis is closely associated with the development of type 2 diabetes, liver lipid content was evaluated. Hepatic triglyceride (TG) concentration was increased in the SE group compared to the Sham group ( $p < 0.05$ ), which was normalised in the SE + MQ group ( $p < 0.05$  vs. SE, Table 1). Hepatic fatty acid synthase (FASN) mRNA expression was significantly increased in the SE group compared to the Sham group ( $p < 0.05$ ) which again was normalised in the SE + MQ offspring ( $p < 0.01$  vs. SE, Figure 2h). Adipose triglyceride lipase (ATGL) and carnitine palmitoyltransferase 1a (CPT1a) mRNA levels were only increased in the SE + MQ group ( $p < 0.05$  vs. Sham, Figure 2i,j).

From lipidomics analysis, liver concentrations of certain phosphatidylethanolamine (PE) species, specifically PE 34:1, PE 38:1, PE 38:2, and PE 40:5 were increased in the SE group compared to the Sham group ( $p < 0.05$ ), with PE 38:2 being normalised in the SE+ MQ group ( $p < 0.05$  vs. SE, Table 1). No differences in other lipid species detected during lipidomics analysis were observed (see Table S2). In addition, plasma TG concentrations were not different among the three groups (Table 1). Overall, increased hepatic de novo lipogenesis could be responsible for elevated hepatic TG concentrations in the SE group. Furthermore, maternal MitoQ supplementation normalised liver TG concentration in the offspring via a normalisation of de novo lipogenesis and an increase in mitochondrial fatty acid  $\beta$ -oxidation.

### 3.4. Liver Injury Markers

Plasma ALT activity and hepatic markers of inflammation and fibrosis are often elevated during liver injury. Plasma ALT was significantly increased in the SE group compared to the Sham group ( $p < 0.05$ ); this was reversed in the SE + MQ group ( $p < 0.05$  vs. SE, Table 1). Hepatic tumour necrosis factor (TNF)- $\alpha$  mRNA expression was significantly increased in the SE group compared to the Sham group ( $p < 0.01$ , Figure 3a) and was nearly normalised in the SE + MQ offspring ( $p = 0.06$  vs. SE, Figure 3a). However, mRNA expression of interleukin (IL)-1 $\beta$  was not different between the groups (Figure 3b). Protein expression of surface macrophage markers, CD68 and F4/80, and mRNA expression of the macrophage chemokine, monocyte chemoattractant protein 1 (MCP-1), were not different among the three groups (Figure 3c–e). Stellate cell activity marker,  $\alpha$ -smooth muscle actin ( $\alpha$ -SMA), was increased in the SE group ( $p < 0.05$  vs. Sham, Figure 3f) which was reversed in the SE + MQ group ( $p < 0.05$  vs. SE, Figure 3f). The deposition of hepatic collagen 1a1, collagen III and total collagen was increased in the SE group compared to the Sham group ( $p < 0.05$ , Figure 3g–i), with collagen1a1 deposition being normalised in the SE + MQ group ( $p < 0.05$  vs. SE, Figure 3g). Elevated liver injury markers in the offspring from the SE dams were mostly reversed by maternal MitoQ supplementation during pregnancy. However, this did not seem to be associated with changes in resident macrophages.

### 3.5. Oxidative Stress and Mitochondrial Integrity

Oxidative stress and mitochondrial damage are implicated in the development of metabolic disorders and hepatic steatosis. There was a significant decrease in mitochondrial density in the SE group compared to the Sham group ( $p < 0.05$ ) which was normalised in the SE + MQ group ( $p < 0.05$  vs. SE, Figure 4a). Furthermore, an increase in total ROS and mitochondrial ROS levels was observed in the SE group compared to the Sham group ( $p < 0.05$ ), which was normalised in the SE + MQ group ( $p < 0.05$  vs. SE, Figure 4b,c). Protein expression of the endogenous antioxidant MnSOD was reduced in both SE and SE + MQ groups compared to the Sham group ( $p < 0.05$  and  $p < 0.01$  respectively, Figure 4d); whereas, GPx1 protein was increased in the SE + MQ offspring compared to both the Sham and SE offspring ( $p < 0.05$ , Figure 4e). Mitochondrial biogenesis marker peroxisome proliferator-activated receptor gamma coactivator (PGC)-1a mRNA expression was increased in the SE + MQ group ( $p < 0.01$  vs. Sham, Figure 4f).

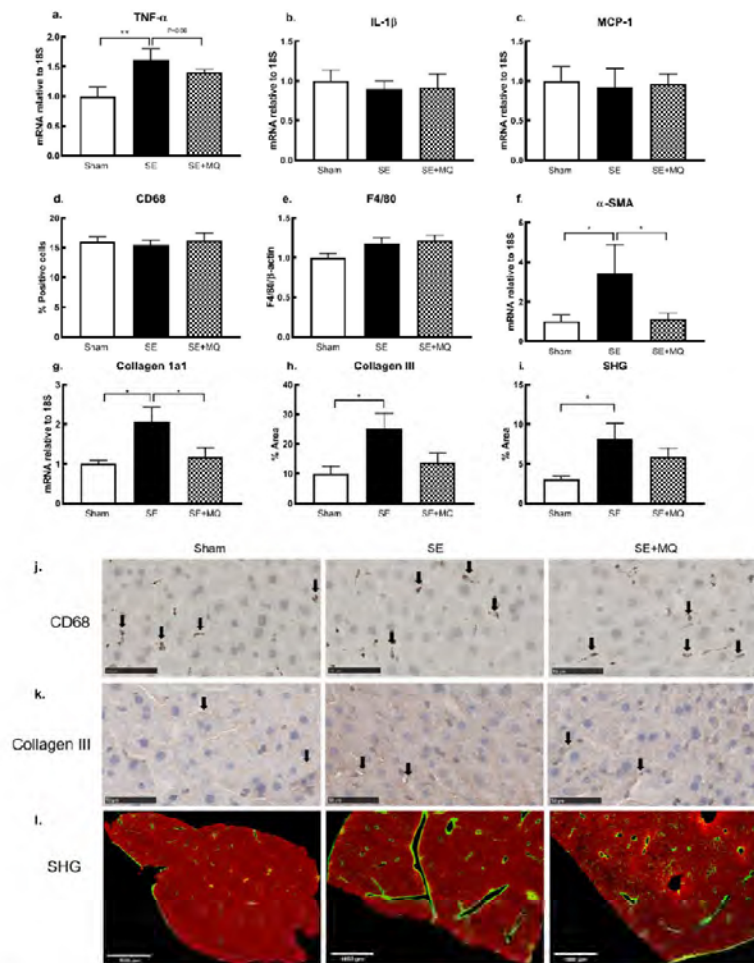


**Figure 3.** Markers of liver inflammation TNF- $\alpha$ , IL-1 $\beta$  (a,b), macrophage markers MCP-1, CD68 and F4/80 (c–e), stellate cell activation marker  $\alpha$ -SMA (f) and fibrous deposition of collagen 1 $\alpha$ 1, collagen III, and total collagen (g–i) in 13 weeks old male offspring. Results are expressed as mean  $\pm$  SEM ( $n = 4–8$ ). \*  $p < 0.05$ , \*\*  $p < 0.01$ . Representative images of hepatic CD68 (j, positive staining indicated by arrows) and collagen III (k, positive staining indicated by arrows) immunohistochemistry staining in 13 weeks old male offspring, bar = 50  $\mu$ m. (l) Representative images of SHG showing total collagen staining after gamma correction (collagen is green/yellow), bar = 1000  $\mu$ m.  $\alpha$ -SMA: alpha-smooth muscle actin, CD68: cluster of differentiation 68, F4/80: EGF-like module-containing mucin-like hormone receptor-like 1, IL-1 $\beta$ : interleukin 1 beta, MCP-1: monocyte chemoattractant protein 1, SE: cigarette smoke exposure, SE + MQ: SE with MitoQ supplementation, SHG: second harmonic generation, TNF- $\alpha$ : tumour necrosis factor- $\alpha$ .

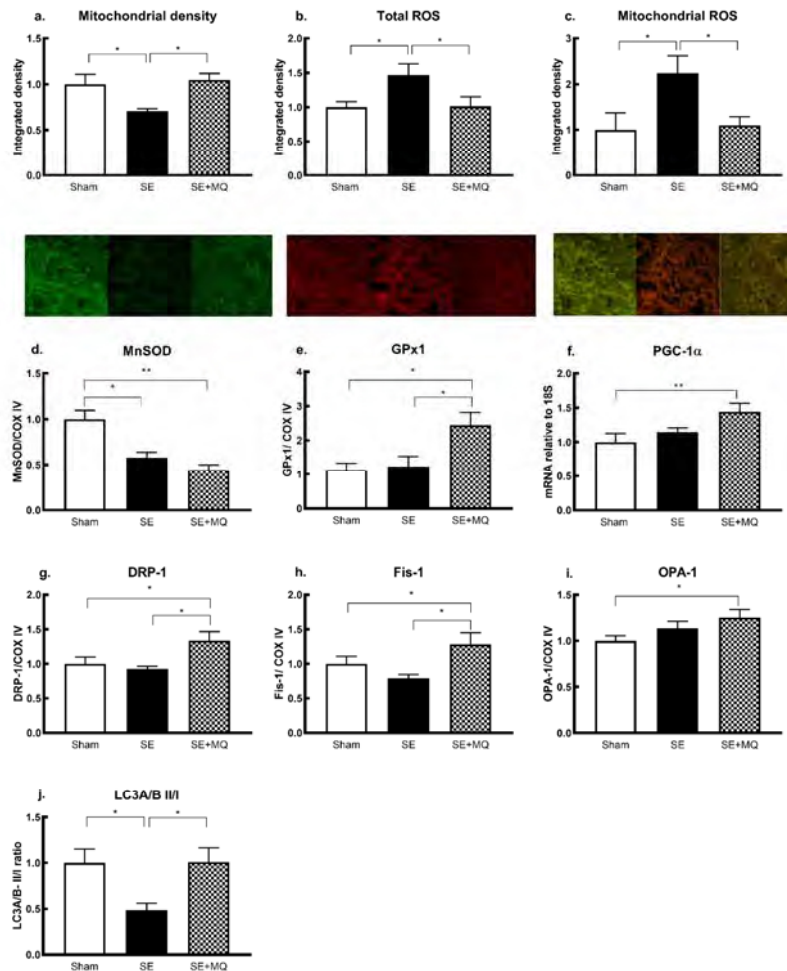


**Figure 4.** Hepatic mitochondrial density (a, green signal), ROS (b, red signal) and mitochondrial specific ROS (c, orange signal), endogenous mitochondrial antioxidants MnSOD (d) and GPx1 (e), marker of mitochondrial biogenesis PGC-1 $\alpha$  (f) and markers of mitophagy (g–j) in 13 weeks old male offspring. Results are expressed as mean  $\pm$  SEM ( $n = 6-8$ ). \*  $p < 0.05$ , \*\*  $p < 0.01$ . DRP-1: dynamin related protein 1, Fis-1: fission 1 protein, GPx1: glutathione peroxidase 1, LC3A/B II/I: microtubule associated 1A/1B light chain protein 3, MnSOD: manganese superoxide dismutase, OPA-1: mitochondrial dynamin like GTPase, PGC-1 $\alpha$ : peroxisome proliferator-activated receptor gamma coactivator 1- $\alpha$ , ROS: reactive oxygen species, SE: cigarette smoke exposure, SE + MQ: SE with MitoQ supplementation.

Both mitochondrial fission markers DRP-1 and Fis-1 were not significantly changed in the SE offspring, but increased in the SE + MQ group compared to both the Sham and SE groups ( $p < 0.05$ , Figure 4g,h). Mitochondrial fusion marker OPA-1 was not altered in the SE offspring, but significantly increased in the SE + MQ group ( $p < 0.05$  vs. Sham, Figure 4i). The ratio of LC3A/B II



to LC3A/B I was reduced in the SE group ( $p < 0.05$  vs. Sham) but normalised in the SE + MQ group ( $p < 0.05$  vs. SE, Figure 4j). Increased liver steatosis and damage in the SE offspring could be due to increased mitochondrial injury and impaired mitochondrial antioxidant defense capacity, leading to mitochondrial ROS accumulation. Increased liver markers of mitophagy and mitochondrial biogenesis by maternal MitoQ supplementation suggest an improvement in mitochondrial repair machinery. This was associated with a normalisation of mitochondrial ROS level, and improved hepatic steatosis and liver damage.

#### 4. Discussion

The mechanisms underlying intrauterine underdevelopment and disease induced by maternal smoking are not well understood. Evidence from genetically modified mice suggests that these changes could be due to increased oxidative stress, rather than nicotine [22]. In this study, increased mitochondrial oxidative stress and resulting mitochondrial insufficiency are proposed as the underlying mechanisms. In our model, the offspring from the SE mothers had low birth weight, glucose intolerance, hepatic steatosis, inflammation, and fibrosis in adulthood. Maternal supplementation with the mitochondrial-targeted antioxidant, MitoQ, during gestation and lactation rescued body weight at birth, and decreased mitochondrial oxidative stress in the offspring's liver, preventing hepatic changes in the offspring. As MitoQ reduces mitochondrial oxidative stress, our results suggest that it could be used as a novel treatment to prevent the metabolic dysfunction and liver damage induced by maternal SE.

In humans, intrauterine exposure to tobacco cigarette smoke leads to intrauterine growth restriction [23], insulin resistance [24], and hepatic steatosis [25], which were all observed in this study. In conjunction with our previous studies, this indicates the reproducibility and reliability of our model in reflecting human pathophysiology [1,8,9,15,25–29]. Cigarette smoke exposure causes vasoconstriction, limiting placental nutrient delivery and increasing the risk of low birth weight, leading to the development of type 2 diabetes and non-alcoholic fatty liver disease (NAFLD) in adulthood [25,26]. Inflammation is also important, as it leads to insulin resistance, interrupting lipid metabolism and causing liver steatosis and cellular damage, leading to fibrosis [30]. However, previous studies have only found modifications of genes related to fibrosis in the human male foetus, suggesting an increased risk of cirrhosis, but not steatosis [31]. In the present study, although hepatic glucose metabolic markers were not affected by maternal SE, *de novo* lipogenesis as indicated by upregulated FASN expression in adult SE offspring, contributing to increased liver triglyceride accumulation. Plasma PE levels are increased in patients with non-alcoholic steatohepatitis (NASH) [32]. We found increased PE levels in the SE offspring, accompanied by increased inflammation and fibrosis, suggesting an increased risk of NASH.

Of particular interest, maternal MitoQ supplementation reversed intrauterine growth restriction in the offspring. MitoQ has been shown to improve vascular function in both human and animal studies [33,34]. Therefore, we postulate that MitoQ may prevent the vasoconstriction induced by maternal SE, restoring nutrient supply to the foetus. This was reflected by an increase in birth weight in the SE + MQ offspring compared to the SE offspring, indicating better nutrient supply and intrauterine development. This may be due to increased uterine vasodilation since oxidative stress is closely related to smoking-induced vasoconstriction [35]. Previous studies have shown that MitoQ supplementation or increased cellular CoQ10 levels can reverse hepatic steatosis by inhibiting *de novo* lipogenesis and enhancing fatty acid  $\beta$ -oxidation [36–38]. Consistently, maternal MitoQ supplementation not only normalised systemic glucose metabolism and a marker of *de novo* lipogenesis (FASN), but also increased expression of lipid catabolism markers (ATGL and CPT-1 $\alpha$ ) in the offspring.

Mitochondrial oxidative stress and injury have been observed in patients with NAFLD and NASH [39,40]. In this study, we identified mitochondrial oxidative stress and mitochondrial insufficiency as a critical mechanism in the foetal origin of hepatic steatosis and fibrosis resulting from maternal smoking. In addition, a similar situation was found in the brain and kidneys, associated with

functional disorders [8,9,13,28]. We found maternal SE impaired markers of mitophagy, which may be due to both oxidative stress and lipid overaccumulation [41]. Mitochondrial oxidative stress is a well-known trigger of inflammation and in this study was reflected by increased production of TNF- $\alpha$  in the SE offspring. Interestingly, this did not appear to be the result of increased macrophage numbers (CD68 and F4/80 positive cells). Thus, the increase in TNF- $\alpha$  expression could be due to increased macrophage activity, or increased inflammatory responses within hepatocytes or stellate cells [42]. Reduced levels of the endogenous mitochondrial antioxidant MnSOD has been consistently observed in multiple organs from in utero cigarette smoke exposure in murine [13,14,43] and non-human primate models [44]. This study, together with those from a series of studies in the same model [13,14], have established the key role of systemic mitochondrial insufficiency and mitochondrial specific oxidative stress in foetal underdevelopment induced by maternal smoking [27].

Unlike other conventional antioxidants, MitoQ rapidly accumulates within the inner mitochondrial membrane to suppress oxidative stress [10]. In the MitoQ treated mothers, the offspring had a normal hepatic mitochondrial function, accompanied by reduced inflammation, fibrosis and lipid profiles. We suggest that this is an effect not driven by the inhibition of inflammation, as previous studies have found that depletion of Kupffer cells (resident liver macrophages) failed to protect the liver from fibrotic injury [33]; thus, normalising mitochondrial oxidative stress is the key. Oxidative stress may promote the activation of fibrogenic myofibroblasts, as indicated by  $\alpha$ -SMA expression which was associated with ROS and fibrosis levels [45]. Here, there was an increase in the endogenous mitochondrial antioxidant GPx1, the mitochondrial biogenesis mediator PGC1 $\alpha$ , and the mitochondrial self-renew machinery—DRP-1, Fis-1, OPA-1, and LC3A/B. However, another mitochondrial antioxidant MnSOD was not changed. It has been suggested that MitoQ mimics the function of MnSOD, which neutralises superoxide radicals. Therefore, there may be no need to increase MnSOD in the presence of MitoQ. However, the level of GPx1, which acts downstream of MnSOD, was increased, suggesting enhanced ROS scavenging capacity. Increased DRP-1 and Fis-1 by maternal MitoQ supplementation can facilitate the separation of healthy and damaged mitochondrial fragments due to oxidative injury. Increased OPA-1 can improve the recycling of healthy mitochondrial fragments to generate new mitochondria. The damaged fragments are further degraded by autophagosomes formed by LC3A/B to protect cells from their toxic effects [4]. Thus, taken together, maternal MitoQ supplementation restored mitochondrial integrity and oxidative stress level in the offspring's liver and prevented the development of metabolic disorders. MitoQ also appears to protect offspring from liver steatosis better than the non-mitochondrial targeted antioxidant L-carnitine as we showed previously [27].

In this study, a low dosage of tobacco cigarette smoke was administered to the mothers, which may only apply to light smokers who continue to smoke during pregnancy. The effect of maternal MitoQ supplementation in mice exposed to high doses of cigarette smoke requires further investigation. In addition, the offspring were fed a balanced diet after weaning. Future studies can add a secondary insult (e.g., high fat diet or high carbohydrate diet [46]) to determine whether the risk of metabolic disorders in the liver can be mitigated.

We suggest that MitoQ can inhibit some of the detrimental effects of in utero cigarette smoke exposure on liver health. We are not suggesting that it is safe to smoke and use MitoQ, but in situations where mothers are unable to quit smoking there might be a beneficial effect of using MitoQ. Similarly, there might be efficacy against the detrimental effects of other endogenous inhaled oxidants, such as pollution or workplace noxious gasses. Although sold as an over-the-counter supplement, the safety of MitoQ during pregnancy has not been evaluated in humans. Nevertheless, the current study provides evidence for MitoQ supplementation in women who are unable to quit smoking during pregnancy to protect offspring from metabolic dysfunction.

**Supplementary Materials:** The following are available online at <http://www.mdpi.com/2072-6643/11/7/1669/s1>, Table S1: TaqMan Probe sequence (Life Technologies, CA, USA) used for rt-PCR, Table S2: Lipid species in the liver detected by lipidomics analysis.

**Author Contributions:** Conceptualisation, B.G.O., S.S. (Sonia Saad), and H.C.; investigation, G.L., Y.L.C., S.S. (Supom Sukjamnong), A.G.A., H.V., M.P., and R.Z.; writing, G.L., J.G., B.G.O., S.S. (Sonia Saad), and H.C.

**Funding:** This study was supported by a postgraduate research support provided by the Faculty of Science, University of Technology Sydney. This work was partially supported by the Australian Research Council/ Centre of Excellence for Nanoscale Biophotonics (CE140100003). Mr Gerard Li is supported by a Strategic Scholarship provided by the Faculty of Science, University of Technology Sydney. Ms Razia Zakarya is supported by an Australia Postgraduate Award. Dr Yik Lung Chan is supported by National Health and Medical Research Council Peter Doherty Fellowship. A/Prof Oliver is supported by National Health and Medical Research Council Career Development II Fellowship (APP1110368). Professor Jacob George is supported by the Robert W Storr Bequest to the University of Sydney.

**Acknowledgments:** The authors acknowledge the facilities and technical assistance of Microscopy Australia at the Australian Centre for Microscopy and Microanalysis at the University of Sydney and Cherie Xia for her assistance with image analysis. The MitoQ was provided by Greg Macpherson from MitoQ Limited, New Zealand.

**Conflicts of Interest:** The authors declare no conflict of interest.

## References

- Jaddoe, V.W.; De Jonge, L.L.; Van Dam, R.M.; Willett, W.C.; Harris, H.; Stampfer, M.J.; Hu, F.B.; Michels, K.B. Fetal exposure to parental smoking and the risk of type 2 diabetes in adult women. *Diabetes Care* **2014**, *37*, 2966–2973. [[CrossRef](#)] [[PubMed](#)]
- Izzotti, A.; Balansky, R.M.; Cartiglia, C.; Camoirano, A.; Longobardi, M.; De Flora, S. Genomic and transcriptional alterations in mouse fetus liver after transplacental exposure to cigarette smoke. *FASEB J.* **2003**, *17*, 1127–1129. [[CrossRef](#)] [[PubMed](#)]
- Pisoschi, A.M.; Pop, A. The role of antioxidants in the chemistry of oxidative stress: A review. *Eur. J. Med. Chem.* **2015**, *97*, 55–74. [[CrossRef](#)] [[PubMed](#)]
- Palikaras, K.; Tavernarakis, N. Mitochondrial homeostasis: The interplay between mitophagy and mitochondrial biogenesis. *Exp. Gerontol.* **2014**, *56*, 182–188. [[CrossRef](#)] [[PubMed](#)]
- Hu, F.; Liu, F. Mitochondrial stress: A bridge between mitochondrial dysfunction and metabolic diseases? *Cell. Signal.* **2011**, *23*, 1528–1533. [[CrossRef](#)] [[PubMed](#)]
- Yang, Z.; Harrison, C.M.; Chuang, G.C.; Ballinger, S.W. The role of tobacco smoke induced mitochondrial damage in vascular dysfunction and atherosclerosis. *Mutat. Res.* **2007**, *621*, 61–74. [[CrossRef](#)] [[PubMed](#)]
- Chan, Y.L.; Saad, S.; Al-Odat, I.; Oliver, B.G.; Pollock, C.; Jones, N.M.; Chen, H. Maternal l-carnitine supplementation improves brain health in offspring from cigarette smoke exposed mothers. *Front. Mol. Neurosci.* **2017**, *10*, 33. [[CrossRef](#)]
- Chan, Y.L.; Saad, S.; Pollock, C.; Oliver, B.; Al-Odat, I.; Zaky, A.A.; Jones, N.; Chen, H. Impact of maternal cigarette smoke exposure on brain inflammation and oxidative stress in male mice offspring. *Sci. Rep.* **2016**, *6*, 25881. [[CrossRef](#)]
- Stangenberg, S.; Nguyen, L.T.; Chen, H.; Al-Odat, I.; Killingsworth, M.C.; Gosnell, M.E.; Anwer, A.G.; Goldys, E.M.; Pollock, C.A.; Saad, S. Oxidative stress, mitochondrial perturbations and fetal programming of renal disease induced by maternal smoking. *Int. J. Biochem. Cell Biol.* **2015**, *64*, 81–90. [[CrossRef](#)]
- Smith, R.A.; Murphy, M.P. Animal and human studies with the mitochondria-targeted antioxidant mitoq. *Ann. N. Y. Acad. Sci.* **2010**, *1201*, 96–103. [[CrossRef](#)]
- Al-Bazi, M.M.; Elshal, M.F.; Khoja, S.M. Reduced coenzyme q(10) in female smokers and its association with lipid profile in a young healthy adult population. *Arch. Med. Sci.* **2011**, *7*, 948–954. [[CrossRef](#)]
- Lim, S.C.; Tan, H.H.; Goh, S.K.; Subramaniam, T.; Sum, C.F.; Tan, I.K.; Lee, B.L.; Ong, C.N. Oxidative burden in prediabetic and diabetic individuals: Evidence from plasma coenzyme q(10). *Diabet. Med. A J. Br. Diabet. Assoc.* **2006**, *23*, 1344–1349. [[CrossRef](#)]
- Sukjamnong, S.; Chan, Y.L.; Zakarya, R.; Saad, S.; Sharma, P.; Santianont, R.; Chen, H.; Oliver, B.G. Effect of long-term maternal smoking on the offspring's lung health. *Am. J. Physiol. Lung Cell. Mol. Physiol.* **2017**, *313*, L416–L423. [[CrossRef](#)]
- Sukjamnong, S.; Chan, Y.L.; Zakarya, R.; Nguyen, L.T.; Anwer, A.G.; Zaky, A.A.; Santianont, R.; Oliver, B.G.; Goldys, E.; Pollock, C.A.; et al. Mitoq supplementation prevent long-term impact of maternal smoking on renal development, oxidative stress and mitochondrial density in male mice offspring. *Sci. Rep.* **2018**, *8*, 6631. [[CrossRef](#)]

15. Al-Odat, I.; Chen, H.; Chan, Y.L.; Amgad, S.; Wong, M.G.; Gill, A.; Pollock, C.; Saad, S. The impact of maternal cigarette smoke exposure in a rodent model on renal development in the offspring. *PLoS ONE* **2014**, *9*, e103443. [[CrossRef](#)]
16. Vivekanandarajah, A.; Chan, Y.L.; Chen, H.; Machaalani, R. Prenatal cigarette smoke exposure effects on apoptotic and nicotinic acetylcholine receptor expression in the infant mouse brainstem. *Neurotoxicology* **2016**, *53*, 53–63. [[CrossRef](#)]
17. Smith, R.A.; Porteous, C.M.; Gane, A.M.; Murphy, M.P. Delivery of bioactive molecules to mitochondria in vivo. *Proc. Natl. Acad. Sci. USA* **2003**, *100*, 5407–5412. [[CrossRef](#)]
18. Chen, H.; Simar, D.; Pegg, K.; Saad, S.; Palmer, C.; Morris, M.J. Exendin-4 is effective against metabolic disorders induced by intrauterine and postnatal overnutrition in rodents. *Diabetologia* **2014**, *57*, 614–622. [[CrossRef](#)]
19. Folch, J.; Lees, M.; Sloane Stanley, G.H. A simple method for the isolation and purification of total lipides from animal tissues. *J. Biol. Chem.* **1957**, *226*, 497–509.
20. Matyash, V.; Liebisch, G.; Kurzchalia, T.V.; Shevchenko, A.; Schwudke, D. Lipid extraction by methyl-tert-butyl ether for high-throughput lipidomics. *J. Lipid Res.* **2008**, *49*, 1137–1146. [[CrossRef](#)]
21. Hutchins, P.D.; Russell, J.D.; Coon, J.J. Lipidex: An integrated software package for high-confidence lipid identification. *Cell Syst.* **2018**, *6*, 621–625. [[CrossRef](#)]
22. Owens, L.; Laing, I.A.; Murdzoska, J.; Zhang, G.; Turner, S.W.; Le Souef, P.N. Glutathione s-transferase genotype protects against in utero tobacco linked lung function deficits. *Am. J. Respir. Crit. Care Med.* **2019**. [[CrossRef](#)]
23. Horta, B.L.; Victora, C.G.; Menezes, A.M.; Halpern, R.; Barros, F.C. Low birthweight, preterm births and intrauterine growth retardation in relation to maternal smoking. *Paediatr. Perinat. Epidemiol.* **1997**, *11*, 140–151. [[CrossRef](#)]
24. Thiering, E.; Brüske, I.; Kratzsch, J.; Thiery, J.; Sausenthaler, S.; Meisinger, C.; Koletzko, S.; Bauer, C.-P.; Schaaf, B.; Von Berg, A.; et al. Prenatal and postnatal tobacco smoke exposure and development of insulin resistance in 10 year old children. *Int. J. Hyg. Environ. Health* **2011**, *214*, 361–368. [[CrossRef](#)]
25. Ayonrinde, O.T.; Adams, L.A.; Mori, T.A.; Beilin, L.J.; De Klerk, N.; Pennell, C.E.; White, S.; Olynyk, J.K. Sex differences between parental pregnancy characteristics and nonalcoholic fatty liver disease in adolescents. *Hepatology* **2018**, *67*, 108–122. [[CrossRef](#)]
26. Chen, H.; Morris, M.J. Maternal smoking—a contributor to the obesity epidemic? *Obes. Res. Clin. Pract.* **2007**, *1*, 155–163. [[CrossRef](#)]
27. Saad, S.; Al-Odat, I.; Chan, Y.L.; McGrath, K.C.; Pollock, C.A.; Oliver, B.G.; Chen, H. Maternal l-carnitine supplementation improves glucose and lipid profiles in female offspring of dams exposed to cigarette smoke. *Clin. Exp. Pharmacol. Physiol.* **2018**, *45*, 694–703. [[CrossRef](#)]
28. Nguyen, L.T.; Stangenberg, S.; Chen, H.; Al-Odat, I.; Chan, Y.L.; Gosnell, M.E.; Anwer, A.G.; Goldys, E.M.; Pollock, C.A.; Saad, S. L-carnitine reverses maternal cigarette smoke exposure-induced renal oxidative stress and mitochondrial dysfunction in mouse offspring. *Am. J. Physiol. Ren. Physiol.* **2015**, *308*, F689–F696. [[CrossRef](#)]
29. Montgomery, S.M.; Ekblom, A. Smoking during pregnancy and diabetes mellitus in a british longitudinal birth cohort. *BMJ* **2002**, *324*, 26–27. [[CrossRef](#)]
30. Song, M.; Schuschke, D.A.; Zhou, Z.; Zhong, W.; Zhang, J.; Zhang, X.; Wang, Y.; McClain, C.J. Kupffer cell depletion protects against the steatosis, but not the liver damage, induced by marginal-copper, high-fructose diet in male rats. *Am. J. Physiol. Gastrointest. Liver Physiol.* **2015**, *308*, G934–G945. [[CrossRef](#)]
31. Filis, P.; Nagrath, N.; Fraser, M.; Hay, D.C.; Iredale, J.P.; O’Shaughnessy, P.; Fowler, P.A. Maternal smoking dysregulates protein expression in second trimester human fetal livers in a sex-specific manner. *J. Clin. Endocrinol. Metab.* **2015**, *100*, E861–E870. [[CrossRef](#)]
32. Ma, D.W.; Arendt, B.M.; Hillyer, L.M.; Fung, S.K.; McGilvray, I.; Guindi, M.; Allard, J.P. Plasma phospholipids and fatty acid composition differ between liver biopsy-proven nonalcoholic fatty liver disease and healthy subjects. *Nutr. Diabetes* **2016**, *6*, e220. [[CrossRef](#)]
33. Rossman, M.J.; Santos-Parker, J.R.; Steward, C.A.C.; Bispham, N.Z.; Cuevas, L.M.; Rosenberg, H.L.; Woodward, K.A.; Chonchol, M.; Gioscia-Ryan, R.A.; Murphy, M.P.; et al. Chronic supplementation with a mitochondrial antioxidant (mitoq) improves vascular function in healthy older adults. *Hypertension* **2018**, *71*, 1056–1063. [[CrossRef](#)]



34. Gioscia-Ryan, R.A.; LaRocca, T.J.; Sindler, A.L.; Zigler, M.C.; Murphy, M.P.; Seals, D.R. Mitochondria-targeted antioxidant (mitoq) ameliorates age-related arterial endothelial dysfunction in mice. *J. Physiol.* **2014**, *592*, 2549–2561. [[CrossRef](#)]
35. Toda, N.; Okamura, T. Cigarette smoking impairs nitric oxide-mediated cerebral blood flow increase: Implications for alzheimer's disease. *J. Pharmacol. Sci.* **2016**, *131*, 223–232. [[CrossRef](#)]
36. Xu, Z.; Huo, J.; Ding, X.; Yang, M.; Li, L.; Dai, J.; Hosoe, K.; Kubo, H.; Mori, M.; Higuchi, K.; et al. Coenzyme q10 improves lipid metabolism and ameliorates obesity by regulating camkii-mediated pde4 inhibition. *Sci. Rep.* **2017**, *7*, 8253. [[CrossRef](#)]
37. Feillet-Coudray, C.; Fouret, G.; Ebabe Elle, R.; Rieusset, J.; Bonafos, B.; Chabi, B.; Crouzier, D.; Zarkovic, K.; Zarkovic, N.; Ramos, J.; et al. The mitochondrial-targeted antioxidant mitoq ameliorates metabolic syndrome features in obesogenic diet-fed rats better than apocynin or allopurinol. *Free Radic. Res.* **2014**, *48*, 1232–1246. [[CrossRef](#)]
38. Mercer, J.R.; Yu, E.; Figg, N.; Cheng, K.K.; Prime, T.A.; Griffin, J.L.; Masoodi, M.; Vidal-Puig, A.; Murphy, M.P.; Bennett, M.R. The mitochondria-targeted antioxidant mitoq decreases features of the metabolic syndrome in atm<sup>+/−</sup>/apoe<sup>−/−</sup> mice. *Free Radic. Biol. Med.* **2012**, *52*, 841–849. [[CrossRef](#)]
39. Caldwell, S.H.; Swerdlow, R.H.; Khan, E.M.; Iezzoni, J.C.; Hespeneheide, E.E.; Parks, J.K.; Parker, W.D., Jr. Mitochondrial abnormalities in non-alcoholic steatohepatitis. *J. Hepatol.* **1999**, *31*, 430–434. [[CrossRef](#)]
40. Seki, S.; Kitada, T.; Yamada, T.; Sakaguchi, H.; Nakatani, K.; Wakasa, K. In situ detection of lipid peroxidation and oxidative DNA damage in non-alcoholic fatty liver diseases. *J. Hepatol.* **2002**, *37*, 56–62. [[CrossRef](#)]
41. Amir, M.; Czaja, M.J. Autophagy in nonalcoholic steatohepatitis. *Expert Rev. Gastroenterol. Hepatol.* **2011**, *5*, 159–166. [[CrossRef](#)]
42. Spencer, N.Y.; Zhou, W.; Li, Q.; Zhang, Y.; Luo, M.; Yan, Z.; Lynch, T.J.; Abbott, D.; Banfi, B.; Engelhardt, J.F. Hepatocytes produce tnf-alpha following hypoxia-reoxygenation and liver ischemia-reperfusion in a nadph oxidase-and c-src-dependent manner. *Am. J. Physiol. Gastrointest. Liver Physiol.* **2013**, *305*, G84–G94. [[CrossRef](#)]
43. Fetterman, J.L.; Pompilius, M.; Westbrook, D.G.; Uyeminami, D.; Brown, J.; Pinkerton, K.E.; Ballinger, S.W. Developmental exposure to second-hand smoke increases adult atherogenesis and alters mitochondrial DNA copy number and deletions in apoe<sup>−/−</sup> mice. *PLoS ONE* **2013**, *8*, e66835. [[CrossRef](#)]
44. Westbrook, D.G.; Anderson, P.G.; Pinkerton, K.E.; Ballinger, S.W. Perinatal tobacco smoke exposure increases vascular oxidative stress and mitochondrial damage in non-human primates. *Cardiovasc. Toxicol.* **2010**, *10*, 216–226. [[CrossRef](#)]
45. Sanchez-Valle, V.; Chavez-Tapia, N.C.; Uribe, M.; Mendez-Sanchez, N. Role of oxidative stress and molecular changes in liver fibrosis: A review. *Curr. Med. Chem.* **2012**, *19*, 4850–4860. [[CrossRef](#)]
46. Sethi, R.K.; Kumar, A.; Das, S.; Kadiiska, M.B.; Michelotti, G.; Diehl, A.M.; Chatterjee, S. Environmental toxin-linked nonalcoholic steatohepatitis and hepatic metabolic reprogramming in obese mice. *Toxicol. Sci.* **2013**, *134*, 291–303. [[CrossRef](#)]



© 2019 by the authors. Licensee MDPI, Basel, Switzerland. This article is an open access article distributed under the terms and conditions of the Creative Commons Attribution (CC BY) license (<http://creativecommons.org/licenses/by/4.0/>).

## ORIGINAL RESEARCH

# Dietary Fatty Acids Amplify Inflammatory Responses to Infection through p38 MAPK Signaling

Sandra Rutting<sup>1,2</sup>, Razia Zakarya<sup>1,3</sup>, Jack Bozier<sup>1,3</sup>, Dia Xenaki<sup>1</sup>, Jay C. Horvat<sup>2</sup>, Lisa G. Wood<sup>2</sup>, Philip M. Hansbro<sup>2,4,5</sup>, and Brian G. Oliver<sup>1,3</sup>

<sup>1</sup>Respiratory Cellular and Molecular Biology, Woolcock Institute of Medical Research, The University of Sydney, Sydney, Australia;

<sup>2</sup>Priority Research Centre for Healthy Lungs, Hunter Medical Research Institute and University of Newcastle, Newcastle, Australia;

<sup>3</sup>School of Life Sciences and <sup>5</sup>University of Technology Sydney, Faculty of Science, Ultimo, Australia; and <sup>4</sup>Centre for Inflammation, Centenary Institute, Sydney, Australia

### Abstract

Obesity is an important risk factor for severe asthma exacerbations, which are mainly caused by respiratory infections. Dietary fatty acids, which are increased systemically in obese patients and are further increased after high-fat meals, affect the innate immune system and may contribute to dysfunctional immune responses to respiratory infection. In this study we investigated the effects of dietary fatty acids on immune responses to respiratory infection in pulmonary fibroblasts and a bronchial epithelial cell line (BEAS-2B). Cells were challenged with BSA-conjugated fatty acids ( $\omega$ -6 polyunsaturated fatty acids [PUFAs],  $\omega$ -3 PUFAs, or saturated fatty acids [SFAs]) +/− the viral mimic polyinosinic:polycytidylic acid (poly[I:C]) or bacterial compound lipoteichoic acid (LTA), and release of proinflammatory cytokines was measured. In both cell types, challenge with arachidonic acid (AA) ( $\omega$ -6 PUFA) and poly(I:C) or LTA led to substantially greater IL-6 and CXCL8 release than either challenge alone, demonstrating synergy. In epithelial cells, palmitic acid (SFA) combined with poly(I:C) also led to greater IL-6 release. The underlying signaling pathways of AA and poly(I:C)- or LTA-induced cytokine release were examined using specific signaling inhibitors and IB. Cytokine production in pulmonary fibroblasts was prostaglandin

dependent, and synergistic upregulation occurred via p38 mitogen-activated protein kinase signaling, whereas cytokine production in bronchial epithelial cell lines was mainly mediated through JNK and p38 mitogen-activated protein kinase signaling. We confirmed these findings using rhinovirus infection, demonstrating that AA enhances rhinovirus-induced cytokine release. This study suggests that during respiratory infection, increased levels of dietary  $\omega$ -6 PUFAs and SFAs may lead to more severe airway inflammation and may contribute to and/or increase the severity of asthma exacerbations.

**Keywords:** viral infection; asthma exacerbations; dietary fatty acids; primary lung fibroblasts; obese asthma

### Clinical Relevance

Obesity is an important risk factor for severe asthma exacerbations, which are most commonly caused by respiratory infections. We show for the first time that dietary fatty acids, which are increased in obese individuals, enhance immune responses to bacterial and viral infection in human lung cells.

(Received in original form June 28, 2018; accepted in final form November 26, 2018)

Supported by a fellowship from the National Health and Medical Research Council of Australia, a Brawn Fellowship from the Faculty of Health and Medicine (University of Newcastle), and funding from the Rainbow Foundation (P.M.H.) and by a fellowship from the National Health and Medical Research Council of Australia (APP1110368) (B.G.O.).

Author Contributions: S.R., R.Z., J.B., D.X., P.M.H., and B.G.O. conceived and planned the experiments. S.R. and R.Z. performed the experiments. S.R., R.Z., J.C.H., L.G.W., P.M.H., and B.G.O. contributed to the interpretation of the results. S.R. took the lead in writing the manuscript. All authors provided critical feedback and helped shape the research, analysis, and manuscript.

Correspondence and requests for reprints should be addressed to Brian G. Oliver, B.Sc., M.Sc., Ph.D., Woolcock Institute of Medical Research, Level 3 Cell Biology, 431 Glebe Point Road, Glebe, NSW 2037, Australia. E-mail: brian.oliver@uts.edu.au

This article has a data supplement, which is accessible from this issue's table of contents at [www.atsjournals.org](http://www.atsjournals.org).

Am J Respir Cell Mol Biol Vol 60, Iss 5, pp 554–568, May 2019

Copyright © 2019 by the American Thoracic Society

Originally Published in Press as DOI: 10.1165/rcmb.2018-0215OC on January 16, 2019

Internet address: [www.atsjournals.org](http://www.atsjournals.org)

More than 2 billion people around the world are overweight or obese with a body mass index (BMI) of 25 kg/m<sup>2</sup> or more (1). This global epidemic is associated with many chronic diseases, including asthma. A number of epidemiological studies show that obesity is an important risk factor for asthma development, increasing the risk by 2.7-fold compared with normal body weight (2). However, the underlying mechanisms are still poorly understood.

Clinical studies suggest that asthma in obese individuals differs from the classical phenotype of the disease. The obese asthma phenotype is characterized by greater severity, poorer control and quality of life, and lack of atopy, with neutrophilic inflammation being specifically reported in obese women (2–5). Obesity also increases the risk of exacerbations and obese patients are almost five times more likely to be hospitalized for asthma exacerbations than lean patients (3, 6, 7). A higher BMI appears to particularly increase the risk of autumn/winter exacerbations in more severe forms of asthma (6).

The major cause of asthma exacerbations is respiratory infection with rhinovirus (RV), which accounts for up to 80% of all exacerbations (8). Viral-induced exacerbations in asthma are associated with increased levels of IL-6, the neutrophil chemoattractant CXCL8, and neutrophilic inflammation (9, 10). Some studies have reported that bacterial infection is also related to asthma exacerbations (11, 12); however, this relationship is less evident. The impact of obesity on immune responses to infections is not clear, but obesity is associated with more severe outcomes after respiratory infection (13, 14). Several studies showed associations between obesity and hospitalization and mortality after infection with pandemic influenza A/H1N1 2009 (15, 16). A recent study by Campitelli and colleagues showed that obesity increases the risk of outpatient visits after respiratory infection compared with a normal body weight (14).

The innate immune system is the first line of defense against pathogens and its aim is to rapidly clear the body of pathogens. To do so, the innate immune system triggers an immediate inflammatory response that induces migration and activation of immune cells into infected sites. However, an excessive inflammatory response may induce greater tissue damage than that caused by pathogens and can

contribute to the cause and severity of exacerbations (8).

Obesity is the result of a continuous overconsumption of nutrients. The Western diet contributes to obesity, being rich in saturated fatty acids (SFAs) and  $\omega$ -6 polyunsaturated fatty acids (PUFAs) and low in  $\omega$ -3 PUFAs (17). It has been shown that the consumption of high-fat meals leads to increased levels of circulating fatty acids and modulates the innate immune system, as shown by increases in the levels of CXCL8 as well as the proportion of neutrophils in the circulation and sputum (18, 19). Obesity itself is also associated with increased fatty acid levels (20). The serum levels of SFAs and  $\omega$ -6 PUFAs are substantially higher than those of  $\omega$ -3 PUFAs (21–23).  $\omega$ -6 PUFAs and SFAs have predominantly been associated with proinflammatory effects, and current evidence suggests that SFAs promote inflammation through activation of a family of receptors involved in innate immunity, known as Toll-like receptors (TLRs) (24). Several studies have suggested that  $\omega$ -3 PUFAs have antiinflammatory and immunosuppressive properties and may be beneficial in treating infectious diseases.  $\omega$ -3 and  $\omega$ -6 PUFAs act as bioactive molecules that are metabolized by cyclooxygenase (COX) and lipoxygenase into prostaglandins (PGs) and leukotrienes, respectively, which have potential anti- and proinflammatory actions of their own (25).

An emerging hypothesis to explain why obese patients have more frequent and severe asthma exacerbations is dysfunctional innate immune responses to viral and/or bacterial respiratory infections. Increased levels of dietary fatty acids could potentially contribute to these dysfunctional immune responses.

The bronchial epithelium has always been considered as the primary site of infection. However, *in vivo* evidence shows that infection also occurs in submucosal cells, including pulmonary fibroblasts (26). In this study we investigated the effect of dietary fatty acids on primary human pulmonary fibroblasts (HPFs) and a bronchial epithelial cell line (BEAS-2B) *in vitro*, and specifically examined the possible enhancement of respiratory infection by measuring the release of inflammatory mediators involved in immune responses against infection.

## Methods

### Cell Culture

HPFs were isolated from the parenchyma of lungs from patients undergoing lung transplantation or lung resection for thoracic malignancies, as previously described (27). Ethical approval for all experiments involving the use of human lung tissue was provided by the Sydney South West Area Health Service, and written informed consent was obtained. Table 1 shows the patient demographics. We also used the bronchial cell line BEAS-2B (ATCC). Details regarding the methods used for culture of HPFs and BEAS-2B are provided in the data supplement.

### Preparation of BSA-conjugated Fatty Acids

Stock solutions of 0.5 M  $\omega$ -3 PUFAs (docosahexaenoic acid [DHA], eicosapentaenoic acid [EPA], and  $\alpha$ -linolenic acid [ALA]), saturated fatty acid (SFA) (palmitic acid [PA]), and 0.3 M  $\omega$ -6 PUFA (arachidonic acid [AA]) (Sigma Aldrich) were prepared in 100% ethanol and stored at  $-20^{\circ}\text{C}$ . Working water-soluble solutions of 10 mM were generated by incubating the fatty acids in 10% endotoxin and fatty acid-free BSA (Sigma Aldrich) as previously described by Gupta and colleagues (28).

### Treatment of Cells

The cells were challenged with DHA, EPA, ALA, PA, or AA (100  $\mu\text{M}$ ) or vehicle (ethanol/BSA/cell culture medium) 4 hours before stimulation with or without the viral mimic polyinosinic:polycytidylic acid (poly[I:C]) (10  $\mu\text{g}/\text{ml}$ ) or the bacterial compound lipoteichoic acid (LTA) (10  $\mu\text{g}/\text{ml}$ ) (Sigma Aldrich). All cells were incubated at  $37^{\circ}\text{C}$  with 5%  $\text{CO}_2$  for 24 hours.

### Determination of IL-6, CXCL8, Granulocyte-Macrophage Colony-Stimulating Factor, and CCL5 Levels

The levels of supernatant IL-6, CXCL8, granulocyte-macrophage colony-stimulating factor (GM-CSF), and chemokine (C-C motif) ligand 5 (CCL5) were measured using commercial ELISA kits (R&D Systems) according to the manufacturer's instructions.

### Western Blotting

Total protein concentrations were obtained using a bicinchoninic acid assay (Sigma-Aldrich) according to the manufacturer's

Table 1. Summary of Patient Demographics

Donor #	Diagnosis	Age	Sex	Surgery	Experiment
1	Emphysema	61	F	Explanted lung	Fatty acids and bacterial/viral mimics
3	BOS	43	M	Explanted lung	Fatty acids and bacterial/viral mimics
4	COPD	60	F	Explanted lung	Fatty acids and bacterial/viral mimics
5	NSCLC	62	F	Lung resection	Fatty acids and bacterial/viral mimics
6	Adenocarcinoma	60	F	Lung resection	Fatty acids and bacterial/viral mimics
7	Emphysema	65	F	Explanted lung	Fatty acids and bacterial/viral mimics
8	Healthy	65	M	Explanted lung	Fatty acids and bacterial/viral mimics
9	Healthy	41	F	Explanted lung	Fatty acids and bacterial/viral mimics
10	COPD	65	M	Explanted lung	Fatty acids and bacterial/viral mimics
11	Adenocarcinoma	72	F	Lung resection	Fatty acids and bacterial/viral mimics
12	COPD	61	F	Explanted lung	Western blotting, inhibitors, fatty acids and bacterial/viral mimics
13	COPD	62	F	Explanted lung	Western blotting, inhibitors
14	Emphysema	65	F	Explanted lung	Western blotting, inhibitors
15	Adenocarcinoma	57	F	Lung resection	Western blotting, inhibitors
16	PAH	57	F	Explanted lung	Western blotting, inhibitors
17	IPF	67	M	Explanted lung	Western blotting
18	Adenocarcinoma	76	F	Lung resection	Western blotting, inhibitors, RV16 infection
19	Adenocarcinoma	64	F	Lung resection	Western blotting, inhibitors, RV16 infection
20	IPF	63	M	Explanted lung	Western blotting, inhibitors, RV16 infection
21	Emphysema	59	M	Explanted lung	Western blotting, inhibitors, RV16 infection
22	PAH	57	F	Explanted lung	Western blotting, inhibitors, RV16 infection
23	COPD	62	F	Explanted lung	Western blotting, inhibitors, RV16 infection
24	PAH	30	F	Explanted lung	Western blotting, inhibitors, RV16 infection
25	Emphysema	62	F	Explanted lung	Inhibitors
26	Emphysema	59	M	Explanted lung	Inhibitors
27	COPD	56	F	Explanted lung	Inhibitors
28	IPF	58	F	Explanted lung	Inhibitors
29	Emphysema	64	M	Explanted lung	Inhibitors
30	NSCLC and COPD	58	M	Lung resection	Inhibitors
31	IPF	64	M	Explanted lung	Inhibitors, RV16 infection
32	Emphysema	61	M	Explanted lung	Inhibitors, RV16 infection
33	COPD	69	F	Explanted lung	Mixed $\omega$ -6: $\omega$ -3 PUFAs, ALA and EPA
34	Interstitial pneumonitis	59	M	Explanted lung	Mixed $\omega$ -6: $\omega$ -3 PUFAs, ALA and EPA
35	IPF	64	M	Explanted lung	Mixed $\omega$ -6: $\omega$ -3 PUFAs, ALA and EPA
36	NSCLC	71	F	Lung resection	Mixed $\omega$ -6: $\omega$ -3 PUFAs, ALA and EPA
37	Adenocarcinoma and COPD	75	F	Lung resection	Mixed $\omega$ -6: $\omega$ -3 PUFAs, ALA and EPA
38	IPF	63	F	Explanted lung	Mixed $\omega$ -6: $\omega$ -3 PUFAs, ALA and EPA
39	Squamous cell carcinoma	65	M	Lung resection	Mixed $\omega$ -6: $\omega$ -3 PUFAs, ALA and EPA
40	Adenocarcinoma	72	F	Lung resection	Mixed $\omega$ -6: $\omega$ -3 PUFAs, ALA and EPA
41	IPF	54	M	Explanted lung	Mixed $\omega$ -6: $\omega$ -3 PUFAs, ALA and EPA

*Definition of abbreviations:* ALA =  $\alpha$ -linolenic acid; BOS = bronchiolitis obliterans syndrome; COPD = chronic obstructive pulmonary disease; EPA = eicosapentaenoic acid; IPF = idiopathic pulmonary fibrosis; F = female; M = male; NSCLC = non-small cell lung carcinoma; PAH = pulmonary arterial hypertension; PUFAs = polyunsaturated fatty acids; RV16 = human rhinovirus 16.

instructions. Cell lysates (10  $\mu$ g) were separated by SDS-PAGE on 10% gels and transferred to polyvinylidene fluoride membranes. The membranes were incubated with rabbit monoclonal antibodies against total and phosphorylated NF- $\kappa$ B p65, p38 mitogen-activated protein kinase (MAPK), or stress-activated protein kinase/c-Jun NH2-terminal kinase (SAPK/JNK) (all 1:1,000; Cell Signaling Technology) and anti-mouse GAPDH (1:5,000; Merck Millipore). Primary antibodies were detected with goat anti-rabbit or rabbit anti-mouse horseradish peroxidase (HRP)-conjugated secondary antibodies (DAKO) and visualized by

enhanced chemiluminescence (Image Station 4000MM; Kodak Digital Science). GAPDH served as the loading control. Details regarding the methods used are provided in the data supplement.

#### Signaling Pathway Inhibition

HPFs and BEAS-2Bs were treated with inhibitors of p38 MAPK (SB239063, 3  $\mu$ M, IC<sub>50</sub> = 44 nM) (Tocris), JNK (SP600125, 10  $\mu$ M, IC<sub>50</sub> = 40 nM for JNK-1 and JNK-2, and 90 nM for JNK-3) (Calbiochem), COX (indomethacin, 10  $\mu$ M, IC<sub>50</sub> = 0.23  $\mu$ M for COX-1 and IC<sub>50</sub> = 0.63  $\mu$ M for COX-2) (Sigma), and NF- $\kappa$ B (BAY-117082, 10  $\mu$ M, IC<sub>50</sub> = 10  $\mu$ M) (Sigma) for 1 hour before

stimulation with AA (100  $\mu$ M) with or without poly(I:C) (10  $\mu$ g/ml) or LTA (10  $\mu$ g/ml).

#### RV Infection

Major group human RV serotype-16 (RV16) was a kind gift from Prof. S. Johnston (Imperial College UK).

RV16 was grown in HeLa cells and infectivity titer was determined using a titration assay as previously described (29, 30). HPFs were unstimulated or treated with AA (100  $\mu$ M) 4 hours before infection with or without live RV16 at a multiplicity of infection (MOI) of 1. Plates were incubated at 37°C with 5% CO<sub>2</sub> for 24 hours.



**Statistical Analysis**

Statistical analysis was conducted using GraphPad Prism version 7 software. Comparisons of the data were performed by one-way ANOVA with repeated measures followed by a Bonferroni post test when appropriate unless otherwise specified. A *P* value of <0.05 was considered significant.

**Results****Stimulation with AA and poly(I:C) Leads to Greater Cytokine Release from Fibroblasts**

To assess whether dietary fatty acids modulate the response to viral infection, HPFs were challenged with 100  $\mu$ M of DHA, PA, or AA before stimulation with poly(I:C) (10  $\mu$ g/ml), and IL-6, CXCL8, GM-CSF, and CCL5 release was measured. AA alone, but not DHA or PA, induced IL-6 and CXCL8 release ( $n = 11$ ,  $P < 0.05$ ) (Figure 1). poly(I:C) alone also induced IL-6 and CXCL8 release ( $n = 11$ ,  $P < 0.05$ ). Challenge with the combination of AA and poly(I:C) resulted in substantially greater IL-6 and CXCL8 release than AA alone ( $n = 11$ ,  $P < 0.01$ ) (Figures 1A and 1B). The effect of the combination of AA with poly(I:C) on IL-6 and CXCL8 release was greater than the sum of the individual effects of AA and poly(I:C), demonstrating a synergistic effect. There was no interaction between DHA or PA and poly(I:C) on IL-6 and CXCL8 release. None of the treatments induced GM-CSF release from the HPFs (data not shown). CCL5 was induced upon poly(I:C) challenge and, interestingly, AA and DHA suppressed poly(I:C)-induced CCL5 release ( $n = 5-8$ ,  $P < 0.05$ ) (Figures 1C and 1F).

**Stimulation with AA and LTA Leads to Greater Cytokine Release from Fibroblasts**

To evaluate whether there is an interaction between dietary fatty acids and bacterial infection, HPFs were treated with dietary fatty acids before stimulation with LTA (10  $\mu$ g/ml). LTA alone did not induce IL-6 or CXCL8 release (Figure 2). However, release of both IL-6 and CXCL8 ( $n = 11$ ,  $P < 0.05$ ) was greater upon challenge with the combination of AA and LTA than with AA alone (Figures 2A and 2B), also demonstrating synergistic effects. Again, there was no interaction between DHA or PA and LTA. In addition, there was no

induction of GM-CSF or CCL5 with any of these treatments (data not shown).

 **$\omega$ -3 PUFAs Do Not Suppress Combined AA and poly(I:C)-induced Cytokine Release**

The  $\omega$ -3 PUFA DHA did not affect poly(I:C)-induced IL-6 and CXCL8 release in HPFs. To confirm that  $\omega$ -3 PUFAs do not affect IL-6 and CXCL8 release, we investigated the effects of the other  $\omega$ -3 PUFAs, ALA and EPA, and found that these fatty acids also did not affect the response to poly(I:C) (see Figure E1 in the data supplement). Because nutrients do not occur in isolation, and a healthy diet consists of  $\omega$ -3 PUFAs: $\omega$ -6 PUFAs in a 1:4 ratio (31), we next investigated the effects of DHA:AA, EPA:AA, and ALA:AA in a 1:4 ratio on poly(I:C)-induced cytokine release. There was no difference in the response to AA with or without DHA, EPA, or ALA in combination with poly(I:C) (see Figure E2), showing that  $\omega$ -3 PUFAs do not suppress AA and poly(I:C)-mediated inflammatory responses in HPFs.

**Stimulation with AA and poly(I:C) or LTA also Leads to Greater Cytokine Release from Epithelial Cells**

To explore whether other structural lung cells respond similarly to HPFs, we repeated selected experiments in the bronchial epithelial cell line BEAS-2B. AA alone did not induce IL-6 or CXCL8 release from BEAS-2Bs; however, AA in combination with poly(I:C) resulted in greater IL-6 release ( $n = 6$ ,  $P < 0.05$ ) than poly(I:C) alone (Figure 3A), showing responses similar to those observed in HPFs. PA in combination with poly(I:C) also resulted in greater IL-6 release ( $n = 6$ ,  $P < 0.05$ ) than poly(I:C) alone (Figure 3G). DHA did not affect poly(I:C)-induced IL-6 or CXCL8 release, but suppressed poly(I:C)-induced CCL5 release ( $n = 7$ ,  $P < 0.05$ ) (Figure 3F). Furthermore, LTA alone did not induce cytokine release from BEAS-2Bs. However, the combination of AA and LTA resulted in significant IL-6 and CXCL8 release ( $n = 6$ ,  $P < 0.01$ ) (Figures 4A and 4B). There was no interaction between DHA or PA and LTA (Figures 4C-4F).

**p38 MAPK Hyperactivation in Pulmonary Fibroblasts upon Challenge with AA and poly(I:C)**

To investigate the mechanisms underlying the effects of AA- and combined AA and poly(I:C) or LTA-induced IL-6 and CXCL8 release in HPFs, we used protein IB to

investigate the activation of three main signaling pathways (p38, NF- $\kappa$ B, and SAPK/JNK), all of which have been shown to play a role in PG- or infection-mediated inflammatory responses (32, 33). Phosphorylation of p38 MAPK was increased after stimulation with AA alone ( $n = 8$ ,  $P < 0.01$ ) and in combination with poly(I:C) ( $P < 0.001$ ) or LTA ( $P < 0.01$ ), whereas poly(I:C) and LTA alone did not affect p38 MAPK phosphorylation (Figure 5A). The combination of AA and poly(I:C) led to greater phosphorylation of p38 MAPK than AA alone ( $n = 8$ ,  $P < 0.05$ ), indicating that hyperactivation of this pathway is the mechanism by which synergism occurs. NF- $\kappa$ B phosphorylation was increased upon challenge with poly(I:C) ( $n = 8$ ,  $P < 0.01$ ) and LTA alone ( $n = 8$ ,  $P < 0.01$ ), but not in combination with AA (Figure 5B). Phosphorylation of SAPK/JNK was increased upon challenge with AA in combination with poly(I:C) ( $n = 7$ ,  $P < 0.05$ ), but not with any other challenge (Figure 5C). Total p38 MAPK, NF- $\kappa$ B, and SAPK/JNK did not change with any treatment (Figures 5D-5F).

**AA and poly(I:C) or LTA-induced Cytokine Release in Pulmonary Fibroblasts Is Mediated via p38 MAPK Signaling**

To further investigate and confirm the mechanisms underlying the effects of AA- and combined AA and poly(I:C) or LTA-induced IL-6 and CXCL8 release, specific inhibitors were used to block p38 MAPK, JNK, and NF- $\kappa$ B activation. Inhibition of p38 MAPK suppressed IL-6 and CXCL8 ( $n = 9-14$ ,  $P < 0.01$ ) release induced by AA alone (Figures 6A and 6B) or the combinations of AA and poly(I:C) (Figures 6E and 6F) and AA and LTA (Figures 6G and 6H), but did not affect cytokine release induced by poly(I:C) alone. Inhibition of JNK attenuated IL-6 release induced by poly(I:C) alone ( $n = 10$ ,  $P < 0.0001$ ) (Figure 6C) and AA combined with poly(I:C) ( $n = 10$ ,  $P < 0.01$ ) (Figure 6E). Inhibition of NF- $\kappa$ B only suppressed IL-6 release induced by AA in combination with LTA ( $n = 14$ ,  $P < 0.01$ ) (Figure 6G).

**Inhibition of COX Suppresses AA and poly(I:C) or LTA-induced Cytokine Release in Pulmonary Fibroblasts**

AA is a bioactive molecule and is a precursor that is metabolized by COX to produce eicosanoids, including the PGs (25, 34). PGs are known to play a key role in the

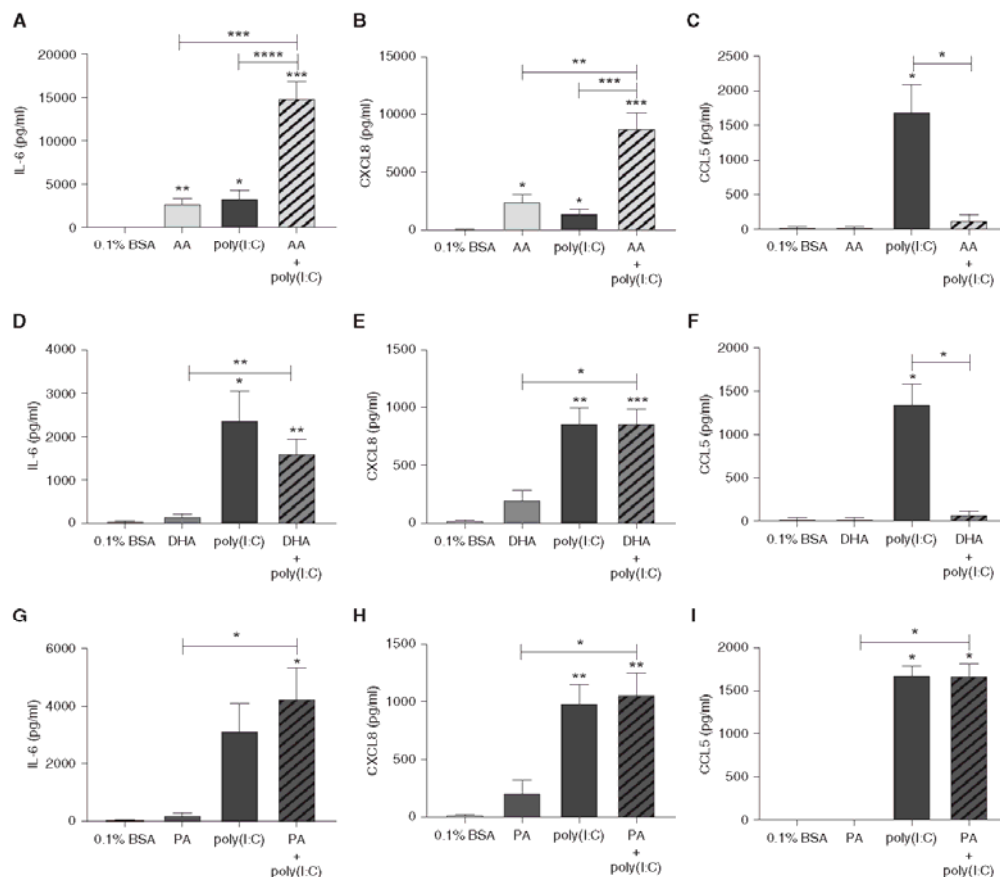


**Figure 1.** Greater cytokine release was achieved with combined arachidonic acid (AA) and polyinosinic:polycytidylic acid (poly(I:C)) challenge than with either alone. (A–C) Human primary pulmonary fibroblasts were unstimulated or challenged with the  $\omega$ -6 polyunsaturated fatty acid (PUFA) AA ( $n = 8–11$ ) (patients), (D–F) the  $\omega$ -3 PUFA docosahexaenoic acid (DHA), ( $n = 5–9$ ) (patients), or (G–I) the saturated fatty acid (SFA) palmitic acid (PA), ( $n = 3–9$ ) (patients) in 0.1% BSA–Dulbecco’s modified Eagle medium (BSA–DMEM, 100  $\mu$ M) for 4 hours with or without the viral mimic poly(I:C) (10  $\mu$ g/ml) for another 24 hours. Cell-free supernatants were collected and (A, D, and G) IL-6, (B, E, and H) CXCL8, or (C, F, and I) CCL5 release was measured using ELISA. All data are represented as mean  $\pm$  SEM. All challenges are compared with control, and challenges with poly(I:C) are compared with their respective challenge without poly(I:C) and challenge with poly(I:C) alone, using a one-way ANOVA with a Bonferroni post test. Significance is represented as \* $P < 0.05$ , \*\* $P < 0.01$ , \*\*\* $P < 0.001$ , or \*\*\*\* $P < 0.0001$ .

generation of inflammatory responses. To investigate whether COX-mediated PGs contribute to the induction of IL-6 and CXCL8 release, we pretreated HPFs with the nonselective COX inhibitor indomethacin. We found that indomethacin ( $10^{-5}$  M) pretreatment suppressed IL-6 and CXCL8 release induced by AA alone (Figures 6A and 6B), AA in combination with poly(I:C)

(Figures 6E and 6F), and AA in combination with LTA (Figures 6G and 6H) ( $n = 9–14$ ,  $P < 0.01$ ). However, indomethacin pretreatment did not affect cytokine release induced by poly(I:C) alone. The COX and p38 MAPK signaling pathways were the only two involved in both AA and poly(I:C)- as well as AA and LTA-induced IL-6 and IL-8 release.

#### AA and poly(I:C) or LTA-induced Cytokine Release in BEAS-2Bs Is Mainly Mediated by JNK and p38 MAPK Signaling

We also investigated the underlying mechanisms in BEAS-2Bs and found that phosphorylation of p38 MAPK was increased 30 minutes after stimulation with AA alone, and with AA in combination

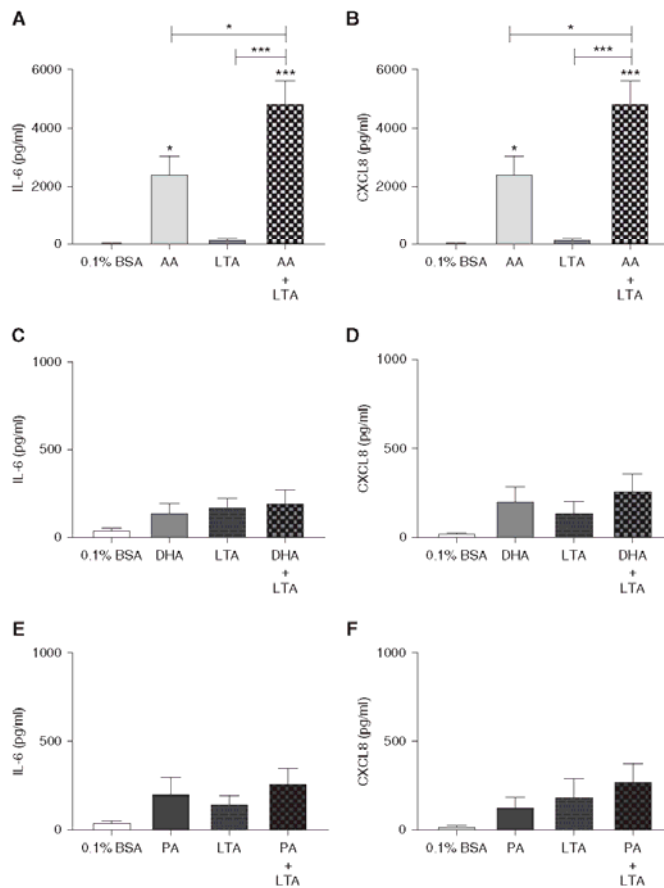


**Figure 2.** Greater cytokine release was achieved with combined AA and lipoteichoic acid (LTA) challenge than with either alone. (A and B) Human primary pulmonary fibroblasts were unstimulated (control) or challenged with the  $\omega$ -6 PUFA AA ( $n = 11$ ) (patients), (C and D) the  $\omega$ -3 PUFA DHA ( $n = 10$ ) (patients), or (E and F) the SFA PA ( $n = 9$ ) (patients) in 0.1% BSA-DMEM (100  $\mu$ M) for 4 hours prior to 24 hours with or without the bacterial compound LTA (10 mg/ml). Cell-free supernatants were collected and (A, C, and E) IL-6 and (B, D, and F) CXCL8 release was measured using ELISA. All data are represented as mean  $\pm$  SEM. All challenges are compared with control, and challenges with LTA are compared with their respective challenge without LTA and challenge with LTA alone, using a one-way ANOVA with a Bonferroni post test. Significance is represented as \* $P < 0.05$  or \*\*\* $P < 0.001$ .

with poly(I:C) or LTA ( $n = 8$ ,  $P < 0.05$ ) (Figure 7A). NF- $\kappa$ B phosphorylation was increased upon challenge with poly(I:C) and LTA alone, and with AA in combination with poly(I:C) ( $n = 7$ ,  $P < 0.05$ ) (Figure 7B). Phosphorylation of

SAPK/JNK was increased upon challenge with AA in combination with LTA ( $n = 7$ ,  $P < 0.05$ ) (Figure 7C).

In addition, inhibition of p38 MAPK or JNK suppressed IL-6 and CXCL8 release induced by poly(I:C) alone, AA in

combination with poly(I:C), and AA in combination with LTA ( $n = 7$ ,  $P < 0.05$ ) (Figure 8). Inhibition of NF- $\kappa$ B suppressed IL-6 and CXCL8 release induced by AA in combination with poly(I:C) ( $n = 7$ ,  $P < 0.05$ ) (Figures 8A and 8B), and CXCL8 release induced by poly(I:C) alone ( $P < 0.05$ ) (Figure 8D). Inhibition of JNK resulted in the greatest suppression of combined AA and poly(I:C)- or LTA-induced IL-6 and CXCL8 release. Inhibition of COX did not suppress IL-6 or CXCL8 release in BEAS-2Bs. These results show that the responses in BEAS-2Bs are different from those in HPFs and are mediated through NF- $\kappa$ B, JNK, and p38 MAPK (but not COX) signaling, and suggest that JNK signaling is the dominant pathway.

### Infection with Human RV16 Leads to Greater AA-induced Cytokine Release

To ensure that the results we obtained with pathogen components are reflective of a live infection, we next assessed whether the innate immune response to RV was modulated by AA. RV was chosen because it is the most common cause of common colds and has been shown to be a major cause of asthma exacerbations (8). Challenge with AA (100  $\mu$ M) in combination with RV16 infection at an MOI of 1.0 resulted in substantially greater IL-6 and CXCL8 ( $P < 0.05$ ) release than AA or RV alone from HPFs ( $n = 9$ ) (Figures 9A and 9B) and BEAS-2Bs ( $n = 7$ ) (replicates) (Figures 9C and 9D). The effect of the combination of AA with RV16 on IL-6 and CXCL8 release was greater than the sum of the individual effects of AA and RV16 in both cell types, demonstrating synergistic effects.

## Discussion

Obese patients with asthma have more frequent and severe exacerbations, which may be a result of excess dietary fatty acids enhancing the innate immune response to viral and/or bacterial infection. This study is the first to examine the effects of dietary fatty acids in this context.

This study demonstrates that the  $\omega$ -6 PUFA AA in combination with the viral mimic poly(I:C) results in greater IL-6 and CXCL8 release than either AA or poly(I:C) alone. Interestingly, the effect of the combination on cytokine release was substantially greater than the sum of the individual effects of AA and poly(I:C),

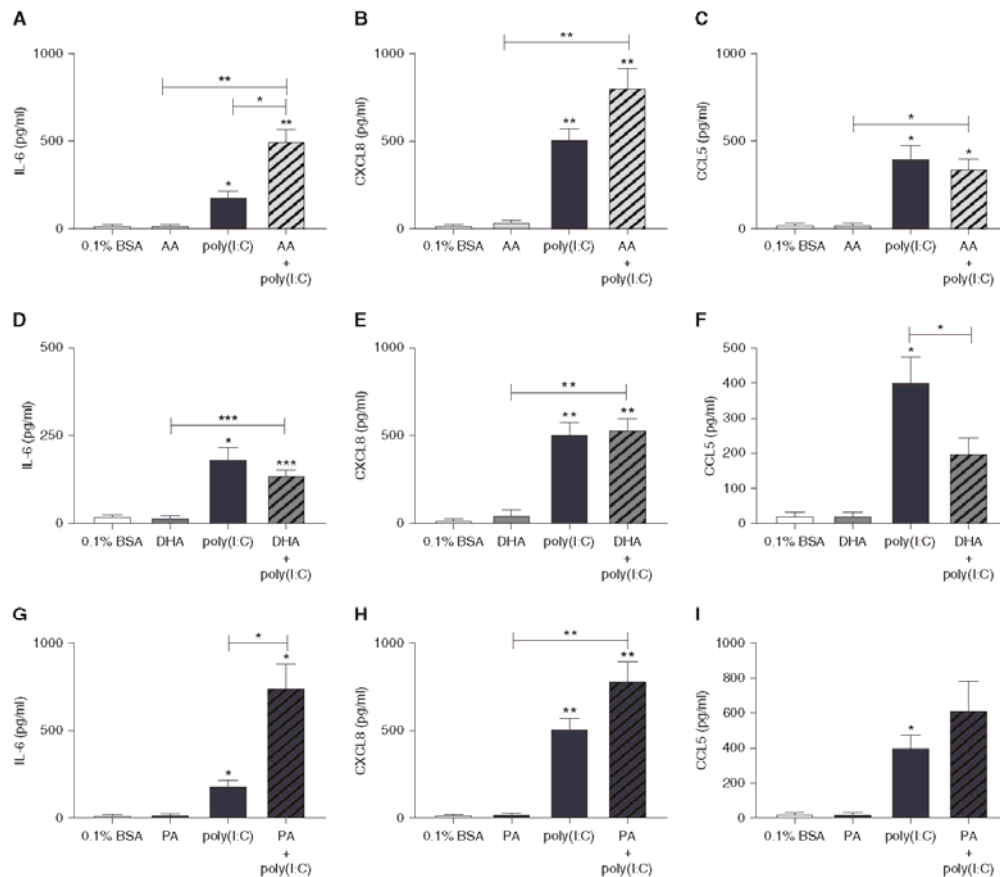


**Figure 3.** Greater IL-6 release was achieved with combined AA or PA and poly(I:C) challenge than with either alone in BEAS-2Bs. (A–C) The human bronchial epithelial cell line BEAS-2B was unstimulated (control) or challenged with the  $\omega$ -6 PUFA AA ( $n = 6-7$ ) (replicates), (D–F) the  $\omega$ -3 PUFA DHA ( $n = 6-7$ ) (replicates), or (G–I) the SFA PA ( $n = 6-7$ ) (replicates) in 0.1% BSA-DMEM (100  $\mu$ M) for 4 hours prior to 24 hours with or without the viral mimic poly(I:C) (10 mg/ml). Cell-free supernatants were collected and (A, D, and G) IL-6, (B, E, and H) CXCL8, and (C, F, and I) CCL5 release was measured using ELISA. All data are represented as mean  $\pm$  SEM. All challenges are compared with control, and challenges with poly(I:C) are compared with their respective challenge without poly(I:C) and challenge with poly(I:C) alone, using a one-way ANOVA with a Bonferroni post test. Significance is represented as \* $P < 0.05$ , \*\* $P < 0.01$ , or \*\*\* $P < 0.001$ .

which indicates that these effects are synergistic. We also examined the effects of dietary fatty acids on respiratory infection in epithelial cells. Interestingly, we found that epithelial cells were unresponsive to AA alone, but the combination with poly(I:C) resulted in synergistic cytokine release. In addition, PA enhanced poly(I:C)-induced cytokine release from epithelial

cells. These results show that dietary fatty acids have different effects on different lung cells, and suggest that increased levels of AA and PA during viral infection may lead to more severe airway inflammation.

The current study focused mainly on the cytokines IL-6 and CXCL8, as these are crucial drivers of neutrophilic inflammation and are clinically important in both the

pathogenesis of asthma and clinical outcomes in severe and obese asthma, including virus-induced exacerbations. However, multiple cytokines and chemokines are important for driving granulocyte recruitment and activation in asthma. We also measured CCL5 (RANTES) and GM-CSF release. There was no induction of GM-CSF in both cell types.

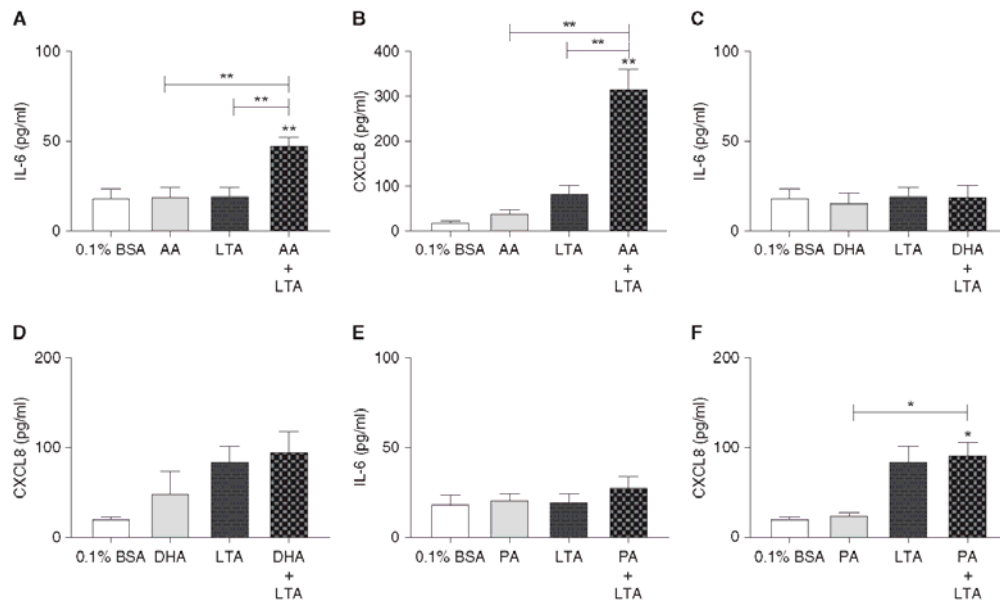


**Figure 4.** Greater cytokine release was achieved with combined AA and LTA challenge than with either alone in BEAS-2Bs. (A and B) The human bronchial epithelial cell line BEAS-2B was unstimulated (control) or challenged with the  $\omega$ -6 PUFA AA ( $n = 6$ ) (replicates), (C and D) the  $\omega$ -3 PUFA DHA ( $n = 6$ ) (replicates), or (E and F) the SFA PA ( $n = 6$ ) (replicates) in 0.1% BSA-DMEM (100  $\mu$ M) for 4 hours prior to 24 hours with or without the bacterial compound LTA (10 mg/ml). Cell-free supernatants were collected and (A, C, and E) IL-6 and (B, D, and F) CXCL8 release was measured using ELISA. All data are represented as mean  $\pm$  SEM. All challenges are compared with control, and challenges with LTA are compared with their respective challenge without LTA and challenge with LTA alone, using a one-way ANOVA with a Bonferroni post test. Significance is represented as \* $P < 0.05$  or \*\* $P < 0.01$ .

However, DHA reduced poly(I:C)-induced RANTES in HPFs and BEAS-2Bs. In addition, AA reduced poly(I:C)-induced RANTES in fibroblasts, but not BEAS-2Bs. We interpret these results as further evidence that the immune response in obese asthma is skewed toward neutrophilic inflammation. If GM-CSF induction had occurred, this would have been evidence of a granulocytic response, as it promotes the proliferation, differentiation, and activation of monocytes, neutrophils, eosinophils, and dendritic cells, and acts as a cofactor for superoxide production and degranulation (35, 36). The suppression of CCL5 (RANTES) by AA further reinforces neutrophilic inflammation, as it typically recruits monocytes, T cells, and eosinophils, and has been associated with eosinophilic airway inflammation in asthma (37, 38).

RV is the most common cause of virus-induced exacerbations in both children and adults with asthma (8, 39). In the past, RV

was considered as an upper-respiratory pathogen only. However, *in vivo* studies have conclusively shown that RV can also replicate in the lower airways (26, 40) and can infect submucosal cells, including pulmonary fibroblasts and airway smooth muscle cells. Other investigators and we have shown that RV infects primary pulmonary fibroblasts, inducing proinflammatory mediators such as IL-6 and CXCL8 (41, 42). Fibroblasts are located within the airway submucosa where airway blood vessels are found, and therefore are directly exposed to constituents of tissue fluids (plasma), including dietary fatty acids, and are likely to be key cells in driving inflammatory responses to serum-derived factors. As such, this study focused primarily on pulmonary fibroblasts.

Viruses activate the innate immune response through activation of the molecular pattern recognition receptors TLR3, TLR7, and TLR8 (43) via the

activation of specific transcription factors, including NF- $\kappa$ B and AP-1. poly(I:C) is a synthetic analog of double-stranded RNA (dsRNA) and is known to activate TLR3 (44). TLR7 and TLR8 detect single-stranded RNA, whereas TLR3 detects dsRNA, which occurs when single-stranded RNA viruses, including RV, replicate (43). We used an agonist for TLR3 rather than TLR7 or TLR8 based on previous studies showing that RV induces cytokines via activation of TLR3, but not TLR7 or TLR8, in bronchial epithelial cells. Furthermore, we have previously shown that RV-induced cytokine release in fibroblasts is replication dependent (i.e., the cells detect and respond only to dsRNA) (41). To confirm that AA increases RV-induced inflammation, we also assessed the response to AA in combination with RV16 infection. We found that challenge with AA in combination with RV16 infection resulted in substantially greater cytokine release

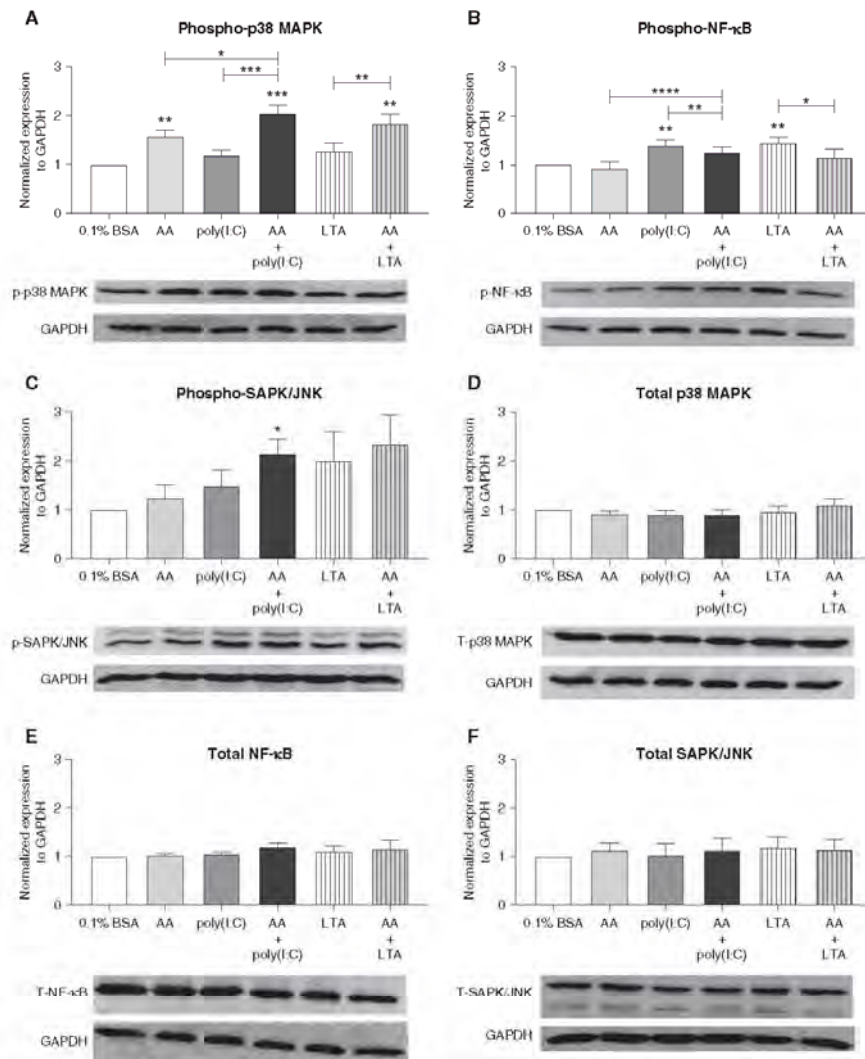


**Figure 5.** Activation of p38 mitogen-activated protein kinase (MAPK), NF- $\kappa$ B, and stress-activated protein kinase/c-Jun NH2-terminal kinase (SAPK/JNK) upon challenge with AA and poly(I:C) or LTA. (A–C) Primary human pulmonary fibroblasts ( $n = 7–8$ ) (patients) were unstimulated (control) or challenged with AA (100  $\mu$ M), the viral mimic poly(I:C) (10  $\mu$ g/ml), the bacterial compound LTA (10  $\mu$ g/ml), AA (100  $\mu$ M) in combination with poly(I:C) (1 ng/ml), or AA (100  $\mu$ M) in combination with LTA for 30 minutes before whole-cell lysates were collected and p38 MAPK (A), NF- $\kappa$ B p65 (B), or JNK (C) phosphorylation was assessed by Western blotting. (D–F) Total p38 MAPK (D), NF- $\kappa$ B p65 (E), or SAPK/JNK (F) was also assessed. All values were normalized to GAPDH (housekeeping protein) detected on the same blots. Data are expressed as fold increase of control, mean  $\pm$  SEM. All challenges are compared with control, and challenges with poly(I:C) or LTA are compared with their respective challenge without poly(I:C) or LTA and challenge with poly(I:C) or LTA alone, using a one-way ANOVA (Fisher's least significant difference test). Significance is represented as \* $P < 0.05$ , \*\* $P < 0.01$ , \*\*\* $P < 0.001$ , or \*\*\*\* $P < 0.0001$ . Representative Western blots of phosphorylated and total p38 MAPK, NF- $\kappa$ B p65, and SAPK/JNK are shown under each graph.



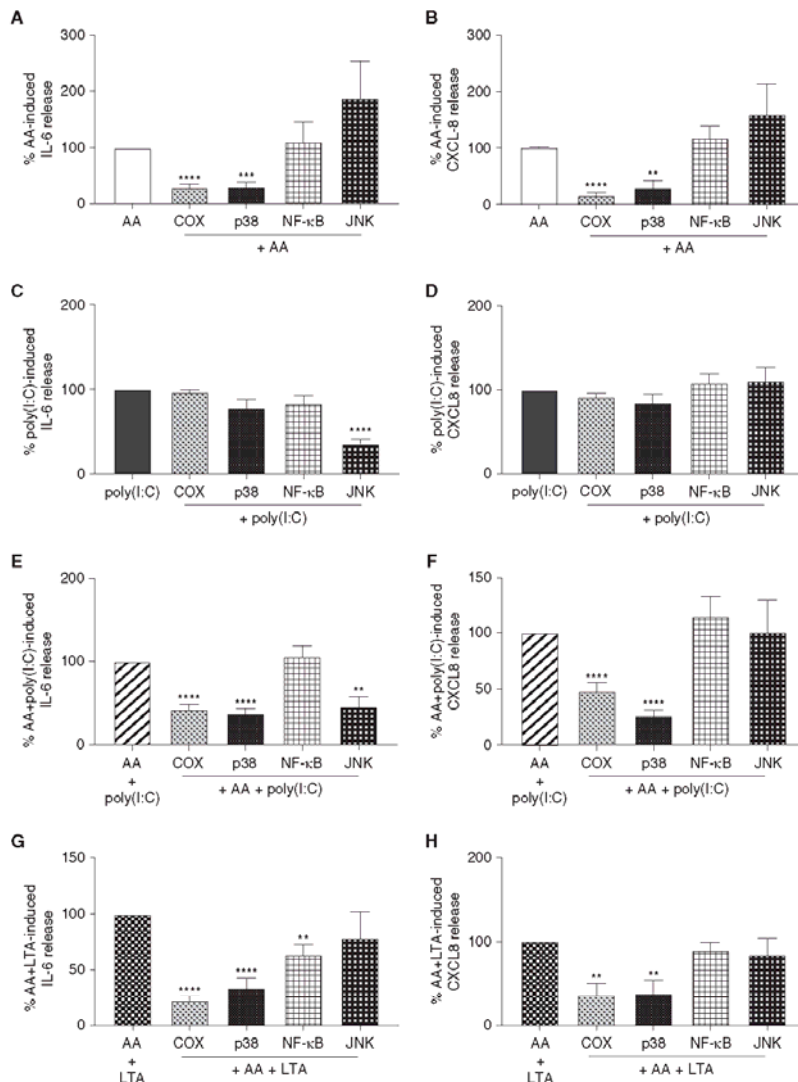


**Figure 6.** Inhibition of cyclooxygenase (COX) or p38 MAPK suppresses cytokine release induced by AA alone and in combination with viral or bacterial surrogates from fibroblasts. Primary human pulmonary fibroblasts ( $n = 9-14$ ) (patients) were treated with or without the COX inhibitor indomethacin ( $10^{-5}$  M), the p38 MAPK signaling inhibitor SB238063 ( $3 \mu\text{M}$ ), the NF- $\kappa$ B inhibitor BAY-117082 ( $1 \mu\text{M}$ ), or (A and B) the JNK inhibitor SP600125 ( $10 \mu\text{M}$ ) for 60 minutes before challenge with AA ( $100 \mu\text{M}$ ), (C and D) the viral mimic poly(I:C) ( $10 \mu\text{g}/\text{ml}$ ), (E and F) AA ( $100 \mu\text{M}$ ) in combination with poly(I:C), or (G and H) AA ( $100 \mu\text{M}$ ) in combination with LTA ( $10 \mu\text{g}/\text{ml}$ ). Cell-free supernatants were collected after 24 hours and (A, C, E, and G) IL-6 and (B, D, F, and H) CXCL8 release was measured using ELISA. All data are represented as percent cytokine release  $\pm$  SEM. All treatments with an inhibitor are compared with their respective control in the absence of the inhibitor using one-way ANOVA with a Bonferroni post test. Significance is represented as \*\* $P < 0.01$ , \*\*\* $P < 0.001$ , or \*\*\*\* $P < 0.0001$ .

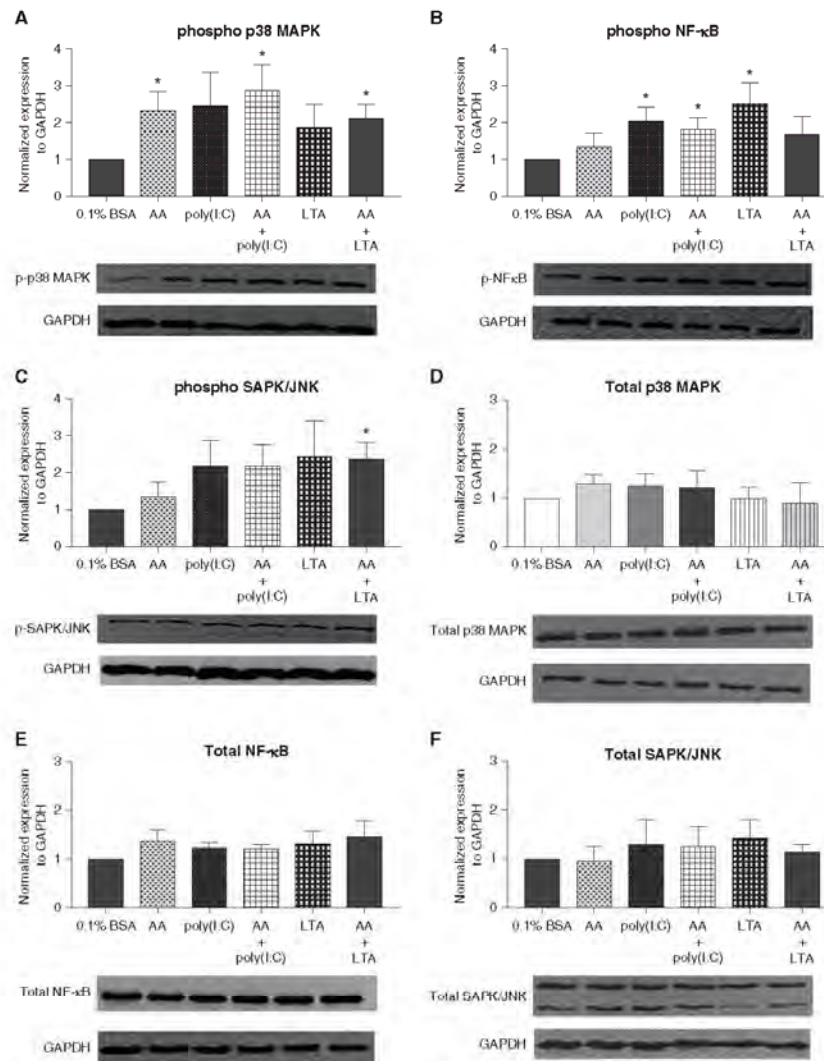


**Figure 7.** Activation of p38 MAPK, NF- $\kappa$ B, and SAPK/JNK upon challenge with AA and poly(I:C) or LTA in BEAS-2Bs. (A–C) The human bronchial epithelial cell line BEAS-2B ( $n = 4$ –8) (replicates) was unstimulated or challenged with AA (100  $\mu$ M), the viral mimic poly(I:C) (10  $\mu$ g/ml), the bacterial compound LTA (10  $\mu$ g/ml), AA (100  $\mu$ M) in combination with poly(I:C) (1 ng/ml), or AA (100  $\mu$ M) in combination with LTA for 30 minutes before whole-cell lysates were collected and p38 MAPK (A), NF- $\kappa$ B p65 (B), or SAPK/JNK (C) phosphorylation was assessed by Western blotting. (D–F) Total p38 MAPK (D), NF- $\kappa$ B p65 (E), or SAPK/JNK (F) was also assessed. All values were normalized to GAPDH (housekeeping protein) detected on the same blots. Data are expressed as fold increase of control, mean  $\pm$  SEM. All challenges are compared with control, and challenges with poly(I:C) or LTA are compared with their respective challenge without poly(I:C) or LTA and challenge with poly(I:C) or LTA alone, using a one-way ANOVA (Fisher's least significant difference test). Significance is represented as \* $P < 0.05$ . Representative Western blots of phosphorylated and total p38 MAPK, NF- $\kappa$ B p65, and SAPK/JNK are shown under each graph.



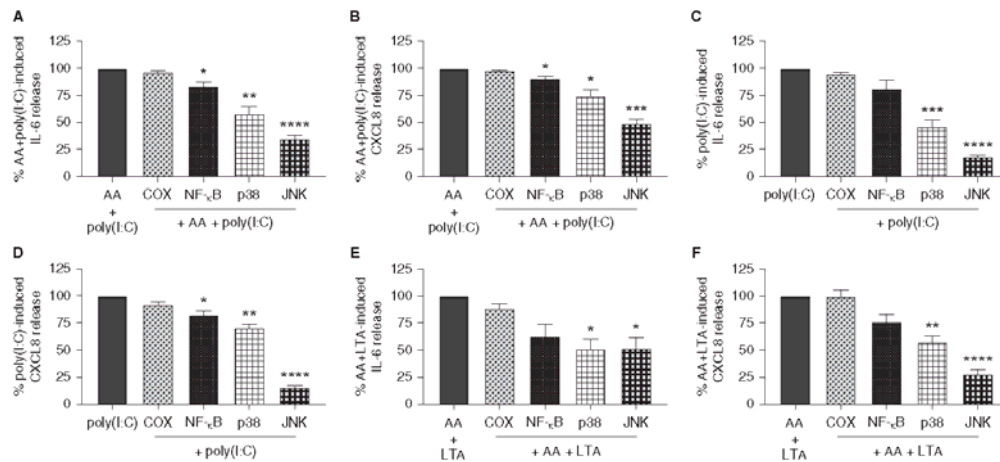


**Figure 8.** Inhibition of p38 MAPK or JNK suppresses cytokine release induced by AA in combination with poly(I:C) or LTA from BEAS-2Bs. The human bronchial epithelial cell line BEAS-2B ( $n = 7$ ) (replicates) was treated with or without the COX inhibitor indomethacin ( $10^{-5}$  M), the p38 MAPK signaling inhibitor SB239063 ( $3 \mu\text{M}$ ), the NF- $\kappa$ B inhibitor BAY-117082 ( $1 \mu\text{M}$ ), or (A and B) the JNK inhibitor SP600125 ( $10 \mu\text{M}$ ) for 60 minutes before challenge with AA ( $100 \mu\text{M}$ ) in combination with the viral mimic poly(I:C), (C and D) poly(I:C) alone, or (E and F) AA ( $100 \mu\text{M}$ ) in combination with LTA ( $10 \mu\text{g/ml}$ ). Cell-free supernatants were collected after 24 hours and (A, C, and E) IL-6 and (B, D, and F) CXCL8 release was measured using ELISA. All data are represented as percent cytokine release  $\pm$  SEM. All treatments with an inhibitor are compared with their respective control in the absence of the inhibitor using one-way ANOVA with a Bonferroni post test. Significance is represented as \* $P < 0.05$ , \*\* $P < 0.01$ , \*\*\* $P < 0.001$ , or \*\*\*\* $P < 0.0001$ .

than either AA or RV16 alone in HPFs and BEAS-2Bs.

Less is known about bacterial infections in asthma. Some bacterial pathogens are more frequently found in the airways of patients with asthma than in healthy individuals (12), but their role in exacerbations is unclear. Studies have reported mycoplasma infection in up to 25% of children with wheezing (11) and in 20% of children with asthma requiring hospitalization due to exacerbations. However, not all studies have confirmed these findings (45). In the current study, we also investigated the effect of dietary fatty acids on bacterial infection. To model bacterial infection, we challenged cells with the bacterial endotoxin LTA. We found that challenge with AA in combination with LTA resulted in greater IL-6 and CXCL8 release from pulmonary fibroblasts and epithelial cells than either alone. The effect of the combination on cytokine release was substantially greater than the sum of the individual effects of AA and LTA, which indicates that these effects are synergistic. These results indicate that exposure to AA during bacterial infection may lead to more severe

airway inflammation. There was no interaction between the other dietary fatty acids and LTA. Bacterial recognition is dependent on TLR2 and TLR4. TLR4 mainly senses LPS, which is a major component of the outer membrane of gram-negative bacteria. TLR2 is the primary innate immune receptor for gram-positive bacteria. We used LTA, an important cell wall polymer found in gram-positive bacteria that has been shown to cause innate immune responses mediated through TLR2 (46).

LTA alone, however, did not induce cytokine release from either HPFs or BEAS-2Bs. Presumably, even though bronchial epithelial cells express TLR2, challenge with LTA is not potent enough to induce the production of IL-6 or CXCL8 in epithelial cells, and a cochallenge is needed. Other studies have reported similar findings. Armstrong and colleagues found that LTA alone did not induce the production of CXCL8 or IL-6 in bronchial epithelial cells (47), and a low responsiveness of lung epithelial cells to LTA (small increase in CXCL8 release) was observed in another *in vitro* study (48).

The effects of dietary fatty acids on immune responses have been an area of interest for many years. However, there is a great deal of conflicting data. DHA and AA serve as important cell membrane components as well as precursors for biologic mediators with many effects, including numerous roles in immune function and inflammation. In general,  $\omega$ -6 PUFAs and SFAs have predominantly been associated with proinflammatory effects, whereas the  $\omega$ -3 PUFAs are associated with antiinflammatory and immunosuppressive effects (25, 34). None of the  $\omega$ -3 PUFAs (DHA, EPA, and ALA) suppressed poly(I:C)-induced cytokine release, or combined AA and poly(I:C)-induced inflammatory responses in HPFs, suggesting that  $\omega$ -3 PUFAs do not have antiinflammatory effects in these lung cells. SFAs, including PA, initiate innate immune responses through activation of TLR2 and TLR4 in adipocytes and macrophages (24, 49, 50). These results have been replicated in human studies, which showed that within 4 hours of consumption of a high-fat meal, innate immune responses were activated with increased TLR2, TLR4, and NF- $\kappa$ B activity in mononuclear and

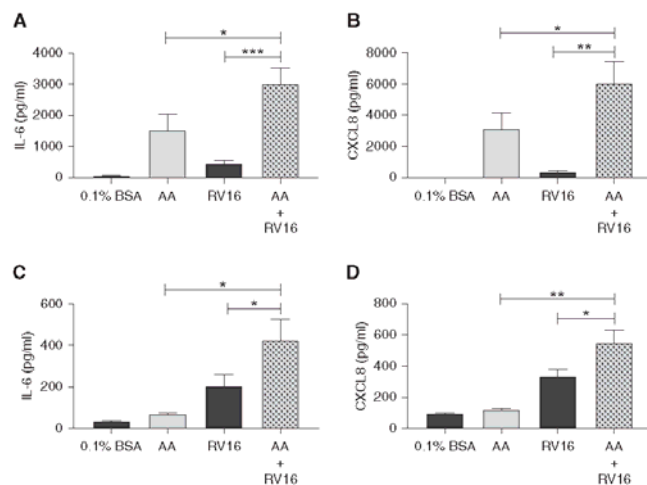


**Figure 9.** Greater cytokine release was achieved with combined AA and human rhinovirus 16 (RV16) challenge than with either alone in human pulmonary fibroblasts and BEAS-2Bs. (A and B) Human primary pulmonary fibroblasts ( $n = 9$ ) (patients) or (C and D) BEAS-2Bs ( $n = 7$ ) (replicates) were unstimulated (control) or challenged with AA in 0.1% BSA-DMEM (100  $\mu$ M) for 4 hours before infection with RV16 at a multiplicity of infection of 1 for another 24 hours. Cell-free supernatants were collected and (A and C) IL-6 and (B and D) CXCL8 release was measured using ELISA. All data are represented as mean  $\pm$  SEM. All challenges with RV16 are compared with their respective challenge without RV16 and with RV16 alone, using a one-way ANOVA with a Bonferroni post test. Significance is represented as \* $P < 0.05$ , \*\* $P < 0.01$ , or \*\*\* $P < 0.001$ .

polymorphonuclear cells (51, 52). The nonresponsiveness to PA observed in this study may be explained by the lack of functional TLR4 signaling in pulmonary fibroblasts. Lung mesenchymal cells do not express CD14, which acts as a coreceptor for TLR4 (53, 54). This is also why we used LTA (TLR2 agonist) and not LPS (TLR4 agonist). SFAs were previously shown to inhibit virus replication in a mouse model of chronic hepatitis B infection (55); however, another mouse model study showed that SFAs increase bacterial load in *Staphylococcus aureus* infection (56). Studies looking at the effects of  $\omega$ -6 PUFAs on inflammatory processes and infections have reported conflicting data. A study in healthy men found that supplementation with  $\omega$ -6 PUFAs significantly increased the number of circulating neutrophils and production of LPS-induced leukotriene B4 from leukocytes (57). Conversely, supplementation with AA did not affect *in vitro* secretion of TNF- $\alpha$  by peripheral mononuclear cells, nor did it affect peripheral blood mononuclear cell

proliferation and natural killer cell activity. A study by Jordao and colleagues found that AA enhanced bacterial killing of *Mycobacterium tuberculosis* in macrophages, but increased pathogen survival in a mouse model of tuberculosis (58). In the current study, a clear proinflammatory effect of AA on bacterial and viral infection was observed.

To understand the underlying mechanisms involved in (synergistic) AA and poly(I:C)- or LTA-induced IL-6 and CXCL8 production, signaling pathways were investigated. We observed activation of p38 MAPK upon challenge with AA alone and in combination with poly(I:C) or LTA. Challenge with poly(I:C) and LTA alone led to increased phosphorylation of NF- $\kappa$ B, while challenge with the combination of AA and poly(I:C) caused increased phosphorylation of SAPK/JNK. AA in combination with poly(I:C) led to greater phosphorylation of p38 MAPK than challenge with AA alone, indicating p38 MAPK signaling to be the mechanism by which synergism occurs. We further

investigated and confirmed the underlying mechanisms involved in AA and poly(I:C)- or LTA-induced IL-6 and CXCL8 release using specific signaling inhibitors at concentrations previously shown to be effective in human airway cells (26–28). SB239063 is a potent and selective inhibitor of p38 MAPK and displays specific and high-affinity binding ( $IC_{50} = 44$  nM) (59). It suppressed IL-6 and CXCL8 release induced by AA alone and the combinations of AA and poly(I:C) or LTA. These data suggest that AA in combination with poly(I:C) or LTA activates the p38 MAPK pathway, leading to both IL-6 and CXCL8 release. Inhibition of JNK with SP600125 suppressed IL-6 release induced by poly(I:C) alone and in combination with AA, but did not affect CXCL8 release. Inhibition of NF- $\kappa$ B with BAY-117082 partially suppressed IL-6 release induced by the combination of AA and LTA, again indicating the involvement of multiple pathways. These results, which showed that BAY-117082 suppressed AA and LTA-induced IL-6 but not CXCL8 release while SP600125 suppressed poly(I:C)- and AA/poly(I:C)-induced IL-6 but not CXCL8 release, are unexpected. Previous studies have shown IL-6 and CXCL8 transcription to be regulated by the same transcription factors: NF- $\kappa$ B, CREB protein, AP-1, and CCAAT/enhancer binding protein (C/EBP) (60, 61). However, it appears that in this study the dominant transcription factors regulating CXCL8 are different to those regulating IL-6 with p38 MAPK being the only common transcription factor for both cytokines.

PGs, including PGE<sub>2</sub>, are COX metabolites of AA. PGE<sub>2</sub> induces IL-6 release from bronchial epithelial cells, and CXCL8 release from lung mesenchymal cells (62, 63). To investigate whether COX-mediated PGs contribute to IL-6 and CXCL8 release, we pretreated pulmonary fibroblasts with indomethacin, which inhibits both COX-1 and COX-2. Indomethacin inhibited AA-induced IL-6 and CXCL8 release alone and in combination with poly(I:C) or LTA. However, indomethacin did not affect cytokine release induced by poly(I:C) alone. Our data suggest that IL-6 and CXCL8 production in HPFs is PG mediated. We consider these effects to be mediated through COX-2 rather than COX-1, as COX-1 is responsible for constitutive production under basal conditions, whereas COX-2 is upregulated during inflammation and is responsible for PGE<sub>2</sub> biosynthesis at

sites of inflammation (64). We consider the combination of the production of COX-mediated PGs and the activation of transcription factors to be the most logical mechanism for synergistic cytokine release in HPFs.

We also investigated the underlying mechanisms in BEAS-2Bs and found that p38 MAPK signaling is involved in poly(I:C)-, combined poly(I:C) and AA-, and combined LTA and AA-induced IL-6 and CXCL8 release in BEAS-2Bs. However, inhibition of COX did not suppress IL-6 or CXCL8 release in BEAS-2Bs, which is different from what we observed in fibroblasts. This is consistent with the lack of cytokine induction by AA in BEAS-2B. In addition, inhibition of JNK signaling resulted in the greatest suppression of combined AA and poly(I:C)- or LTA-induced IL-6 and CXCL8 release in BEAS-2Bs. These results suggest that there

is a differential response in BEAS-2Bs compared with fibroblasts. Although we used primary HPFs here, an important limitation of this study is that all experiments were done *in vitro*. In future studies, we plan to investigate the effects of dietary fatty acids on immune responses to infection using an *in vivo* model.

In summary, this study demonstrates that exposure of HPFs and epithelial cells to  $\omega$ -6 PUFAs causes an amplification of the inflammatory responses to viral and bacterial components, as measured by IL-6 and CXCL8 release. In HPFs the responses were PG dependent and mediated through p38 MAPK signaling, whereas the responses in BEAS-2Bs were mainly mediated through JNK and p38 MAPK signaling, suggesting that p38 MAPK inhibitors might be effective in obese patients with asthma to prevent exacerbations. In epithelial cells, exposure

to PA also enhanced the inflammatory response to viral infection. These results suggest that during respiratory infection, increased levels of dietary  $\omega$ -6 PUFAs and SFAs may lead to more severe airway inflammation and might contribute to and/or increase the severity of asthma exacerbations in obese patients with asthma. ■

**Author disclosures** are available with the text of this article at [www.atsjournals.org](http://www.atsjournals.org).

**Acknowledgment:** The authors would like to thank the collaborative effort of the cardiopulmonary transplant team and the pathologists at St. Vincent's Hospital (Sydney, Australia), and the thoracic physicians and pathologists at the Royal Prince Alfred Hospital (Sydney) and Strathfield Private Hospital (Strathfield, Australia). They also thank F. Thomson and M. Thomson for their continued support.

References

- Ng M, Fleming T, Robinson M, Thomson B, Graetz N, Margono C, et al. Global, regional, and national prevalence of overweight and obesity in children and adults during 1980-2013: a systematic analysis for the global burden of disease study 2013. *Lancet* 2014;384:766-781.
- Gruchala-Niedoszytko M, Malgorzewicz S, Niedoszytko M, Gnacinska M, Jassem E. The influence of obesity on inflammation and clinical symptoms in asthma. *Adv Med Sci* 2013;58:15-21.
- Mosen DM, Schatz M, Magid DJ, Camargo CA Jr. The relationship between obesity and asthma severity and control in adults. *J Allergy Clin Immunol* 2008;122:507-511.e6.
- Telenga ED, Tideman SW, Kerstjens HA, Hacken NH, Timens W, Postma DS, et al. Obesity in asthma: more neutrophilic inflammation as a possible explanation for a reduced treatment response. *Allergy* 2012; 67:1060-1068.
- Scott HA, Gibson PG, Garg ML, Wood LG. Airway inflammation is augmented by obesity and fatty acids in asthma. *Eur Respir J* 2011; 38:594-602.
- Schatz M, Zeiger RS, Zhang F, Chen W, Yang SJ, Camargo CA Jr. Overweight/obesity and risk of seasonal asthma exacerbations. *J Allergy Clin Immunol Pract* 2013;1:618-622.
- Rodrigo GJ, Plaza V. Body mass index and response to emergency department treatment in adults with severe asthma exacerbations: a prospective cohort study. *Chest* 2007;132:1513-1519.
- Wark PA, Gibson PG. Asthma exacerbations: 3. Pathogenesis. *Thorax* 2006;61:909-915.
- Yamaya M. Virus infection-induced bronchial asthma exacerbation. *Pulm Med* 2012;2012:834826.
- Kim CK, Callaway Z, Gern JE. Viral infections and associated factors that promote acute exacerbations of asthma. *Allergy Asthma Immunol Res* 2018;10:12-17.
- Henderson FW, Clyde WA Jr, Collier AM, Denny FW, Senior RJ, Sheaffer CI, et al. The etiologic and epidemiologic spectrum of bronchiolitis in pediatric practice. *J Pediatr* 1979;95:183-190.
- Nisar N, Guleria R, Kumar S, Chand Chawla T, Ranjan Biswas N. *Mycoplasma pneumoniae* and its role in asthma. *Postgrad Med J* 2007;83:100-104.
- Dhurandhar NV, Bailey D, Thomas D. Interaction of obesity and infections. *Obes Rev* 2015;16:1017-1029.
- Campitelli MA, Rosella LC, Kwong JC. The association between obesity and outpatient visits for acute respiratory infections in Ontario, Canada. *Int J Obes (Lond)* 2014;38:113-119.
- Louie JK, Acosta M, Samuel MC, Schechter R, Vugia DJ, Harriman K, et al.; California Pandemic (H1N1) Working Group. A novel risk factor for a novel virus: obesity and 2009 pandemic influenza A (H1N1). *Clin Infect Dis* 2011;52:301-312.
- Morgan OW, Bramley A, Fowlkes A, Freedman DS, Taylor TH, Gargiullo P, et al. Morbid obesity as a risk factor for hospitalization and death due to 2009 pandemic influenza A(H1N1) disease. *PLoS One* 2010;5: e9694.
- Wood LG. Diet, obesity, and asthma. *Ann Am Thorac Soc* 2017;14 (Suppl 5):S332-S338.
- van Oostrom AJ, Sijmonsma TP, Verseyden C, Jansen EH, de Koning EJ, Rabelink TJ, et al. Postprandial recruitment of neutrophils may contribute to endothelial dysfunction. *J Lipid Res* 2003;44:576-583.
- Wood LG, Garg ML, Gibson PG. A high-fat challenge increases airway inflammation and impairs bronchodilator recovery in asthma. *J Allergy Clin Immunol* 2011;127:1133-1140.
- Boden G. Obesity and free fatty acids. *Endocrinol Metab Clin North Am* 2008;37:635-646, viii-ix.
- Abdelmagid SA, Clarke SE, Nielsen DE, Badawi A, El-Sohemy A, Mutch DM, et al. Comprehensive profiling of plasma fatty acid concentrations in young healthy Canadian adults. *PLoS One* 2015; 10:e0116195.
- Feng R, Luo C, Li C, Du S, Okeunle AP, Li Y, et al. Free fatty acids profile among lean, overweight and obese non-alcoholic fatty liver disease patients: a case-control study. *Lipids Health Dis* 2017;16: 165.
- Guereñdiain M, Montes R, López-Belmonte G, Martín-Matillas M, Castellote AI, Martín-Bautista E, et al. Changes in plasma fatty acid composition are associated with improvements in obesity and related metabolic disorders: a therapeutic approach to overweight adolescents. *Clin Nutr* 2018;37:149-156.
- Huang S, Rutkowski JM, Snodgrass RG, Ono-Moore KD, Schneider DA, Newman JW, et al. Saturated fatty acids activate TLR-mediated proinflammatory signaling pathways. *J Lipid Res* 2012;53:2002-2013.
- Calder PC. Polyunsaturated fatty acids and inflammatory processes: new twists in an old tale. *Biochimie* 2009;91:791-795.

26. Papadopoulos NG, Bates PJ, Bardin PG, Papi A, Leir SH, Fraenkel DJ, et al. Rhinoviruses infect the lower airways. *J Infect Dis* 2000;181:1875–1884.
27. Krimmer D, Ichimaru Y, Burgess J, Black J, Oliver B. Exposure to biomass smoke extract enhances fibronectin release from fibroblasts. *PLoS One* 2013;8:e83938.
28. Gupta S, Knight AG, Gupta S, Keller JN, Bruce-Keller AJ. Saturated long-chain fatty acids activate inflammatory signaling in astrocytes. *J Neurochem* 2012;120:1060–1071.
29. Kuo C, Lim S, King NJ, Bartlett NW, Walton RP, Zhu J, et al. Rhinovirus infection induces expression of airway remodeling factors *in vitro* and *in vivo*. *Respirology* 2011;16:367–377.
30. Bartlett NW, Walton RP, Edwards MR, Aniscenko J, Caramori G, Zhu J, et al. Mouse models of rhinovirus-induced disease and exacerbation of allergic airway inflammation. *Nat Med* 2008;14:199–204.
31. Simopoulos AP. The importance of the ratio of omega-6/omega-3 essential fatty acids. *Biomed Pharmacother* 2002;56:365–379.
32. Huang G, Shi LZ, Chi H. Regulation of JNK and p38 MAPK in the immune system: signal integration, propagation and termination. *Cytokine* 2009;48:161–169.
33. Guven-Maiorov E, Keskin O, Gursoy A, VanWaes C, Chen Z, Tsai CJ, et al. The architecture of the TIR domain signalosome in the Toll-like receptor-4 signaling pathway. *Sci Rep* 2015;5:13128.
34. Calder PC. Omega-3 polyunsaturated fatty acids and inflammatory processes: nutrition or pharmacology? *Br J Clin Pharmacol* 2013;75:645–662.
35. Sanders SP, Kim J, Connolly KR, Porter JD, Siekierski ES, Proud D. Nitric oxide inhibits rhinovirus-induced granulocyte macrophage colony-stimulating factor production in bronchial epithelial cells. *Am J Respir Cell Mol Biol* 2001;24:317–325.
36. Becher B, Tugues S, Greter M. GM-CSF: from growth factor to central mediator of tissue inflammation. *Immunity* 2016;45:963–973.
37. Marques RE, Guabiraba R, Russo RC, Teixeira MM. Targeting CCL5 in inflammation. *Expert Opin Ther Targets* 2013;17:1439–1460.
38. Koya T, Takeda K, Kodama T, Miyahara N, Matsubara S, Balhorn A, et al. Rantes (CCL5) regulates airway responsiveness after repeated allergen challenge. *Am J Respir Cell Mol Biol* 2006;35:147–154.
39. Kurai D, Saraya T, Ishii H, Takizawa H. Virus-induced exacerbations in asthma and COPD. *Front Microbiol* 2013;4:293.
40. Wos M, Sanak M, Soja J, Olechnowicz H, Busse WW, Szczeklik A. The presence of rhinovirus in lower airways of patients with bronchial asthma. *Am J Respir Crit Care Med* 2008;177:1082–1089.
41. Van Ly D, King NJ, Moir LM, Burgess JK, Black JL, Oliver BG. Effects of  $\beta(2)$  agonists, corticosteroids, and novel therapies on rhinovirus-induced cytokine release and rhinovirus replication in primary airway fibroblasts. *J Allergy (Cairo)* 2011;2011:457169.
42. Ghildyal R, Dagher H, Donninger H, de Silva D, Li X, Freezer NJ, et al. Rhinovirus infects primary human airway fibroblasts and induces a neutrophil chemokine and a permeability factor. *J Med Virol* 2005;75:608–615.
43. Muralidharan S, Mandrekar P. Cellular stress response and innate immune signaling: integrating pathways in host defense and inflammation. *J Leukoc Biol* 2013;94:1167–1184.
44. Zhou Y, Guo M, Wang X, Li J, Wang Y, Ye L, et al. TLR3 activation efficiency by high or low molecular mass poly I:C. *Innate Immun* 2013;19:184–192.
45. Cunningham AF, Johnston SL, Julious SA, Lampe FC, Ward ME. Chronic *Chlamydia pneumoniae* infection and asthma exacerbations in children. *Eur Respir J* 1998;11:345–349.
46. Seo HS, Michalek SM, Nahm MH. Lipoteichoic acid is important in innate immune responses to Gram-positive bacteria. *Infect Immun* 2008;76:206–213.
47. Armstrong L, Medford AR, Uppington KM, Robertson J, Witherden IR, Tetley TD, et al. Expression of functional Toll-like receptor-2 and -4 on alveolar epithelial cells. *Am J Respir Cell Mol Biol* 2004;31:241–245.
48. Mayer AK, Muehner M, Mages J, Gueinzus K, Hess C, Heeg K, et al. Differential recognition of TLR-dependent microbial ligands in human bronchial epithelial cells. *J Immunol* 2007;178:3134–3142.
49. Ajuwon KM, Spurlock ME. Palmitate activates the NF-kappaB transcription factor and induces IL-6 and TNFalpha expression in 3T3-L1 adipocytes. *J Nutr* 2005;135:1841–1846.
50. Lee JY, Zhao L, Youn HS, Weatherill AR, Tapping R, Feng L, et al. Saturated fatty acid activates but polyunsaturated fatty acid inhibits toll-like receptor 2 dimerized with Toll-like receptor 6 or 1. *J Biol Chem* 2004;279:16971–16979.
51. Patel C, Ghanim H, Ravishanker S, Sia CL, Viswanathan P, Mohanty P, et al. Prolonged reactive oxygen species generation and nuclear factor-kappaB activation after a high-fat, high-carbohydrate meal in the obese. *J Clin Endocrinol Metab* 2007;92:4476–4479.
52. Ghanim H, Sia CL, Upadhyay M, Korzeniewski K, Viswanathan P, Abuaysheh S, et al. Orange juice neutralizes the proinflammatory effect of a high-fat, high-carbohydrate meal and prevents endotoxin increase and toll-like receptor expression. *Am J Clin Nutr* 2010;91:940–949.
53. Alt E, Yan Y, Gehrmet S, Song YH, Altman A, Gehrmet S, et al. Fibroblasts share mesenchymal phenotypes with stem cells, but lack their differentiation and colony-forming potential. *Biol Cell* 2011;103:197–208.
54. Xing Z, Jordana M, Braciak T, Ohtoshi T, Gauldie J. Lipopolysaccharide induces expression of granulocyte/macrophage colony-stimulating factor, interleukin-8, and interleukin-6 in human nasal, but not lung, fibroblasts: evidence for heterogeneity within the respiratory tract. *Am J Respir Cell Mol Biol* 1993;9:255–263.
55. Zhang RN, Pan Q, Zhang Z, Cao HX, Shen F, Fan JG. Saturated fatty acid inhibits viral replication in chronic hepatitis B virus-infected with nonalcoholic fatty liver disease by toll-like receptor 4-mediated innate immune response. *Hepat Mon* 2015;15:e27909.
56. Svahn SL, Grahnmø L, Palsdottir V, Nookaew I, Wendt K, Gabrielson B, et al. Dietary polyunsaturated fatty acids increase survival and decrease bacterial load during septic *Staphylococcus aureus* infection and improve neutrophil function in mice. *Infect Immun* 2015;83:514–521.
57. Kelley DS, Taylor PC, Nelson GJ, Mackey BE. Arachidonic acid supplementation enhances synthesis of eicosanoids without suppressing immune functions in young healthy men. *Lipids* 1998;33:125–130.
58. Jordao L, Lengeling A, Bordat Y, Boudou F, Gicquel B, Neyrolles O, et al. Effects of omega-3 and -6 fatty acids on *Mycobacterium tuberculosis* in macrophages and in mice. *Microbes Infect* 2008;10:1379–1386.
59. Underwood DC, Osborn RR, Kotzer CJ, Adams JL, Lee JC, Webb EF, et al. SB 239063, a potent p38 MAP kinase inhibitor, reduces inflammatory cytokine production, airways eosinophil infiltration, and persistence. *J Pharmacol Exp Ther* 2000;293:281–288.
60. Ammit AJ, Lazaar AL, Irani C, O'Neill GM, Gordon ND, Amrani Y, et al. Tumor necrosis factor-alpha-induced secretion of rantes and interleukin-6 from human airway smooth muscle cells: modulation by glucocorticoids and beta-agonists. *Am J Respir Cell Mol Biol* 2002;26:465–474.
61. Terry CF, Loukaci V, Green FR. Cooperative influence of genetic polymorphisms on interleukin 6 transcriptional regulation. *J Biol Chem* 2000;275:18138–18144.
62. Bonanno A, Albano GD, Siena L, Montalbano AM, Riccobono L, Anzalone G, et al. Prostaglandin E<sub>2</sub> possesses different potencies in inducing vascular endothelial growth factor and interleukin-8 production in COPD human lung fibroblasts. *Prostaglandins Leukot Essent Fatty Acids* 2016;106:11–18.
63. Tavakoli S, Cowan MJ, Benfield T, Logun C, Shelhamer JH. Prostaglandin E<sub>2</sub>-induced interleukin-6 release by a human airway epithelial cell line. *Am J Physiol Lung Cell Mol Physiol* 2001;280:L127–L133.
64. Ricciotti E, FitzGerald GA. Prostaglandins and inflammation. *Arterioscler Thromb Vasc Biol* 2011;31:986–1000.

Reprinted with permission of the American Thoracic Society. Copyright © 2019 American Thoracic Society.

The *American Journal of Respiratory and Critical Care Medicine* is an official journal of the American Thoracic Society.



# SCIENTIFIC REPORTS

## OPEN MitoQ supplementation prevent long-term impact of maternal smoking on renal development, oxidative stress and mitochondrial density in male mice offspring

Received: 18 October 2017  
Accepted: 26 March 2018  
Published online: 26 April 2018

Suporn Sukjamnong<sup>1,2</sup>, Yik Lung Chan<sup>1,3</sup>, Razia Zakarya<sup>1,3</sup>, Long The Nguyen<sup>4</sup>, Ayad G. Anwer<sup>5</sup>, Amgad A. Zaky<sup>4</sup>, Rachana Santiyanont<sup>2</sup>, Brian G. Oliver<sup>2,3</sup>, Ewa Goldys<sup>5</sup>, Carol A. Pollock<sup>4</sup>, Hui Chen<sup>1</sup> & Sonia Saad<sup>4,1</sup>

To investigate the effect of maternal MitoQ treatment on renal disorders caused by maternal cigarette smoke exposure (SE). We have demonstrated that maternal SE during pregnancy increases the risk of developing chronic kidney disease (CKD) in adult offspring. Mitochondrial oxidative damage contributes to the adverse effects of maternal smoking on renal disorders. MitoQ is a mitochondria-targeted antioxidant that has been shown to protect against oxidative damage-related pathologies in many diseases. Female Balb/c mice (8 weeks) were divided into Sham (exposed to air), SE (exposed to cigarette smoke) and SEMQ (exposed to cigarette smoke with MitoQ supplemented from mating) groups. Kidneys from the mothers were collected when the pups weaned and those from the offspring were collected at 13 weeks. Maternal MitoQ supplementation during gestation and lactation significantly reversed the adverse impact of maternal SE on offspring's body weight, kidney mass and renal pathology. MitoQ administration also significantly reversed the impact of SE on the renal cellular mitochondrial density and renal total reactive oxygen species in both the mothers and their offspring in adulthood. Our results suggested that MitoQ supplementation can mitigate the adverse impact of maternal SE on offspring's renal pathology, renal oxidative stress and mitochondrial density in mice offspring.

It has been increasingly recognised that maternal programming during fetal development predisposes the offspring to future disease. Maternal smoking imposes a significant adverse impact on fetal renal development that determines the future risk of chronic kidney disease (CKD) in adulthood<sup>1</sup>. Human studies have shown that intrauterine exposure to cigarette smoke (SE) is closely linked to impaired fetal renal growth<sup>2</sup>. Maternal smoking is associated with a 1.24-times increased risk of child proteinuria compared with offspring of non-smoking mothers<sup>3</sup>. These phenomena have also been confirmed in our mouse model of maternal smoking, which demonstrated that maternal SE leads to renal underdevelopment in offspring at birth and renal dysfunction in adulthood<sup>4</sup>.

Mitochondria are intracellular organelles that generate the energy required for cellular functions through oxidative phosphorylation, which involves a series of oxidation-reduction reactions. During this process, reactive oxygen species (ROS) are released as a by-product. Thus, mitochondria are the major source of ROS during energy synthesis<sup>5</sup>, which is subsequently cleared by the endogenous antioxidants, such as manganese superoxide dismutase (MnSOD). Mitochondrial abnormalities, such as the accumulation of mitochondrial DNA mutations

<sup>1</sup>School of Life Sciences, Faculty of Science, University of Technology Sydney, Sydney, NSW, 2007, Australia.

<sup>2</sup>Department of Clinical Chemistry, Faculty of Allied Health Sciences, Chulalongkorn University, Bangkok, Thailand.

<sup>3</sup>Respiratory Cellular and Molecular Biology, Woolcock Institute of Medical Research, Sydney, NSW, 2037, Australia.

<sup>4</sup>Renal group Kolling Institute, Royal North Shore Hospital, St Leonards, NSW, 2065, Australia. <sup>5</sup>ARC

Centre of Excellence for Nanoscale Biophotonics, Macquarie University, North Ryde, 2109, NSW, Australia. Suporn

Sukjamnong and Yik Lung Chan contributed equally to this work. Correspondence and requests for materials should

be addressed to S. Saad (email: [sonia.saad@sydney.edu.au](mailto:sonia.saad@sydney.edu.au))

and damaged mitochondria structure due to metabolic stress, can overconsume the antioxidant enzymes or impair the production of antioxidants leading to oxidative stress which in turn triggers pro-inflammatory response<sup>6,7</sup>. Renal tubular cells contain abundant mitochondria, therefore mitochondrial density plays a fundamental role in the pathogenesis of kidney diseases. Growing evidence suggests that mitochondrial damage is implicated in the pathophysiology of renal diseases<sup>8,9</sup>. It has been reported that nicotine can accumulate in the kidney<sup>10</sup>. Several studies indicated that maternal smoking is closely related to increased levels of oxidative stress in the mothers, infants and newborns<sup>11,12</sup>, and reduced levels of the antioxidant enzymes superoxide dismutase (SOD) in the arteries of offspring from nicotine treated rats<sup>13</sup>. Moreover, we also demonstrated that oxidative stress and mitochondrial dysfunction are closely associated with the adverse effects of maternal smoking on the kidney pathology in the male offspring<sup>14,15</sup>.

Coenzyme Q10 (CoQ10) is a mitochondrial endogenous antioxidant. It has been shown that CoQ10 supplementation in mice can lower hepatic oxidative stress and inflammation associated with diet-induced obesity in mice<sup>16</sup>. Amniotic fluid CoQ10 levels are significantly lower among women delivering preterm babies, a risk which is increased by maternal smoking<sup>17,18</sup>. In addition, plasma CoQ10 levels are reduced in smokers<sup>19</sup>. However CoQ10 is not a viable treatment option due to poor bioavailability and delayed mitochondrial uptake<sup>20</sup>. Mitoquinone mesylate, also known as MitoQ, is a mitochondria-targeted antioxidant. It consists of a ubiquinone moiety, the same structure to the ubiquinone found in CoQ10, which allows its rapid uptake and accumulation in the mitochondria to restore the antioxidant efficacy of the mitochondrial respiratory complex<sup>21</sup>. As such, it has been reported that MitoQ has a protective role against oxidative damage-related pathologies in metabolic<sup>22</sup> and neurodegenerative diseases<sup>23</sup>. Moreover, our previous study demonstrated that maternal MitoQ supplementation during pregnancy and lactation is beneficial in reducing lung inflammatory and oxidative stress responses caused by maternal SE in the adult offspring<sup>24</sup>. Therefore, this study aimed to investigate whether maternal MitoQ supplementation can also mitigate the adverse impact on renal disorders caused by SE and whether the benefits of MitoQ administered to the SE mother are transmitted to the fetus and result in reduced future risk of CKD.

## Materials and Methods

**Animal experiments.** The animal experiments were approved by the Animal Care and Ethics Committee at the University of Technology Sydney (ACEC#2014-638 and #2016-419). All protocols were performed according to the Australian National Health & Medical Research Council Guide for the Care and Use of Laboratory Animals. Female Balb/c mice (8 weeks) were housed at  $20 \pm 2^\circ\text{C}$  and maintained on a 12:12 hour light/dark cycle with ad libitum access to standard laboratory chow and water. After the acclimatization period, mice were divided into three groups: SHAM (exposed to air), SE (exposed to cigarette smoke from 2 cigarettes twice daily, 6 weeks before mating and throughout gestation and lactation, as previously described<sup>9</sup>), and SEMQ (SE mothers supplied with MitoQ (500  $\mu\text{M}$  in drinking water<sup>25-27</sup>) during gestation and lactation). Male breeders and suckling pups stayed in the home cage when the mothers were exposed to normal air or cigarette smoke. Pups were weaned at postnatal day 20 and maintained without additional intervention.

Since we have previously demonstrated that maternal SE have a greater impact on the male offspring<sup>28</sup>, only male offspring were assessed in this study. One cohort of pups were randomly selected at postnatal day 1 from each litter to prevent selection bias<sup>29</sup>. The rest of the pups were kept to week 13. The birthweight of the latter group was not measured to avoid disturbance to the new born litter and mothers and problems with attachment which may influence later results<sup>30</sup>. Briefly, male offspring were euthanized (4% isoflurane, 1%  $\text{O}_2$ , Veterinary companies of Australia, Kings Park, NSW) at adulthood (13 weeks). A terminal urine collection was undertaken via direct bladder puncture and the blood was collected via cardiac puncture after mice were anesthetized. The kidney tissues were collected and stored at  $-80^\circ\text{C}$  for later analysis.

**Albumin and creatinine assays.** The levels of urinary albumin and creatinine were measured using Murine Microalbuminuria ELISA kit (Albuwell M) and Creatinine Companion kit, respectively (Exocell Inc, PA, USA) following the manufacturer's instructions.

**Kidney histology.** Kidney structure was examined in the male offspring at 13 weeks as previously described. Briefly, fixed kidney samples were embedded in paraffin and sectioned. Kidney sections were stained with hematoxylin and eosin (H&E) and periodic acid-Schiff (PAS). Glomerular number and size were assessed as we have previously described<sup>4</sup> and quantitated using ImageJ software (National Institute of Health, Bethesda, Maryland, USA).

**Confocal Microscopy Imaging.** Confocal laser scanning microscopy images of frozen kidney sections were acquired using Leica SP2 confocal laser scanning microscope (Leica, Wetzlar, Germany). Data was generated from 5–6 animals/group. Four to 6 Images were collected from each kidney and averaged before the analysis. All imaging parameters including laser intensities, Photomultiplier tubes voltage and pinholes were kept constant during imaging. For total reactive oxygen species (ROS) detection, CellROX Deep Red (Thermo Fisher Scientific, Australia) was used at 5  $\mu\text{M}$  final concentration, images were acquired at 633 nm excitation wavelength and detected in the 640–680 nm emission range. MitoTracker Green (Thermo Fisher Scientific, Australia) was used for staining the mitochondria at 200 nM final concentration, Images were acquired at 488 nm excitation wavelength and detected in the 510–550 nm emission range.

**Western blotting.** Kidney tissues were homogenized in lysis buffer with phosphatase inhibitors (Thermo Fisher Scientific, CA, USA). Protein concentrations were measured using DC Protein assay (Bio-rad, Hercules, CA, USA). Equal amount of proteins (20  $\mu\text{g}$ ) were separated on 4–12% Criterion™ XT Bis-Tris Protein Gel (Bio-rad, Hercules, CA, USA) and transferred to PVDF membranes. The membranes were blocked with TBS-0.05% Tween 20 (TBS-T) containing 5% BSA or skim milk for 1 h, before incubation with primary antibodies against endogenous antioxidant Manganese superoxide dismutase (MnSOD, 1:2000, Millipore, Billerica,

MA, USA), translocase of the outer membrane-20 (TOM-20, 1:2000, Santa Cruz Biotechnology), fibronectin (1:1000, Abcam, Cambridge, UK), phospho-extracellular signal-regulated kinase-1/2 (Erk1/2, 1:1000, Cell Signaling Technology Inc), phospho-INK (1:1000, Cell Signaling Technology Inc), phospho-p38 Mitogen-activated protein kinase (MAPK, 1:1000, Cell Signaling Technology Inc), p38 MAPK (1:1000, Cell Signaling Technology Inc), transcription factor nuclear factor- $\kappa$ -light-chain-enhancer of activated B cells (NF $\kappa$ B, 1:1000, Cell Signaling Technology Inc), phospho-NF $\kappa$ B (1:1000, Cell Signaling Technology Inc), F4/80 (1:1000, Sigma Aldrich, New South Wales, Australia), Collagen I (1:500, Santa Cruz Biotechnology, Texas, USA), Collagen III (1:500, Santa Cruz Biotechnology, Texas, USA) and Collagen IV (1:500, Santa Cruz Biotechnology, Texas, USA) overnight at 4 °C, then followed by secondary antibodies (peroxidase-conjugated goat anti-mouse or anti-rabbit IgG or rabbit anti-goat IgG, 1:2000, Santa Cruz Biotechnology Inc). The blots were then incubated in Super Signal West Pico Chemiluminescent substrate (Thermo Fisher Scientific, CA, USA) and the membranes were then visualized by an Amersham Imager 600 (GE Healthcare, NSW, Australia). Protein band density determined using ImageJ software (National Institute of Health, Maryland, USA) was used for densitometry, and  $\beta$ -actin (1:5000, Santa Cruz Biotechnology, Texas, USA) was used as the control.

**Quantitative real-time PCR.** Total mRNA was isolated from kidney tissues using TRIzol Reagent (Life Technologies, CA, USA). First strand cDNA was generated using M-MLV Reverse Transcriptase, RNase H, Point Mutant Kit (Promega, Madison, WI, USA). Genes of interest were measured using pre-optimized SYBR green primers (Sigma-Aldrich) and RT-PCR master mix (Life Technologies, CA, USA). The primers used in real-time RT-PCR experiments were as follows: macrophage chemoattractant protein (MCP)-1 forward primer: 5'-GTTGTTACAGTTGCTGCCT-3', and reverse primer: 5'-CTCTGTCATCTGGTCACTTCTAC-3'. Interleukin (IL)-1 $\alpha$ , IL-6 and cluster of differentiation (CD) 68 mRNA expressions were measured using Taqman probe (IL-1 $\alpha$ : ACCTGCAACAGGAAGTAAATTGA, NCBI gene references: NM\_010554.4, mCT192405.0, BC003727.1, ID: Mm00439620\_m1; IL-6: ATGAGAAAAGAGTTGTGCAATGGCA, NCBI gene references: NM\_031168.1, X06203.1, X54542.1, ID: Mm00446190\_m1; CD68: CACTTCGGGCCATGTTCTCTTGCA, NCBI gene references: NM\_001291058.1, ID: Mm03047343\_m1). The average expression of the control group was assigned as the calibrator against which all other samples were expressed as fold difference. The 18S rRNA was used as the house-keeping gene for all gene of interest.

**Mitochondrial DNA copy number.** Genomic DNA was extracted from renal tissue using the DNeasy blood and tissue kit (Qiagen). The content of mtDNA was calculated using real-time quantitative PCR by measuring the threshold cycle ratio ( $\Delta$ Ct) of the mitochondrial-encoded gene cytochrome c oxidase subunit 1 (COX1) (forward primers 5'-ACTATACTACTACTAA-CAGACCG-3', reverse primers 5'-GGTTCTTTTTTCCGGAGTA-3') vs. the nuclear-encoded gene cyclophilin A (forward primers 5'-ACACGCCATAATGGCACTGG-3', reverse primers 5'-CAGTCTTGGCAGTGCAGAT-3' as we have previously shown<sup>15</sup>).

**ATP assay.** ATP determination kit (Thermo Fisher Scientific, CA, USA) was used to extract ATP according to manufacturer instructions. In brief, kidney tissues (15–20 mg) were homogenized in 0.5 ml ice-cold Phenol-TE (Sigma-Aldrich, New South Wales, Australia). Chloroform (200  $\mu$ l) and de-ionised water (200  $\mu$ l) were added and followed by twenty seconds shaking. Aqueous phase was extracted and ATP was determined with luciferin-luciferase assay.

**Statistical analysis.** Results are presented as the mean  $\pm$  S.E.M. The differences between the groups were analysed by one-way ANOVA followed by post hoc Bonferroni test (Prism 7, Graphpad CA, USA). The differences were considered statistically significant at  $P < 0.05$ .

## Results

**Effects of cigarette smoke exposure on the mothers.** Results in Table 1 show that body weight was not different between the SE mothers and control mothers. Kidney mass was marginally reduced without statistical significance in the SE mothers. Mitochondrial density, total ROS levels, and mitochondrial copy number were significantly increased in the kidney's from the SE mothers ( $P < 0.01$  vs SHAM, Fig. 1).

MitoQ supplementation during gestation and lactation significantly reversed the impact of SE on mitochondrial density ( $P < 0.01$  vs SE, Fig. 1a). In addition, renal DNA copy number in the SEMQ mothers was similar as the SHAM mothers (Fig. 1b). Maternal MitoQ administration also significantly ameliorated ROS level in the kidneys ( $P < 0.01$  SEMQ vs SE, Fig. 1c).

**Effect of maternal cigarette smoke exposure on the growth of the male offspring.** At postnatal day 1, body weight and kidney mass were significantly reduced in the male offspring from the SE mothers ( $P < 0.01$  and  $P < 0.05$  vs SHAM, respectively; Table 1). A lower body weight was maintained until 13 weeks of age ( $P < 0.01$ , Table 1) but kidney mass was only marginally reduced without statistical significance in offspring of SE mothers. This is consistent with our previous study using the same model<sup>4</sup>.

Maternal MitoQ supplementation significantly enhanced body weight at P1 and normalised the body weight at week 13 of the SEMQ offspring ( $P < 0.01$ , Table 1). Moreover, kidney mass was significantly normalised in the SEMQ offspring at P1 ( $P < 0.05$  vs SE, Table 1). Interestingly, there were fewer male offspring in the SEMQ group in comparison to both SE and control groups.

**Effect of maternal cigarette smoke exposure on kidney development.** At 13 weeks, the average number of glomeruli was significantly decreased in the SE offspring compared to the SHAM offspring ( $P < 0.01$ , Fig. 2a). The mature glomerular size in the SE offspring was also significantly larger than those of the offspring



Mother	Control (n = 9)	SE (n = 10)	SEMQ (n = 9)
Body weight (g)	21.8 ± 0.7	21.1 ± 0.9	21.2 ± 0.3
Kidney weight (g)	0.166 ± 0.006	0.148 ± 0.006	0.157 ± 0.003
Kidney % body weight	0.77 ± 0.04	0.71 ± 0.03	0.73 ± 0.02
<b>Offspring P1</b>	<b>(n = 14)</b>	<b>(n = 11)</b>	<b>(n = 7)</b>
Body weight (g)	1.51 ± 0.03	1.50 ± 0.06**	1.65 ± 0.05**
Kidney weight (g)	0.009 ± 0.0005	0.007 ± 0.0004*	0.009 ± 0.0006 <sup>†</sup>
Kidney % body weight	0.57 ± 0.03	0.53 ± 0.04	0.55 ± 0.03
<b>Offspring 13 weeks</b>	<b>(n = 19)</b>	<b>(n = 20)</b>	<b>(n = 14)</b>
Body weight (g)	25.2 ± 0.2	24.2 ± 0.2**	25.1 ± 0.2**
Kidney weight (g)	0.195 ± 0.004	0.186 ± 0.003	0.198 ± 0.004
Kidney % body weight	0.77 ± 0.02	0.77 ± 0.02	0.79 ± 0.02

**Table 1.** Body weight and kidney weights of the mothers and offspring at postnatal day 1 and 13 weeks. Results are expressed as mean ± SE. \*\* $P < 0.01$  SE vs Sham, <sup>†</sup> $P < 0.01$  SEMQ vs SE.

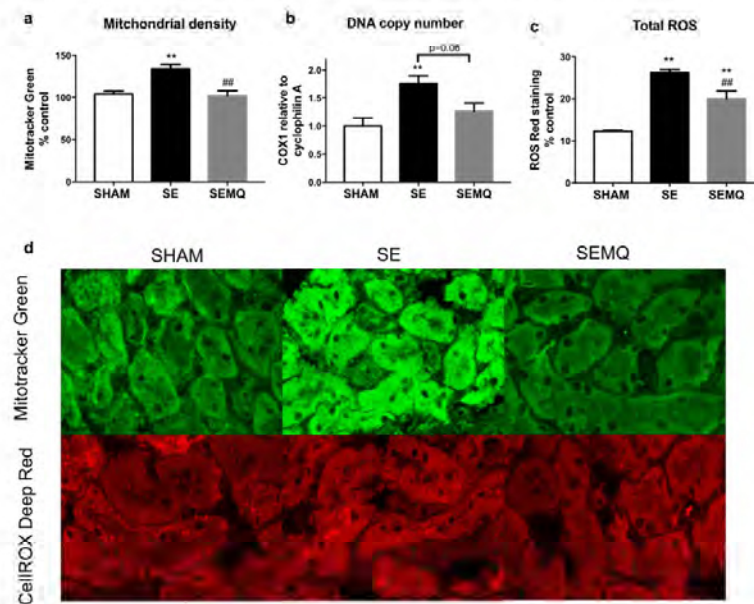


**Figure 1.** Renal mitochondrial density (a), mitochondrial DNA copy number (b) and total ROS level (c) in the mothers. Results are expressed as mean ± SE. \*\* $P < 0.01$  SE vs Sham, <sup>†</sup> $P < 0.01$  SEMQ vs SE. SE: cigarette smoke exposure; SEMQ: cigarette smoke exposure with MitoQ supplementation. Representative confocal images of (a and c) showing Mitotracker and Cell Rox staining in the SHAM, SE and SEMQ groups respectively (d).

from the SHAM mothers ( $P < 0.05$ , Fig. 2b). Maternal MitoQ supplementation normalised glomerular number ( $P < 0.01$  vs SE) and size in the SEMQ offspring (Fig. 2a,b).

**Effect on renal inflammatory and fibrotic markers and kidney function.** Renal mRNA expression of the pro-inflammatory markers MCP-1 and CD68, in addition to the protein levels of F4/80, mice macrophage marker were significantly increased in the offspring kidneys due to maternal SE ( $P < 0.05$  vs SHAM offspring, Fig. 3a,d,e). The levels of the pro-fibrotic marker fibronectin and collagen IV protein were also significantly increased in the offspring kidneys due to maternal SE ( $P < 0.05$  vs SHAM offspring, Fig. 4a,d). IL-1 $\alpha$  and IL-6 expression, as well as Collagen I,III protein levels were not changed by maternal SE (Figs 3b,c, 4b,c). Maternal MitoQ administration ameliorated MCP-1 expression although this did not reach statistical significance (Fig. 3a); whereas CD68 expression and F4/80 protein level were normalised in the SEMQ offspring ( $P < 0.01$  vs SE, Fig. 3d;  $P < 0.05$  vs SE, Fig. 3e).



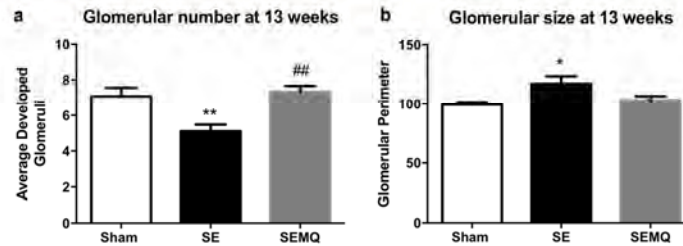


**Figure 2.** Glomerular number and size in the male offspring at 13 weeks. Results are expressed as mean  $\pm$  SE. \* $P < 0.05$ , \*\* $P < 0.01$  SE vs Sham, ## $P < 0.01$  SEMQ vs SE. SE: cigarette smoke exposure; SEMQ: cigarette smoke exposure with MitoQ supplementation.

The urinary albumin-to-creatinine ratio as a marker of renal damage was significantly higher in the SE group ( $P < 0.05$ , Fig. 4c). Maternal MitoQ supplementation showed a trend to normalization of urinary albumin-to-creatinine ratio. However, this was not significant (Fig. 4c).

**Effect on renal mitochondrial and stress markers in the offspring.** Altered mitochondrial number and DNA content have been proposed as a surrogate of mitochondrial function. Here, mitochondrial density and DNA copy number were significantly increased in the offspring from the SE mothers ( $P < 0.01$  and  $P < 0.05$  vs SHAM offspring, respectively; Fig. 5a,b). As such, total ROS level was significantly increased in SE offspring's kidneys ( $P < 0.01$  vs SE offspring, Fig. 5c), with reduced endogenous antioxidant MnSOD level ( $P < 0.01$  vs SHAM offspring, Fig. 5c). We also investigated TOM-20, a mitochondrial outer membrane receptor for the translocation of cytosolically synthesized mitochondrial pre-proteins. Renal TOM-20 protein level was significantly reduced in the SE offspring ( $P < 0.05$  vs SHAM offspring, Fig. 5f).

Cellular oxidative stress level was significantly reduced by maternal MitoQ treatment. Maternal MitoQ treatment normalised cellular mitochondrial density ( $P < 0.01$  vs SE offspring) and total ROS level ( $P < 0.05$  vs SE offspring, Fig. 5a,c) although no change in copy number was seen. It also marginally improved TOM-20 level (Fig. 5f). There was a trend of increased ATP levels in the SE offspring's kidneys ( $P = 0.27$  vs SHAM), which was significantly reduced by maternal MitoQ supplementation ( $P < 0.05$  SEMQ vs SE, Fig. 5g).

**Effect on Receptors for Advanced Glycation End-products (RAGE) pathway.** RAGE is a multi-ligand receptor of the immunoglobulin superfamily, which plays a role in cigarette smoke-related disease through the AGEs-RAGE axis<sup>31,32</sup>. Our data demonstrated that maternal SE has no effect on RAGE, p38 MAPK, ERK1/2, JNK, and NF- $\kappa$ B in the offspring's kidneys at week 13. MitoQ administration also has no effect on these markers (Supplementary Fig. 1).

## Discussion

Maternal smoking during pregnancy affects fetal renal development which is linked to an increased risk of CKD in the offspring in the adulthood. We have previously demonstrated that maternal SE significantly reduced renal development in the male offspring and induced renal pathology in adulthood associated with increased oxidative stress and mitochondrial dysregulation<sup>4,11</sup>. Such effects were male specific<sup>28</sup>. However, it is not clear whether this is due to the direct effect of cigarette smoke on maternal mitochondrial DNA, which can be transmitted to the offspring.

In this study, we demonstrated that SE increased mitochondrial density and maternal renal DNA copy number and as a consequence increased total ROS levels in the mothers' kidneys. We additionally demonstrated that the administration of the mitochondrial-targeted antioxidant MitoQ during gestation and lactation can significantly reverse the impact of SE on the abovementioned renal changes. Furthermore, we demonstrated that maternal SE induced renal underdevelopment and renal dysfunction in the male offspring at adulthood associated with increased renal inflammatory markers, mitochondrial alteration and oxidative stress, which were also ameliorated by maternal MitoQ supplementation. Interestingly, mitochondrial DNA copy number and density were increased in both SE mothers and their offspring suggesting that smoking during pregnancy can alter mitochondrial DNA predisposing the offspring to future kidney disease through foetal programming.

Maternal MitoQ administration reversed the effect of maternal SE on the offspring body weight, kidney size at birth, renal development, as well as renal function in the adult offspring. Interestingly, although maternal MitoQ administration was able to reverse the effect of maternal SE on renal mitochondrial density and total ROS levels in the offspring, it had no effect on mitochondrial DNA copy number. This finding suggests that the effect of SE on mitochondrial DNA copy number in the mothers may be transmitted to the offspring as mitochondrial DNA is inherited from the maternal lineage. Such change can't be reversed by gestational MitoQ supplementation. However, whether such effect occurs prior to gestation requires further validation by examining the females before mating, which is beyond the scope of this study. It is important to note that there were less male offspring in the SEMQ group in comparison to both SE and control groups. The reason for that is to date unclear and is worth further investigation.

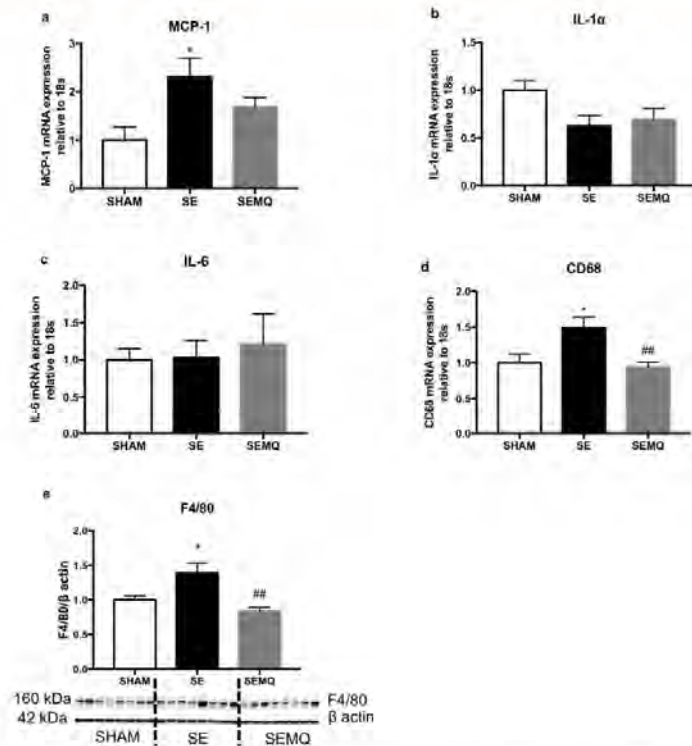


**Figure 3.** Renal MCP-1 mRNA expression (a), IL-1 $\alpha$  mRNA expression (b), IL-6 mRNA expression (c), CD68 mRNA expression (d), F4/80 protein levels (e) in the offspring at 13 weeks. Whole gel images (e) in Supplementary Fig. 3. Results are expressed as mean  $\pm$  SE. \* $P < 0.05$ , SE vs Sham. \*\* $P < 0.01$ ; # $P < 0.05$ , SEMQ vs SE. SE: cigarette smoke exposure; SEMQ: cigarette smoke exposure with MitoQ supplementation.

Several studies have indicated that maternal cigarette smoking during pregnancy was the most common cause of fetal growth restriction and reduced size of the fetal organs<sup>23,24</sup>. We have previously shown, using the same animal model, that maternal SE is linked to smaller glomerular size and delayed kidney development in the male offspring<sup>1,4</sup>. In addition, oxidative stress and mitochondrial dysfunction are closely associated with the adverse effects of maternal smoking on offspring's kidney pathology<sup>14,15</sup>. Such phenotype has also been presented in the SE offspring in this study, reflected by smaller glomerular number with adaptive enlargement of glomerular size and impaired renal function. Mitochondrial DNA can only be inherited from the mothers, not the fathers<sup>25</sup>. Indeed in this study, the changes in renal mitochondrial DNA copy number and density in the SE offspring mirrored that in the SE mothers. While mitochondrial number and DNA copy number were deregulated by maternal SE, renal total ROS were increased in such offspring in line with increased mitochondrial activity of ATP production, suggesting oxidative stress, which is consistent with our previous studies<sup>14,15</sup>. Correlatively, the level of mitochondrial endogenous antioxidant MnSOD was reduced in the offspring's kidney in response to increased oxidative stress, with lower expression of the mitochondrial import receptor subunit (TOM-20) which may be induced by increased workload for ATP synthesis.

Oxidative stress is often linked to inflammatory responses and fibrotic changes, which were also observed in the SE offspring with increased levels of inflammatory (MCP-1, CD68 and F4/80) and fibrotic markers (fibronectin and collagen IV). The AGEs-RAGE interaction has also been shown to associate with enhanced production of intracellular ROS, which can mediate further inflammatory response<sup>26,27</sup>. Several studies have suggested that RAGE can also influence the pathogenesis of renal disorders<sup>28,29</sup>. Our previous study demonstrated that maternal SE can increase RAGE and its signalling elements, as well as promoting oxidative stress and inflammatory responses in offspring's lung<sup>24</sup>. However in this study, none of the RAGE signalling elements including RAGE, p38 MAPK, ERK1/2, JNK, and NFrB, were changed in the SE offspring's kidney. These findings suggest that the

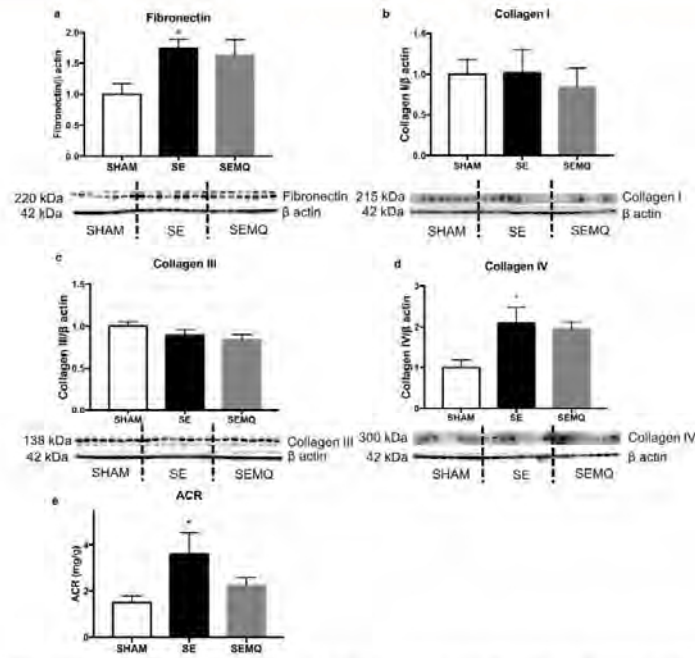


**Figure 4.** Renal fibronectin protein levels (a), collagen I protein levels (b), collagen III protein levels (c), collagen IV protein levels (d), and Urinary Albumin to creatinine ratio (ACR) in the offspring (e) at 13 weeks. Whole gel images (a–d) in Supplementary Fig. 4. (a,b). Results are expressed as mean  $\pm$  SE. \* $P < 0.05$ , SE vs Sham, SE: cigarette smoke exposure; SEMQ: cigarette smoke exposure with MitoQ supplementation.

RAGE pathway does not seem to be involved in maternal SE induced inflammatory response in the offspring's kidney. There is also evidence suggesting that inflammatory cell infiltration correlates with both the extent of renal fibrosis and the severity of renal damage in CKD<sup>40</sup>. Irreversible renal fibrosis is a common consequence after renal injury and leads to a gradual loss of kidney function, which is a hallmark of CKD. In this study, there was a significant increase in fibronectin level in the SE offspring's kidney. We have previously demonstrated that maternal SE induced subtle pathological changes in the offspring's kidneys at 13 weeks. Increased risk of CKD may prevail if the offspring are exposed to additional insult after weaning, such as obesity or diabetes. Such hypothesis requires validation in future studies.

Mitochondrial dysfunction occurs in several human disorders, which is considered as the major driver for cellular and organ failure. Adverse effects of cigarette smoke have been attributed to increased oxidative stress together with mitochondrial dysregulation, which play a key role in the progression of renal injury and development of CKD<sup>41–43</sup>. Therefore, therapeutic application of mitochondrial-targeted therapies may offer potential alternatives for the prevention and treatment of such conditions, instead of the generic antioxidants which are normally poorly taken up by the mitochondria. The most widely investigated mitochondria-specific antioxidant to date is MitoQ<sup>21,44</sup>. The beneficial effects of MitoQ have been reported in various disorders, such as metabolic disease<sup>45</sup>, neurodegenerative diseases<sup>46</sup>, kidney damage related to diabetes<sup>47</sup>, Parkinson's disease<sup>48</sup>, and liver inflammation in hepatitis C virus infection<sup>49</sup>. Importantly, our previous study using the same cohort of mice demonstrated that maternal MitoQ supplementation during pregnancy and lactation is beneficial in reducing lung inflammatory and oxidative stress responses in the adult offspring caused by maternal SE<sup>21</sup>. As we have demonstrated that oxidative stress plays an important role in maternal SE related renal disorders in the male offspring<sup>45,47</sup>, this study extended the investigation of the impact of maternal MitoQ supplementation on renal disorders.

In the current study, our results showed that MitoQ supplementation during pregnancy can significantly mitigate small body weight due to in-utero SE. Moreover, we demonstrated that MitoQ treatment can restore smaller kidney size and glomerular numbers with nearly normalised renal function in adult offspring from the SE mother. These results suggested that MitoQ exert beneficial effects on offspring's health, despite continuing maternal SE during gestation and lactation. Our results are consistent with earlier reports that showed that MitoQ treatment prevented renal disorders in a mouse model of type 1 diabetes<sup>46</sup>. Mukhopadhyay and colleagues also found that

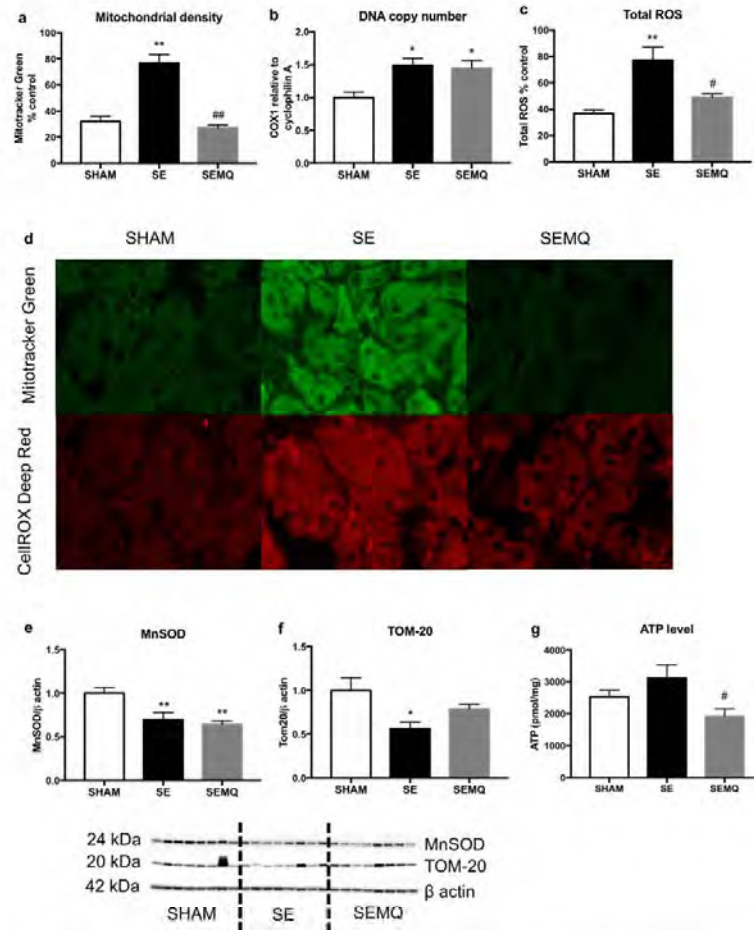


**Figure 5.** Renal cellular mitochondrial density (a), mitochondrial DNA copy number (b), total ROS (c). Representative confocal images of (a and c) showing Mitotracker and Cell Rox staining in the SHAM, SE and SEMQ groups respectively (d), mitochondrial MnSOD (e), and TOM-20 (f), and ATP (g) in the male offspring at 13 weeks. Whole gel images of (e,f) in Supplementary Fig. 5. Results are expressed as mean ± SE. \* $P < 0.05$ ; \*\* $P < 0.01$  SE vs Sham, # $P < 0.05$ , ## $P < 0.01$  SEMQ vs SE. SE: cigarette smoke exposure; SEMQ: cigarette smoke exposure with MitoQ supplementation.

MitoQ treatment prevented renal dysfunction caused by cisplatin nephrotoxicity<sup>49</sup>. Such improvement in the offspring is closely related to reduced renal ROS level and normalised mitochondrial density in both mothers and offspring. Interestingly, renal MnSOD level was not increased in the offspring as a consequence of maternal administration of MitoQ. This was different to that observed in the lungs<sup>24</sup>, suggesting that ROS was suppressed by other antioxidative mechanisms or due to reduced mitochondrial ATP production. The impact of maternal SE on TOM-20, the mitochondrial outer membrane receptor for the translocation of cytosolically synthesized mitochondrial preproteins, was partially reversed in SE offspring, suggesting some improvement in mitochondrial function. However, mitochondrial DNA copy number was not reversed in the SEMQ offspring compared with the SEMQ mothers, suggesting oxidative stress may not be the only factor to damage mitochondrial DNA in the offspring. Foetal kidneys are likely to be more vulnerable to the damage from the chemicals in the cigarette



smoke, since nicotine level is 15% higher in the foetal blood than the maternal blood<sup>49</sup>. This may also affect the fibronectin level in the offspring's kidney<sup>51</sup>, which was also unaffected by maternal MitoQ supplementation although the inflammatory markers MCP-1, CD68, F4/80 and ROS level were reduced. As the aim of the study was to determine whether MitoQ protects the offspring from maternal smoking we did not include a sham group treated with MitoQ. Hence we are unable to be definitive about whether MitoQ may cause changes in the parameters studied in "normal" animals. However, Rodriguez-Cuenca *et al.*, have previously examined the long-term consequences of MitoQ on wild-type mice in the absence of injury and demonstrated that MitoQ has no effect on mitochondrial function, mitochondrial DNA, food consumption or whole body metabolism<sup>25</sup>.

In summary, our study demonstrates the beneficial effects of maternal MitoQ supplementation during gestation and lactation on renal under development and pathology by maternal SE. It also reduced renal ROS accumulation and mitochondrial density in both mothers' and offspring's kidneys. Although MitoQ was unable to reverse the increase in fibrotic markers, it may still protect the offspring against maternal SE induced renal pathology and potentially future CKD through reduction of inflammation and oxidative stress. This is yet to be confirmed in future human clinical trials.

## References

1. Taal, H. R. *et al.* Maternal smoking during pregnancy and kidney volume in the offspring: the Generation R Study. *Pediatr Nephrol* **26**, 1275–1283. <https://doi.org/10.1007/s00467-011-1848-3> (2011).
2. Anblagan, D. *et al.* Maternal smoking during pregnancy and fetal organ growth: a magnetic resonance imaging study. *PLoS One* **8**, e67223. <https://doi.org/10.1371/journal.pone.0067223> (2013).
3. Shinzawa, M. *et al.* Maternal Smoking during Pregnancy, Household Smoking after the Child's Birth, and Childhood Proteinuria at Age 3 Years. *Clinical Journal of the American Society of Nephrology: CJASN* **12**, 253–260. <https://doi.org/10.2215/cjn.05980616> (2017).
4. Al-Odat, I. *et al.* The impact of maternal cigarette smoke exposure in a rodent model on renal development in the offspring. *PLoS One* **9**, e103443. <https://doi.org/10.1371/journal.pone.0103443> (2014).
5. Arany, I. *et al.* Chronic nicotine exposure exacerbates acute renal ischemic injury. *American journal of physiology. Renal physiology* **301**, F125–133. <https://doi.org/10.1152/ajprenal.00041.2011> (2011).
6. Piecznik, S. R. & Neustadt, J. Mitochondrial dysfunction and molecular pathways of disease. *Experimental and molecular pathology* **83**, 84–92. <https://doi.org/10.1016/j.yexmp.2006.09.008> (2007).
7. Bulua, A. C. *et al.* Mitochondrial reactive oxygen species promote production of proinflammatory cytokines and are elevated in TNFR1-associated periodic syndrome (TRAPS). *The Journal of experimental medicine* **208**, 519–533. <https://doi.org/10.1084/jem.20102049> (2011).
8. Che, R., Yuan, Y., Huang, S. & Zhang, A. Mitochondrial dysfunction in the pathophysiology of renal diseases. *Am J Physiol Renal Physiol* **306**, F367–378. <https://doi.org/10.1152/ajprenal.00571.2013> (2014).
9. Granata, S. *et al.* Mitochondrial dysregulation and oxidative stress in patients with chronic kidney disease. *BMC Genomics* **10**, 388. <https://doi.org/10.1186/1471-2164-10-388> (2009).
10. Liu, J. P., Baker, J., Perkins, A. S., Robertson, E. J. & Efstratiadis, A. Mice carrying null mutations of the genes encoding insulin-like growth factor I (Igf-1) and type I IGF receptor (Igf1r). *Cell* **75**, 59–72. [https://doi.org/10.1016/S0092-8674\(05\)80084-4](https://doi.org/10.1016/S0092-8674(05)80084-4) (1993).
11. Ermis, B. *et al.* Influence of Smoking on Maternal and Neonatal Serum Malondialdehyde, Superoxide Dismutase, and Glutathione Peroxidase Levels. *Annals of Clinical & Laboratory Science* **34**, 405–409 (2004).
12. Noakes, P. S. *et al.* Association of maternal smoking with increased infant oxidative stress at 3 months of age. *Thorax* **62**, 714–717. <https://doi.org/10.1136/thx.2006.061630> (2007).
13. Xiao, D., Huang, X., Yang, S. & Zhang, L. Antenatal nicotine induces heightened oxidative stress and vascular dysfunction in rat offspring. *Br J Pharmacol* **164**, 1400–1409. <https://doi.org/10.1111/j.1476-5381.2011.01437.x> (2011).
14. Nguyen, L. T. *et al.* L-Carnitine reverses maternal cigarette smoke exposure-induced renal oxidative stress and mitochondrial dysfunction in mouse offspring. *Am J Physiol Renal Physiol* **308**, F689–696. <https://doi.org/10.1152/ajprenal.00417.2014> (2015).
15. Stangenberg, S. *et al.* Oxidative stress, mitochondrial perturbations and fetal programming of renal disease induced by maternal smoking. *Int J Biochem Cell Biol* **64**, 81–90. <https://doi.org/10.1016/j.biocel.2015.03.017> (2015).
16. Sohet, F. M. *et al.* Coenzyme Q10 supplementation lowers hepatic oxidative stress and inflammation associated with diet-induced obesity in mice. *Biochem Pharmacol* **78**, 1391–1400. <https://doi.org/10.1016/j.bcp.2009.07.008> (2009).
17. Teran, E. *et al.* Maternal plasma and amniotic fluid coenzyme Q10 levels in preterm and term gestations: a pilot study. *Archives of gynecology and obstetrics* **283**(Suppl 1), 67–71. <https://doi.org/10.1007/s00404-011-1894-x> (2011).
18. Kyrklund-Blomborg, N. B., Granath, F. & Cnattingius, S. Maternal smoking and causes of very preterm birth. *Acta obstetrica et gynecologica Scandinavica* **84**, 572–577. <https://doi.org/10.1111/j.0001-6349.2005.00848.x> (2005).
19. Al-Bazi, M. M., Elshal, M. F. & Khoja, S. M. Reduced coenzyme Q(10) in female smokers and its association with lipid profile in a young healthy adult population. *Archives of medical science: AMS* **7**, 948–954. <https://doi.org/10.5114/aoms.2011.26605> (2011).
20. Hirano, M., Garone, C. & Quinzii, C. M. CoQ(10) deficiencies and MNGIE: two treatable mitochondrial disorders. *Biochimica et biophysica acta* **1820**, 625–631. <https://doi.org/10.1016/j.bbagen.2012.01.006> (2012).
21. Kelso, G. F. *et al.* Selective targeting of a redox-active ubiquinone to mitochondria within cells: antioxidant and antiapoptotic properties. *J Biol Chem* **276**, 4588–4596. <https://doi.org/10.1074/jbc.M009993200> (2001).
22. Mercer, J. R. *et al.* The mitochondria-targeted antioxidant MitoQ decreases features of the metabolic syndrome in ATM+/- ApoE-/- mice. *Free radical biology & medicine* **52**, 841–849. <https://doi.org/10.1016/j.freeradbiomed.2011.11.026> (2012).
23. Manczak, M. *et al.* Mitochondria-targeted antioxidants protect against amyloid-beta toxicity in Alzheimer's disease neurons. *J Alzheimers Dis* **20**(Suppl 2), S609–631. <https://doi.org/10.3233/jad-2010-100564> (2010).
24. Sukjammong, S. *et al.* The effect of long-term maternal smoking on the offspring's lung health. *American journal of physiology. Lung cellular and molecular physiology*. <https://doi.org/10.1152/ajplung.00134.2017> (2017).
25. Rodriguez-Cuenca, S. *et al.* Consequences of long-term oral administration of the mitochondria-targeted antioxidant MitoQ to wild-type mice. *Free Radical Biology and Medicine* **48**, 161–172. <https://doi.org/10.1016/j.freeradbiomed.2009.10.039> (2010).
26. Mercer, J. R. *et al.* The mitochondria-targeted antioxidant MitoQ decreases features of the metabolic syndrome in ATM+/- ApoE-/- mice. *Free Radical Biology and Medicine* **52**, 841–849. <https://doi.org/10.1016/j.freeradbiomed.2011.11.026> (2012).
27. Sukjammong, S. *et al.* Effect of long-term maternal smoking on the offspring's lung health. *American Journal of Physiology - Lung Cellular and Molecular Physiology* **313**, L416–L423. <https://doi.org/10.1152/ajplung.00134.2017> (2017).
28. Chan, Y. L. *et al.* Impact of maternal cigarette smoke exposure on brain and kidney health outcomes in female offspring. *Clinical and experimental pharmacology & physiology* **43**, 1168–1176. <https://doi.org/10.1111/1440-1681.12659> (2016).
29. Suresh, K. P. An overview of randomization techniques: An unbiased assessment of outcome in clinical research. *Journal of Human Reproductive Sciences* **4**, 8–11. <https://doi.org/10.4103/0974-1208.82352> (2011).
30. Lambert, M. Breeding strategies for maintaining colonies of laboratory mice. *TJ Laboratory* (2009).
31. Cerami, C. *et al.* Tobacco smoke is a source of toxic reactive glycation products. *Proceedings of the National Academy of Sciences of the United States of America* **94**, 13915–13920 (1997).

32. Prasad, K., Dhar, I. & Caspar-Bell, G. Role of Advanced Glycation End Products and Its Receptors in the Pathogenesis of Cigarette Smoke-Induced Cardiovascular Disease. *The International Journal of Angiology: official publication of the International College of Angiology; Inc* **24**, 75–80, <https://doi.org/10.1055/s-0034-1396413> (2015).
33. Reeves, S. & Bernstein, I. Effects of maternal tobacco-smoke exposure on fetal growth and neonatal size. *Expert review of obstetrics & gynecology* **3**, 719–730, <https://doi.org/10.1586/17474108.3.6.719> (2008).
34. Esposito, E. R., Horn, K. H., Greene, R. M. & Pisano, M. M. An animal model of cigarette smoke-induced in utero growth retardation. *Toxicology* **246**, 193–202, <https://doi.org/10.1016/j.tox.2008.01.014> (2008).
35. Luo, S. M. *et al.* Unique insights into maternal mitochondrial inheritance in mice. *Proceedings of the National Academy of Sciences of the United States of America* **110**, 13038–13043, <https://doi.org/10.1073/pnas.1303231110> (2013).
36. Jiang, I. M., Wang, Z. & Li, D. D. Effects of AGEs on oxidation stress and antioxidation abilities in cultured astrocytes. *Biomedical and environmental sciences: BES* **17**, 79–86 (2004).
37. Lin, L., Park, S. & Lakatta, E. G. RAGE signaling in inflammation and arterial aging. *Frontiers in bioscience (Landmark edition)* **14**, 1403–1413 (2009).
38. Koyama, H. & Nishizawa, Y. AGEs/RAGE in CKD: irreversible metabolic memory road toward CVD? *Eur J Clin Invest* **40**, 623–635, <https://doi.org/10.1111/j.1365-2362.2010.02298.x> (2010).
39. Tomino, Y., Hagihara, S. & Gohda, T. AGE-RAGE interaction and oxidative stress in obesity-related renal dysfunction. *Kidney Int* **80**, 133–135, <https://doi.org/10.1038/kj.2011.86> (2011).
40. Eardley, K. S. *et al.* The role of capillary density, macrophage infiltration and interstitial scarring in the pathogenesis of human chronic kidney disease. *Kidney Int* **74**, 495–504, <https://doi.org/10.1038/kj.2008.183> (2008).
41. Orth, S. R., Schroeder, T., Ritz, E. & Ferrari, P. Effects of smoking on renal function in patients with type 1 and type 2 diabetes mellitus. *Nephrol Dial Transplant* **20**, 2414–2419, <https://doi.org/10.1093/ndt/gf022> (2005).
42. Stengel, B., Couchoud, C., Cenee, S. & Hemon, D. Age, blood pressure and smoking effects on chronic renal failure in primary glomerular nephropathies. *Kidney Int* **57**, 2519–2526, <https://doi.org/10.1046/j.1523-1755.2000.00111.x> (2000).
43. Cigremis, Y., Turkoz, Y., Akgoz, M. & Sozmen, M. The effects of chronic exposure to ethanol and cigarette smoke on the level of reduced glutathione and malondialdehyde in rat kidney. *Urological research* **32**, 213–218, <https://doi.org/10.1007/s00246-004-0406-x> (2004).
44. Mito, O. *et al.* Smoking disturbs mitochondrial respiratory chain function and enhances lipid peroxidation on human circulating lymphocytes. *Carcinogenesis* **20**, 1331–1336 (1999).
45. Smith, R. A., Hartley, R. C., Cocheme, H. M. & Murphy, M. P. Mitochondrial pharmacology. *Trends Pharmacol Sci* **33**, 341–352, <https://doi.org/10.1016/j.tips.2012.03.019> (2012).
46. Chacko, B. K. *et al.* Prevention of diabetic nephropathy in Ins2(+/-)(Akita) mice by the mitochondria-targeted therapy MitoQ. *The Biochemical Journal* **432**, 9–19, <https://doi.org/10.1042/bj20100308> (2010).
47. Snow, B. I. *et al.* A double-blind, placebo-controlled study to assess the mitochondria-targeted antioxidant MitoQ as a disease-modifying therapy in Parkinson's disease. *Mov Disord* **25**, 1670–1674, <https://doi.org/10.1002/mds.23148> (2010).
48. Gane, E. I. *et al.* The mitochondria-targeted anti-oxidant mitoquinone decreases liver damage in a phase II study of hepatitis C patients. *Liver Int* **30**, 1019–1026, <https://doi.org/10.1111/j.1478-3231.2010.02250.x> (2010).
49. Mukhopadhyay, P. *et al.* Mitochondrial-targeted antioxidants represent a promising approach for prevention of cisplatin-induced nephropathy. *Free radical biology & medicine* **52**, 497–506, <https://doi.org/10.1016/j.freeradbiomed.2011.11.001> (2012).
50. Chen, H. & Morris, M. J. Maternal smoking—A contributor to the obesity epidemic? *Obesity research & clinical practice* **1**, 155–163 (2007).
51. Jensen, K. *et al.* General mechanisms of nicotine-induced fibrogenesis. *FASEB journal: official publication of the Federation of American Societies for Experimental Biology* **26**, 4778–4787, <https://doi.org/10.1096/fj.12-206458> (2012).

### Acknowledgements

This study was supported by a postgraduate research support by Faculty of Science, University of Technology Sydney, and a Research grant awarded by Faculty of Allied Health Sciences, Chulalongkorn University support to A/Prof Rachana Santayanont. Ms Razia Zakarya is supported by an Australia Postgraduate Award. Ms Suporn Sukjammong is supported by Overseas Research Experience Scholarship for Graduate Students by Graduate School, Chulalongkorn University and the 90th Anniversary of Chulalongkorn University Fund and Grant for Joint Funding (Ratchadaphiseksomphot Endowment Fund). The MitoQ was provided by MitoQ Limited, New Zealand. A/Prof Oliver is supported by NH&MRC fellowship APP1110368. This work was partially supported by the Australian Research Council (CE140100003).

### Author Contributions


H.C. and S. Saad designed the study. S. Sukjammong Y.L.C., H.C., S. Saad A.A.Z., A.G.A. performed all the experiments. All authors contributed to the writing of the main manuscript text, and S. Sukjammong, Y.L.C., S. Saad and H.C. prepared the figures and table. All authors reviewed the manuscript.

### Additional Information

Supplementary information accompanies this paper at <https://doi.org/10.1038/s41598-018-24949-0>.

Competing Interests: The authors declare no competing interests.

Publisher's note: Springer Nature remains neutral with regard to jurisdictional claims in published maps and institutional affiliations.

 Open Access This article is licensed under a Creative Commons Attribution 4.0 International License, which permits use, sharing, adaptation, distribution and reproduction in any medium or format, as long as you give appropriate credit to the original author(s) and the source, provide a link to the Creative Commons license, and indicate if changes were made. The images or other third party material in this article are included in the article's Creative Commons license, unless indicated otherwise in a credit line to the material. If material is not included in the article's Creative Commons license and your intended use is not permitted by statutory regulation or exceeds the permitted use, you will need to obtain permission directly from the copyright holder. To view a copy of this license, visit <http://creativecommons.org/licenses/by/4.0/>.

© The Author(s) 2018



Article

## Biomass Smoke Exposure Enhances Rhinovirus-Induced Inflammation in Primary Lung Fibroblasts

Sarah J. Capistrano<sup>1,2</sup>, Razia Zakarya<sup>1,2</sup>, Hui Chen<sup>1</sup> and Brian G. Oliver<sup>1,2,\*</sup>

<sup>1</sup> Molecular Biosciences, School of Life Sciences, University of Technology Sydney, Sydney, NSW 2007, Australia; Sarah.Capistrano@student.uts.edu.au (S.J.C.); Razia.zakarya@student.uts.edu.au (R.Z.); Hui.Chen-1@uts.edu.au (H.C.)

<sup>2</sup> Respiratory Cellular and Molecular Biology, Woolcock Institute of Medical Research, Sydney, NSW 2037, Australia

\* Correspondence: Brian.oliver@uts.edu.au; Tel.: +61-2-9114-0367; Fax: +61-2-9114-0399

Academic Editors: Paul R. Reynolds and Benjamin T. Bikman

Received: 1 July 2016; Accepted: 22 August 2016; Published: 25 August 2016

**Abstract:** Biomass smoke is one of the major air pollutants and contributors of household air pollution worldwide. More than 3 billion people use biomass fuels for cooking and heating, while other sources of exposure are from the occurrence of bushfires and occupational conditions. Persistent biomass smoke exposure has been associated with acute lower respiratory infection (ALRI) as a major environmental risk factor. Children under the age of five years are the most susceptible in developing severe ALRI, which accounts for 940,000 deaths globally. Around 90% of cases are attributed to viral infections, such as influenza, adenovirus, and rhinovirus. Although several epidemiological studies have generated substantial evidence of the association of biomass smoke and respiratory infections, the underlying mechanism is still unknown. Using an in vitro model, primary human lung fibroblasts were stimulated with biomass smoke extract (BME), specifically investigating hardwood and softwood types, and human rhinovirus-16 for 24 h. Production of pro-inflammatory mediators, such as IL-6 and IL-8, were measured via ELISA. Firstly, we found that hardwood and softwood smoke extract (1%) up-regulate IL-6 and IL-8 release ( $p \leq 0.05$ ). In addition, human rhinovirus-16 further increased biomass smoke-induced IL-8 in fibroblasts, in comparison to the two stimulatory agents alone. We also investigated the effect of biomass smoke on viral susceptibility by measuring viral load, and found no significant changes between BME exposed and non-exposed infected fibroblasts. Activated signaling pathways for IL-6 and IL-8 production by BME stimulation were examined using signaling pathway inhibitors. p38 MAPK inhibitor SB239063 significantly attenuated IL-6 and IL-8 release the most ( $p \leq 0.05$ ). This study demonstrated that biomass smoke can modulate rhinovirus-induced inflammation during infection, which can alter the severity of the disease. The mechanism by which biomass smoke exposure increases inflammation in the lungs can be targeted and inhibited via p38 MAP kinase pathway.

**Keywords:** Chronic obstructive pulmonary disease; Biomass smoke; Rhinovirus

### 1. Introduction

Biomass smoke is the result of the combustion of different types of biomass fuels, such as wood, animal dung, crop residues, and coal generated by more than 3 billion people for cooking and heating. As such, biomass smoke is one of the major air pollutants and contributors of household air pollution worldwide. In developing countries where poverty is prevalent, burning biomass fuels is a cheaper alternative compared to liquefied petroleum gas (LPG) or electricity. Biomass fuels are also more

accessible, especially for people living rurally [1]. As much as 97% of the population, living in rural areas in the least developed countries, rely solely on biomass fuels for household energy purposes [2].

Several studies have shown that women and children have the highest biomass smoke exposure due to cultural practices, such as indoor cooking in housing with very poor air ventilation [3]. The absence of chimneys or pipes prevents the smoke from venting outside and, therefore, particles become trapped and fuse to the surroundings [4,5]. During the burning of these fuels, people indoors can be exposed with up to 30,000  $\mu\text{g}/\text{m}^3$  of particulate matter (PM) sized 10  $\mu\text{m}$  or smaller ( $\text{PM}_{10}$ ), while an average concentration throughout the day is approximately 300–5000  $\mu\text{g}/\text{m}^3$ . Since most women and children stay indoors, they are exposed to these high concentrations of particulate matter and other toxic air pollutants for about 3–7 h a day [6]. The WHO guideline for  $\text{PM}_{10}$  concentration is only 50  $\mu\text{g}/\text{m}^3$  for a 24-h period. The Global Burden of Disease 2010 study found that household air pollution is the second highest risk factor of ill health for women and girls globally [7].

Children exposed to biomass smoke have an increased risk (1.8-fold) of developing acute lower respiratory disease (ALRI) [8,9]. Younger children, especially aged five years or younger, are more susceptible and have a higher mortality rate. ALRI accounts for 940,000 deaths of children under five per year [10]. Biomass smoke-associated ALRI causes 455,000 deaths and a loss of 39.1 million disability-adjusted life years annually [5,11]. However, diagnosis of ALRI is often based on parent-reported symptoms which can compromise etiological specificity [4]. Generally, ALRI is characterized by acute bronchitis, bronchiolitis, and pneumonia, caused by respiratory bacterial or viral infections. Around 90% of cases are attributed to viral infections, such as influenza, adenovirus, and rhinovirus. Although epidemiological studies have shown that biomass smoke is a considerable risk factor for the development of ALRI, the exact mechanism of the resulting increase in susceptibility is still unknown. Therefore, this study aims to investigate the effect of biomass smoke exposure on primary human lung cells in vitro, specifically examining possible enhancement of respiratory infection such as rhinovirus, by measuring production of inflammatory mediators involved in immune responses against infection.

## 2. Results

### 2.1. Hardwood and Softwood Smoke Extract Are Cytotoxic at Higher Concentrations

To assess the potential toxicological effect of biomass smoke, cells were exposed to 1%–10% of hardwood and softwood smoke for 24 h stimulation. Cell viability was measured via MTT assay, and confirmed by trypan blue exclusion assays. We found a trend of decreasing number of viable cells with increasing concentrations of hardwood and softwood smoke extract stimulation (Figure 1). We then investigated lower concentrations (0.01%, 0.1%, and 1%) of hardwood and softwood smoke extract and found no toxic effects of biomass smoke extract by trypan blue exclusion assays (Figure 2A,B) and LDH assays (Figure 2C,D). Overall we observed no differences in the toxicity of hardwood and softwood smoke extract.

### 2.2. Hardwood and Softwood Smoke Extract Upregulates IL-6 and IL-8 Production at Low Concentrations

Cell free supernatants were collected from fibroblasts stimulated with hardwood and softwood smoke extract (0.01%, 0.1%, and 1%) and IL-6 and IL-8 release was assessed via ELISA. We found a significant increase of both IL-6 and IL-8 release from 1% hardwood and softwood smoke extract stimulation (Figure 3).



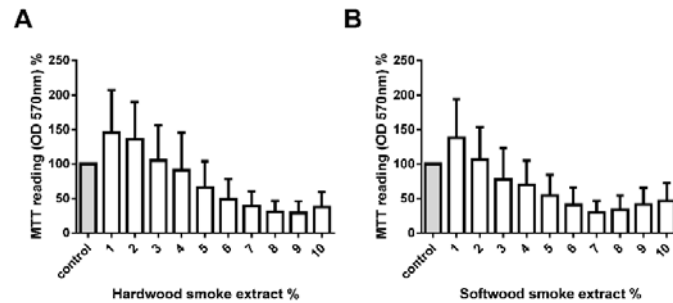


**Figure 1.** Measurement of cell viability with different hardwood and softwood smoke extract concentrations. Human primary lung fibroblasts ( $n = 5$ ) were stimulated with hardwood (A) and softwood (B) smoke extract (1%–10%) in 0.1% FBS/DMEM. Cell viability was measured using MTT assay at 24 h after stimulation. Data expressed as the percent of unstimulated fibroblasts and bars represent mean  $\pm$  SEM. Statistical analysis was executed using one-way ANOVA with Tukey's post-test. No significant differences were found.

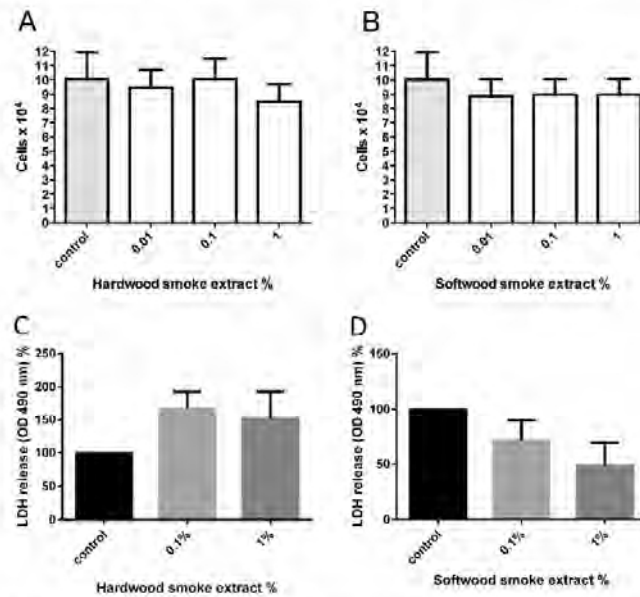


**Figure 2.** Measurement of cell viability from hardwood (A,C) and softwood (B,D) smoke extract stimulation at lower concentrations. Cell viability was measured via Manual cell count with trypan blue (0.02% *w/v*) and LDH assay from hardwood and softwood smoke extract stimulation at 0.01%, 0.1%, and 1% diluted in 0.1% FBS/DMEM in primary human lung fibroblasts ( $n = 6$ ). Manual cell count and LDH assay was executed after 24 h post-stimulation. Data is expressed in cells/mL. (A,B), percent of LDH release from control (C,D), and bars represent mean  $\pm$  SEM. Comparison between cell counts from control and different concentrations of hardwood and softwood smoke extract stimulation made by one-way ANOVA with Tukey's post-test. No significant differences were found.

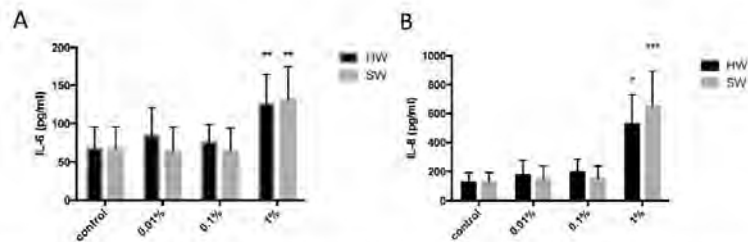


**Figure 3.** IL-6 (A) and IL-8 (B) induction from Hardwood and Softwood smoke exposure at lower concentrations. Human primary lung fibroblasts ( $n = 6$ ) were stimulated with hardwood and softwood smoke extract (0.01%, 0.1% and 1%) in 0.1% FBS/DMEM for 24 h. Cell free supernatants were collected and IL-6 (A) and IL-8 (B) release was measured via ELISA. Data were expressed in pg/mL and bars represent mean  $\pm$  SEM. Comparisons between IL-6/IL-8 release from control and different concentrations of hardwood and softwood smoke extract made by one-way ANOVA with Tukey's post-test. Significance is represented as \*  $p < 0.05$ , \*\*  $p < 0.01$  vs. control, \*\*\*  $p < 0.001$  vs. control.

### 2.3. Biomass Smoke Exposure Enhances RV-16 Induced IL-8 Production

Since epidemiological evidence suggests an interaction between biomass smoke and viral infection, we modelled this interaction *in vitro*. Fibroblasts were stimulated with biomass smoke extract initially (0.1% or 1%) and the infected with RV-16. As expected, hardwood and softwood smoke extract, and RV-16 alone, induced IL-6 and IL-8 release. Interestingly, RV increased IL-8 (Figure 4), but not IL-6 production (Figure 5) in both hardwood and softwood smoke exposed fibroblasts. In cells first infected with RV and then stimulated with biomass smoke extract, cytokine induction was not greater in comparison to RV alone.

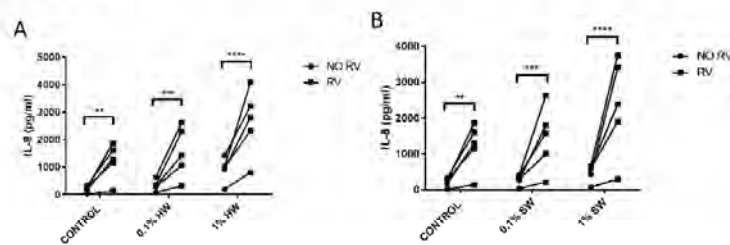


**Figure 4.** Measurement of IL-8 production from hardwood (A) and softwood (B) smoke exposure and RV-16 infection. Primary human lung fibroblasts ( $n = 5$ ) were stimulated with hardwood and softwood smoke extract at 0.1% and 1% concentration alone, RV-16 infection alone (MOI = 1), or both, and incubated for 24 h. Unstimulated fibroblasts were also measured for IL-8 constitutive release. Supernatants were collected for IL-8 concentration analysis via ELISA. Data expressed as pg/mL. Statistical analysis was executed using two-way ANOVA with Sidak's post-test. Significance is represented as \*\*  $p < 0.01$ , \*\*\*  $p < 0.001$ , \*\*\*\*  $p < 0.0001$ .

### 2.4. Biomass Smoke Exposure Did Not Affect RV-16 Load

We further investigated the role of biomass smoke exposure on modulating RV-16 infection by measuring viral load of infected fibroblasts with or without biomass smoke exposure. There were no significant differences between the viral load of biomass smoke exposed and non-exposed RV-16 infected fibroblasts (Figure S1). We also measured viral load from RV-16 infected fibroblasts that were exposed to biomass smoke extract after infection and found no significant difference between the groups (data not shown).

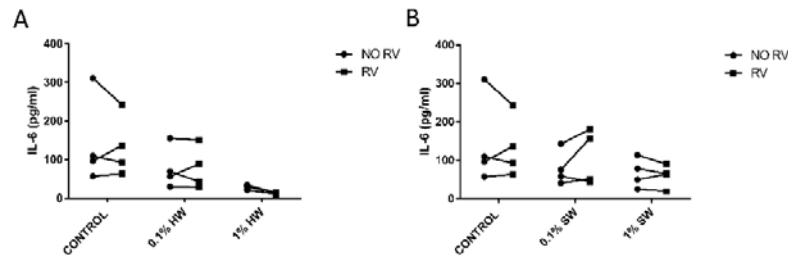


**Figure 5.** Measurement of IL-6 production from hardwood (A) and softwood (B) smoke exposure and RV-16 infection. Primary human lung fibroblasts ( $n = 4$ ) were stimulated with hardwood and softwood smoke extract at 0.1% and 1% concentration alone, RV-16 infection alone (MOI = 1), or both and incubated for 24 h. Unstimulated fibroblasts were also measured for IL-6 constitutive release. Supernatants were collected for IL-6 concentration via ELISA. Data expressed as pg/mL. Statistical analysis was executed using two-way ANOVA with Sidak's post-test.

### 2.5. Hardwood and Softwood Smoke Induced IL-6 and IL-8 Are Attenuated by Different Signalling Pathway Inhibitors

There are different potential signaling pathways being activated by biomass smoke to induce IL-6 and IL-8 production. PI3 kinase, ERK, SMAD, p38 MAP kinase, NF $\kappa$ B, JNK and COX signaling pathways have all been previously shown to play a role in up-regulating inflammation from oxidative stimuli such as cigarette smoke. To examine this, chemical inhibitors were used, which are specific to the signaling pathways mentioned above. PI3 kinase, NF $\kappa$ B, JNK, and COX inhibitors were unable to attenuate IL-6 and IL-8 production from both hardwood and softwood smoke extract stimulation (data not shown). Softwood smoke-induced IL-6 and IL-8 was significantly attenuated by p38 MAP kinase inhibitor (Figures 6 and 7). In addition, softwood smoke-induced IL-8 was also inhibited by ERK and SMAD inhibitors (Figure 7). Surprisingly, hardwood smoke-induced IL-6 was not inhibited by any of the signaling inhibitors used (Figure 6), however, hardwood smoke-induced IL-8 solely involved p38 MAP kinase pathway (Figure 7).

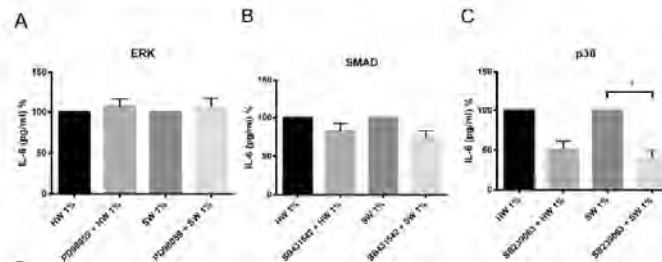


**Figure 6.** The effects of ERK (A), SMAD (B), and p38 MAP kinase (C) inhibitors on IL-6 production by hardwood and softwood smoke extract. Primary human lung fibroblasts ( $n = 4$ ) were pretreated for an hour with signaling inhibitors, PD98059 (10  $\mu$ M), SB431542 (10  $\mu$ M), and SB239063 (3  $\mu$ M) in DMSO (vehicle control) for ERK, SMAD, and p38 MAP kinase pathway, respectively, then stimulated with 1% hardwood and softwood smoke extract for 24 h. Supernatant was collected and IL-6 concentration analysis was executed via ELISA. Data are expressed as the percent of inhibition from control and bars represent mean  $\pm$  SEM. Statistical analysis was executed by using repeated measures, one-way ANOVA with Tukey's post-test. Significance is represented as \*  $p < 0.05$ .

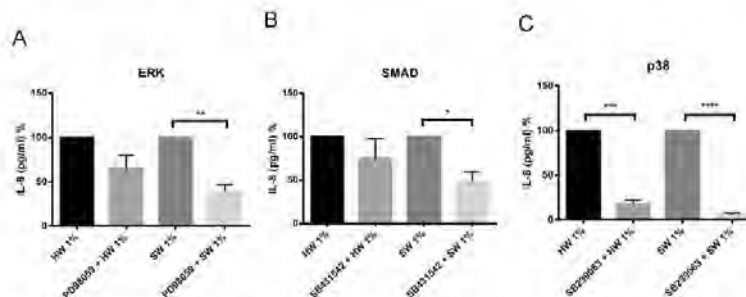


**Figure 7.** The effects of ERK (A), SMAD (B), and p38 MAP kinase (C) inhibitors on IL-8 production by hardwood and softwood smoke extract. Primary human lung fibroblasts ( $n = 4$ ) were pretreated for an hour with signaling inhibitors, PD98059 (10  $\mu$ M), SB431542 (10  $\mu$ M), and SB203683 (3  $\mu$ M) in DMSO (vehicle control) for ERK, SMAD, and p38 MAP kinase pathway respectively, then stimulated with 1% hardwood and softwood smoke extract for 24 h. Supernatant was collected and IL-8 concentration analysis was executed via ELISA. Data expressed as the percent of inhibition from control and bars represent mean  $\pm$  SEM. Statistical analysis executed by using repeated measures, one-way ANOVA with Tukey's post-test. Significance is represented as \*  $p < 0.05$ , \*\*  $p < 0.01$ , \*\*\*  $p < 0.001$ , \*\*\*\*  $p < 0.0001$ .

### 3. Discussion

As expected, this study found that hardwood and softwood smoke extract up-regulates IL-6 and IL-8 release from primary human lung fibroblasts, suggesting that biomass smoke exposure promotes airway inflammation. Interestingly, in the presence of biomass smoke, rhinovirus (RV) was able to further increase IL-8 production, but had no effect on IL-6 production. Biomass smoke exposure did not affect RV replication. To understand the underlying mechanisms involved in biomass smoke-induced IL-6 and IL-8 production, activated signaling pathways were also investigated by using signaling pathway inhibitors. Despite relatively similar toxicity and cytokine induction, the signaling pathways activated by softwood and hardwood biomass smoke were very different. IL-6 production is mainly driven by p38 MAPK. However, softwood smoke extract induced IL-8 via SMAD, ERK, and p38 MAPK, whilst hardwood extract induced IL-8 via p38 MAPK only.

The assessment of cellular toxicology to hardwood and softwood smoke was made using a number of biochemical and biological assays. The aim of these experiments was to choose a concentration of biomass smoke that was non-toxic for further immunogenic analysis. For screening purposes, we chose to use a MTT assay with biomass smoke at 1%–10%. The MTT assay measures mitochondrial activity and not cellular viability, per se. The assay overall showed no statistical change, but a trend towards increased MTT with low concentrations of biomass extract and reduced MTT with higher concentrations was observed. The increased MTT readings could represent either proliferation or increased mitochondrial biogenesis, and the lower readings reduced number of cells or mitochondria. To investigate this further, we chose to count the actual number of viable cells over the concentration range 0.01%–1% biomass smoke extract. No increase or decrease in cell number was found, leading us to assume that the trend towards increased MTT readings at 1% biomass smoke extract is the result of greater mitochondrial activity and/or number. To thoroughly investigate if cell viability was compromised by 1% biomass extract we carried out LDH assays. No significant release of LDH occurred with biomass extract stimulation, although the data were variable and a trend towards increased LDH with hardwood smoke and decreased LDH with softwood smoke extract was observed. These data do have limitations. The gold standard assay of cellular viability is direct microscopic assessment with an exclusion dye, such as trypan blue. The MTT assay and the LDH assay could both be effected by the presence of oxidants, particulate matter, and other chemicals in hardwood and

softwood smoke extract. We are confident that biomass smoke at 1% is nontoxic, but are not certain what the potential changes in MTT or LDH measurements represent.

This study is the first to investigate the interaction of biomass smoke exposure and rhinovirus infection *in vitro*. Epithelial cells and fibroblasts are often the first non-immune cells within the respiratory tract to encounter both viral pathogens and toxic components of air and are essential for innate and subsequent adaptive immune response. Upon RV infection, the cells produce various cytokines and chemokines, such as IL-6 and IL-8 [12] that are capable of activating and recruiting a variety of other cells such as lymphocytes, eosinophils, and neutrophils [13]. We found that prior biomass smoke exposure enhances rhinovirus-induced IL-8 production. As IL-8 production *in vivo* is known to be positively correlated to respiratory symptoms in rhinovirus infected children [14]. We believe that this enhanced secretion of IL-8 may, in part, explain the enhanced severity of virus infections in biomass smoke exposed people.

It was interesting that rhinovirus replication was not altered in biomass smoke exposed fibroblasts. This suggests that the oxidative environment of the biomass smoke extract does not affect the virus capsid enough to alter infection. As IL-8 can be induced by RV-16, independent of viral replication, intracellular adhesion molecule (ICAM) [15], we cannot definitively state that RV-induced IL-8 occurred as a consequence of replication. However, it is reasonable to assume that IL-8 production was in-part induced by RV replication as replication occurred, even in the presence of biomass smoke extract.

Biomass smoke, specifically wood smoke, has been well characterized of its chemical and physical composition. There are over 200 different compounds, including toxic chemicals, such as polycyclic aromatic hydrocarbons (PAH), nitrogen oxides (NO<sub>x</sub>), and particulate matter of varying sizes (e.g., PM<sub>2.5</sub>, 10). These compounds are well studied and are toxicologically indistinguishable despite different wood sources. Since we observed similar responses in hardwood and softwood smoke extract stimulated fibroblasts, we did not attempt to identify specific compounds in biomass smoke extract responsible for the changes evident in our study. It is most likely that these different compounds simultaneously contribute to the aftermath of physiological changes involved; therefore, it is more beneficial to study the entire biomass smoke as a physiological stimulus, similar to other studies involving cigarette smoke. The majority of the toxic components identified in biomass smoke are also present in cigarette smoke and, hence, both stimuli can be comparable in causing similar diseases. Several studies have shown increased susceptibility to ALRI in children from second-hand tobacco smoke [16–18]. Proud et al. have shown an additive increase of IL-8 production from cigarette smoke and rhinovirus stimulation in primary human bronchial epithelial cells, parallel to our findings with biomass smoke [19]. However, current publications have conflicting data on the effect of cigarette smoke on viral replication. Several studies have shown increased rhinovirus replication after cigarette smoke exposure compared to control [20–22]. However, other studies infecting the airway epithelial cell line BEAS-2B with RV-16 [19,23] reported that addition of CSE during and after infection had no effect on viral titer which is consistent with our results with biomass smoke exposure. Since this is the first study to investigate the interaction between biomass smoke exposure and rhinovirus infection, we can only compare our results to studies investigating cigarette smoke exposure. More research on biomass smoke exposure in cell culture models is crucial to understand mechanisms in causing and increasing risk in disease.

We have used an *in vitro* model to attempt to replicate the effects of exposure to biomass smoke *in vivo*. In women exposed to biomass smoke the equivalent exposure to cigarette is calculated as 20 cigarettes per day. In our model system we use the same mass of biomass as tobacco leaf found in a cigarette. However, cigarettes are directly inhaled whilst this is not the intention with biomass smoke. If we assume that 5 kg of wood would be used as a biomass heating source, our model of 1% biomass smoke extraction (from <1 g of wood), would equate to 1/500,000 of the total particles emitted from the 5 kg of biomass wood. We think that this is a reasonable approximation for what might occur *in vivo*, but acknowledge that room size, ventilation and breathing rate would all effect exposure. Interestingly, peak indoor particulate matter (PM10) whilst cooking often exceeded 2 mg/m<sup>3</sup> [24].



Our model of biomass smoke extract does have advantages over direct smoke exposure. For example, it is easier to standardize exposure in comparison to direct smoke exposure, and when modelling effects on cells distal to the epithelium may be a closer approximation to what these cells are exposed to. However, it does have limitations. Volatile organic compounds (VOCs) are produced during biomass combustion. As we collect the soluble component of biomass smoke, it is possible that some VOCs will not be collected due to limited solubility and/or if collected they may not be present at the time of stimulation due to their short half-life. It would be interesting in future studies to look at the relative and separate contribution of particulate matter and VOCs in in vitro and in vivo models.

This study also investigated the possible differences between hardwood and softwood as two types of biomass source. Previous studies have characterized smoke compositions between different woods, and have found that the greatest variation occurs between hard wood and soft wood, rather than between different types of either. Hardwood and softwood have varying levels of resin acid and substituted phenols. More specifically, resin acid is more prominent in softwood types than hardwood [25]; and polycyclic aromatic hydrocarbon profiles between hardwood and softwood [26] Our study shows that 1% hardwood and softwood smoke extract both induce IL-6 and IL-8 release in primary human lung fibroblasts, and is cytotoxic at higher concentrations.

We also investigated the underlying mechanism involved in hardwood and softwood-induced IL-6 and IL-8 production by identifying activated signaling pathways using specific signaling inhibitors. p38 MAPK inhibitor SB239063 significantly attenuated IL-6 and IL-8 release the most. Interestingly, hardwood smoke extract might only be activating the p38 MAP kinase pathway to induce IL-8 production, while softwood smoke extract activates ERK, SMAD, and p38 MAP kinase pathways simultaneously to induce IL-8 production. These data have limitations. The use of specific pathway inhibitors is a good indication of the involvement of a specific pathway in a given response, but measurement of protein phosphorylation, translocation and binding to gene promoter regions is needed to confirm the direct involvement of the pathway. Despite similar cytotoxic and inflammatory effects of hardwood and softwood, different mechanisms might be involved in promoting inflammation. This suggests that the effect of biomass smoke can be source-specific and potentially require different therapeutic targets to inhibit inflammation.

#### 4. Materials and Methods

##### 4.1. Ethics Statement

Ethical approval for all experiments with lung tissue from donors undergoing resections or transplantations provided by the Human Ethics Committees of the University of Sydney and the Sydney South West Area Health Service with written consent forms.

##### 4.2. Isolation and Culture of Primary Human Lung Fibroblasts

Primary human lung fibroblasts were isolated from lung tissue resection for thoracic malignancies or transplantation for interstitial lung disease or emphysema (mean age 63) as previously stated [27]. There were no available data on donor's exposure to environmental pollution or biomass smoke prior to sample collection, although this was unlikely to be significant in Australian donors.

##### 4.3. Cell Culture

Primary human lung fibroblasts were seeded at  $4.2 \times 10^4$  cells/mL in 5% FBS DMEM, at 37 °C with 5% CO<sub>2</sub> for 72 h. Cells were synchronized into G0 phase in 0.1% FBS DMEM for 24 h before stimulation.

##### 4.4. Biomass Smoke Extract Preparation and Stimulation

Two types of biomass were used in these experiments representing hardwood and softwood. The hardwood source was Merbau wood (*Intsia bijuga*), while the softwood source was standard pine

(*Pinus radiata*). Both are commonly found in the Indo-pacific region and Asia where biomass smoke exposure is most prevalent. Both wood sources were untreated.

Biomass smoke extract (BME) was prepared fresh by using a custom built smoking apparatus, which allows the soluble components of biomass smoke to be collected in media. 730 mg of shredded biomass (hardwood/softwood) was combusted and the resulting biomass smoke was bubbled through 25 mL of DMEM, this was defined as 100% BME solution. This solution was then diluted in 0.1% FBS/DMEM to the desired concentration for experiments and used within 30 min after preparation.

#### 4.5. ELISA Detection of IL-6 and IL-8

The concentration of IL-6 and IL-8 in cell free samples was measured using commercial ELISA kits specific for human IL-6 and IL-8 (BD Biosciences, North Ryde, Australia) and ELISA plates (NUNC Maxisorp, Naperville, IL, USA). All antibodies were used at concentrations recommended by manufacturer's instructions and the following protocol was used.

#### 4.6. Cell Viability Assay

Cell viability was estimated using 3-(4,5-Dimethylthiazol-2-yl)-2,5-Diphenyl-tetrazolium Bromide (MTT) assays and lactate dehydrogenase assays according to the manufacturer's instructions (Sigma-Aldrich, St. Louis, MO, USA). In addition, manual cell counting with Trypan blue exclusion (0.02% *w/v*) was performed to confirm cell viability results.

#### 4.7. Viral Propagation, Titration, and Stimulation

Major group human rhinovirus serotype-16 (RV-16) was obtained from Johnston at Imperial College, UK and propagated and titrated in Ohio HeLa cells [28]. Cells were infected with RV-16 (MOI of 1) after the medium was replaced with fresh 0.1% FBS/DMEM. Viral load was also measured from cell free supernatant samples collected from primary human lung fibroblasts that were infected with RV-16 alone, and with hardwood or softwood smoke extract stimulation using titration assay [28].

#### 4.8. Biomass Smoke Extract and Human Rhinovirus-16 Stimulation

Primary human lung fibroblasts were stimulated with either 0.1% or 1% hardwood or softwood smoke extract alone for 24 h, or with RV-16 infection. Cells were either first stimulated with biomass smoke or infected for 4 h, and then the second stimulus (biomass or RV as appropriate) for another 20 h.

#### 4.9. Signalling Pathway Inhibition Using Specific Inhibitors

To investigate the possible signaling pathways activated by biomass and resulting in cytokine production in primary human lung fibroblasts, inhibitors of the PI3 kinase, ERK, JNK, SMAD, p38 MAP kinase, NF $\kappa$ B, and COX pathways were used. The signaling pathway inhibitors were used at the following concentrations which have been shown to be specific and effective in human airway cells [29–33]—L294002 (3  $\mu$ M), PD98059 (10  $\mu$ M), SP600125 (10  $\mu$ M) (Chalbiochem, San Diego, CA, USA), SB431542 (10  $\mu$ M), SB239063 (3  $\mu$ M) (Tocris, Ellisville, MO, USA), BAY117085 (10<sup>-3</sup>  $\mu$ M), and acetylsalicylic acid (0.1  $\mu$ M) (Sigma-Aldrich).

Signaling inhibitors were added to primary human lung fibroblasts for one hour prior to biomass smoke stimulation. A vehicle control (0.06% DMSO) was also used. Supernatant was collected after 24 h.

#### 4.10. Statistical Analysis

Statistical analysis was performed using Graph Pad Prism (version 6, La Jolla, CA, USA). Data were initially checked for normality. To assess statistical significance, One-way repeated measures ANOVA with Tukey's post-test were used for unpaired data. Two-way repeated measures ANOVA with Sidak's post-test were used for paired data. All data on bar graphs were presented as

mean  $\pm$  standard error of the mean (SEM). Significance was shown with \* for  $p$  value  $\leq 0.05$ , \*\* for  $p \leq 0.01$ , \*\*\* for  $p \leq 0.001$ , and \*\*\*\* for  $p \leq 0.0001$ .

**Supplementary Materials:** Supplementary materials can be found at [www.mdpi.com/1422-0067/17/9/1403/s1](http://www.mdpi.com/1422-0067/17/9/1403/s1).

**Acknowledgments:** Supported by NHMRC Australia # APP1026880.

**Author Contributions:** Sarah J. Capistrano, Razia Zakarya, Hui Chen and Brian G. Oliver conceived and wrote the manuscript. Sarah J. Capistrano, Razia Zakarya carried out the experiments.

**Conflicts of Interest:** The authors declare no conflict of interest.

## References

- Dutta, A.; Ray, M.R.; Banerjee, A. Systemic inflammatory changes and increased oxidative stress in rural indian women cooking with biomass fuels. *Toxicol. Appl. Pharmacol.* **2012**, *261*, 255–262. [[CrossRef](#)] [[PubMed](#)]
- Kurmi, O.P.; Lam, K.B.; Ayres, J.G. Indoor air pollution and the lung in low- and medium-income countries. *Eur. Respir. J.* **2012**, *40*, 239–254. [[CrossRef](#)] [[PubMed](#)]
- Kodgule, R.; Salvi, S. Exposure to biomass smoke as a cause for airway disease in women and children. *Curr. Opin. Allergy Clin. Immunol.* **2012**, *12*, 82–90. [[CrossRef](#)] [[PubMed](#)]
- Gordon, S.B.; Bruce, N.G.; Grigg, J.; Hibberd, P.L.; Kurmi, O.P.; Lam, K.B.; Mortimer, K.; Asante, K.P.; Balakrishnan, K.; Balmes, J.; et al. Respiratory risks from household air pollution in low and middle income countries. *Lancet Respir. Med.* **2014**, *2*, 823–860. [[CrossRef](#)]
- Smith, K.R.; Bruce, N.; Balakrishnan, K.; Adair-Rohani, H.; Balmes, J.; Chafe, Z.; Dherani, M.; Hosgood, H.D.; Mehta, S.; Pope, D.; et al. Millions dead: How do we know and what does it mean? Methods used in the comparative risk assessment of household air pollution. *Annu. Rev. Public Health* **2014**, *35*, 185–206. [[CrossRef](#)] [[PubMed](#)]
- Torres-Duque, C.; Maldonado, D.; Perez-Padilla, R.; Ezzati, M.; Viegli, G. Biomass fuels and respiratory diseases: A review of the evidence. *Proc. Am. Thorac. Soc.* **2008**, *5*, 577–590. [[CrossRef](#)] [[PubMed](#)]
- Lim, S.S.; Vos, T.; Flaxman, A.D.; Danaei, G.; Shibuya, K.; Adair-Rohani, H.; Amann, M.; Anderson, H.R.; Andrews, K.G.; Aryee, M.; et al. A comparative risk assessment of burden of disease and injury attributable to 67 risk factors and risk factor clusters in 21 regions, 1990–2010: A systematic analysis for the global burden of disease study 2010. *Lancet* **2012**, *380*, 2224–2260. [[CrossRef](#)]
- Gurley, E.S.; Homaira, N.; Salje, H.; Ram, P.K.; Haque, R.; Petri, W.; Bresee, J.; Moss, W.J.; Breyse, P.; Luby, S.P.; et al. Indoor exposure to particulate matter and the incidence of acute lower respiratory infections among children: A birth cohort study in urban bangladesh. *Indoor Air* **2013**, *23*, 379–386. [[CrossRef](#)] [[PubMed](#)]
- Dherani, M.; Pope, D.; Mascarenhas, M.; Smith, K.R.; Weber, M.; Bruce, N. Indoor air pollution from unprocessed solid fuel use and pneumonia risk in children aged under five years: A systematic review and meta-analysis. *Bull. World Health Organ.* **2008**, *86*, 390C–398C.
- Upadhyay, A.K.; Singh, A.; Kumar, K.; Singh, A. Impact of indoor air pollution from the use of solid fuels on the incidence of life threatening respiratory illnesses in children in India. *BMC Public Health* **2015**, *15*, 300. [[CrossRef](#)] [[PubMed](#)]
- Lee, A.; Kinney, P.; Chillrud, S.; Jack, D. A systematic review of innate immunomodulatory effects of household air pollution secondary to the burning of biomass fuels. *Ann. Glob. Health* **2015**, *81*, 368–374. [[CrossRef](#)] [[PubMed](#)]
- Lopez-Souza, N.; Dolganov, G.; Dubin, R.; Sachs, L.A.; Sassina, L.; Sporer, H.; Yagi, S.; Schnurr, D.; Boushey, H.A.; Widdicombe, J.H. Resistance of differentiated human airway epithelium to infection by rhinovirus. *Am. J. Physiol. Lung Cell. Mol. Physiol.* **2004**, *286*, L373–L381. [[CrossRef](#)] [[PubMed](#)]
- Ghildyal, R.; Dagher, H.; Donninger, H.; de Silva, D.; Li, X.; Freezer, N.J.; Wilson, J.W.; Bardin, P.G. Rhinovirus infects primary human airway fibroblasts and induces a neutrophil chemokine and a permeability factor. *J. Med. Virol.* **2005**, *75*, 608–615. [[CrossRef](#)] [[PubMed](#)]
- Gem, J.E.; Martin, M.S.; Anklam, K.A.; Shen, K.; Roberg, K.A.; Carlson-Dakes, K.T.; Adler, K.; Gilbertson-White, S.; Hamilton, R.; Shult, P.A.; et al. Relationships among specific viral pathogens, virus-induced interleukin-8, and respiratory symptoms in infancy. *Pediatr. Allergy Immunol.* **2002**, *13*, 386–393. [[CrossRef](#)] [[PubMed](#)]



15. Wang, X.; Lau, C.; Wiehler, S.; Pow, A.; Mazzulli, T.; Gutierrez, C.; Proud, D.; Chow, C.W. Syk is downstream of intercellular adhesion molecule-1 and mediates human rhinovirus activation of p38 MAPK in airway epithelial cells. *J. Immunol.* **2006**, *177*, 6859–6870. [[CrossRef](#)] [[PubMed](#)]
16. Claude, J.A.; Grimm, A.; Savage, H.P.; Pinkerton, K.E. Perinatal exposure to environmental tobacco smoke (ETS) enhances susceptibility to viral and secondary bacterial infections. *Int. J. Environ. Res. Public Health* **2012**, *9*, 3954–3964. [[CrossRef](#)] [[PubMed](#)]
17. Du Preez, K.; Mandalakas, A.M.; Kirchner, H.L.; Grewal, H.M.; Schaaf, H.S.; van Wyk, S.S.; Hesselning, A.C. Environmental tobacco smoke exposure increases mycobacterium tuberculosis infection risk in children. *Int. J. Tuberc. Lung Dis.* **2011**, *15*, 1490–1497. [[CrossRef](#)] [[PubMed](#)]
18. Kariya, C.; Chu, H.W.; Huang, J.; Leitner, H.; Martin, R.J.; Day, B.J. Mycoplasma pneumoniae infection and environmental tobacco smoke inhibit lung glutathione adaptive responses and increase oxidative stress. *Infect. Immun.* **2008**, *76*, 4455–4462. [[CrossRef](#)] [[PubMed](#)]
19. Hudy, M.H.; Traves, S.L.; Wiehler, S.; Proud, D. Cigarette smoke modulates rhinovirus-induced airway epithelial cell chemokine production. *Eur. Respir. J.* **2010**, *35*, 1256–1263. [[CrossRef](#)] [[PubMed](#)]
20. Logan, J.; Chen, L.; Gangell, C.; Sly, P.D.; Fantino, E.; Liu, K. Brief exposure to cigarette smoke impairs airway epithelial cell innate anti-viral defence. *Toxicol. In Vitro* **2014**, *28*, 1430–1435. [[CrossRef](#)] [[PubMed](#)]
21. Eddleston, J.; Lee, R.U.; Doerner, A.M.; Herschbach, J.; Zuraw, B.L. Cigarette smoke decreases innate responses of epithelial cells to rhinovirus infection. *Am. J. Respir. Cell Mol. Biol.* **2011**, *44*, 118–126. [[CrossRef](#)] [[PubMed](#)]
22. Groskreutz, D.J.; Monick, M.M.; Babor, E.C.; Nyunoya, T.; Varga, S.M.; Look, D.C.; Hunninghake, G.W. Cigarette smoke alters respiratory syncytial virus-induced apoptosis and replication. *Am. J. Respir. Cell Mol. Biol.* **2009**, *41*, 189–198. [[CrossRef](#)] [[PubMed](#)]
23. Proud, D.; Hudy, M.H.; Wiehler, S.; Zaheer, R.S.; Amin, M.A.; Pelikan, J.B.; Tacon, C.E.; Tonsaker, T.O.; Walker, B.L.; Kooi, C.; et al. Cigarette smoke modulates expression of human rhinovirus-induced airway epithelial host defense genes. *PLoS ONE* **2012**, *7*, e40762. [[CrossRef](#)] [[PubMed](#)]
24. Regalado, J.; Pérez-Padilla, R.; Sansores, R.; Páramo Ramírez, J.I.; Brauer, M.; Paré, P.; Vedral, S. The effect of biomass burning on respiratory symptoms and lung function in rural Mexican women. *Am. J. Respir. Crit. Care Med.* **2006**, *174*, 901–905. [[CrossRef](#)] [[PubMed](#)]
25. Fine, P.M.; Cass, G.R.; Simoneit, B.R. Chemical characterization of fine particle emissions from fireplace combustion of woods grown in the Northeastern United States. *Environ. Sci. Technol.* **2001**, *35*, 2665–2675. [[CrossRef](#)] [[PubMed](#)]
26. Zou, L.Y.; Zhang, W.; Atkiston, S. The characterisation of polycyclic aromatic hydrocarbons emissions from burning of different firewood species in Australia. *Environ. Pollut.* **2003**, *124*, 283–289. [[CrossRef](#)]
27. Krimmer, D.I.; Burgess, J.K.; Wooi, T.K.; Black, J.L.; Oliver, B.G. Matrix proteins from smoke-exposed fibroblasts are pro-proliferative. *Am. J. Respir. Cell Mol. Biol.* **2012**, *46*, 34–39. [[CrossRef](#)] [[PubMed](#)]
28. Oliver, B.G.; Johnston, S.L.; Baraket, M.; Burgess, J.K.; King, N.J.; Roth, M.; Lim, S.; Black, J.L. Increased proinflammatory responses from asthmatic human airway smooth muscle cells in response to rhinovirus infection. *Respir. Res.* **2006**, *7*, 71. [[CrossRef](#)] [[PubMed](#)]
29. Griego, S.D.; Weston, C.B.; Adams, J.L.; Tal-Singer, R.; Dillon, S.B. Role of p38 mitogen-activated protein kinase in rhinovirus-induced cytokine production by bronchial epithelial cells. *J. Immunol.* **2000**, *165*, 5211–5220. [[CrossRef](#)] [[PubMed](#)]
30. Pelaia, G.; Cuda, G.; Vatrella, A.; Fratto, D.; Grembale, R.D.; Tagliaferri, P.; Maselli, R.; Costanzo, F.S.; Marsico, S.A. Effects of transforming growth factor- $\beta$  and budesonide on mitogen-activated protein kinase activation and apoptosis in airway epithelial cells. *Am. J. Respir. Cell Mol. Biol.* **2003**, *29*, 12–18. [[CrossRef](#)] [[PubMed](#)]
31. Ip, W.K.; Wong, C.K.; Lam, C.W. Interleukin (IL)-4 and IL-13 up-regulate monocyte chemoattractant protein-1 expression in human bronchial epithelial cells: Involvement of p38 mitogen-activated protein kinase, extracellular signal-regulated kinase 1/2 and janus kinase-2 but not c-Jun NH2-terminal kinase 1/2 signalling pathways. *Clin. Exp. Immunol.* **2006**, *145*, 162–172. [[PubMed](#)]

32. Johnson, P.R.; Burgess, J.K.; Ge, Q.; Poniris, M.; Boustany, S.; Twigg, S.M.; Black, J.L. Connective tissue growth factor induces extracellular matrix in asthmatic airway smooth muscle. *Am. J. Respir. Crit. Care Med.* **2006**, *173*, 32–41. [[CrossRef](#)] [[PubMed](#)]
33. Zhong, J.; Gencay, M.M.; Bubendorf, L.; Burgess, J.K.; Parson, H.; Robinson, B.W.; Tamm, M.; Black, J.L.; Roth, M. ERK1/2 and p38 Map kinase control MMP-2, MT1-MMP, and TIMP action and affect cell migration: A comparison between mesothelioma and mesothelial cells. *J. Cell. Physiol.* **2006**, *207*, 540–552. [[CrossRef](#)] [[PubMed](#)]



© 2016 by the authors; licensee MDPI, Basel, Switzerland. This article is an open access article distributed under the terms and conditions of the Creative Commons Attribution (CC-BY) license (<http://creativecommons.org/licenses/by/4.0/>).

## Appendix B – Genes Located on ECM Microarray

<b>ECM Gene</b>	<b>Chromosomal location</b>
VCAM1	Chr1p
COL11A1	Chr1p
COL16A1	Chr1p
ECM1	Chr1q
LAMB3	Chr1q
LAMC1	Chr1q
SELE	Chr1q
SELL	Chr1q
SELP	Chr1q
THBS3	Chr1q
FN1	Chr2q
ITGA4	Chr2q
ITGA6	Chr2q
ITGAV	Chr2q
COL7A1	Chr3p
CLEC3B	Chr3p
COL8A1	Chr3q
CTNNB1	Chr3q
ITGB5	Chr3q
SPP1	Chr4q
CTNND2	Chr5p
VCAN	Chr5q
CTNNA1	Chr5q
ITGA1	Chr5q
ITGA2	Chr5q
SPARC	Chr5q
TBP	Chr6q
COL12A1	Chr6q
CTGF aka CCN2	Chr6q
LAMA2	Chr6q
THBS2	Chr6q
ACTB	Chr7p
PPIA	Chr7p
LAMB1	Chr7q
SGCE	Chr7q
COL14A1	Chr8q
MMP16	Chr8q
ADAMTS13	Chr9q
COL15A1	Chr9q
COL5A1	Chr9q
TNC	Chr9q

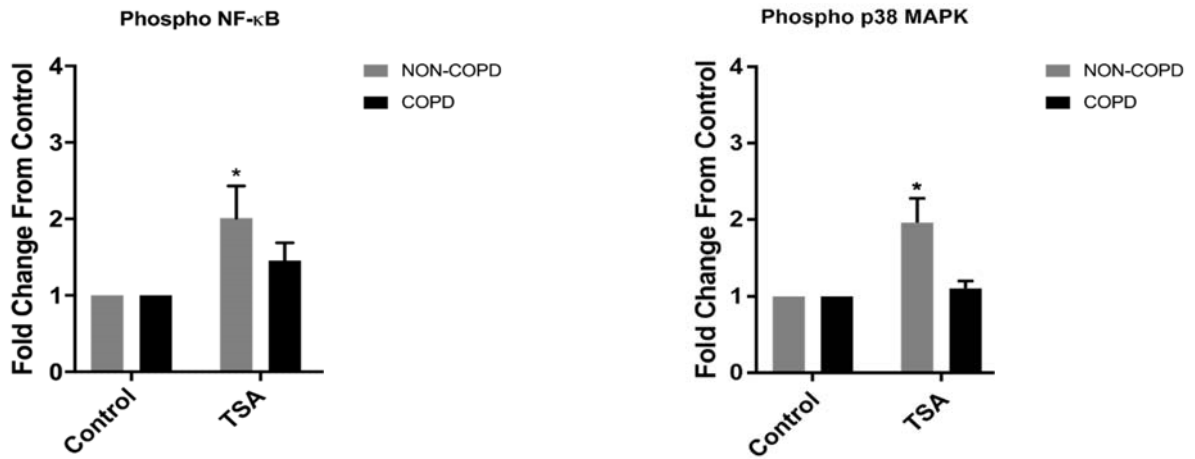
ITGA8	Chr10p
ITGB1	Chr10p
CD44	Chr11p
HMBS	Chr11q
ADAMTS8	Chr11q
CTNND1	Chr11q
MMP1	Chr11q
MMP10	Chr11q
MMP12	Chr11q
MMP13	Chr11q
MMP3	Chr11q
MMP7	Chr11q
MMP8	Chr11q
NCAM1	Chr11q
RPLP0	Chr12q
UBC	Chr12q
CNTN1	Chr12q
ITGA5	Chr12q
ITGA7	Chr12q
COL4A2	Chr13q
MMP14	Chr14q
B2M	Chr15q
THBS1	Chr15q
ITGAL	Chr16p
ITGAM	Chr16p
CDH1	Chr16q
MMP15	Chr16q
MMP2	Chr16q
SPG7	Chr16q
COL1A1	Chr17q
ITGA3	Chr17q
ITGB3	Chr17q
ITGB4	Chr17q
PECAM1	Chr17q
TIMP2	Chr17q
VTN	Chr17q
LAMA1	Chr18p
LAMA3	Chr18q
ICAM1	Chr19p
HAS1	Chr19q
TGFBI	Chr19q
MMP9	Chr20q

ADAMTS1	Chr21q
COL6A1	Chr21q
COL6A2	Chr21q
ITGB2	Chr21q
MMP11	Chr22q
TIMP3	Chr22q
KAL1 aka ANOS1	ChrXp
TIMP1	ChrXp
PGK1	ChrXq

– End Table –

## Appendix C – Data from Study into Off-target Effects of Epigenetic Inhibitors

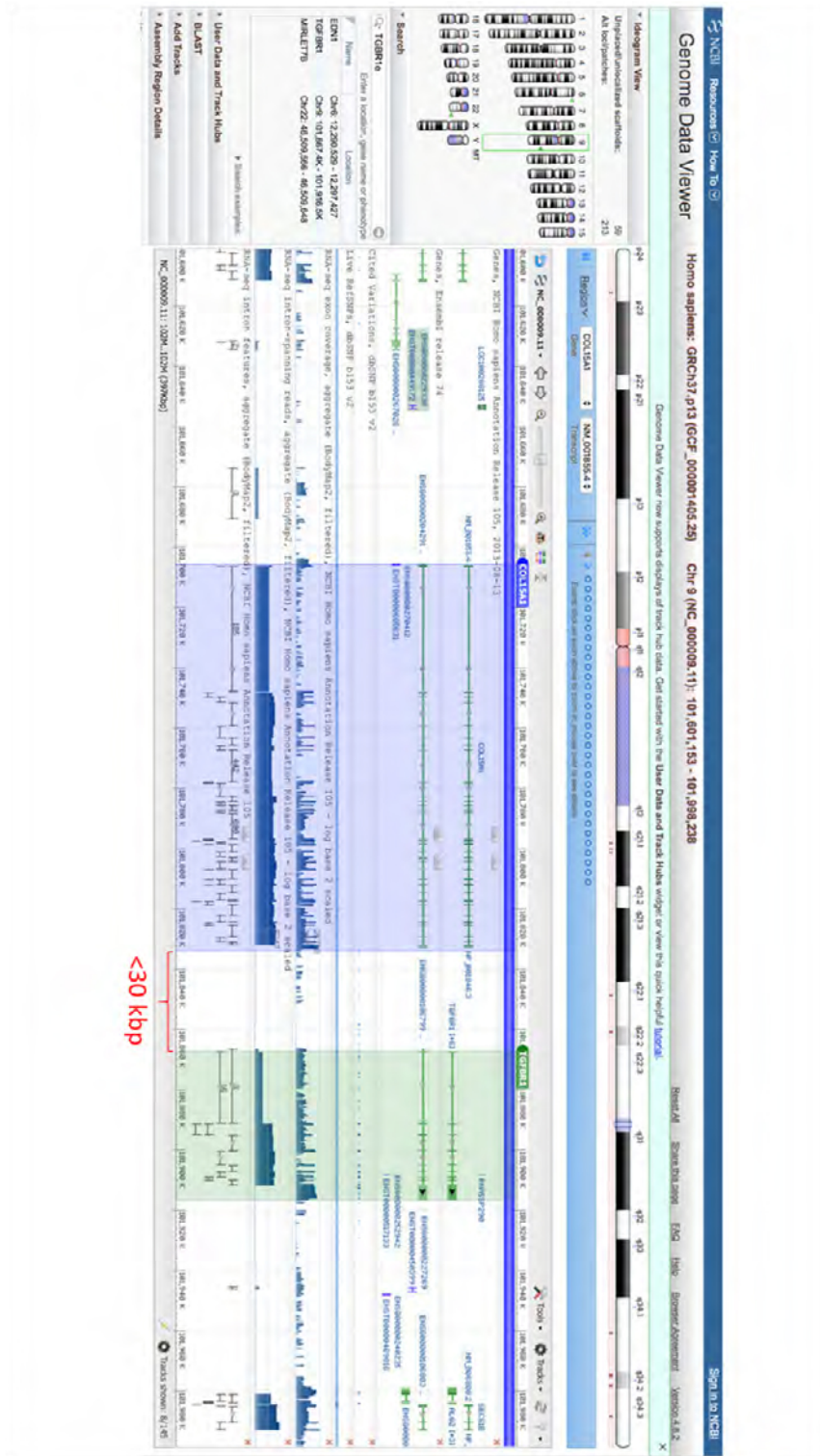
The following data was generated by Karosham Reddy (2018) under the supervision of A/Prof Brian Oliver and Razia Zakarya. Reproduced with permission.



Primary human ASM cells from non-COPD and COPD smokers were stimulated with TSA alone for 24 hours. Western blot analyses of protein abundance and phosphorylation showed that TSA treatment lead to significant increase in NF-κB p65 subunit and p38 MAPK phosphorylation in non-COPD cells only. These findings demonstrate off target effects of TSA treatment for HDAC inhibition.



Appendix D – Genome Data Viewer: Chromosomal Proximity of  
COL15A1 and TGFBR1



*COL15A1* highlighted in blue whilst *TGFBR1* highlighted in green. With <30 kbp between them, it is evident that *COL15A1* and *TGFBR1* are proximal genes, allowing for factors mediating the transcription of one to affect the other.

## Chapter 6 Reference

1. Disease GfCOL. Guide to COPD Diagnosis, Management, and Prevention. 2019.
2. Disease GfCOL. Global strategy for the diagnosis, management, and prevention of chronic obstructive pulmonary disease. 2016.
3. Krimmer DI, Burgess JK, Wooi TK, Black JL, Oliver BG. Matrix proteins from smoke-exposed fibroblasts are pro-proliferative. *Am J Respir Cell Mol Biol*. 2012;46(1):34-9.
4. Organisation WH. Global Burden of Disease. 2015.
5. AIHW. Australia's Health. Australian Institute of Health & Welfare; 2012.
6. Ltd AEP. Economic Impact of COPD and cost effective solutions. 2008.
7. Sezer H, Akkurt I, Guler N, Marakoglu K, Berk S. A case-control study on the effect of exposure to different substances on the development of COPD. *Ann Epidemiol*. 2006;16(1):59-62.
8. Boman C, Forsberg B, Sandstrom T. Shedding new light on wood smoke: a risk factor for respiratory health. *Eur Respir J*. 2006;27(3):446-7.
9. Ezzati M. Indoor air pollution and health in developing countries. *Lancet*. 2005;366(9480):104-6.
10. Mishra V, Dai X, Smith KR, Mika L. Maternal exposure to biomass smoke and reduced birth weight in Zimbabwe. *Ann Epidemiol*. 2004;14(10):740-7.
11. Tam A, Churg A, Wright JL, Zhou S, Kirby M, Coxson HO, et al. Sex Differences in Airway Remodeling in a Mouse Model of Chronic Obstructive Pulmonary Disease. *Am J Respir Crit Care Med*. 2016;193(8):825-34.
12. Fletcher C, Peto R. The natural history of chronic airflow obstruction. *Br Med J*. 1977;1(6077):1645-8.
13. Hersh CP, Hokanson JE, Lynch DA, Washko GR, Make BJ, Crapo JD, et al. Family History Is a Risk Factor for COPD. *Chest*. 2011;140(2):343-50.
14. McCLOSKEY SC, Patel BD, Hinchliffe SJ, Reid ED, Wareham NJ, Lomas DA. Siblings of patients with severe chronic obstructive pulmonary disease have a significant risk of airflow obstruction. *American Journal of Respiratory and Critical Care Medicine*. 2001;164(8):1419-24.
15. Cantani A, Micera M. A study on 300 asthmatic children, 300 controls and their parents confirms the genetic transmission of allergy and asthma. *Eur Rev Med Pharmacol Sci*. 2011;15(9):1051-6.
16. Kurzius-Spencer M, Guerra S, Sherrill DL, Halonen M, Elston RC, Martinez FD. Familial aggregation of allergen-specific sensitization and asthma. *Pediatric Allergy and Immunology*. 2012;23(1):21-7.
17. Shrine N, Portelli MA, John C, Artigas MS, Bennett N, Hall R, et al. Moderate-to-severe asthma in individuals of European ancestry: a genome-wide association study. *The Lancet Respiratory Medicine*. 2018.
18. Loveridge B, West P, Kryger MH, Anthonisen NR. Alteration in breathing pattern with progression of chronic obstructive pulmonary disease. *Am Rev Respir Dis*. 1986;134(5):930-4.
19. Arango E, Espinosa D, Illana J, Carrasco G, Moreno P, Algar FJ, et al. Lung volume reduction surgery after lung transplantation for emphysema-chronic obstructive pulmonary disease. *Transplant Proc*. 2012;44(7):2115-7.
20. Kessler R, Partridge MR, Miravittles M, Cazzola M, Vogelmeier C, Leynaud D, et al. Symptom variability in patients with severe COPD: a pan-European cross-sectional study. *Eur Respir J*. 2011;37(2):264-72.
21. Hogg JC, Chu F, Utokaparch S, Woods R, Elliott WM, Buzatu L, et al. The nature of small-airway obstruction in chronic obstructive pulmonary disease. *N Engl J Med*. 2004;350(26):2645-53.
22. Brashier B, Salvi S. Measuring lung function using sound waves: role of the forced oscillation technique and impulse oscillometry system. *Breathe*. 2015;11(1):57-65.

23. Barnes PJ. Small airways in COPD. *N Engl J Med.* 2004;350(26):2635-7.
24. Hogg JC. Pathophysiology of airflow limitation in chronic obstructive pulmonary disease. *Lancet.* 2004;364(9435):709-21.
25. McDonough JE, Yuan R, Suzuki M, Seyednejad N, Elliott WM, Sanchez PG, et al. Small-airway obstruction and emphysema in chronic obstructive pulmonary disease. *N Engl J Med.* 2011;365(17):1567-75.
26. Hogg JC, Macklem PT, Thurlbeck WM. Site and nature of airway obstruction in chronic obstructive lung disease. *N Engl J Med.* 1968;278(25):1355-60.
27. Van Brabant H, Cauberghs M, Verbeken E, Moerman P, Lauweryns JM, Van de Woestijne KP. Partitioning of pulmonary impedance in excised human and canine lungs. *J Appl Physiol Respir Environ Exerc Physiol.* 1983;55(6):1733-42.
28. Yanai M, Sekizawa K, Ohrui T, Sasaki H, Takishima T. Site of airway obstruction in pulmonary disease: direct measurement of intrabronchial pressure. *J Appl Physiol (1985).* 1992;72(3):1016-23.
29. Hulbert WC, Walker DC, Jackson A, Hogg JC. Airway permeability to horseradish peroxidase in guinea pigs: the repair phase after injury by cigarette smoke. *Am Rev Respir Dis.* 1981;123(3):320-6.
30. Jones JG, Minty BD, Lawler P, Hulands G, Crawley JC, Veall N. Increased alveolar epithelial permeability in cigarette smokers. *Lancet.* 1980;1(8159):66-8.
31. Simani AS, Inoue S, Hogg JC. Penetration of the respiratory epithelium of guinea pigs following exposure to cigarette smoke. *Lab Invest.* 1974;31(1):75-81.
32. Barnes PJ. New concepts in chronic obstructive pulmonary disease. *Annu Rev Med.* 2003;54:113-29.
33. Di Stefano A, Turato G, Maestrelli P, Mapp CE, Ruggieri MP, Roggeri A, et al. Airflow limitation in chronic bronchitis is associated with T-lymphocyte and macrophage infiltration of the bronchial mucosa. *Am J Respir Crit Care Med.* 1996;153(2):629-32.
34. Tomita K, Caramori G, Lim S, Ito K, Hanazawa T, Oates T, et al. Increased p21(CIP1/WAF1) and B cell lymphoma leukemia-x(L) expression and reduced apoptosis in alveolar macrophages from smokers. *Am J Respir Crit Care Med.* 2002;166(5):724-31.
35. Russell RE, Thorley A, Culpitt SV, Dodd S, Donnelly LE, Demattos C, et al. Alveolar macrophage-mediated elastolysis: roles of matrix metalloproteinases, cysteine, and serine proteases. *Am J Physiol Lung Cell Mol Physiol.* 2002;283(4):L867-73.
36. Saetta M, Di Stefano A, Maestrelli P, Turato G, Ruggieri MP, Roggeri A, et al. Airway eosinophilia in chronic bronchitis during exacerbations. *Am J Respir Crit Care Med.* 1994;150(6 Pt 1):1646-52.
37. Pascoe S, Locantore N, Dransfield MT, Barnes NC, Pavord ID. Blood eosinophil counts, exacerbations, and response to the addition of inhaled fluticasone furoate to vilanterol in patients with chronic obstructive pulmonary disease: a secondary analysis of data from two parallel randomised controlled trials. *The Lancet Respiratory Medicine.* 2015;3(6):435-42.
38. Criner GJ, Celli BR, Brightling CE, Agusti A, Papi A, Singh D, et al. Benralizumab for the Prevention of COPD Exacerbations. 2019.
39. Pavord ID, Chanez P, Criner GJ, Kerstjens HA, Korn S, Lugogo N, et al. Mepolizumab for eosinophilic chronic obstructive pulmonary disease. 2017;377(17):1613-29.
40. Brightling C, Greening N. Airway inflammation in COPD-progress to precision medicine. *European Respiratory Journal.* 2019:1900651.
41. Neutra MR, Mantis NJ, Kraehenbuhl JP. Collaboration of epithelial cells with organized mucosal lymphoid tissues. *Nat Immunol.* 2001;2(11):1004-9.
42. Holt PG, Stumbles PA. Regulation of immunologic homeostasis in peripheral tissues by dendritic cells: the respiratory tract as a paradigm. *J Allergy Clin Immunol.* 2000;105(3):421-9.
43. Stick SM, Holt PG. The airway epithelium as immune modulator: the LARC ascending. *Am J Respir Cell Mol Biol.* 2003;28(6):641-4.
44. Liu YJ. Dendritic cell subsets and lineages, and their functions in innate and adaptive immunity. *Cell.* 2001;106(3):259-62.

45. Aaron SD, Angel JB, Lunau M, Wright K, Fex C, Le Saux N, et al. Granulocyte inflammatory markers and airway infection during acute exacerbation of chronic obstructive pulmonary disease. *Am J Respir Crit Care Med.* 2001;163(2):349-55.
46. de Boer WI, van Schadewijk A, Sont JK, Sharma HS, Stolk J, Hiemstra PS, et al. Transforming growth factor beta1 and recruitment of macrophages and mast cells in airways in chronic obstructive pulmonary disease. *Am J Respir Crit Care Med.* 1998;158(6):1951-7.
47. Keatings VM, Collins PD, Scott DM, Barnes PJ. Differences in interleukin-8 and tumor necrosis factor-alpha in induced sputum from patients with chronic obstructive pulmonary disease or asthma. *Am J Respir Crit Care Med.* 1996;153(2):530-4.
48. O'Shaughnessy TC, Ansari TW, Barnes NC, Jeffery PK. Inflammation in bronchial biopsies of subjects with chronic bronchitis: inverse relationship of CD8+ T lymphocytes with FEV1. *Am J Respir Crit Care Med.* 1997;155(3):852-7.
49. Pesci A, Balbi B, Majori M, Cacciani G, Bertacco S, Alciato P, et al. Inflammatory cells and mediators in bronchial lavage of patients with chronic obstructive pulmonary disease. *Eur Respir J.* 1998;12(2):380-6.
50. Takizawa H, Tanaka M, Takami K, Ohtoshi T, Ito K, Satoh M, et al. Increased expression of transforming growth factor-beta1 in small airway epithelium from tobacco smokers and patients with chronic obstructive pulmonary disease (COPD). *Am J Respir Crit Care Med.* 2001;163(6):1476-83.
51. Hasday JD, Bascom R, Costa JJ, Fitzgerald T, Dubin W. Bacterial endotoxin is an active component of cigarette smoke. *Chest.* 1999;115(3):829-35.
52. Dragon S, Rahman MS, Yang J, Unruh H, Halayko AJ, Gounni AS. IL-17 enhances IL-1 $\beta$ -mediated CXCL-8 release from human airway smooth muscle cells. *American Journal of Physiology-Lung Cellular and Molecular Physiology.* 2007;292(4):L1023-L9.
53. Létuvé S, Lajoie-Kadoch S, Audusseau S, Rothenberg ME, Fiset P-O, Ludwig MS, et al. IL-17E upregulates the expression of proinflammatory cytokines in lung fibroblasts. *Journal of Allergy and Clinical Immunology.* 2006;117(3):590-6.
54. Langen RC, Schols AM, Kelders MC, Wouters EF, Janssen-Heininger YM. Inflammatory cytokines inhibit myogenic differentiation through activation of nuclear factor-kappaB. *FASEB J.* 2001;15(7):1169-80.
55. de Godoy I, Donahoe M, Calhoun WJ, Mancino J, Rogers RM. Elevated TNF-alpha production by peripheral blood monocytes of weight-losing COPD patients. *Am J Respir Crit Care Med.* 1996;153(2):633-7.
56. Kim PH, Kagnoff MF. Transforming growth factor beta 1 increases IgA isotype switching at the clonal level. *J Immunol.* 1990;145(11):3773-8.
57. Blobel GC, Schiemann WP, Lodish HF. Role of transforming growth factor beta in human disease. *N Engl J Med.* 2000;342(18):1350-8.
58. Königshoff M, Kneidinger N, Eickelberg O. TGF- $\beta$  signaling in COPD: deciphering genetic and cellular susceptibilities for future therapeutic regimen. *Swiss medical weekly.* 2009;139(3940).
59. Coker R, Laurent G, Shahzeidi S, Hernandez-Rodriguez N, Pantelidis P, Du Bois R, et al. Diverse cellular TGF-beta 1 and TGF-beta 3 gene expression in normal human and murine lung. *European Respiratory Journal.* 1996;9(12):2501-7.
60. Annes JP, Munger JS, Rifkin DB. Making sense of latent TGF $\beta$  activation. *Journal of cell science.* 2003;116(2):217-24.
61. Schmierer B, Hill CS. TGF $\beta$ -SMAD signal transduction: molecular specificity and functional flexibility. *Nature reviews Molecular cell biology.* 2007;8(12):970.
62. Redhu NS, Gounni AS. Function and mechanisms of TSLP/TSLPR complex in asthma and COPD. *Clin Exp Allergy.* 2012;42(7):994-1005.
63. Ying S, O'Connor B, Ratoff J, Meng Q, Fang C, Cousins D, et al. Expression and cellular provenance of thymic stromal lymphopoietin and chemokines in patients with severe asthma and chronic obstructive pulmonary disease. *J Immunol.* 2008;181(4):2790-8.
64. Barnes PJ. Targeting cytokines to treat asthma and chronic obstructive pulmonary disease. *Nature Reviews Immunology.* 2018;18(7):454-66.

65. James AL, Elliot JG, Jones RL, Carroll ML, Mauad T, Bai TR, et al. Airway smooth muscle hypertrophy and hyperplasia in asthma. *Am J Respir Crit Care Med.* 2012;185(10):1058-64.
66. Woodruff PG, Dolganov GM, Ferrando RE, Donnelly S, Hays SR, Solberg OD, et al. Hyperplasia of smooth muscle in mild to moderate asthma without changes in cell size or gene expression. *Am J Respir Crit Care Med.* 2004;169(9):1001-6.
67. Jones RL, Noble PB, Elliot JG, Mitchell HW, McFawn PK, Hogg JC, et al. Airflow obstruction is associated with increased smooth muscle extracellular matrix. *Eur Respir J.* 2016;47(6):1855-7.
68. Chen L, Ge Q, Tjin G, Alkhoury H, Deng L, Brandsma C-A, et al. Effects of cigarette smoke extract on human airway smooth muscle cells in COPD. *European Respiratory Journal.* 2014;44(3):634-46.
69. Jones FS, Jones PL. The tenascin family of ECM glycoproteins: structure, function, and regulation during embryonic development and tissue remodeling. *Dev Dyn.* 2000;218(2):235-59.
70. Jones RL, Noble PB, Elliot JG, James AL. Airway remodelling in COPD: It's not asthma! *Respirology.* 2016.
71. Dekkers BG, Maarsingh H, Meurs H, Gosens R. Airway structural components drive airway smooth muscle remodeling in asthma. *Proc Am Thorac Soc.* 2009;6(8):683-92.
72. Johnson PR, Black JL, Carlin S, Ge Q, Underwood PA. The production of extracellular matrix proteins by human passively sensitized airway smooth-muscle cells in culture: the effect of beclomethasone. *Am J Respir Crit Care Med.* 2000;162(6):2145-51.
73. Hynes RO. Integrins: bidirectional, allosteric signaling machines. *Cell.* 2002;110(6):673-87.
74. Bonacci JV, Harris T, Stewart AG. Impact of extracellular matrix and strain on proliferation of bovine airway smooth muscle. *Clin Exp Pharmacol Physiol.* 2003;30(5-6):324-8.
75. Hirst SJ, Twort CH, Lee TH. Differential effects of extracellular matrix proteins on human airway smooth muscle cell proliferation and phenotype. *Am J Respir Cell Mol Biol.* 2000;23(3):335-44.
76. Peng Q, Lai D, Nguyen TT, Chan V, Matsuda T, Hirst SJ. Multiple beta 1 integrins mediate enhancement of human airway smooth muscle cytokine secretion by fibronectin and type I collagen. *J Immunol.* 2005;174(4):2258-64.
77. Shibuya H, Okamoto O, Fujiwara S. The bioactivity of transforming growth factor-beta1 can be regulated via binding to dermal collagens in mink lung epithelial cells. *J Dermatol Sci.* 2006;41(3):187-95.
78. Burgess JK, Weckmann M. Matrikines and the lungs. *Pharmacology & therapeutics.* 2012;134(3):317-37.
79. Akthar S, Patel DF, Beale RC, Peiró T, Xu X, Gaggar A, et al. Matrikines are key regulators in modulating the amplitude of lung inflammation in acute pulmonary infection. *Nature communications.* 2015;6:8423.
80. Burgess JK, Weckmann M, Karsdal MA. The message from the matrix—should we listen more closely? *Journal of thoracic disease.* 2019;11(Suppl 3):S230.
81. Joehanes R, Just AC, Marioni RE, Pilling LC, Reynolds LM, Mandaviya PR, et al. Epigenetic Signatures of Cigarette Smoking. *Circ Cardiovasc Genet.* 2016.
82. Zeilinger S, Kuhnel B, Klopp N, Baurecht H, Kleinschmidt A, Gieger C, et al. Tobacco smoking leads to extensive genome-wide changes in DNA methylation. *PLoS One.* 2013;8(5):e63812.
83. Feng X-H, Derynck R. Specificity and versatility in TGF- $\beta$  signaling through Smads. *Annu Rev Cell Dev Biol.* 2005;21:659-93.
84. ten Dijke P, Hill CS. New insights into TGF- $\beta$ -Smad signalling. *Trends in biochemical sciences.* 2004;29(5):265-73.
85. Shi Y, Massagué J. Mechanisms of TGF- $\beta$  signaling from cell membrane to the nucleus. *cell.* 2003;113(6):685-700.
86. Massagué J, Seoane J, Wotton D. Smad transcription factors. *Genes & development.* 2005;19(23):2783-810.
87. Sapkota G, Alarcón C, Spagnoli FM, Brivanlou AH, Massagué J. Balancing BMP signaling through integrated inputs into the Smad1 linker. *Molecular cell.* 2007;25(3):441-54.

88. Liu F. Smad3 phosphorylation by cyclin-dependent kinases. *Cytokine & growth factor reviews*. 2006;17(1-2):9-17.
89. Dyson S, Gurdon J. The interpretation of position in a morphogen gradient as revealed by occupancy of activin receptors. *Cell*. 1998;93(4):557-68.
90. Jullien J, Gurdon J. Morphogen gradient interpretation by a regulated trafficking step during ligand-receptor transduction. *Genes & development*. 2005;19(22):2682-94.
91. Li M, Krishnaveni MS, Li C, Zhou B, Xing Y, Banfalvi A, et al. Epithelium-specific deletion of TGF- $\beta$  receptor type II protects mice from bleomycin-induced pulmonary fibrosis. *The Journal of clinical investigation*. 2011;121(1):277-87.
92. Di Guglielmo GM, Le Roy C, Goodfellow AF, Wrana JL. Distinct endocytic pathways regulate TGF- $\beta$  receptor signalling and turnover. *Nature cell biology*. 2003;5(5):410.
93. Hayes S, Chawla A, Corvera S. TGF $\beta$  receptor internalization into EEA1-enriched early endosomes: role in signaling to Smad2. *The Journal of cell biology*. 2002;158(7):1239-49.
94. Mitchell H, Choudhury A, Pagano RE, Leof EB. Ligand-dependent and-independent transforming growth factor- $\beta$  receptor recycling regulated by clathrin-mediated endocytosis and Rab11. *Molecular biology of the cell*. 2004;15(9):4166-78.
95. Zhao B, Wang Q, Du J, Luo S, Xia J, Chen Y-G. PICK1 promotes caveolin-dependent degradation of TGF- $\beta$  type I receptor. *Cell research*. 2012;22(10):1467.
96. Runyan CE, Schnaper HW, Poncelet A-C. The role of internalization in transforming growth factor  $\beta$ 1-induced Smad2 association with Smad anchor for receptor activation (SARA) and Smad2-dependent signaling in human mesangial cells. *Journal of Biological Chemistry*. 2005;280(9):8300-8.
97. Zuo W, Chen Y-G. Specific activation of mitogen-activated protein kinase by transforming growth factor- $\beta$  receptors in lipid rafts is required for epithelial cell plasticity. *Molecular biology of the cell*. 2009;20(3):1020-9.
98. He K, Yan X, Li N, Dang S, Xu L, Zhao B, et al. Internalization of the TGF- $\beta$  type I receptor into caveolin-1 and EEA1 double-positive early endosomes. *Cell research*. 2015;25(6):738.
99. Sanderson N, Factor V, Nagy P, Kopp J, Kondaiah P, Wakefield L, et al. Hepatic expression of mature transforming growth factor beta 1 in transgenic mice results in multiple tissue lesions. *Proc Natl Acad Sci U S A*. 1995;92(7):2572-6.
100. Kenyon N, Ward R, McGrew G, Last JA. TGF- $\beta$ 1 causes airway fibrosis and increased collagen I and III mRNA in mice. *Thorax*. 2003;58(9):772-7.
101. Aubert J-D, Dalal BI, Bai TR, Roberts CR, Hayashi S, Hogg J. Transforming growth factor beta 1 gene expression in human airways. *Thorax*. 1994;49(3):225-32.
102. Takizawa H, TANAKA M, Takami K, OHTOSHI T, ITO K, SATOH M, et al. Increased expression of transforming growth factor- $\beta$  1 in small airway epithelium from tobacco smokers and patients with chronic obstructive pulmonary disease (COPD). *American journal of respiratory and critical care medicine*. 2001;163(6):1476-83.
103. Vignola AM, Chanez P, Chiappara G, Merendino A, Pace E, Rizzo A, et al. Transforming growth factor- $\beta$  expression in mucosal biopsies in asthma and chronic bronchitis. *American journal of respiratory and critical care medicine*. 1997;156(2):591-9.
104. Vignola A, Chanez P, Chiappara G, Merendino A, Zinnanti E, Bousquet J, et al. Release of transforming growth factor-beta (TGF- $\beta$ ) and fibronectin by alveolar macrophages in airway diseases. *Clinical & Experimental Immunology*. 1996;106(1):114-9.
105. Zhao Y. Transforming growth factor- $\beta$  (TGF- $\beta$ ) type I and type II receptors are both required for TGF- $\beta$ -mediated extracellular matrix production in lung fibroblasts. *Molecular and cellular endocrinology*. 1999;150(1-2):91-7.
106. Baarsma HA, Menzen MH, Halayko AJ, Meurs H, Kerstjens HA, Gosens R.  $\beta$ -Catenin signaling is required for TGF- $\beta$ 1-induced extracellular matrix production by airway smooth muscle cells. *American Journal of Physiology-Lung Cellular and Molecular Physiology*. 2011;301(6):L956-L65.
107. Kumawat K, Menzen MH, Bos IST, Baarsma HA, Borger P, Roth M, et al. Noncanonical WNT-5A signaling regulates TGF- $\beta$ -induced extracellular matrix production by airway smooth muscle cells. *The FASEB journal*. 2013;27(4):1631-43.

108. Issa JP. CpG-island methylation in aging and cancer. *Curr Top Microbiol Immunol.* 2000;249:101-18.
109. Strahl BD, Allis CD. The language of covalent histone modifications. *Nature.* 2000;403(6765):41-5.
110. Law JA, Jacobsen SE. Establishing, maintaining and modifying DNA methylation patterns in plants and animals. *Nat Rev Genet.* 2010;11(3):204-20.
111. Qiu W, Baccarelli A, Carey VJ, Boutaoui N, Bacherman H, Klanderman B, et al. Variable DNA methylation is associated with chronic obstructive pulmonary disease and lung function. *Am J Respir Crit Care Med.* 2012;185(4):373-81.
112. Bestor TH. The DNA methyltransferases of mammals. *Hum Mol Genet.* 2000;9(16):2395-402.
113. Lei H, Oh SP, Okano M, Juttermann R, Goss KA, Jaenisch R, et al. De novo DNA cytosine methyltransferase activities in mouse embryonic stem cells. *Development.* 1996;122(10):3195-205.
114. Hermann A, Goyal R, Jeltsch A. The Dnmt1 DNA-(cytosine-C5)-methyltransferase methylates DNA processively with high preference for hemimethylated target sites. *J Biol Chem.* 2004;279(46):48350-9.
115. Kangaspeska S, Stride B, Metivier R, Polycarpou-Schwarz M, Ibberson D, Carmouche RP, et al. Transient cyclical methylation of promoter DNA. *Nature.* 2008;452(7183):112-5.
116. Kwon NH, Kim JS, Lee JY, Oh MJ, Choi DC. DNA methylation and the expression of IL-4 and IFN-gamma promoter genes in patients with bronchial asthma. *J Clin Immunol.* 2008;28(2):139-46.
117. Li J, Lin LH, Wang J, Peng X, Dai HR, Xiao H, et al. Interleukin-4 and interleukin-13 pathway genetics affect disease susceptibility, serum immunoglobulin E levels, and gene expression in asthma. *Ann Allergy Asthma Immunol.* 2014;113(2):173-9 e1.
118. Fukuda T, Fukushima Y, Numao T, Ando N, Arima M, Nakajima H, et al. Role of interleukin-4 and vascular cell adhesion molecule-1 in selective eosinophil migration into the airways in allergic asthma. *Am J Respir Cell Mol Biol.* 1996;14(1):84-94.
119. Rabinovich EI, Kapetanaki MG, Steinfeld I, Gibson KF, Pandit KV, Yu G, et al. Global methylation patterns in idiopathic pulmonary fibrosis. *PLoS One.* 2012;7(4):e33770.
120. Rabinovich EI, Selman M, Kaminski N. Epigenomics of idiopathic pulmonary fibrosis: evaluating the first steps. *Am J Respir Crit Care Med.* 2012;186(6):473-5.
121. Sanders YY, Ambalavanan N, Halloran B, Zhang X, Liu H, Crossman DK, et al. Altered DNA methylation profile in idiopathic pulmonary fibrosis. *Am J Respir Crit Care Med.* 2012;186(6):525-35.
122. Vucic EA, Chari R, Thu KL, Wilson IM, Cotton AM, Kennett JY, et al. DNA methylation is globally disrupted and associated with expression changes in chronic obstructive pulmonary disease small airways. *Am J Respir Cell Mol Biol.* 2014;50(5):912-22.
123. Vucic EA, Chari R, Thu KL, Wilson IM, Cotton AM, Kennett JY, et al. DNA methylation is globally disrupted and associated with expression changes in chronic obstructive pulmonary disease small airways. *American journal of respiratory cell and molecular biology.* 2014;50(5):912-22.
124. Meek PM, Sood A, Petersen H, Belinsky SA, Tesfaigzi Y. Epigenetic change (GATA-4 gene methylation) is associated with health status in chronic obstructive pulmonary disease. *Biological research for nursing.* 2015;17(2):191-8.
125. Sood A, Petersen H, Blanchette CM, Meek P, Picchi MA, Belinsky SA, et al. Wood smoke exposure and gene promoter methylation are associated with increased risk for COPD in smokers. *American journal of respiratory and critical care medicine.* 2010;182(9):1098-104.
126. Ransom M, Dennehey BK, Tyler JK. Chaperoning histones during DNA replication and repair. *Cell.* 2010;140(2):183-95.
127. Shahbazian MD, Grunstein M. Functions of site-specific histone acetylation and deacetylation. *Annu Rev Biochem.* 2007;76:75-100.
128. Luger K, Mader AW, Richmond RK, Sargent DF, Richmond TJ. Crystal structure of the nucleosome core particle at 2.8 Å resolution. *Nature.* 1997;389(6648):251-60.



129. Ito K, Yamamura S, Essilfie-Quaye S, Cosio B, Ito M, Barnes PJ, et al. Histone deacetylase 2-mediated deacetylation of the glucocorticoid receptor enables NF-kappaB suppression. *J Exp Med*. 2006;203(1):7-13.
130. Vollmuth F, Geyer M. Interaction of propionylated and butyrylated histone H3 lysine marks with Brd4 bromodomains. *Angew Chem Int Ed Engl*. 2010;49(38):6768-72.
131. Brook PO, Perry MM, Adcock IM, Durham AL. Epigenome-modifying tools in asthma. *Epigenomics*. 2015;7(6):1017-32.
132. Tessarz P, Kouzarides T. Histone core modifications regulating nucleosome structure and dynamics. *Nat Rev Mol Cell Biol*. 2014;15(11):703-8.
133. Dumuis-Kervabon A, Encontre I, Etienne G, Jauregui-Adell J, Mery J, Mesnier D, et al. A chromatin core particle obtained by selective cleavage of histones by clostripain. *EMBO J*. 1986;5(7):1735-42.
134. Xu WS, Parmigiani RB, Marks PA. Histone deacetylase inhibitors: molecular mechanisms of action. *Oncogene*. 2007;26(37):5541-52.
135. Li Z, Nie F, Wang S, Li L. Histone H4 Lys 20 monomethylation by histone methylase SET8 mediates Wnt target gene activation. *Proc Natl Acad Sci U S A*. 2011;108(8):3116-23.
136. Simon JA, Lange CA. Roles of the EZH2 histone methyltransferase in cancer epigenetics. *Mutat Res*. 2008;647(1-2):21-9.
137. Wei G, Wei L, Zhu J, Zang C, Hu-Li J, Yao Z, et al. Global mapping of H3K4me3 and H3K27me3 reveals specificity and plasticity in lineage fate determination of differentiating CD4+ T cells. *Immunity*. 2009;30(1):155-67.
138. Seumois G, Chavez L, Gerasimova A, Lienhard M, Omran N, Kalinke L, et al. Epigenomic analysis of primary human T cells reveals enhancers associated with TH2 memory cell differentiation and asthma susceptibility. *Nat Immunol*. 2014;15(8):777-88.
139. Zhu Y, van Essen D, Sacconi S. Cell-type-specific control of enhancer activity by H3K9 trimethylation. *Mol Cell*. 2012;46(4):408-23.
140. Clifford RL, Patel JK, John AE, Tatler AL, Mazengarb L, Brightling CE, et al. CXCL8 histone H3 acetylation is dysfunctional in airway smooth muscle in asthma: regulation by BET. *Am J Physiol Lung Cell Mol Physiol*. 2015;308(9):L962-72.
141. Matsushita I, Hasegawa K, Nakata K, Yasuda K, Tokunaga K, Keicho N. Genetic variants of human  $\beta$ -defensin-1 and chronic obstructive pulmonary disease. *Biochemical and biophysical research communications*. 2002;291(1):17-22.
142. Andresen E, Günther G, Bullwinkel J, Lange C, Heine H. Increased expression of beta-defensin 1 (DEFB1) in chronic obstructive pulmonary disease. *PLoS One*. 2011;6(7):e21898.
143. Young MD, Willson TA, Wakefield MJ, Trounson E, Hilton DJ, Blewitt ME, et al. ChIP-seq analysis reveals distinct H3K27me3 profiles that correlate with transcriptional activity. *Nucleic Acids Res*. 2011;39(17):7415-27.
144. Choudhary C, Kumar C, Gnad F, Nielsen ML, Rehman M, Walther TC, et al. Lysine acetylation targets protein complexes and co-regulates major cellular functions. *Science*. 2009;325(5942):834-40.
145. Kouzarides T. Acetylation: a regulatory modification to rival phosphorylation? *EMBO J*. 2000;19(6):1176-9.
146. Falkenberg KJ, Johnstone RW. Histone deacetylases and their inhibitors in cancer, neurological diseases and immune disorders. *Nat Rev Drug Discov*. 2014;13(9):673-91.
147. Bantscheff M, Hopf C, Savitski MM, Dittmann A, Grandi P, Michon AM, et al. Chemoproteomics profiling of HDAC inhibitors reveals selective targeting of HDAC complexes. *Nat Biotechnol*. 2011;29(3):255-65.
148. Ito K, Barnes PJ, Adcock IM. Glucocorticoid receptor recruitment of histone deacetylase 2 inhibits interleukin-1beta-induced histone H4 acetylation on lysines 8 and 12. *Mol Cell Biol*. 2000;20(18):6891-903.
149. Ito K, Ito M, Elliott WM, Cosio B, Caramori G, Kon OM, et al. Decreased histone deacetylase activity in chronic obstructive pulmonary disease. *N Engl J Med*. 2005;352(19):1967-76.
150. Ito K, Caramori G, Lim S, Oates T, Chung KF, Barnes PJ, et al. Expression and activity of histone deacetylases in human asthmatic airways. *Am J Respir Crit Care Med*. 2002;166(3):392-6.

151. Ito K, Lim S, Caramori G, Chung KF, Barnes PJ, Adcock IM. Cigarette smoking reduces histone deacetylase 2 expression, enhances cytokine expression, and inhibits glucocorticoid actions in alveolar macrophages. *FASEB J*. 2001;15(6):1110-2.
152. Shakespear MR, Halili MA, Irvine KM, Fairlie DP, Sweet MJ. Histone deacetylases as regulators of inflammation and immunity. *Trends Immunol*. 2011;32(7):335-43.
153. Grausenburger R, Bilic I, Boucheron N, Zupkovitz G, El-Housseiny L, Tschisnarov R, et al. Conditional deletion of histone deacetylase 1 in T cells leads to enhanced airway inflammation and increased Th2 cytokine production. *J Immunol*. 2010;185(6):3489-97.
154. Halili MA, Andrews MR, Sweet MJ, Fairlie DP. Histone deacetylase inhibitors in inflammatory disease. *Curr Top Med Chem*. 2009;9(3):309-19.
155. Tamaru H, Selker EU. A histone H3 methyltransferase controls DNA methylation in *Neurospora crassa*. *Nature*. 2001;414(6861):277-83.
156. You A, Tong JK, Grozinger CM, Schreiber SL. CoREST is an integral component of the CoREST- human histone deacetylase complex. *Proc Natl Acad Sci U S A*. 2001;98(4):1454-8.
157. Kim HP, Leonard WJ. CREB/ATF-dependent T cell receptor-induced FoxP3 gene expression: a role for DNA methylation. *J Exp Med*. 2007;204(7):1543-51.
158. Floess S, Freyer J, Siewert C, Baron U, Olek S, Polansky J, et al. Epigenetic control of the foxp3 locus in regulatory T cells. *PLoS Biol*. 2007;5(2):e38.
159. Filippakopoulos P, Picaud S, Mangos M, Keates T, Lambert JP, Barsyte-Lovejoy D, et al. Histone recognition and large-scale structural analysis of the human bromodomain family. *Cell*. 2012;149(1):214-31.
160. Owen DJ, Ornaghi P, Yang JC, Lowe N, Evans PR, Ballario P, et al. The structural basis for the recognition of acetylated histone H4 by the bromodomain of histone acetyltransferase gcn5p. *EMBO J*. 2000;19(22):6141-9.
161. Zeng L, Zhou MM. Bromodomain: an acetyl-lysine binding domain. *FEBS Lett*. 2002;513(1):124-8.
162. Wu SY, Lee AY, Hou SY, Kemper JK, Erdjument-Bromage H, Tempst P, et al. Brd4 links chromatin targeting to HPV transcriptional silencing. *Genes Dev*. 2006;20(17):2383-96.
163. Jang MK, Mochizuki K, Zhou M, Jeong H-S, Brady JN, Ozato K. The bromodomain protein Brd4 is a positive regulatory component of P-TEFb and stimulates RNA polymerase II-dependent transcription. *Molecular cell*. 2005;19(4):523-34.
164. Dey A, Chitsaz F, Abbasi A, Misteli T, Ozato K. The double bromodomain protein Brd4 binds to acetylated chromatin during interphase and mitosis. *Proceedings of the National Academy of Sciences*. 2003;100(15):8758-63.
165. Dey A, Ellenberg J, Farina A, Coleman AE, Maruyama T, Sciortino S, et al. A bromodomain protein, MCAP, associates with mitotic chromosomes and affects G2-to-M transition. *Molecular and cellular biology*. 2000;20(17):6537-49.
166. Dey A, Nishiyama A, Karpova T, McNally J, Ozato K. Brd4 marks select genes on mitotic chromatin and directs postmitotic transcription. *Molecular biology of the cell*. 2009;20(23):4899-909.
167. Wu S-Y, Chiang C-M. The double bromodomain-containing chromatin adaptor Brd4 and transcriptional regulation. *Journal of Biological Chemistry*. 2007;282(18):13141-5.
168. Khan YM, Kirkham P, Barnes PJ, Adcock IM. Brd4 is essential for IL-1beta-induced inflammation in human airway epithelial cells. *PLoS One*. 2014;9(4):e95051.
169. Perry MM, Durham AL, Austin PJ, Adcock IM, Chung KF. BET bromodomains regulate transforming growth factor-beta-induced proliferation and cytokine release in asthmatic airway smooth muscle. *J Biol Chem*. 2015;290(14):9111-21.
170. Filippakopoulos P, Qi J, Picaud S, Shen Y, Smith WB, Fedorov O, et al. Selective inhibition of BET bromodomains. *Nature*. 2010;468(7327):1067-73.
171. Tripathi S, Stelmack GL, Shan L, Unruh H, Gounni AS, Halayko AJ, et al. Epigenetic Control By Bromodomain Proteins Drives Increased Release Of Thymic Stromal Lymphopoietin (TSLP) By Human COPD Lung Fibroblasts. C21 MECHANISMS THAT LINK AGING WITH LUNG DISEASE: THE CUTTING EDGE: Am Thoracic Soc; 2014. p. A3981-A.

172. Malhotra R, Kurian N, Zhou X-H, Jiang F, Monkley S, DeMicco A, et al. Altered regulation and expression of genes by BET family of proteins in COPD patients. *PloS one*. 2017;12(3):e0173115.
173. Kendzioriski C, Irizarry R, Chen K-S, Haag J, Gould MJPotNAoS. On the utility of pooling biological samples in microarray experiments. 2005;102(12):4252-7.
174. Annoni R, Lanças T, Tanigawa RY, de Medeiros Matsushita M, de Moraes Fernezlian S, Bruno A, et al. Extracellular matrix composition in COPD. 2012;40(6):1362-73.
175. Löfdahl M, Kaarteenaho R, Lappi-Blanco E, Tornling G, Sköld MCJRr. Tenascin-C and alpha-smooth muscle actin positive cells are increased in the large airways in patients with COPD. 2011;12(1):48.
176. Gocheva V, Naba A, Bhutkar A, Guardia T, Miller KM, Li CM-C, et al. Quantitative proteomics identify Tenascin-C as a promoter of lung cancer progression and contributor to a signature prognostic of patient survival. 2017;114(28):E5625-E34.
177. Carey WA, Taylor GD, Dean WB, Bristow JDJAJoP-LC, Physiology M. Tenascin-C deficiency attenuates TGF- $\beta$ -mediated fibrosis following murine lung injury. 2010;299(6):L785-L93.
178. Bhattacharyya S, Wang W, Morales-Nebreda L, Feng G, Wu M, Zhou X, et al. Tenascin-C drives persistence of organ fibrosis. 2016;7:11703.
179. Trebault A, Chan E, Midwood K. Regulation of fibroblast migration by tenascin-C. Portland Press Limited; 2007.
180. Tomono Y, Naito I, Ando K, Yonezawa T, Sado Y, Hirakawa S, et al. Epitope-defined monoclonal antibodies against multiplexin collagens demonstrate that type XV and XVIII collagens are expressed in specialized basement membranes. 2002;27(1):9-20.
181. Hägg P, Hägg P, Peltonen S, Autio-Harmainen H, Pihlajaniemi TJTAjop. Location of type XV collagen in human tissues and its accumulation in the interstitial matrix of the fibrotic kidney. 1997;150(6):2075.
182. Akthar S, Patel DF, Beale RC, Peiro T, Xu X, Gaggar A, et al. Matrikines are key regulators in modulating the amplitude of lung inflammation in acute pulmonary infection. *Nature communications*. 2015;6:8423.
183. Patel DF, Snelgrove RJJERR. The multifaceted roles of the matrikine Pro-Gly-Pro in pulmonary health and disease. 2018;27(148):180017.
184. Abdul Roda M, Fernstrand AM, Redegeld FA, Blalock JE, Gaggar A, Folkerts GJAJoP-LC, et al. The matrikine PGP as a potential biomarker in COPD. 2015;308(11):L1095-L101.
185. Ramchandran R, Dhanabal M, Volk R, Waterman MJ, Segal M, Lu H, et al. Antiangiogenic activity of restin, NC10 domain of human collagen XV: comparison to endostatin. 1999;255(3):735-9.
186. Bilbe G, Delabie J, Bruggen J, Richener H, Asselbergs FA, Cerletti N, et al. Restin: a novel intermediate filament-associated protein highly expressed in the Reed-Sternberg cells of Hodgkin's disease. *Embo j*. 1992;11(6):2103-13.
187. Gardiner-Garden M, Frommer MJJomb. CpG islands in vertebrate genomes. 1987;196(2):261-82.
188. Deaton AM, Bird AJG, development. CpG islands and the regulation of transcription. 2011;25(10):1010-22.
189. Jin B, Robertson KD. DNA methyltransferases, DNA damage repair, and cancer. *Epigenetic Alterations in Oncogenesis*: Springer; 2013. p. 3-29.
190. Svedružić ŽM. Dnmt1: structure and function. *Progress in molecular biology and translational science*. 101: Elsevier; 2011. p. 221-54.
191. Christman JKJO. 5-Azacytidine and 5-aza-2'-deoxycytidine as inhibitors of DNA methylation: mechanistic studies and their implications for cancer therapy. 2002;21(35):5483.
192. Kaminskas E, Farrell AT, Wang Y-C, Sridhara R, Pazdur RJTo. FDA drug approval summary: azacitidine (5-azacytidine, Vidaza™) for injectable suspension. 2005;10(3):176-82.
193. Khorasanizadeh SJC. The nucleosome: from genomic organization to genomic regulation. 2004;116(2):259-72.
194. Allfrey V, Faulkner R, Mirsky AJPotNAoS. Acetylation and methylation of histones and their possible role in the regulation of RNA synthesis. 1964;51(5):786-94.

195. Nightingale KP, O'Neill LP, Turner BMJCoig, development. Histone modifications: signalling receptors and potential elements of a heritable epigenetic code. 2006;16(2):125-36.
196. Peterson CL, Laniel M-AJCB. Histones and histone modifications. 2004;14(14):R546-R51.
197. Spencer VA, Davie JRJG. Role of covalent modifications of histones in regulating gene expression. 1999;240(1):1-12.
198. Berndsen CE, Denu JMCoisb. Catalysis and substrate selection by histone/protein lysine acetyltransferases. 2008;18(6):682-9.
199. Devaiah BN, Case-Borden C, Gegonne A, Hsu CH, Chen Q, Meerzaman D, et al. BRD4 is a histone acetyltransferase that evicts nucleosomes from chromatin. 2016;23(6):540.
200. Kuo Y-M, Andrews AJJPo. Quantitating the specificity and selectivity of Gcn5-mediated acetylation of histone H3. 2013;8(2):e54896.
201. Schiltz RL, Mizzen CA, Vassilev A, Cook RG, Allis CD, Nakatani YJJoBC. Overlapping but distinct patterns of histone acetylation by the human coactivators p300 and PCAF within nucleosomal substrates. 1999;274(3):1189-92.
202. Balasubramanyam K, Varier RA, Altaf M, Swaminathan V, Siddappa NB, Ranga U, et al. Curcumin, a novel p300/CREB-binding protein-specific inhibitor of acetyltransferase, represses the acetylation of histone/nonhistone proteins and histone acetyltransferase-dependent chromatin transcription. 2004;279(49):51163-71.
203. Kang S-K, Cha S-H, Jeon H-GJSc, development. Curcumin-induced histone hypoacetylation enhances caspase-3-dependent glioma cell death and neurogenesis of neural progenitor cells. 2006;15(2):165-74.
204. Morimoto T, Sunagawa Y, Kawamura T, Takaya T, Wada H, Nagasawa A, et al. The dietary compound curcumin inhibits p300 histone acetyltransferase activity and prevents heart failure in rats. 2008;118(3):868-78.
205. Yao Y-L, Yang W-MJBRI. Beyond histone and deacetylase: an overview of cytoplasmic histone deacetylases and their nonhistone substrates. 2010;2011.
206. Di Giorgio E, Brancolini CJE. Regulation of class IIa HDAC activities: it is not only matter of subcellular localization. 2016;8(2):251-69.
207. Gallinari P, Di Marco S, Jones P, Pallaoro M, Steinkühler CJCr. HDACs, histone deacetylation and gene transcription: from molecular biology to cancer therapeutics. 2007;17(3):195.
208. Frye RAJB, communications br. Phylogenetic classification of prokaryotic and eukaryotic Sir2-like proteins. 2000;273(2):793-8.
209. De Ruijter AJ, Van Gennip AH, Caron HN, Stephan K, Van Kuilenburg ABJBJ. Histone deacetylases (HDACs): characterization of the classical HDAC family. 2003;370(3):737-49.
210. Sakuma T, Uzawa K, Onda T, Shiiba M, Yokoe H, Shibahara T, et al. Aberrant expression of histone deacetylase 6 in oral squamous cell carcinoma. 2006;29(1):117-24.
211. Barneda-Zahonero B, Parra MJMo. Histone deacetylases and cancer. 2012;6(6):579-89.
212. Barnes P. Theophylline for COPD. BMJ Publishing Group Ltd; 2006.
213. Ito K, Lim S, Caramori G, Cosio B, Chung KF, Adcock IM, et al. A molecular mechanism of action of theophylline: induction of histone deacetylase activity to decrease inflammatory gene expression. 2002;99(13):8921-6.
214. Cosio BG, Tsaprouni L, Ito K, Jazrawi E, Adcock IM, Barnes PJJJoEM. Theophylline restores histone deacetylase activity and steroid responses in COPD macrophages. 2004;200(5):689-95.
215. Cosío BG, Shafiek H, Iglesias A, Yanez A, Córdova R, Palou A, et al. Oral low-dose theophylline on top of inhaled fluticasone-salmeterol does not reduce exacerbations in patients with severe COPD: a pilot clinical trial. 2016;150(1):123-30.
216. Götz R, Köster R, Winkler C, Raulf F, Lottspeich F, Schartl M, et al. Neurotrophin-6 is a new member of the nerve growth factor family. 1994;372(6503):266.
217. Yoshida M, Kijima M, Akita M, Beppu TJJoBC. Potent and specific inhibition of mammalian histone deacetylase both in vivo and in vitro by trichostatin A. 1990;265(28):17174-9.
218. Alam H, Gu B, Lee MGJC, sciences ml. Histone methylation modifiers in cellular signaling pathways. 2015;72(23):4577-92.
219. Ng S, Yue W, Oppermann U, Klose RJC, Sciences ML. Dynamic protein methylation in chromatin biology. 2009;66(3):407.
220. Strahl BD, Allis CDJN. The language of covalent histone modifications. 2000;403(6765):41.

221. Cavalli G. Chromatin and epigenetics in development: blending cellular memory with cell fate plasticity. The Company of Biologists Ltd; 2006.
222. Minard ME, Jain AK, Barton MCJG. Analysis of epigenetic alterations to chromatin during development. 2009;47(8):559-72.
223. Briggs SD, Xiao T, Sun Z-W, Caldwell JA, Shabanowitz J, Hunt DF, et al. Gene silencing: trans-histone regulatory pathway in chromatin. 2002;418(6897):498.
224. Frederiks F, Tzouros M, Oudgenoeg G, Van Welsem T, Fornerod M, Krijgsveld J, et al. Nonprocessive methylation by Dot1 leads to functional redundancy of histone H3K79 methylation states. 2008;15(6):550.
225. Margueron R, Trojer P, Reinberg DJCoig, development. The key to development: interpreting the histone code? 2005;15(2):163-76.
226. Pokholok DK, Harbison CT, Levine S, Cole M, Hannett NM, Lee TI, et al. Genome-wide map of nucleosome acetylation and methylation in yeast. 2005;122(4):517-27.
227. Kouzarides TJCoig, development. Histone methylation in transcriptional control. 2002;12(2):198-209.
228. Bedford MT, Richard SJMc. Arginine methylation: an emerging regulator of protein function. 2005;18(3):263-72.
229. Garcia BA, Hake SB, Diaz RL, Kauer M, Morris SA, Recht J, et al. Organismal differences in post-translational modifications in histones H3 and H4. 2007;282(10):7641-55.
230. Chen M-W, Hua K-T, Kao H-J, Chi C-C, Wei L-H, Johansson G, et al. H3K9 histone methyltransferase G9a promotes lung cancer invasion and metastasis by silencing the cell adhesion molecule Ep-CAM. 2010;70(20):7830-40.
231. Rodriguez-Paredes M, De Paz AM, Simo-Riudalbas L, Sayols S, Moutinho C, Moran S, et al. Gene amplification of the histone methyltransferase SETDB1 contributes to human lung tumorigenesis. 2014;33(21):2807.
232. Matsushita I, Hasegawa K, Nakata K, Yasuda K, Tokunaga K, Keicho NJB, et al. Genetic variants of human  $\beta$ -defensin-1 and chronic obstructive pulmonary disease. 2002;291(1):17-22.
233. Andresen E, Günther G, Bullwinkel J, Lange C, Heine HJPO. Increased expression of beta-defensin 1 (DEFB1) in chronic obstructive pulmonary disease. 2011;6(7):e21898.
234. Smitheman KN, Severson TM, Rajapurkar SR, McCabe MT, Karpnich N, Foley J, et al. Lysine specific demethylase 1 inactivation enhances differentiation and promotes cytotoxic response when combined with all-trans retinoic acid in acute myeloid leukemia across subtypes. 2019;104(6):1156-67.
235. Huang R, Sun J, Li M, Dong Y, Zhang Y, Yan J. UNC0642 inhibits G9a and induces apoptosis of human bladder cancer cells. AACR; 2019.
236. Menon VP, Sudheer AR. Antioxidant and anti-inflammatory properties of curcumin. The molecular targets and therapeutic uses of curcumin in health and disease: Springer; 2007. p. 105-25.
237. Ak T, Gülçin İJC-bi. Antioxidant and radical scavenging properties of curcumin. 2008;174(1):27-37.
238. Ashburner BP, Westerheide SD, Baldwin ASJM, biology c. The p65 (RelA) subunit of NF- $\kappa$ B interacts with the histone deacetylase (HDAC) corepressors HDAC1 and HDAC2 to negatively regulate gene expression. 2001;21(20):7065-77.
239. Saccani S, Pantano S, Natoli GJJoEM. Two waves of nuclear factor  $\kappa$ B recruitment to target promoters. 2001;193(12):1351-60.
240. Spannhoff A, Machmur R, Heinke R, Trojer P, Bauer I, Brosch G, et al. A novel arginine methyltransferase inhibitor with cellular activity. 2007;17(15):4150-3.
241. Devaiah BN, Singer DSJT. Two faces of brd4: mitotic bookmark and transcriptional lynchpin. 2013;4(1):13-7.
242. Dey A, Ellenberg J, Farina A, Coleman AE, Maruyama T, Sciortino S, et al. A bromodomain protein, MCAP, associates with mitotic chromosomes and affects G2-to-M transition. 2000;20(17):6537-49.
243. Kanno T, Kanno Y, Siegel RM, Jang MK, Lenardo MJ, Ozato KJMc. Selective recognition of acetylated histones by bromodomain proteins visualized in living cells. 2004;13(1):33-43.

244. Crowe BL, Larue RC, Yuan C, Hess S, Kvaratskhelia M, Foster MPJPotNAoS. Structure of the Brd4 ET domain bound to a C-terminal motif from  $\gamma$ -retroviral integrases reveals a conserved mechanism of interaction. 2016;113(8):2086-91.
245. Kwak H, Lis JTJArog. Control of transcriptional elongation. 2013;47:483-508.
246. Adelman K, Lis JTJNRG. Promoter-proximal pausing of RNA polymerase II: emerging roles in metazoans. 2012;13(10):720.
247. Yang X-JJO. Multisite protein modification and intramolecular signaling. 2005;24(10):1653.
248. Yang Z, Yik JH, Chen R, He N, Jang MK, Ozato K, et al. Recruitment of P-TEFb for stimulation of transcriptional elongation by the bromodomain protein Brd4. 2005;19(4):535-45.
249. Zhou Q, Li T, Price DHJArob. RNA polymerase II elongation control. 2012;81:119-43.
250. Jang MK, Mochizuki K, Zhou M, Jeong H-S, Brady JN, Ozato KJMc. The bromodomain protein Brd4 is a positive regulatory component of P-TEFb and stimulates RNA polymerase II-dependent transcription. 2005;19(4):523-34.
251. Liu W, Ma Q, Wong K, Li W, Ohgi K, Zhang J, et al. Brd4 and JMJD6-associated anti-pause enhancers in regulation of transcriptional pause release. 2013;155(7):1581-95.
252. Zhou M, Huang K, Jung K-J, Cho W-K, Klase Z, Kashanchi F, et al. Bromodomain protein Brd4 regulates human immunodeficiency virus transcription through phosphorylation of CDK9 at threonine 29. 2009;83(2):1036-44.
253. Wu S-Y, Lee A-Y, Lai H-T, Zhang H, Chiang C-MJMc. Phospho switch triggers Brd4 chromatin binding and activator recruitment for gene-specific targeting. 2013;49(5):843-57.
254. Kruhlak MJ, Hendzel MJ, Fischle W, Bertos NR, Hameed S, Yang X-J, et al. Regulation of global acetylation in mitosis through loss of histone acetyltransferases and deacetylases from chromatin. 2001;276(41):38307-19.
255. Long JJ, Leresche A, Kriwacki RW, Gottesfeld JMJM, biology c. Repression of TFIID transcriptional activity and TFIID-associated cdk7 kinase activity at mitosis. 1998;18(3):1467-76.
256. Segil N, Guermah M, Hoffmann A, Roeder RG, Heintz NJG, Development. Mitotic regulation of TFIID: inhibition of activator-dependent transcription and changes in subcellular localization. 1996;10(19):2389-400.
257. Dey A, Chitsaz F, Abbasi A, Misteli T, Ozato KJPotNAoS. The double bromodomain protein Brd4 binds to acetylated chromatin during interphase and mitosis. 2003;100(15):8758-63.
258. Zhao R, Nakamura T, Fu Y, Lazar Z, Spector DLJNcb. Gene bookmarking accelerates the kinetics of post-mitotic transcriptional re-activation. 2011;13(11):1295.
259. Zuber J, Shi J, Wang E, Rappaport AR, Herrmann H, Sison EA, et al. RNAi screen identifies Brd4 as a therapeutic target in acute myeloid leukaemia. 2011;478(7370):524.
260. Delmore JE, Issa GC, Lemieux ME, Rahl PB, Shi J, Jacobs HM, et al. BET bromodomain inhibition as a therapeutic strategy to target c-Myc. 2011;146(6):904-17.
261. Mertz JA, Conery AR, Bryant BM, Sandy P, Balasubramanian S, Mele DA, et al. Targeting MYC dependence in cancer by inhibiting BET bromodomains. 2011;108(40):16669-74.
262. Perry MM, Durham AL, Austin PJ, Adcock IM, Chung KFJJoBC. BET bromodomains regulate transforming growth factor- $\beta$ -induced proliferation and cytokine release in asthmatic airway smooth muscle. 2015;290(14):9111-21.
263. Mumby S, Gambaryan N, Meng C, Perros F, Humbert M, Wort SJ, et al. Bromodomain and extra-terminal protein mimic JQ1 decreases inflammation in human vascular endothelial cells: Implications for pulmonary arterial hypertension. *Respirology*. 2017;22(1):157-64.
264. Migeot V, Hermand D. Chromatin Immunoprecipitation-Polymerase Chain Reaction (ChIP-PCR) Detects Methylation, Acetylation, and Ubiquitylation in *S. pombe*. *Schizosaccharomyces pombe*: Springer; 2018. p. 25-34.
265. Ross S, Cheung E, Petrakis TG, Howell M, Kraus WL, Hill CSJTEj. Smads orchestrate specific histone modifications and chromatin remodeling to activate transcription. 2006;25(19):4490-502.
266. Massagué J, Wotton DJTEj. Transcriptional control by the TGF- $\beta$ /Smad signaling system. 2000;19(8):1745-54.
267. Levy GG, Motto DG, Ginsburg DJB. ADAMTS13 turns 3. 2005;106(1):11-7.

268. Marwick JA, Kirkham PA, Stevenson CS, Danahay H, Giddings J, Butler K, et al. Cigarette smoke alters chromatin remodeling and induces proinflammatory genes in rat lungs. 2004;31(6):633-42.
269. Yang S-R, Valvo S, Yao H, Kode A, Rajendrasozhan S, Edirisinghe I, et al. IKK $\alpha$  causes chromatin modification on pro-inflammatory genes by cigarette smoke in mouse lung. 2008;38(6):689-98.
270. Szulakowski P, Crowther AJ, Jiménez LA, Donaldson K, Mayer R, Leonard TB, et al. The effect of smoking on the transcriptional regulation of lung inflammation in patients with chronic obstructive pulmonary disease. 2006;174(1):41-50.
271. Estève P-O, Chin HG, Smallwood A, Feehery GR, Gangisetty O, Karpf AR, et al. Direct interaction between DNMT1 and G9a coordinates DNA and histone methylation during replication. 2006;20(22):3089-103.
272. Tamaru H, Selker EUJN. A histone H3 methyltransferase controls DNA methylation in *Neurospora crassa*. 2001;414(6861):277.
273. Llinàs L, Peinado VI, Goni JR, Rabinovich R, Pizarro S, Rodriguez-Roisin R, et al. Similar gene expression profiles in smokers and patients with moderate COPD. 2011;24(1):32-41.
274. Hebbes T, Clayton A, Thorne A, Crane-Robinson CJTEj. Core histone hyperacetylation co-maps with generalized DNase I sensitivity in the chicken beta-globin chromosomal domain. 1994;13(8):1823-30.
275. Forsberg EC, Bresnick EHJB. Histone acetylation beyond promoters: long-range acetylation patterns in the chromatin world. 2001;23(9):820-30.
276. Riggs AD, Porter TNJCSHMA. Overview of epigenetic mechanisms. 1996;32:29-45.